SCUOLA DI DOTTORATO

UNIVERSITÀ DEGLI STUDI DI MILANO-BICOCCA

MISSIONE 4
ISTRUZIONE
RICERCA

Department of Earth and Environmental Sciences (DISAT)

PhD program in Marine Sciences, Technology and Management (MTM) Cycle XXXVIII

DEVELOPMENT OF SUSTAINABLE SEMI-SOLID COSMETIC EMULSION BASED ON PLANT-DERIVED BIOACTIVE EXTRACTS

DE SANTES BEATRICE

Registration number 876124

Tutor: Prof. Miriam COLOMBO

Co-tutor: Dr. Lucia SALVIONI

Supervisor: Prof. Paolo GALLI

Coordinator: Prof. Paolo Galli

ACADEMIC YEAR 2024-2025

Finanziato dall'Unione europea NextGenerationEU

Ministero dell'Università e della Ricerca

Italiadomani
PIANO NAZIONALE DI RIPRESA E RESILIENZA

INDEX

Abstract

The cosmetic industry is currently undergoing rapid expansion, driven by the increasing demand for skincare products, particularly anti-aging formulations aimed at counteracting visible signs of skin aging in an increasingly aging population. In parallel, this sector is facing unprecedented challenges linked to the global climate crisis, which has fostered heightened consumer awareness regarding sustainability and environmental impact. As a result, there is growing pressure to develop cosmetic products that combine efficacy, safety, and sustainability, spanning from raw material selection and extraction processes to formulation design and final product performance.

Within this context, the main objective of this PhD project was the development of an innovative and sustainable semi-solid anti-aging cosmetic formulation through an integrated and multidisciplinary approach. The project covered the bioprospecting and selection of plant-based active ingredients adapted to extreme environments, the use of low-impact extraction techniques, the evaluation of relevant biological activities, and the development of a functional cosmetic formulation. In parallel, recognizing that not all selected extracts might be suitable for cosmetic anti-aging applications, alternative biological uses were explored to ensure their scientific and functional valorization.

Two plant species native to or dominant in the United Arab Emirates (UAE) were selected as case studies: *Prosopis cineraria* (Ghaf), the national tree of the UAE, and *Avicennia marina*, the only mangrove species naturally occurring in the region. Both species thrive under harsh environmental conditions, including high salinity, drought, and extreme temperatures, which are known to drive the biosynthesis of distinctive secondary metabolites with potential biological relevance.

In the first phase of the project, hydroalcoholic extracts obtained from different plant parts of both species were screened for their potential anti-aging properties. Antioxidant activity was evaluated alongside the inhibitory capacity against key enzymes involved in extracellular matrix (ECM) remodeling, namely elastase, collagenase, and hyaluronidase. Ghaf extracts consistently exhibited outstanding radical scavenging activity and robust, biologically relevant inhibition of all tested enzymes, regardless of the plant portion. These results highlighted Ghaf as a highly promising multifunctional anti-aging candidate and supported the feasibility of using a single extract

representative of the whole plant. In contrast, *A. marina* extracts showed only moderate antioxidant activity and limited enzyme inhibition, insufficient to justify further cosmetic formulation development.

Based on these findings, the second phase of the project focused on Ghaf extract as an anti-aging active ingredient and its incorporation into a sustainable cosmetic formulation. A representative whole-plant Ghaf extract was chemically characterized by UHPLC–DAD–HRMS/MS, revealing a polyphenol-rich profile dominated by catechins and flavonoid derivatives. The extract confirmed strong antioxidant activity and exhibited inhibitory effects against elastase, collagenase, hyaluronidase, and tyrosinase, addressing multiple biochemical pathways involved in skin aging. In parallel, a sustainable oil-in-water Pickering emulsion was developed using natural stabilizers and a Design of Experiments (DoE) approach. The selected formulation featured a minimal INCI list, avoided heating, and maintained excellent physical stability. Importantly, incorporation of Ghaf extract did not compromise the physicochemical, rheological, or microstructural properties of the emulsion, resulting in a stable semi-solid cosmetic prototype.

Finally, given the limited cosmetic anti-aging potential of *A. marina*, a third phase adopted a bioprospecting-oriented strategy to explore alternative biological applications. Comprehensive phytochemical profiling of extracts from different plant parts identified 49 compounds, including several phenylethanoid glycosides and triterpene saponins reported for the first time in *A. marina* and mangroves. Antioxidant assays and *in vitro* cytotoxicity tests against cancer and normal cell lines revealed strong, plant-part-specific bioactivities, particularly for root and pericarp extracts. These findings highlighted *A. marina* as a valuable source of bioactive compounds with antioxidant and anticancer potential, supporting its further investigation beyond cosmetic applications.

Overall, this PhD project demonstrates the value of an integrated, evidence-based, and sustainability-oriented approach to the valorization of plant resources. By combining bioprospecting, biological screening, phytochemical characterization, and formulation development, the work provides a comprehensive framework for the development of natural cosmetic actives while remaining adaptable to alternative biomedical applications when appropriate.

1 Introduction

1.1 Global context: wellness, luxury market, and personal care evolution

Wellness and personal care have become increasingly central themes in contemporary society. In the context of growing environmental stressors, urban pollution, and lifestyle-related challenges, self-care is no longer perceived as a secondary or purely aesthetic practice, but rather as an essential component of individual health and well-being [1]. This shift has been further amplified by the COVID-19 pandemic, which represented a critical turning point in public awareness of personal health. Beyond its systemic effects, COVID-19 was also associated with dermatological manifestations and skin barrier alterations in certain individuals, contributing to increased attention toward skin health and protective care routines[2].

Within this framework, cosmetic products have played an important role as accessible tools for daily self-care[3]. Together with the effects of globalization, digitalization, and expanding consumer access to information, this renewed focus on personal well-being has contributed to the global growth of the cosmetic industry[4]. According to the European Commission Regulation No. 1223/2009, cosmetics are defined as "any substance or mixture intended to be placed in contact with the external parts of the human body (epidermis, hair system, nails, lips and external genital organs) or with the teeth and the mucous membranes of the oral cavity with a view exclusively or mainly to cleaning them, perfuming them, changing their appearance, protecting them, keeping them in good condition or correcting body odours"[5]. While this regulatory definition frames cosmetics primarily as external-use products, consumer perception has progressively evolved toward recognizing skincare as an integral component of overall wellness rather than a purely appearance-driven practice. Indeed, although many personal care products formally fall under the cosmetic category, consumer demand has increasingly shifted toward skincare-oriented products[6]. Traditionally associated with aesthetic enhancement, skincare today encompasses broader concepts such as prevention, skin health maintenance, comfort, and self-esteem, reflecting a wider sociocultural transformation that spans all genders and age groups[7]. In parallel, economic development and technological progress have contributed to reshaping the concept of "healthy skin," fostering demand for products capable of improving hydration, preventing premature aging, and mitigating visible signs of photoaging[8].

Demographic trends further reinforce this expansion. Population aging and increased life expectancy have generated a growing consumer demand for effective strategies aimed at preserving a youthful and healthy appearance over time[9]. Consequently, anti-aging skincare has emerged as one of the most dynamic segments of the cosmetic market, driving continuous research into novel ingredients, mechanisms of action, and scientifically substantiated claims[10].

Alongside these developments, growing lifestyle and fashion trends, strongly influenced by social media impact and communication explosion, have fueled the expansion of the luxury market, including the luxury cosmetics sector[11]. Whereas luxury was historically associated primarily with the possession of material goods, contemporary luxury increasingly emphasizes personal experience, meaningfulness, and self-expression. In line with this sociological shift, luxury has progressively moved from a paradigm of "having" to one of "being," where products are expected to deliver not only performance but also values, identity, and emotional engagement[11].

In this evolving context, luxury cosmetics have transitioned from an exclusive focus on sensory experience to a more holistic approach that integrates efficacy, ingredient quality, ethical sourcing, and environmental responsibility[12]. As consumers become more attentive to sustainability and transparency, even the luxury segment has embraced natural, high-quality ingredients and scientifically validated formulations[13]. Consequently, luxury skincare products have attained a dominant position within the broader cosmetic market, driven by their emphasis on innovation, performance, and perceived added value[14].

Overall, the growing centrality of personal well-being, combined with demographic changes and the expansion of the luxury sector, continues to drive the evolution of the cosmetic industry. Within this landscape, skincare stands out as a key area of innovation, where the pursuit of effective, high-quality, and scientifically supported products aligns with contemporary notions of wellness, self-care, and sustainable luxury.

1.2 Sustainability as a driver in modern cosmetics

Sustainability is one of the most urgent challenges faced by modern societies, representing one of the most impacting drivers shaping contemporary industrial development[15]. The current climate emergency has resulted in disastrous and interconnected consequences including soil desertification and degradation, loss of biodiversity, and depletion of water resources. As a result, consumer

awareness and attitudes have progressively evolved. Modern consumers are increasingly conscious of the environmental footprint associated with everyday products and are actively seeking cosmetic formulations that align with sustainability principles, ethical sourcing, and reduced ecological impact[16]. In addition, the constant increase in world's population further intensifies the demand for natural resources and accelerates resource depletion[17]. Consequently, industries characterized by large-scale consumption of raw materials, including the cosmetic industry, are facing an urgent need to undergo a comprehensive ecological transition.

In particular, the continuous market expansion that the cosmetic sector is experiencing, driven by both the growing centrality of personal care and the demographic trends such as population aging and increased life expectancy, amplifies the environmental responsibility associated with cosmetic production, making long-term sustainability vision not just a marketing advantage but a strategic requirement for sectoral resilience and regulatory compliance[15]. Indeed, some current regulations have further reinforced this transition such as, for instance, the banned use of microplastics in rinse-off cosmetic products that have pushed manufacturers to reformulate existing products and rethink ingredient selection and formulation strategies[18].

Importantly, sustainability in cosmetics must be addressed through a holistic perspective, involving all stages of the product supply chain[19]. At the design and sourcing stage, sustainability considerations embrace the selection of renewable, traceable, and responsibly sourced raw materials, with increasing attention toward plant-based ingredients and waste products[20][21] . During manufacturing, sustainable practices focus on reducing energy consumption, minimizing waste generation, and favoring low-impact processing technologies, including the use of renewable energy sources and mild processing conditions[22]. Packaging represents another critical aspect, as cosmetic packaging must ensure product stability and safety while minimizing environmental pollution, leading to growing interest in recyclable, biodegradable, or refillable packaging solutions[23] . Finally, distribution, consumer use, and post-use phases are increasingly considered, with efforts directed toward reducing carbon emissions, improving product biodegradability, and facilitating proper waste management [24]. Among all these steps, the selection of ingredients remains one of the most critical and challenging steps. While consumers strongly associate sustainability with natural-origin ingredients, the use of botanical raw materials does not inherently guarantee environmental sustainability or product performance. Balancing ecological responsibility

with formulation efficacy, stability, and safety represents a major scientific and technological challenge for cosmetic research and development [19].

Recent market analyses estimate that the global natural cosmetics sector reached approximately USD 33 billion in 2025, and natural-ingredient formulations currently account for a substantial portion of the 'clean beauty' segment (32.6%), reflecting a strong consumer-driven demand for sustainably sourced products [25]. Consequently, cosmetic companies are progressively favoring plant-based, eco-friendly ingredients and are investing in environmentally responsible extraction and processing technologies. In this context, green extraction approaches, such as ultrasound-assisted extraction, microwave-assisted extraction, and the use of low-toxicity or renewable solvent systems, have gained considerable attention as viable strategies to reduce environmental impact while preserving bioactive compound integrity[26]. Nevertheless, despite this growing interest, botanical-derived actives still represent a relatively limited fraction of the global cosmetic ingredient market. This gap highlights the need for continued research into new plant sources, as well as for the development of innovative extraction and formulation strategies capable of translating sustainability principles into effective cosmetic products.

Overall, the ecological transition of the cosmetic sector has transformed sustainability from a secondary consideration into a central driver of innovation. The increasing demand for sustainable, high-performance cosmetic products has therefore intensified the search for novel natural ingredients and environmentally responsible processing methods, positioning bioprospecting and green chemistry at the core of modern cosmetic research.

1.3 Microplastics in cosmetics

Microplastics are small plastic particles (0.1–5 mm) that have emerged over the last decade as a major global environmental and public health concern[27]. They originate from multiple sources, including plastic packaging, textiles, fishing gear, and cosmetic and personal care products (PCCPs), with the latter representing a significant contributor due to the rapid expansion of the cosmetic market[28].

In cosmetics, microplastics are classified as primary, when intentionally added to formulations, or secondary, when generated through the degradation of plastic packaging[29]. Since their introduction in the 1980s, primary microplastics have been widely used to improve product

performance, serving as exfoliating agents, texture modifiers, opacifiers, and rheology enhancers, owing to their durability, low cost, and formulation versatility[30]. However, their insolubility, resistance to degradation, and environmental persistence, have led to their widespread accumulation in aquatic and terrestrial ecosystems, air, food chains, and ultimately in the human body[31].

Growing evidence suggests that microplastics may impair skin barrier function, trigger inflammatory responses, alter the skin microbiome, and potentially accelerate skin aging processes[32]. In response to these environmental and health concerns, regulatory actions and public awareness initiatives have intensified worldwide, driving the cosmetic industry toward the progressive elimination of microplastics from PCCPs[33].

As a result, considerable research efforts are now focused on the development of sustainable alternatives, including biodegradable polymers and natural materials such as cellulose- and starch-based systems, capable of replacing microplastics without compromising formulation performance[34]. The phase-out of microplastics therefore represents one of the key challenges for modern cosmetic science.

Given the relevance of this topic, during my PhD I helped draft a comprehensive review addressing the microplastic issue, current regulatory actions, and potential eco-friendly alternatives, attached at the end of this thesis.

1.4 Skin aging and the anti-aging role of natural compounds

The skin is the largest, most complex, and most exposed organ of the human body and, as such, it is the tissue in which aging-related alterations become most visibly apparent[35]. Beyond its aesthetic implications, skin aging has gained increasing relevance from a biological, social, and economic perspective, due to its impact on barrier function, immune defense, and overall skin health[36].

The skin is composed of three main layers (**Figure 1.1**)[37]: the epidermis, the outermost barrier primarily constituted by keratinocytes and melanocytes; the dermis, a connective tissue rich in fibroblasts and extracellular matrix (ECM) components; and the hypodermis, a highly vascularized and innervated layer dominated by adipose tissue that provides mechanical and metabolic support[38]. Among these layers, the dermis plays a key role in determining skin mechanical

properties, as it contains a highly organized ECM network composed of collagen fibers, elastic fibers, proteoglycans, and glycosaminoglycans, which collectively confer tensile strength, elasticity, and hydration.

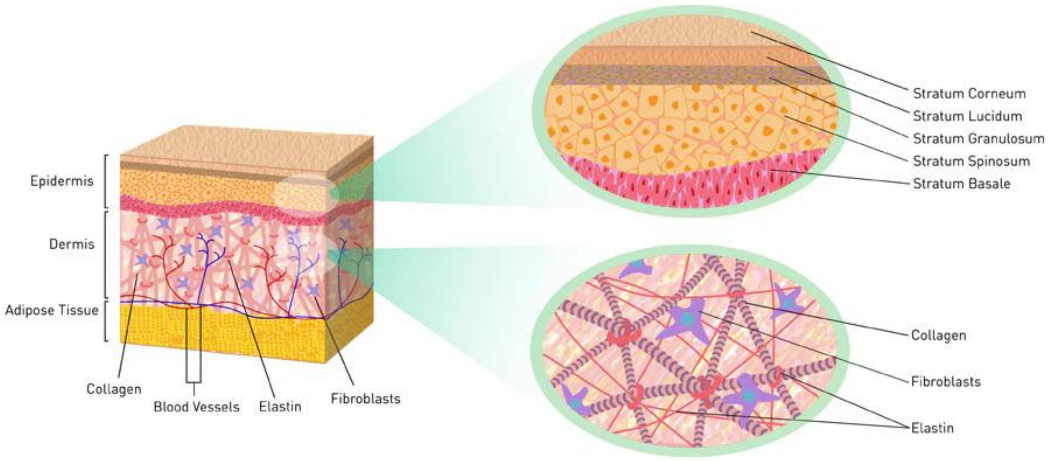

Figure 1.1. Representation of the skin structure composed of epidermis, dermis and adipose tissue (hypodermis).

Skin aging is a complex and irreversible biological process that affects all three skin layers, although dermal alterations are particularly determinant[39]. Age-related changes include dermal thinning, fragmentation and reduction of collagen and elastin fibers, decreased regenerative capacity, altered pigmentation patterns, and progressive loss of skin firmness and elasticity[40]. Clinically, these changes manifest as wrinkles, sagging, dryness, uneven pigmentation, and loss of skin tone and softness[41].

From an etiological point of view, skin aging results from the combined contribution of intrinsic aging, driven by genetic and hormonal factors, and extrinsic aging, caused by environmental stressors[42]. Intrinsic aging is associated with cellular senescence, telomere shortening, physiological hormonal decline, and cumulative oxidative damage generated by normal cellular metabolism[43]. Extrinsic aging, on the other hand, is largely preventable and is predominantly driven by ultraviolet (UV) radiation (photoaging), which accounts for up to 80% of visible skin aging, as well as by air pollution, smoking, poor nutrition, sleep deprivation, and chronic stress[44].

Despite their different origins, intrinsic and extrinsic aging converge on common molecular pathways, most notably oxidative stress, ECM degradation, and skin hyperpigmentation, which

together represent the main biological hallmarks of cutaneous aging and the primary targets for anti-aging cosmetic strategies[45].

1.4.1 Oxidative stress

Oxidative stress is recognized as a key driver of skin aging, representing a primary target for preventive intervention[46]. Reactive oxygen species (ROS) are continuously generated as by-products of cellular metabolism, particularly within mitochondria, and play physiological roles in cell signaling. However, when ROS production exceeds the neutralizing capacity of endogenous antioxidant systems, oxidative stress occurs[47].

The skin comes with endogenous antioxidant defense systems, including superoxide dismutase (SOD), catalase, and glutathione. These defenses progressively decline with age and may become insufficient to contrast ROS accumulation, making skin cells more vulnerable to oxidative damage[48]. Excessive ROS induces lipid peroxidation, protein oxidation[49], and DNA damage, impair mitochondrial function, reduce ATP production, and accelerate cellular senescence[50].

UV radiation represents the most influent extrinsic source of ROS in the skin. UV-induced oxidative stress not only damages cellular components directly but also activates signaling cascades that upregulate matrix metalloproteinases (MMPs), thereby linking oxidative stress to ECM degradation[51]. Elevated ROS levels have been shown to reduce collagen content, disrupt fibroblast function, and promote wrinkle formation and loss of elasticity[52].

For these reasons, scavenging excess ROS is one of the most established and effective approaches to counteract both intrinsic and extrinsic skin aging. Natural antioxidants have therefore gained significant attention in cosmetic science. Plant-derived compounds such as polyphenols, flavonoids, carotenoids, and vitamins exhibit strong radical-scavenging activity and can restore redox balance within skin cells[48]. Botanical extracts from green tea, rosemary[53], turmeric[54], acai berry, resveratrol-rich plants, and quercetin-containing sources have been widely reported to protect against photoaging, reduce inflammation, and improve overall skin appearance[55], [56]. As a result, topical antioxidants are now considered essential components of comprehensive anti-aging skincare strategies.

1.4.2 Extracellular matrix remodeling

The integrity of the ECM is fundamental to maintaining skin structure, elasticity, and mechanical resistance. The dermal ECM is a highly dynamic network composed primarily of collagen fibers, which provide tensile strength; elastic fibers, formed by elastin and fibrillin, which confer resilience and elasticity; and proteoglycans and glycosaminoglycans, such as hyaluronic acid (HA), which regulate hydration and tissue viscoelasticity.

During skin aging, ECM homeostasis is progressively disrupted as a result of increased oxidative stress and cellular senescence. Excess ROS activates intracellular signaling pathways, notably the mitogen-activated protein kinase (MAPK) cascade, leading to activation of the transcription factor activator protein-1 (AP-1)[57]. AP-1 upregulates the expression of several matrix metalloproteinases (MMPs), including collagenases and elastases, while simultaneously suppressing the transforming growth factor-β (TGF-β)/Smad signaling, which is essential for collagen synthesis[58]. In parallel, the expression of tissue inhibitors of metalloproteinases (TIMPs) is reduced, further exacerbating ECM degradation[59].

Senescent fibroblasts contribute to this process through the secretion of a senescence-associated secretory phenotype (SASP), characterized by elevated levels of MMPs and pro-inflammatory cytokines such as IL-6 and IL-8[60]. This chronic inflammatory microenvironment accelerates collagen fragmentation, elastic fiber disorganization, and loss of dermal integrity[61]. As a consequence, aged skin exhibits reduced collagen and elastin content, impaired mechanical strength, and visible sagging.

In addition to collagen and elastin, age-related changes also affect glycosaminoglycans, particularly HA[62]. It plays a crucial role in skin hydration, cell migration, and tissue repair but has a relatively short half-life in the skin[63]. Its levels decline with age due to both oxidative damage and increased activity of hyaluronidases. Excessive HA degradation results in moisture loss, reduced skin volume, and wrinkle formation. Because HA turnover is rapid, modulation of hyaluronidase activity represents an attractive target for observing early anti-aging effects[64].

Nature provides a vast reservoir of bioactive compounds capable of modulating ECM-related enzymes. Polyphenols, flavonoids, cinnamic acid derivatives, terpenoids, and lipid-based phytochemicals have been shown to inhibit collagenase, elastase, and hyaluronidase activities, while

simultaneously exerting antioxidant and anti-inflammatory effects. For example, shea butter has been reported to enhance collagen production while inhibiting proteolytic enzymes[65], and soybean isoflavones, such as genistein, promote elastin and collagen synthesis while reducing elastase activity[66]. These multifunctional properties make plant-derived compounds particularly suitable for preserving ECM integrity in aging skin.

1.4.3 Skin hyperpigmentation

Pigmentary alterations represent another hallmark of skin aging, particularly in photoaged skin. Tyrosinase is the key regulatory enzyme of melanogenesis, catalyzing the initial and rate-limiting steps in melanin synthesis within melanocytes[67]. Although melanin is essential for photoprotection, enhancing the skin's defense against UV radiation and other environmental or hormonal factors, excessive or dysregulated melanin production leads to hyperpigmentation disorders such as solar lentigines, melasma, and age spots[68]. Excessive UV exposure leads to increased ROS generation, which can further stimulate tyrosinase activity and melanogenic signaling pathways. This ROS-mediated hyperactivation of melanogenesis contributes to uneven skin tone and exacerbates visible signs of photoaging[69]. In aged skin, the situation is further complicated by alterations in dermal–epidermal communication. Senescent fibroblasts exhibit reduced insulin-like growth factor-1 (IGF-1) production, impairing the protective DNA damage response of keratinocytes and indirectly affecting melanocyte behavior. This dysregulated paracrine signaling promotes pigmentary instability and increases susceptibility to age-related skin disorders[70].

Consequently, tyrosinase inhibition is a key strategy in cosmetic anti-aging formulations, not only to reduce hyperpigmentation but also to indirectly limit ROS-associated melanogenic pathways. Natural tyrosinase inhibitors, including flavonoids, phenolic acids, and other plant-derived compounds, have emerged as safer alternatives to conventional depigmenting agents, aligning efficacy with improved tolerability and sustainability[71].

Taken together, oxidative stress, ECM remodeling, and skin hyperpigmentation represent tightly interconnected mechanisms that collectively drive skin aging (**Figure 1.2**)[72]. Oxidative stress acts as a common upstream trigger, amplifying enzymatic degradation of the ECM and stimulating

aberrant melanogenesis. As a result, there is a growing demand for cosmetic actives capable of targeting multiple aging-related pathways simultaneously.

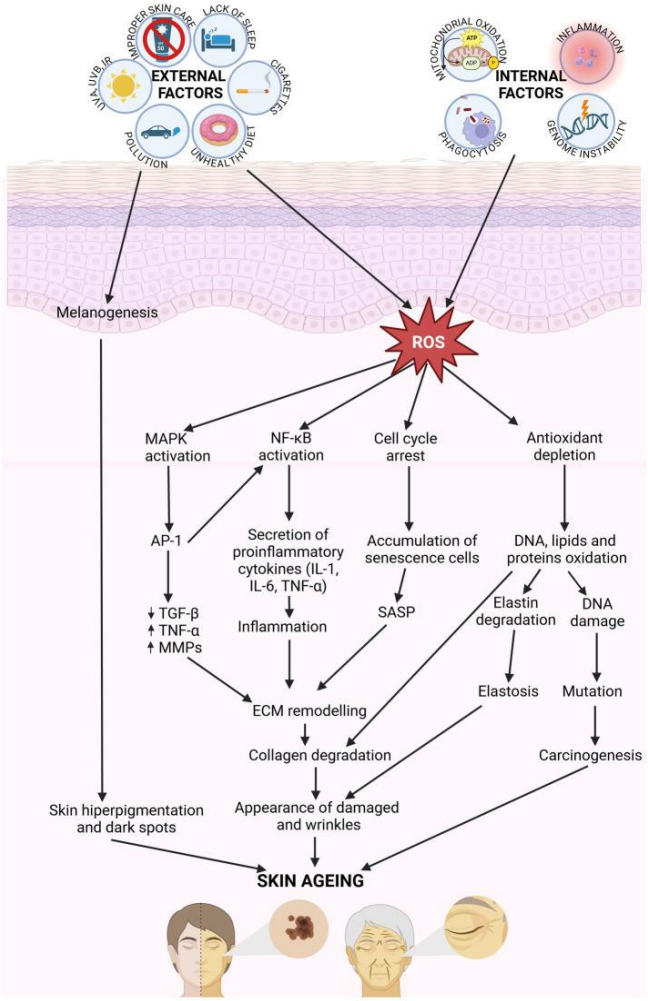

Figure 1.2. Molecular mechanisms involved in skin aging. Internal and external factors generate ROS that activate signaling pathways such as MAPK and AP-1 that affect ECM remodeling. Collagen and elastic fiber break down, and skin collapse leading to wrinkles formation. ROS causes oxidation of DNA, lipids and proteins leading to cellular disfunction.

In this context, natural compounds stand out as particularly promising candidates. Owing to their structural diversity and multifunctional biological activities, plant-derived bioactives can exert antioxidant effects while concomitantly inhibiting collagenase, elastase, hyaluronidase, and tyrosinase activities. The immense chemical diversity offered by natural biodiversity therefore represents an exceptional reservoir for the discovery of innovative anti-aging ingredients, capable of meeting both efficacy and sustainability requirements in modern cosmetic science.

1.5 Other plant bioprospecting applications

While plants have been discovered as valuable sources of ingredients for cosmetic formulations, including anti-aging, moisturizing, anti-inflammatory and antioxidants properties, their potential extends far beyond skin care[73]. The term bioprospecting refers to the systematic exploration of biological diversity to identify organisms, genes, or metabolites with novel and useful applications across a range of scientific and industrial fields, without disruption to nature[74]. In the plant kingdom, bioprospecting has historically served as a cornerstone for drug discovery and biomedical innovation, reflecting the remarkable chemical diversity that evolved through millions of years of adaptation to environmental stressors[75]. The global relevance of medicinal plant research is further underscored by the fact that different geographical regions, characterized by unique ecological pressures, have generated distinct phytochemical reservoir with region-specific biological activities[76]. Over evolutionary time, nature has thus produced a vast array of molecules capable of modulating biological pathways and counteracting a wide spectrum of diseases[77].

At the intersection of ethnobotany and modern pharmacology, plants have been instrumental in the development of numerous therapeutic agents. Classic examples include artemisinin, the potent antimalarial compound isolated from *Artemisia annua*[78], and taxol (paclitaxel), a landmark chemotherapeutic agent originally derived from *Taxus brevifolia*[79]. These compounds have revolutionized clinical practice in their respective fields and clearly exemplify the medical relevance of plant secondary metabolites. Contemporary bioprospecting research continues to uncover new bioactive compounds with diverse pharmacological profiles, including antimicrobial[80], antiviral[81], anti-inflammatory[82], and anticancer activities[83], highlighting plants as enduring reservoirs of clinically relevant chemical diversity.

Among the wide range of biomedical applications, antimicrobial and anti-tumoral activities are the most urgent. Indeed, antimicrobial resistance (AMR)[84], together with cancer, represents one of the most pressing global health challenges[85]. In recent years, the rapid increase in multidrug-resistant infections and the growing incidence of cancer worldwide have positioned these diseases among the current and future major causes of death[86][87]. Recent studies have documented the antibacterial, antibiofilm, and bactericidal properties of extracts from wild edible plants, which are

being explored as potential solutions against resistant pathogens such as methicillin-resistant *Staphylococcus aureus*[88]. Similarly, several established anticancer drugs, including vincristine[89], vinblastine, and etoposide[90], are of natural origin, and many additional plant-derived or plant-inspired antitumoral compounds continue to be discovered and developed[91]. These examples highlight the sustained relevance of natural products as a privileged chemical space for anticancer drug discovery.

In the context of biopharmaceutical research, plant bioprospecting therefore remains a highly productive strategy for the identification of new therapeutic candidates. Typically, this process relies on an integrated workflow that combines phytochemical profiling with targeted biological screening to correlate chemical composition with bioactivity[92]. This approach enables the prioritization of specific plant extracts, tissues, or compound classes for further investigation and supports a rational, mechanism-oriented exploration of plant biodiversity.

Overall, these considerations emphasize that the search for new natural compounds with therapeutic potential, particularly in the oncological field, remains both timely and scientifically compelling. Beyond their established cosmetic applications, plant-derived metabolites continue to offer significant opportunities for biomedical research, reinforcing the rationale for bioprospecting studies aimed at uncovering alternative and high-impact biological activities.

1.6 Desert and halophytic plants

Plants that live in extreme environments represent unique reservoirs of secondary metabolites[93]. It is well known that plant chemical profiles are strongly affected by environmental conditions[94], and among stress-adapted species, desert plants and halophytes are considered some of the most emblematic examples of ecological and metabolic adaptation[95]. These plants are capable of living and thriving under harsh conditions such as high temperatures, drought, soil salinity, and intense solar radiation[96]. Prolonged exposure to these abiotic stressors has imposed strong selective pressure, driving the evolution of distinctive morphological and physiological traits[97]. As a result, these species produce specific secondary metabolites that not only support plant survival but may also be beneficial for human applications[96], as several of the stress-response pathways activated

in plants, such as oxidative stress, inflammation, and dehydration, closely mirror the molecular mechanisms involved in skin aging[98].

Desert plants (xerophytes) are continuously exposed to high temperatures, extreme UV irradiation, low rainfall, and poor soil nutrition. In such environments, the main challenges are to maintain thermoregulation and preserving water[99]. Accordingly, xerophytes have developed characteristic morphological adaptations, such as reduced leaf surface area[100] and the produce of reflective waxes or trichomes [101] that limit transpiration and mitigate excessive light exposure. From a metabolic perspective, several studies have reported that desert plants are particularly rich in phenolic compounds and polyphenols, often associated with strong antioxidant activity[102], as well as flavonoids with UV-absorbing properties. These metabolites play a protective role against oxidative and photo-induced damage and make xerophytic species promising candidates for antioxidant and photoprotective applications in cosmetic formulations[103].

Halophytic plants are a highly specialized group adapted to saline environments characterized by high concentrations of soluble salts, fluctuating water levels, hypoxia, elevated temperatures, and intense UV exposure[104]. Among these stressors, salinity is the most critical, as it causes reduced water uptake, ionic imbalance, and ROS overproduction[105]. Therefore, halophytes developed intensive adaptive mechanisms, including ion exclusion or compartmentalization, osmotic adjustment through compatible solute accumulation, and the enhanced synthesis of stress-related metabolites. Indeed, extracts and isolated compounds from some halophytes species proved the presence of high levels of antioxidants, including phenolic compounds and flavonoids, thus attracting interest as potential multifunctional cosmetic ingredients. For instance, isoorientin isolated from a halophytic species has been reported to exhibit marked antioxidant and photoprotective activities, highlighting its suitability for cosmetic applications[106]. Additional studies have demonstrated that halophytic plants are rich in phenolic and flavonoid compounds capable not only of scavenging free radicals but also of inhibiting key extracellular matrix-degrading enzymes[107]. Moreover, a broader screening of multiple halophytic species has revealed consistent anti-aging-related properties, including antioxidant, anti-wrinkle, and skin-whitening activities[108].

Overall, the strong link between environmental stress and secondary metabolite production gives a boost to the exploration of desert and halophytic plants as reservoirs of natural bioactives. Their stress-driven chemodiversity reflects unique evolutionary adaptations and offers significant opportunities for the development of innovative, nature-inspired cosmetic ingredients targeting skin aging.

1.6.1 United Arab Emirates (UAE) biodiversity

The United Arab Emirates (UAE) lie in the arid subtropical zone, while exposed to the influences of the surrounding Arabian Gulf and the Indian Ocean[109]. The UAE is a federation of seven emirates extending along the northern coast of the Arabian Peninsula between approximately 22°50′ and 26° North latitude and 51° and 56° Est longitude[110]. From a geological and bioclimatic perspective, the country is divided into three main regions: a mountainous area in the east, and a western zone divided into a coastline and an extensive inland desert. The UAE climate is characterized by extreme environmental conditions, including pronounced seasonal temperature fluctuations, with summer temperatures frequently exceeding 48 °C and winter minima occasionally approaching 3 °C[111]. Solar radiation levels are exceptionally high, while annual precipitation is rare and irregular. These conditions result in an extremely arid climate, nutrient-poor soils, and high evaporation rates, which in coastal lagoons and bays contribute to elevated salinity levels. Together, heat stress, water scarcity, intense irradiation, and salinity represent major abiotic constraints shaping both terrestrial and coastal ecosystems[112].

Despite these harsh conditions, the UAE hosts a remarkably variety of native plant species that have successfully adapted to survive and thrive under extreme environmental stress. To date, more than 760 indigenous plant species have been identified, many of which are desert plants and halophytes[113]. Beyond their fundamental ecological roles in providing essential ecosystem services, several of these species have long been recognized in local traditions for their nutritional and medicinal value. Indigenous plants therefore represent important biodiversity resources with ecological, socio-economic, and cultural relevance[114].

Among desert-adapted species, *Vachellia flava* and *Prosopis cineraria* (*P. cineraria*) are particularly notable. These species are rich in nutrients, have traditionally contributed to local diets, and are

highly valued for their resilience, as they require minimal water and maintenance[115], [116]. Their adaptability makes them well suited for sustainable landscaping and urban greening in arid environments, while their long-standing use in traditional medicine suggests the presence of bioactive compounds of potential interest for modern applications[111].

Regarding the halophytic vegetation, the Arabian Gulf coastline of the UAE, together with neighboring regions of Bahrain, Qatar, and Iran, hosts one of the most environmentally extreme mangrove ecosystems[117]. Mangroves in this region are exposed to exceptionally high salinity levels of about 65–70 ppt, beyond the typical tolerance limits of mangrove species[118]. Despite these constraints, mangrove forests form highly productive and unique ecosystems that support diverse biological communities and provide vital ecosystem services, including carbon sequestration, coastal protection, and nursery habitats for commercially important fish species[119]. *Avicennia marina* (*A. marina*) is the only mangrove species naturally occurring in the UAE, where it forms evergreen coastal forests along sheltered shorelines[120]. Recent studies have indicated that halophytic species growing under UAE environmental conditions accumulate distinctive phytochemicals, likely thanks to their adaptation to severe salinity, heat, and oxidative stress[121]. This stress-driven metabolic specialization further supports the bioprospecting potential of UAE-native desert plants and halophytes as sources of natural bioactive compounds.

1.6.1.1 *Prosopis cineraria*

Prosopis cineraria is a small to moderate sized, thorny, evergreen flowering tree characterized by irregular branches, belonging to the family *Fabaceae* (Leguminosae) and the subfamily *Mimosoideae*[122] (**Figure 1.3**)[123]. As one of the most emblematic native plant species of the United Arab Emirates, *P. cineraria*, commonly known as Ghaf, has demonstrated an extraordinary ability to survive under extreme desert conditions. Owing to its ecological resilience and cultural significance, Ghaf was officially declared the national tree of the UAE in 2008. Beyond its symbolic value, representing stability and resilience in the desert environment, *P. cineraria* is an important component of the region's natural and cultural heritage[124].

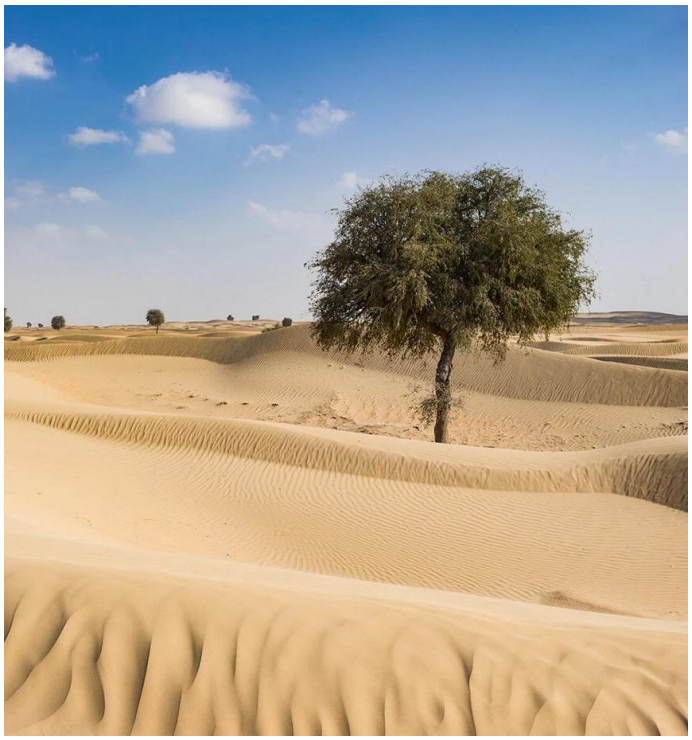

Figure 1.3. Representation of the *Prosopis cineraria* Ghaf tree in UAE desert.

As a xerophytic species adapted to arid and semi-arid climates, *P. cineraria* is widely distributed across many arid and semi-arid regions (mainly Arabia and India), as native or introduced species. In addition to its ecological and cultural relevance, Ghaf has attracted increasing scientific interest as a potential source of raw materials for food, medicinal, and, more recently, high-value applications such as cosmetics and luxury products[125].

The genus *Prosopis* has been extensively reported as a rich source of proteins, carbohydrates, lipids, minerals, and different phytochemical constituents with documented health-promoting effects. *P. cineraria* is particularly appreciated for the versatility of its various plant parts, to the extent that it has been traditionally referred to as the "King of the Desert[116]." Ecologically, the species plays a crucial role in desert ecosystems by preventing soil erosion and stabilizing dunes through its deep and extensive root system[126]. Moreover, it contributes to soil improvement by accumulating organic matter and reducing soil pH, thereby enhancing soil fertility in otherwise nutrient-poor environments[127]. The plant is also widely used as animal feed in arid regions[116].

The medicinal value of *P. cineraria* has been extensively documented in traditional medicine systems, where different parts of the plant have been employed through oral and topical administration such as antivenom, antipyretic, analgesic, antihyperglycemic, wound-healing, antioxidant, anti-inflammatory, and antibacterial agents[128]. These traditional uses highlight the contribution of multiple plant tissues to its overall pharmacological potential. In contrast, scientific knowledge regarding the cosmetic applications of *P. cineraria* remains relatively limited.

Nevertheless, phytochemical investigations of different plant portions suggest that *P. cineraria* represents a highly promising candidate for cosmetic research. Methanolic, hydroalcoholic, and aqueous extracts of the bark have been reported to contain high levels of phenolic compounds and flavonoids, associated with strong antioxidant activity[129], in addition to lignin and starch, which are already exploited in cosmetic formulations. Furthermore, well-known antioxidant molecules such as gallic acid and rutin have been identified in the seeds[130], while leaves have been shown to contain quercetin and related flavonoid derivatives[131]. Although several studies have explored the phytochemical constituents underlying the traditional medicinal uses of *P. cineraria*, substantial gaps remain regarding the systematic evaluation of its cosmetic potential. To date, only one formulation-oriented study has been reported, describing the development of an oil-in-water (O/W) cosmetic emulsion containing 2% *P. cineraria* bark extract as an active ingredient[132]. The resulting formulation demonstrated promising efficacy in terms of skin-whitening, moisturizing, anti-acne, and anti-wrinkle effects[133]. This preliminary evidence further supports the need for more comprehensive investigations into *P. cineraria* as a multifunctional cosmetic active, particularly in light of its stress-adaptive strategies and the presence of well-established antioxidant phytochemical classes.

1.6.1.2 *Avicennia marina*

Avicennia marina (*A. marina*) is a mangrove species belonging to the family *Acanthaceae* (formerly classified within *Verbenaceae*), widely distributed across tropical and subtropical regions worldwide (**Figure 1.4**). Its geographical range extends along the tropical coasts of East Africa, South and Southeast Asia, Australia, the North Island of New Zealand, and several Pacific islands, including Fiji. In addition, *A. marina* occurs in temperate regions, particularly in Southwestern Asia, along the coastline of the Arabian Gulf and the eastern and western coasts of the Red Sea[134].

Figure 1.4. Representation of *A.marina* plant of UAE.

A. marina is the most dominant and widely distributed mangrove species and represents the prevailing coastal vegetation along the Arabian Gulf coasts of the UAE, Saudi Arabia, Bahrain, Qatar, and Iran[135]. Commonly known as the "grey mangrove", this species grows as shrubs or trees ranging from approximately 3 to 14 m in height. It is characterized by a grey bark composed of thin, delicate scales, green leaves bearing fine hairs on the abaxial surface, and small yellow flowers arranged in clusters of three to five, typically blooming in spring. Reproduction occurs through propagules, which function as dispersal units[136].

A. marina is among the most stress-tolerant mangrove species, exhibiting remarkable resistance to extreme environmental conditions such as high salinity, elevated temperatures, strong winds, intense solar radiation, and anaerobic, waterlogged soils[137]. To survive under these harsh conditions, the species has evolved highly specialized morphological and physiological adaptations, including salt-secreting glands on the leaf surface to regulate ionic balance[138] and pneumatophores that facilitate atmospheric oxygen diffusion to submerged root tissues[139].

These adaptive traits are closely associated with the biosynthesis of a variety of secondary metabolites, including aliphatic alcohols, amino acids, carbohydrates, alkaloids, carotenoids, fatty acids, hydrocarbons, iridoid glycosides, abietane diterpenoid glycosides, carboxylic acids, steroids, tannins, triterpenes, naphthalene derivatives, flavones, flavonoids, phorbol esters, phenolic compounds and related metabolites, phytoalexins, inorganic salts, minerals, and vitamins[136]. Collectively, these compounds are considered responsible for the wide range of biological activities attributed to *A. marina*, supporting its extensive use in traditional medicine as an anti-inflammatory, antioxidant, anticancer, antiviral, antimicrobial, and antidiabetic remedy[140].

Despite the growing literature on *A. marina*, most phytochemical and bioactivity studies have been conducted on populations from limited geographical regions, representing a significant constraint in fully understanding the species' chemo diversity. Given the extreme environmental conditions of the Arabian Gulf, characterized by exceptionally high salinity, temperature fluctuations, and intense solar radiation[141], it is plausible that *A. marina* populations growing in the UAE have undergone specific metabolic adaptations, including the upregulation of antioxidant defense systems and the production of distinct secondary metabolites with unique biological activities[137].

For this reason, there is a clear need to further investigate *A. marina* from the UAE, not only to expand current knowledge on its pharmacological potential but also to explore less-studied application areas. Notably, despite the species' exceptionally high content of antioxidants and multifunctional bioactive compounds, its potential use as active ingredient in cosmetic formulations remains largely unexplored. While some studies on Thai mangrove species have begun to investigate anti-aging cosmetic applications[142], evidence for *A. marina* is limited primarily to the use of leaf extracts as cosmetic additives[143]. This substantial knowledge gap highlights *A. marina* as a particularly promising and innovative candidate for bioprospecting-driven research aimed at identifying new natural actives for cosmetic and dermocosmetic applications.

1.7 Cosmetic emulsions

In recent years, there has been a growing demand for cosmetic products designed to meet specific consumer needs. In particular, skincare products aimed at giving a younger and healthy appearance are increasingly in demand. To achieve these effects, specific bioactive ingredients must be

effectively delivered to the skin, while maintaining their stability, bioavailability, and efficacy. Among the delivery systems employed in cosmetic formulations, emulsions represent one of the most widely used platforms due to their remarkable versatility and functional properties [144].

Emulsions are colloidal dispersions composed of two immiscible liquids, in which one (the dispersed phase) is dispersed into the other (the continuous phase) as droplets. The intrinsic immiscibility of the components results in thermodynamically unstable emulsions, making the presence of at least one stabilizing agent essential to ensure adequate kinetic stability. Conventionally, surfactants or amphiphilic polymers are employed for this purpose; by forming a protective layer around droplets, they reduce interfacial tension between the two fluids. Based on the nature of the dispersed and continuous phases, emulsions are typically classified as oil-in-water (O/W) or water-in-oil (W/O) systems, depending on whether oil droplets are dispersed in an aqueous phase or vice versa[145]. This distinction strongly influences the sensory properties of the final formulation: O/W emulsions are generally perceived as more comfortable, whereas W/O emulsions tend to be richer and greasy but are often more effective for the rapid delivery of hydrophobic active ingredients[145]. More complex systems, called "double emulsions", have also been developed like water-in-oil-in-water (W/O/W) and oil-in-water-in-oil (O/W/O), where droplets of the dispersed phase contain smaller droplets within them. These systems are particularly attractive for advanced encapsulation strategies and controlled release applications[146] (**Figure 1.5**)[144].

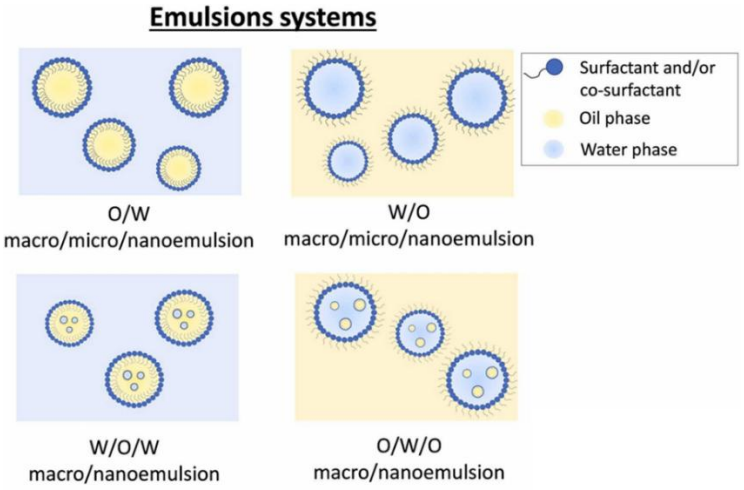

Figure 1.5. Graphical representation of simple and double emulsions.

Emulsions can further be differentiated according to the size of their dispersed droplets, which significantly affects their stability and optical properties. Macroemulsions typically exhibit droplet sizes ranging from approximately 0.1 to 100 μm and have typical creamy white appearance by allowing light scattering[147]. Microemulsions, characterized by droplet sizes between 10 and 100 nm and the presence of both surfactant and co-surfactant, form spontaneously and are transparent systems. Nanoemulsions, with droplet sizes typically between 20 and 200 nm, are translucent systems that also contain surfactant and co-surfactant but, unlike microemulsions, they do not form spontaneously and remain thermodynamically unstable despite their high kinetic stability[148].

Historically, surfactants have been extensively used in cosmetic emulsions due to their effectiveness and relatively low cost. Common examples include polysorbates (e.g., Tween 80), sorbitan esters (e.g., Span 80), sodium laureth sulfate (SLES), sodium dodecyl sulfate (SDS), and polyethylene glycol ethers[149], [150], [151]. However, many of these compounds have been associated with adverse effects, including skin irritation, allergic reactions, and environmental concerns[152]. This has driven the search for alternative stabilization strategies capable of ensuring formulation stability and sensory acceptability while offering improved safety and sustainability profiles.

An innovative and increasingly explored alternative involves replacing conventional surfactants with solid particles, leading to the formation of so-called "Pickering emulsions" (**Figure 1.6**)[153]. This approach offers many advantages, including enhanced formulation stability, reduced sensitivity to external factors such as pH, temperature, and oil phase composition, a lower amount of stabilizing agent required compared to traditional surfactants, and improved biocompatibility, as the solid particles employed are often derived from natural sources[154].

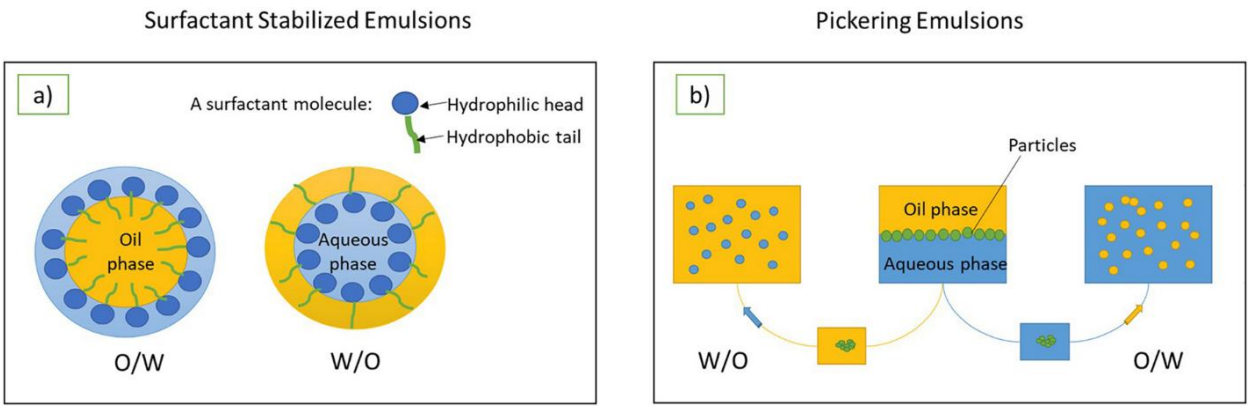

Figure 1.6. Schematic representation of O/W and W/O emulsions stabilized with (a) surfactant (conventional emulsions) and with (b) solid particles (Pickering emulsions).

1.7.1 Pickering emulsions

Pickering emulsions are surfactant-free emulsions stabilized by solid particles that are insoluble in both the aqueous and oil phases but possess partial wettability toward each phase. This allows the particles to adsorb irreversibly at the oil–water interface, where they rearrange on the droplets to form a protective interfacial film. This film provides both physical and, in some cases, electrostatic stabilization, resulting in long-term stability emulsions[155]. The size of the stabilizing particles also plays a crucial role in emulsion stability, as particles in the nanometric to submicrometric range (typically 10–1000 nm) are generally more effective in forming dense interfacial layers. In addition, the particles should typically be at least one order of magnitude smaller than the emulsion droplets to ensure efficient interfacial coverage and stabilization [156]. Depending on the nature and properties of the solid particles employed, Pickering emulsions can be stabilized through three main mechanisms: (i) the formation of a dense interfacial film around individual droplets, (ii) the creation of a three-dimensional network of aggregated particles within the continuous phase that immobilizes the droplets, and (iii) stabilization driven by depletion interactions between particles (**Figure 1.7**)[157].

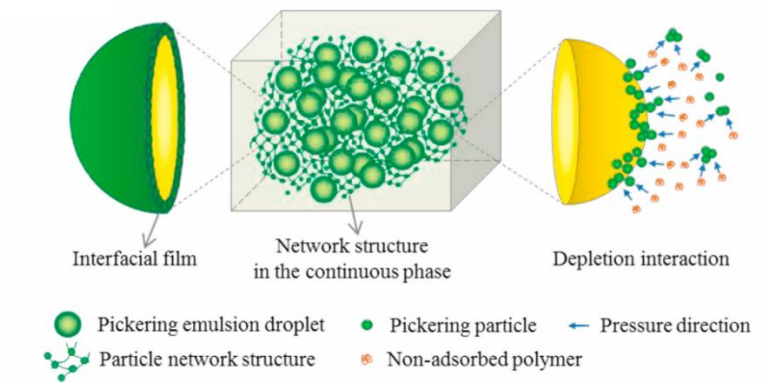

Figure 1.7. Graphical representation of the three mechanisms of stabilizations of Pickering emulsions: interfacial film, network structure and depletion interactions.

Initially, Pickering emulsions were stabilized using inorganic solid particles such as silica, alumina, titanium dioxide, and clays[158]. However, due to concerns related to their limited biodegradability and biocompatibility, the use of these materials has declined significantly[158]. In response to the increasing demand for safer and more sustainable cosmetic products, recent research has focused on natural materials, including proteins (e.g., pea proteins) and polysaccharides, mainly starch, cellulose, and chitosan[159].

Since these biopolymers do not naturally occur in particulate form, chemical, physical, or enzymatic modifications are often required to obtain solid or semi-solid particles suitable for Pickering stabilization[157]. For instance, cellulose which is characterized by a relatively hydrophobic crystalline region and a more hydrophilic non-crystallin region, is frequently modified to increase its hydrophobicity[160]. In other cases, particulate complexes are formed by combining polysaccharides with other polysaccharides, proteins, or polyphenols[155]. However, the preparation of such materials can be resource-intensive, involving multiple extraction, purification, and modification steps. Moreover, isolating a single component from the original matrix may lead to the loss of valuable bioactive compounds, such as polyphenols and flavonoids. In line with sustainability principles that prioritize functionality over purity and aim to minimize waste, an emerging research trend involves the use of food industry by-products as Pickering stabilizers[158]. These materials often function as efficient emulsifiers without requiring extensive purification and may contain both insoluble particles and soluble components with surface-active properties, leading to the formation of so-called “hybrid Pickering emulsions”[161]. For example, apple pomace derived from food processing waste has been shown to effectively stabilize emulsions through the combined

action of insoluble cellulose particles and soluble components such as proteins and pectins[162]. Nevertheless, the use of food by-products may pose challenges in cosmetic applications, particularly regarding color and aesthetic acceptability, depending on the intended use of the final formulation[163].

1.7.2 Emulsion characterizations

Given the key role of emulsions in stabilizing and delivering active ingredients, the characterization of their complex structure, including phase distribution, droplet size and interfacial properties, is crucial to optimize both performance and stability[164].

Although emulsions can be kinetically stabilized through the use of emulsifiers or particulate stabilizers, they are inherently thermodynamically unstable systems. Therefore, what is commonly referred to as emulsion stability is defined by the rate at which destabilization phenomena occur rather than by true equilibrium[165]. Physical instability results in macroscopic phase separation and can be classified into five main mechanisms, as summarized in **Figure 1.8**[166]. Sedimentation and creaming are gravity-driven phenomena in which dispersed droplets migrate toward the bottom or the top of the emulsion, respectively, depending on the relative density of the dispersed and continuous phases. These processes may occur independently or in combination with coalescence, Ostwald ripening, and flocculation, which are instead related to changes in droplet size. Specifically, coalescence refers to the irreversible fusion of small droplets into larger ones, Ostwald ripening involves the slow diffusion of dispersed phase molecules from smaller to larger droplets, while flocculation describes the reversible aggregation of droplets without fusion[167].

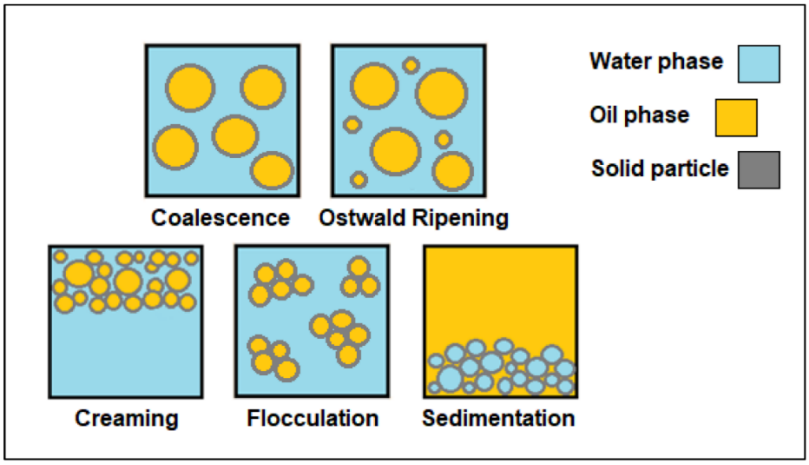

Figure 1.8. Schematic representation of the different physical instability phenomena of emulsions.

The most commonly employed techniques to evaluate physical instability include visual inspection and analytical tools such as microscopy and spectroscopy. However, cosmetic emulsions are often highly concentrated and opaque, which frequently necessitates dilution prior to analysis[168]. This dilution step may alter the native structure of the system and reduce the accuracy and representativeness of the measurements.

1.7.2.1 Static Multiple Light Scattering

Static Multiple Light Scattering (SMLS), implemented in instruments such as the TURBISCAN®, enables the investigation of droplet dispersion and its temporal evolution without the need for sample dilution. This technology is based on the transmission of a photon beam through the sample along the entire height of a glass vial. After interaction with the dispersed droplets, the scattered photons are detected by two synchronized detectors. The transmission detector collects the light passing through the sample (0° from incident beam), while the backscattering detector measures light scattered at an angle of 135° from incident beam[169] (**Figure 1.9**)[170].

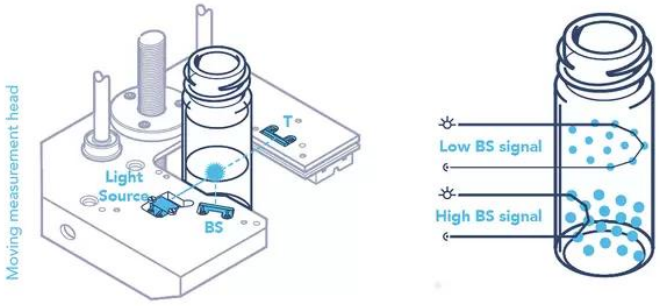

Figure 1.9. Schematic representation of Static Multiple Light Scattering (SMLS) technology adopted by TURBISCAN®.

Both transmission and backscattering intensities depend on droplet size and concentration. By monitoring these signals as a function of sample height and time, Turbiscan allows the detection of early destabilization phenomena, even when they are not yet naked-eye visible. Regions with higher droplet concentration produce increased backscattering signals (BS), whereas less dense regions result in lower BS[171].

1.7.2.2 Accelerated stability tests

Although SMLS provides highly reliable and sensitive information on emulsion stability, long-term studies require repeated measurements over extended time periods. To overcome this limitation, accelerated stability tests are commonly employed to predict long-term stability within a shorter time[172]. These tests consist of subjecting emulsions to controlled mechanical or thermal stresses that simulate the environmental conditions encountered during product life cycle. Typical approaches include centrifugation cycles[173] and storage at different critical temperatures[174], which accelerate destabilization processes.

1.7.2.3 Rheology

The study of their rheological characteristics is a fundamental tool for investigating emulsion structure and stability, as it provides insight into deformation behavior and viscoelastic properties. Rheological parameters reflect the internal organization of the system and are closely related to droplet interactions, phase volume fraction, and interfacial strength[175].

The most commonly performed rheological analyses include flow sweep and strain sweep analysis. Flow sweep analysis evaluates the apparent viscosity as a function of shear rate, allowing the classification of emulsions as non-Newtonian fluids. Cosmetic emulsions typically exhibit either shear-thinning or shear-thickening behavior (**Figure 1.10**)[176], depending on whether viscosity decreases or increases with increasing shear rate. Shear-thinning (pseudoplastic) behavior is the most frequently observed and is generally associated with progressive droplet deformation and alignment along the flow direction, leading to partial disruption of the original microstructure[177].

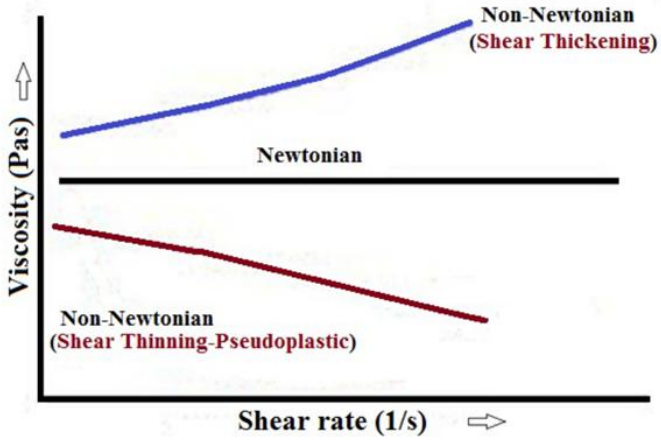

Figure 1.10. Typical rheological behavior of Newtonian and non-Newtonian fluids.

Strain sweep analysis, on the other hand, is used to identify the linear viscoelastic region (LVR**)**, defined as the range of deformation within which the emulsion structure remains intact and responds elastically[178]. This test evaluates the relative contribution of elastic (storage modulus, G′) and viscous (loss modulus, G″) components under increasing strain[179]. Within the LVR, both moduli remain constant until the yield point, beyond which structural breakdown occurs and G′ and G″ begin to change, sometimes intersecting at the flow point[180] (**Figure 1.11**)[181].

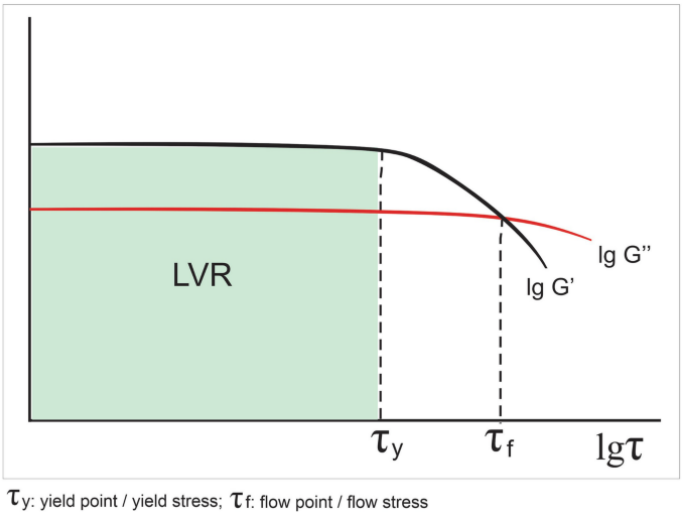

Figure 1.11. Example of strain sweep analysis: the functions of G' and G'' show constant plateau values within the LVR region.

1.7.2.4 Laser diffraction analysis

One of the most widely used techniques for characterizing the size distribution of droplets in emulsions is laser diffraction particle size analysis. Laser diffraction is a rapid, non-destructive optical method commonly applied to powders, suspensions, and emulsions to determine volume-based size distributions over a broad range, typically from tens of nanometers to several millimeters, depending on the instrument configuration[182].

The operating principle of laser diffraction is based on the measurement of light scattering when a collimated laser beam interacts with dispersed droplets in a sample. As the laser passes through a dispersion, droplets of different sizes scatter light at characteristic angles: larger droplets scatter light predominantly at smaller angles relative to the incident beam, whereas smaller droplets scatter light at larger angles. The resulting pattern of scattered light is detected by an array of photodetectors installed at various angles around the sample, and the measured angular intensity distribution is analyzed mathematically using light-scattering models to compute the droplet size distribution[183]. The analysis inherently assumes that droplets behave as equivalent spheres, and the resulting size distribution is reported accordingly as a dimensional distribution, often expressed in terms of parameters such as D10, D50 (median diameter), and D90, which represent the diameters below which 10%, 50%, and 90% of the total volume is contained, respectively[184]. In practice, laser diffraction instruments can be equipped with a wet dispersion module, in which the emulsion

sample is dispersed in a liquid (typically water or SDS solutions) under gentle agitation to ensure representative sampling and prevent droplet coalescence or settling during measurement. The sample flows through the measurement cell while the laser and detectors record the scattered light, allowing for the real-time determination of the droplet size distribution[185], [186].

1.8 References

[1] M. I. M. Khalil, R. S. Shaala, E. F. S. Mousa, M. A. Zoromba, and M. H. R. Atta, "Examining the associations between emotionally charged reactions toward climate change and self-care, quality of life among older adults, coping mechanisms, and pro-environmental practices," *Geriatr. Nurs. (Minneap).*, vol. 61, pp. 353–363, Jan. 2025, doi: 10.1016/j.gerinurse.2024.11.013.

[2] S. Marahatta, A. Singh, and P. Pyakurel, "Self-cosmetic care during the COVID-19 pandemic and its psychological impacts: Facts behind the closed doors," *J. Cosmet. Dermatol.*, vol. 20, no. 10, pp. 3093–3097, Oct. 2021, doi: 10.1111/jocd.14380.

[3] Y. Yayun, "Care as Concern for Oneself Cosme tics in Modern Japan Care as Concern for Oneself Cosmetics in Modern Japan," 2022. [Online]. Available: http://hdl.handle.net/2433/286395

[4] B. Bharatbhai Patel, A. Prajapati, S. Narkhede, and S. Luhar, "Digitalization in Natural Cosmetics: Trends, Opportunities and Challenges," *Asian Journal of Pharmacy and Technology*, pp. 177–180, Apr. 2025, doi: 10.52711/2231-5713.2025.00028.

[5] "Regulation (EC) No 1223/2009 of the European Parliament and of the Council of 30 November 2009 on cosmetic products (recast) (Text with EEA relevance) ."

[6] C. K. Mahendra *et al.*, "The Potential of Sky Fruit as an Anti-Aging and Wound Healing Cosmeceutical Agent," *Cosmetics*, vol. 8, no. 3, p. 79, Aug. 2021, doi: 10.3390/cosmetics8030079.

[7] H.-C. Ho, C. L. Chiu, S. Mansumitrchai, and B. J. Quarles, "Hedonic and utilitarian value as a mediator of men's intention to purchase cosmetics," *Journal of Global Fashion Marketing*, vol. 11, no. 1, pp. 71–89, Jan. 2020, doi: 10.1080/20932685.2019.1682026.

[8] J.-K. Liu, "Natural products in cosmetics," *Nat. Prod. Bioprospect.*, vol. 12, no. 1, p. 40, Dec. 2022, doi: 10.1007/s13659-022-00363-y.

[9] G. Daniels and S. Gupta, "Responsible and Sustainable Beauty Consumption for Wellbeing of Older Adults," *Journal of Macromarketing*, vol. 45, no. 4, pp. 747–761, Dec. 2025, doi: 10.1177/02761467251331440.

[10] A. M. Juncan, C. Morgovan, L.-L. Rus, and F. Loghin, "Development and Evaluation of a Novel Anti-Ageing Cream Based on Hyaluronic Acid and Other Innovative Cosmetic Actives," *Polymers (Basel).*, vol. 15, no. 20, p. 4134, Oct. 2023, doi: 10.3390/polym15204134.

[11] H. Cristini, H. Kauppinen-Räisänen, and A. G. Woodside, "Broadening the Concept of Luxury: Transformations and Contributions to Well-Being," *Journal of Macromarketing*, vol. 42, no. 4, pp. 673–685, Dec. 2022, doi: 10.1177/02761467221116779.

[12] T. Pencarelli, V. Ali Taha, V. Škerháková, T. Valentiny, and R. Fedorko, "Luxury Products and Sustainability Issues from the Perspective of Young Italian Consumers," *Sustainability*, vol. 12, no. 1, p. 245, Dec. 2019, doi: 10.3390/su12010245.

[13] R. Dhillon, B. Agarwal, and N. Rajput, "Experiential marketing strategies used by luxury cosmetics companies," *Innovative Marketing*, vol. 18, no. 1, pp. 49–62, Feb. 2022, doi: 10.21511/im.18(1).2022.05.

[14] A. C. Hodge, Z. G. Romo, I. G. Medina, and A. Fionda-Douglas, "Consumer–brand relationships within the luxury cosmetic domain," *Journal of Brand Management*, vol. 22, no. 8, pp. 631–657, Oct. 2015, doi: 10.1057/bm.2015.36.

[15] R. Rocca, F. Acerbi, L. Fumagalli, and M. Taisch, "Sustainability paradigm in the cosmetics industry: State of the art," *Cleaner Waste Systems*, vol. 3, p. 100057, Dec. 2022, doi: 10.1016/j.clwas.2022.100057.

[16] R. Dhillon, B. Agarwal, and N. Rajput, "Experiential marketing strategies used by luxury cosmetics companies," *Innovative Marketing*, vol. 18, no. 1, pp. 49–62, Feb. 2022, doi: 10.21511/im.18(1).2022.05.

[17] A. Tal, "The Environmental Impacts of Overpopulation," *Encyclopedia*, vol. 5, no. 2, p. 45, Apr. 2025, doi: 10.3390/encyclopedia5020045.

[18] C. Guerranti, T. Martellini, G. Perra, C. Scopetani, and A. Cincinelli, "Microplastics in cosmetics: Environmental issues and needs for global bans," *Environ. Toxicol. Pharmacol.*, vol. 68, pp. 75–79, May 2019, doi: 10.1016/j.etap.2019.03.007.

[19] S. Bom, J. Jorge, H. M. Ribeiro, and J. Marto, "A step forward on sustainability in the cosmetics industry: A review," *J. Clean. Prod.*, vol. 225, pp. 270–290, Jul. 2019, doi: 10.1016/j.jclepro.2019.03.255.

[20] S. Bom, H. M. Ribeiro, and J. Marto, "Sustainability Calculator: A Tool to Assess Sustainability in Cosmetic Products," *Sustainability*, vol. 12, no. 4, p. 1437, Feb. 2020, doi: 10.3390/su12041437.

[21] F. Mellou, A. Varvaresou, and S. Papageorgiou, "Renewable sources: applications in personal care formulations," *Int. J. Cosmet. Sci.*, vol. 41, no. 6, pp. 517–525, Dec. 2019, doi: 10.1111/ics.12564.

[22] C. Xu, M. Jia, M. Xu, Y. Long, and H. Jia, "Progress on environmental and economic evaluation of low-impact development type of best management practices through a life cycle perspective," *J. Clean. Prod.*, vol. 213, pp. 1103–1114, Mar. 2019, doi: 10.1016/j.jclepro.2018.12.272.

[23] M. Dube and S. Dube, "Towards Sustainable Color Cosmetics Packaging," *Cosmetics*, vol. 10, no. 5, p. 139, Oct. 2023, doi: 10.3390/cosmetics10050139.

[24] P. Rachmawati, S. Susanto, and Y. E. Christian, "Integrating Sustainability into Cosmetic Manufacturing and Consumption: Challenges and Innovations," *Jurnal Perkotaan*, vol. 17, no. 2, pp. 83–109, Jan. 2026, doi: 10.25170/perkotaan.v17i2.7353.

[25] Coherent market insights. Available online: https://www.coherentmarketinsights.com/industry-reports/natural-cosmetics-market (accessed on 12 December 2025).

[26] M. Usman, M. Nakagawa, and S. Cheng, "Emerging Trends in Green Extraction Techniques for Bioactive Natural Products," *Processes*, vol. 11, no. 12, p. 3444, Dec. 2023, doi: 10.3390/pr11123444.

[27] P. Wu *et al.*, "Environmental occurrences, fate, and impacts of microplastics," *Ecotoxicol. Environ. Saf.*, vol. 184, p. 109612, Nov. 2019, doi: 10.1016/j.ecoenv.2019.109612.

[28] Y. Lee, J. Cho, J. Sohn, and C. Kim, "Health Effects of Microplastic Exposures: Current Issues and Perspectives in South Korea," *Yonsei Med. J.*, vol. 64, no. 5, p. 301, 2023, doi: 10.3349/ymj.2023.0048.

[29] N. A. S. M Rahim, F. Islahudin, N. Abu Tahrim, and M. Jasamai, "Microplastics in Cosmetics and Personal Care Products: Impacts on Aquatic Life and Rodents with Potential Alternatives," *Sains Malays.*, vol. 51, no. 8, pp. 2495–2506, Aug. 2021, doi: 10.17576/jsm-2022-5108-12.

[30] A. Kukkola, A. J. Chetwynd, S. Krause, and I. Lynch, "Beyond microbeads: Examining the role of cosmetics in microplastic pollution and spotlighting unanswered questions," *J. Hazard. Mater.*, vol. 476, p. 135053, Sep. 2024, doi: 10.1016/j.jhazmat.2024.135053.

[31] S. Chandra and K. B. Walsh, "Microplastics in water: Occurrence, fate and removal," *J. Contam. Hydrol.*, vol. 264, p. 104360, May 2024, doi: 10.1016/j.jconhyd.2024.104360.

[32] M. Aristizabal *et al.*, "Microplastics in dermatology: Potential effects on skin homeostasis," *J. Cosmet. Dermatol.*, vol. 23, no. 3, pp. 766–772, Mar. 2024, doi: 10.1111/jocd.16167.

[33] J. H. Han and H. S. Kim, "Microplastics in Cosmetics: Emerging Risks for Skin Health and the Environment," *Cosmetics*, vol. 12, no. 4, p. 171, Aug. 2025, doi: 10.3390/cosmetics12040171.

[34] A. L. V. Cubas, R. T. Bianchet, I. M. A. S. dos Reis, and I. C. Gouveia, "Plastics and Microplastic in the Cosmetic Industry: Aggregating Sustainable Actions Aimed at Alignment and Interaction with UN Sustainable Development Goals," *Polymers (Basel).*, vol. 14, no. 21, p. 4576, Oct. 2022, doi: 10.3390/polym14214576.

[35] S. H. Shin, Y. H. Lee, N.-K. Rho, and K. Y. Park, "Skin aging from mechanisms to interventions: focusing on dermal aging," *Front. Physiol.*, vol. 14, May 2023, doi: 10.3389/fphys.2023.1195272.

[36] R. S. Hussein, S. Bin Dayel, O. Abahussein, and A. A. El-Sherbiny, "Influences on Skin and Intrinsic Aging: Biological, Environmental, and Therapeutic Insights," *J. Cosmet. Dermatol.*, vol. 24, no. 2, Feb. 2025, doi: 10.1111/jocd.16688.

[37] S. Sibilla, M. Godfrey, S. Brewer, A. Budh-Raja, and L. Genovese, "An Overview of the Beneficial Effects of Hydrolysed Collagen as a Nutraceutical on Skin Properties: Scientific Background and Clinical Studies," *Open Nutraceuticals J.*, vol. 8, no. 1, pp. 29–42, Mar. 2015, doi: 10.2174/1876396001508010029.

[38] E. Hofmann, A. Schwarz, J. Fink, L.-P. Kamolz, and P. Kotzbeck, "Modelling the Complexity of Human Skin In Vitro," *Biomedicines*, vol. 11, no. 3, p. 794, Mar. 2023, doi: 10.3390/biomedicines11030794.

[39] A. Malik and L. J. Hoenig, "Can aging be slowed down?," *Clin. Dermatol.*, vol. 37, no. 4, pp. 306–311, Jul. 2019, doi: 10.1016/j.clindermatol.2019.04.003.

[40] S. Shanbhag, A. Nayak, R. Narayan, and U. Y. Nayak, "Anti-aging and Sunscreens: Paradigm Shift in Cosmetics," *Adv. Pharm. Bull.*, vol. 9, no. 3, pp. 348–359, Aug. 2019, doi: 10.15171/apb.2019.042.

[41] K. A. Khalid, A. F. M. Nawi, N. Zulkifli, Md. A. Barkat, and H. Hadi, "Aging and Wound Healing of the Skin: A Review of Clinical and Pathophysiological Hallmarks," ., vol. 12, no. 12, p. 2142, Dec. 2022, doi: 10.3390/life12122142.

[42] R. S. Hussein, S. Bin Dayel, O. Abahussein, and A. A. El-Sherbiny, "Influences on Skin and Intrinsic Aging: Biological, Environmental, and Therapeutic Insights," *J. Cosmet. Dermatol.*, vol. 24, no. 2, Feb. 2025, doi: 10.1111/jocd.16688.

[43] Z. A. M. Yasin, F. Ibrahim, N. N. Rashid, M. F. M. Razif, and R. Yusof, "The Importance of Some Plant Extracts as Skin Anti-aging Resources: A Review," *Curr. Pharm. Biotechnol.*, vol. 18, no. 11, pp. 864–876, Feb. 2018, doi: 10.2174/1389201019666171219105920.

[44] J. P. de Moura *et al.*, "Targets Involved in Skin Aging and Photoaging and their Possible Inhibitors: A Mini-review," *Curr. Drug Targets*, vol. 24, no. 10, pp. 797–815, Aug. 2023, doi: 10.2174/1389450124666230719105849.

[45] S. Davinelli, J. C. Bertoglio, A. Polimeni, and G. Scapagnini, "Cytoprotective Polyphenols Against Chronological Skin Aging and Cutaneous Photodamage," *Curr. Pharm. Des.*, vol. 24, no. 2, pp. 99–105, Apr. 2018, doi: 10.2174/1381612823666171109102426.

[46] V. Francois-Newton *et al.*, "Antioxidant and Anti-Aging Potential of Indian Sandalwood Oil against Environmental Stressors In Vitro and Ex Vivo," *Cosmetics*, vol. 8, no. 2, p. 53, Jun. 2021, doi: 10.3390/cosmetics8020053.

[47] N. H. amin Hussen, S. K. Abdulla, N. M. Ali, V. A. Ahmed, A. H. Hasan, and E. E. Qadir, "Role of antioxidants in skin aging and the molecular mechanism of ROS: A comprehensive review," *Aspects of Molecular Medicine*, vol. 5, p. 100063, Jun. 2025, doi: 10.1016/j.amolm.2025.100063.

[48] R. R. Kotha, F. S. Tareq, E. Yildiz, and D. L. Luthria, "Oxidative Stress and Antioxidants—A Critical Review on In Vitro Antioxidant Assays," *Antioxidants*, vol. 11, no. 12, p. 2388, Dec. 2022, doi: 10.3390/antiox11122388.

[49] P. Zandi and E. Schnug, "Reactive Oxygen Species, Antioxidant Responses and Implications from a Microbial Modulation Perspective," *Biology (Basel).*, vol. 11, no. 2, p. 155, Jan. 2022, doi: 10.3390/biology11020155.

[50] M. Rinnerthaler, J. Bischof, M. Streubel, A. Trost, and K. Richter, "Oxidative Stress in Aging Human Skin," *Biomolecules*, vol. 5, no. 2, pp. 545–589, Apr. 2015, doi: 10.3390/biom5020545.

[51] X. He, F. Wan, W. Su, and W. Xie, "Research Progress on Skin Aging and Active Ingredients," *Molecules*, vol. 28, no. 14, p. 5556, Jul. 2023, doi: 10.3390/molecules28145556.

[52] S. Dunaway, R. Odin, L. Zhou, L. Ji, Y. Zhang, and A. L. Kadekaro, "Natural Antioxidants: Multiple Mechanisms to Protect Skin From Solar Radiation," *Front. Pharmacol.*, vol. 9, Apr. 2018, doi: 10.3389/fphar.2018.00392.

[53] F. Li Pomi *et al.*, "Rosmarinus officinalis and Skin: Antioxidant Activity and Possible Therapeutical Role in Cutaneous Diseases," *Antioxidants*, vol. 12, no. 3, p. 680, Mar. 2023, doi: 10.3390/antiox12030680.

[54] Y. Nie and Y. Li, "Curcumin: a potential anti-photoaging agent," *Front. Pharmacol.*, vol. 16, May 2025, doi: 10.3389/fphar.2025.1559032.

[55] N. H. amin Hussen, S. K. Abdulla, N. M. Ali, V. A. Ahmed, A. H. Hasan, and E. E. Qadir, "Role of antioxidants in skin aging and the molecular mechanism of ROS: A comprehensive review," *Aspects of Molecular Medicine*, vol. 5, p. 100063, Jun. 2025, doi: 10.1016/j.amolm.2025.100063.

[56] S. Freitas-Rodríguez, A. R. Folgueras, and C. López-Otín, "The role of matrix metalloproteinases in aging: Tissue remodeling and beyond," *Biochimica et Biophysica Acta (BBA) - Molecular Cell Research*, vol. 1864, no. 11, pp. 2015–2025, Nov. 2017, doi: 10.1016/j.bbamcr.2017.05.007.

[57] S. H. Shin, Y. H. Lee, N.-K. Rho, and K. Y. Park, "Skin aging from mechanisms to interventions: focusing on dermal aging," *Front. Physiol.*, vol. 14, May 2023, doi: 10.3389/fphys.2023.1195272.

[58] T. Quan and G. J. Fisher, "Role of Age-Associated Alterations of the Dermal Extracellular Matrix Microenvironment in Human Skin Aging: A Mini-Review," *Gerontology*, vol. 61, no. 5, pp. 427–434, 2015, doi: 10.1159/000371708.

[59] W. Hornebeck, "Down-regulation of tissue inhibitor of matrix metalloprotease-1 (TIMP-1) in aged human skin contributes to matrix degradation and impaired cell growth and survival," *Pathologie Biologie*, vol. 51, no. 10, pp. 569–573, Dec. 2003, doi: 10.1016/j.patbio.2003.09.003.

[60] J. Zhang, H. Yu, M. Man, and L. Hu, "Aging in the dermis: Fibroblast senescence and its significance," *Aging Cell*, vol. 23, no. 2, Feb. 2024, doi: 10.1111/acel.14054.

[61] M. R. Sharma, R. Mitrani, and V. P. Werth, "Effect of TNFα blockade on UVB-induced inflammatory cell migration and collagen loss in mice," *J. Photochem. Photobiol. B*, vol. 213, p. 112072, Dec. 2020, doi: 10.1016/j.jphotobiol.2020.112072.

[62] F. Pintus *et al.*, "Hydroxy-3-Phenylcoumarins as Multitarget Compounds for Skin Aging Diseases: Synthesis, Molecular Docking and Tyrosinase, Elastase, Collagenase and Hyaluronidase Inhibition, and Sun Protection Factor," *Molecules*, vol. 27, no. 20, p. 6914, Oct. 2022, doi: 10.3390/molecules27206914.

[63] S. H. Shin, Y. H. Lee, N.-K. Rho, and K. Y. Park, "Skin aging from mechanisms to interventions: focusing on dermal aging," *Front. Physiol.*, vol. 14, May 2023, doi: 10.3389/fphys.2023.1195272.

[64] A. Fallacara, E. Baldini, S. Manfredini, and S. Vertuani, "Hyaluronic Acid in the Third Millennium," *Polymers (Basel).*, vol. 10, no. 7, p. 701, Jun. 2018, doi: 10.3390/polym10070701.

[65] M. O. Israel, "Effects of Topical and Dietary Use of Shea Butter on Animals," *American Journal of Life Sciences*, vol. 2, no. 5, p. 303, 2014, doi: 10.11648/j.ajls.20140205.18.

[66] M. Wójciak *et al.*, "Protective, Anti-Inflammatory, and Anti-Aging Effects of Soy Isoflavones on Skin Cells: An Overview of In Vitro and In Vivo Studies," *Molecules*, vol. 29, no. 23, p. 5790, Dec. 2024, doi: 10.3390/molecules29235790.

[67] C. D. Papaemmanouil *et al.*, "ANTIAGE-DB: A Database and Server for the Prediction of Anti-Aging Compounds Targeting Elastase, Hyaluronidase, and Tyrosinase," *Antioxidants*, vol. 11, no. 11, p. 2268, Nov. 2022, doi: 10.3390/antiox11112268.

[68] E. Ersoy, E. Eroglu Ozkan, M. Boga, M. A. Yilmaz, and A. Mat, "Anti-aging potential and anti-tyrosinase activity of three Hypericum species with focus on phytochemical composition by LC–MS/MS," *Ind. Crops Prod.*, vol. 141, p. 111735, Dec. 2019, doi: 10.1016/j.indcrop.2019.111735.

[69] A.-Y. Lee, "Skin Pigmentation Abnormalities and Their Possible Relationship with Skin Aging," *Int. J. Mol. Sci.*, vol. 22, no. 7, p. 3727, Apr. 2021, doi: 10.3390/ijms22073727.

[70] A. M. M. Alkawar *et al.*, "Insulin-like Growth Factor-1 Impacts p53 Target Gene Induction in UVB-irradiated Keratinocytes and Human Skin," *Photochem. Photobiol.*, vol. 96, no. 6, pp. 1332–1341, Nov. 2020, doi: 10.1111/php.13279.

[71] J.-K. Liu, "Natural products in cosmetics," *Nat. Prod. Bioprospect.*, vol. 12, no. 1, p. 40, Dec. 2022, doi: 10.1007/s13659-022-00363-y.

[72] N. Dorf and M. Maciejczyk, "Skin senescence—from basic research to clinical practice," *Front. Med. (Lausanne).*, vol. 11, Oct. 2024, doi: 10.3389/fmed.2024.1484345.

[73] L. Krishna Panicker *et al.*, "Bioprospecting for Cosmetics," in *Biodiversity and Business*, Cham: Springer Nature Switzerland, 2024, pp. 143–155. doi: 10.1007/978-3-031-71674-4_8.

[74] N. Mateo, W. Nader, and G. Tamayo, "BIOPROSPECTING I. Bioprospecting: A Tool for Survival and a Source of Inspiration and Innovation II. Economic Value and Benefit Sharing III. Concepts and Practices of Bioprospecting: The Case of Costa Rica."

[75] S. Dixit, A. Shukla, V. Singh, and S. K. Upadhyay, "Bioprospecting of Natural Compounds for Industrial and Medical Applications," in *Bioprospecting of Plant Biodiversity for Industrial Molecules*, Wiley, 2021, pp. 53–71. doi: 10.1002/9781119718017.ch3.

[76] S. S. Dhillion, H. Svarstad, C. Amundsen, and H. C. Bugge, "Bioprospecting: Effects on Environment and Development," *AMBIO: A Journal of the Human Environment*, vol. 31, no. 6, pp. 491–493, Sep. 2002, doi: 10.1579/0044-7447-31.6.491.

[77] G. B. Frisvold, "Bioprospecting and Incentives for Biodiversity Conservation: Lessons from the History of Paclitaxel," 2023, pp. 179–206. doi: 10.1007/978-3-031-24823-8_14.

[78] D. L. Klayman, "*Qinghaosu* (Artemisinin): an Antimalarial Drug from China," *Science (1979).*, vol. 228, no. 4703, pp. 1049–1055, May 1985, doi: 10.1126/science.3887571.

[79] H. J. LONG, "Paclitaxel (Taxol): A Novel Anticancer Chemotherapeutic Drug," *Mayo Clin. Proc.*, vol. 69, no. 4, pp. 341–345, Apr. 1994, doi: 10.1016/S0025-6196(12)62219-8.

[80] A. Indraningrat, H. Smidt, and D. Sipkema, "Bioprospecting Sponge-Associated Microbes for Antimicrobial Compounds," *Mar. Drugs*, vol. 14, no. 5, p. 87, May 2016, doi: 10.3390/md14050087.

[81] A. Naz, A. Chowdhury, S. Pareek, P. Kumar, and N. K. Poddar, "A critical review on the active anti-viral metabolites of bioprospecting traditionally used plant species from semi-arid regions of the subcontinent," *J. Complement. Integr. Med.*, vol. 21, no. 4, pp. 412–439, Dec. 2024, doi: 10.1515/jcim-2024-0186.

[82] A. Katchborian-Neto *et al.*, "Bioprospecting-based untargeted metabolomics identifies alkaloids as potential anti-inflammatory bioactive markers of Ocotea species (Lauraceae)," *Phytomedicine*, vol. 120, p. 155060, Nov. 2023, doi: 10.1016/j.phymed.2023.155060.

[83] S. O. Anifowose *et al.*, "Efforts in Bioprospecting Research: A Survey of Novel Anticancer Phytochemicals Reported in the Last Decade," *Molecules*, vol. 27, no. 23, p. 8307, Nov. 2022, doi: 10.3390/molecules27238307.

[84] K. W. K. Tang, B. C. Millar, and J. E. Moore, "Antimicrobial Resistance (AMR)," *Br. J. Biomed. Sci.*, vol. 80, Jun. 2023, doi: 10.3389/bjbs.2023.11387.

[85] H. Jangid, S. Garg, P. Kashyap, A. Karnwal, A. Shidiki, and G. Kumar, "Bioprospecting of Aspergillus sp. as a promising repository for anti-cancer agents: a comprehensive bibliometric investigation," *Front. Microbiol.*, vol. 15, May 2024, doi: 10.3389/fmicb.2024.1379602.

[86] M. R. Felício, O. N. Silva, S. Gonçalves, N. C. Santos, and O. L. Franco, "Peptides with Dual Antimicrobial and Anticancer Activities," *Front. Chem.*, vol. 5, Feb. 2017, doi: 10.3389/fchem.2017.00005.

[87] M. C. Chifiriuc *et al.*, "Common themes in antimicrobial and anticancer drug resistance," *Front. Microbiol.*, vol. 13, Aug. 2022, doi: 10.3389/fmicb.2022.960693.

[88] E. Donati *et al.*, "Bioprospecting of six polyphenol-rich Mediterranean wild edible plants reveals antioxidant, antibiofilm and bactericidal properties against Methicillin resistant Staphylococcus aureus," *Sci. Rep.*, vol. 15, no. 1, p. 28765, Aug. 2025, doi: 10.1038/s41598-025-03166-6.

[89] N. Garg *et al.*, "Vincristine in Cancer Therapy: Mechanisms, Efficacy, and Future Perspectives," *Curr. Med. Chem.*, vol. 32, no. 32, pp. 6941–6959, Oct. 2025, doi: 10.2174/0109298673319496240911060138.

[90] W. Zhang, P. Gou, J.-M. Dupret, C. Chomienne, and F. Rodrigues-Lima, "Etoposide, an anticancer drug involved in therapy-related secondary leukemia: Enzymes at play," *Transl. Oncol.*, vol. 14, no. 10, p. 101169, Oct. 2021, doi: 10.1016/j.tranon.2021.101169.

[91] M. N. Rosa *et al.*, "Bioprospecting of Natural Compounds from Brazilian Cerrado Biome Plants in Human Cervical Cancer Cell Lines," *Int. J. Mol. Sci.*, vol. 22, no. 7, p. 3383, Mar. 2021, doi: 10.3390/ijms22073383.

[92] K. Singh, A. Kumar, S. Kumar, and S. Gairola, "Bioprospecting of Plants for Phytochemicals: Important for Drugs," in *Phytochemical Genomics*, Singapore: Springer Nature Singapore, 2022, pp. 69–83. doi: 10.1007/978-981-19-5779-6_3.

[93] D. Giordano, "Bioactive Molecules from Extreme Environments," *Mar. Drugs*, vol. 18, no. 12, p. 640, Dec. 2020, doi: 10.3390/md18120640.

[94] "Antioxidant Activity, Total Phenolic, Phytochemical Content, and HPLC Profile of Selected Mangrove Species from Tanjung Api-Api Port Area, South Sumatra, Indonesia," *Tropical Journal of Natural Product Research*, vol. 7, no. 7, Jul. 2023, doi: 10.26538/tjnpr/v7i7.29.

[95] "The Evolutionary Pathways and Ecological Adaptations of Plants: A Comprehensive Analysis of Survival Strategies Over Geological Timescales," *Australian Herbal Insight*, vol. 6, no. 1, pp. 1–5, Jan. 2023, doi: 10.25163/ahi.619966.

[96] T. Dussarrat *et al.*, "Another Tale from the Harsh World: How Plants Adapt to Extreme Environments," in *Annual Plant Reviews online*, Wiley, 2021, pp. 551–603. doi: 10.1002/9781119312994.apr0758.

[97] G. Bartoli, S. Bottega, L. M. C. Forino, D. Ciccarelli, and C. Spanò, "Plant adaptation to extreme environments: The example of Cistus salviifolius of an active geothermal alteration field," *C. R. Biol.*, vol. 337, no. 2, pp. 101–110, Feb. 2014, doi: 10.1016/j.crvi.2013.12.005.

[98] M. Xie, Z. Jiang, X. Lin, and X. Wei, "Application of plant extracts cosmetics in the field of anti-aging," *Journal of Dermatologic Science and Cosmetic Technology*, vol. 1, no. 2, p. 100014, Jun. 2024, doi: 10.1016/j.jdsct.2024.100014.

[99] Q. Ma *et al.*, "Genomic analysis reveals phylogeny of Zygophyllales and mechanism for water retention of a succulent xerophyte," *Plant Physiol.*, vol. 195, no. 1, pp. 617–639, Apr. 2024, doi: 10.1093/plphys/kiae040.

[100] P. K. Yudina, L. A. Ivanova, D. A. Ronzhina, N. V. Zolotareva, and L. A. Ivanov, "Variation of leaf traits and pigment content in three species of steppe plants depending on the climate aridity," *Russian Journal of Plant Physiology*, vol. 64, no. 3, pp. 410–422, May 2017, doi: 10.1134/S1021443717020145.

[101] L.-B. Liu *et al.*, "ZxABCG11 from the xerophyte Zygophyllum xanthoxylum enhances drought tolerance in Arabidopsis thaliana through modulating cuticular wax accumulation," *Environ. Exp. Bot.*, vol. 190, p. 104570, Oct. 2021, doi: 10.1016/j.envexpbot.2021.104570.

[102] R. Ofir, "'Desert Chemotypes': The Potential of Desert Plants-Derived Metabolome to Become a Sustainable Resource for Drug Leads," *Med. Res. Arch.*, vol. 8, no. 7, 2020, doi: 10.18103/mra.v8i7.2169.

[103] A. Bandyopadhyay, S. A. Selvan, P. K. Patial, and T. Pal, "Plant-based ingredients in cosmetic science: Current applications, limitations, and prospects," *Int. J. Cosmet. Sci.*, Oct. 2025, doi: 10.1111/ics.70034.

[104] J. Bose, A. Rodrigo-Moreno, and S. Shabala, "ROS homeostasis in halophytes in the context of salinity stress tolerance," *J. Exp. Bot.*, vol. 65, no. 5, pp. 1241–1257, Mar. 2014, doi: 10.1093/jxb/ert430.

[105] P. Parihar, S. Singh, R. Singh, V. P. Singh, and S. M. Prasad, "Effect of salinity stress on plants and its tolerance strategies: a review," *Environmental Science and Pollution Research*, vol. 22, no. 6, pp. 4056–4075, Mar. 2015, doi: 10.1007/s11356-014-3739-1.

[106] M. Lefahal, E.-H. Makhloufi, A. Boussetla, R. Ayad, S. A. Rayane, and S. Akkal, "Isoorientin Isolated from the Algerian Halophyte Limonium thouinii (Viv.) Kuntze as a Multifunctional Cosmetic Ingredient: Antioxidant and Photoprotective Effects Evaluation," *Proceedings of the National Academy of Sciences, India Section B: Biological Sciences*, vol. 92, no. 4, pp. 889–896, Dec. 2022, doi: 10.1007/s40011-022-01380-0.

[107] A. Correia *et al.*, "Salicornia ramosissima: A New Green Cosmetic Ingredient with Promising Skin Effects," *Antioxidants*, vol. 11, no. 12, p. 2449, Dec. 2022, doi: 10.3390/antiox11122449.

[108] C. Jiratchayamaethasakul *et al.*, "In vitro screening of elastase, collagenase, hyaluronidase, and tyrosinase inhibitory and antioxidant activities of 22 halophyte plant extracts for novel cosmeceuticals," *Fish. Aquatic Sci.*, vol. 23, no. 1, p. 6, Dec. 2020, doi: 10.1186/s41240-020-00149-8.

[109] J. E. Satchell, "Ecology and environment in the United Arab Emirates," *J. Arid Environ.*, vol. 1, no. 3, pp. 201–226, Sep. 1978, doi: 10.1016/S0140-1963(18)31724-5.

[110] Sabitha Sakkir, "Medicinal plants diversity and their conservation status in the United Arab Emirates (UAE)," *Journal of Medicinal Plants Research*, vol. 6, no. 7, Feb. 2012, doi: 10.5897/JMPR11.1412.

[111] N. A. S. A. Alyammahi, F. L. Ridouane, A. A. Almoalla, A. S. S. J. Al Dhanhani, A. Gorashi, and S. B. Mirza, "Exploration of the Native Plants from the Biodiversity of United Arab Emirates for Conservation and Reintroduction Efforts: Collection, Verification, Design, and Implementation of UAE Flora Database," *International Journal of Plant Biology*, vol. 14, no. 2, pp. 493–502, May 2023, doi: 10.3390/ijpb14020038.

[112] S. Gairola, K. I. Al Shaer, E. K. Al Harthi, and K. A. Mosa, "Strengthening desert plant biotechnology research in the United Arab Emirates: a viewpoint," *Physiology and Molecular Biology of Plants*, vol. 24, no. 4, pp. 521–533, Jul. 2018, doi: 10.1007/s12298-018-0551-2.

[113] UAE FLORA. Available online: https://uaeflora.ae/. (Accessed on 7 January 2026).

[114] Sabitha Sakkir, "Medicinal plants diversity and their conservation status in the United Arab Emirates (UAE)," *Journal of Medicinal Plants Research*, vol. 6, no. 7, Feb. 2012, doi: 10.5897/JMPR11.1412.

[115] W. S. O. F. Al Dahmani, S. B. Mirza, M. S. H. Kalathingal, and F. L. Ridouane, "Macro-mineral concentration analysis of Acacia ehrenbergiana (Salam) from the origin of Fujairah, UAE, with staple food items as a mineral rich dietary supplement for arid and semi-arid lands of the world," *Adv. Life Sci.*, vol. 9, no. 4, p. 534, Jan. 2023, doi: 10.62940/als.v9i4.1516.

[116] H. Sobhy Amin Afifi and I. Abu Al-rub, "Prosopis cineraria as an Unconventional Legumes, Nutrition and Health Benefits," in *Legume Seed Nutraceutical Research*, IntechOpen, 2019. doi: 10.5772/intechopen.79291.

[117] G. Meraj *et al.*, "Middle Eastern mangroves at the arid limit (Red Sea and Arabian/Persian Gulf): eco-biophysical dynamics, blue-carbon MRV, climate-risk pathways, and governance for resilient restoration - a comprehensive review," *Front. Mar. Sci.*, vol. 12, Dec. 2025, doi: 10.3389/fmars.2025.1695426.

[118] M. Alzaabi, J. Orpilla, K. M. Hazzouri, L. Li, and K. Amiri, "SOS3 from Avicennia marina Enhances Salt Stress Tolerance of Arabidopsis thaliana," *Cells*, vol. 14, no. 12, p. 935, Jun. 2025, doi: 10.3390/cells14120935.

[119] S. I. Elmahdy and T. A. Ali, "Monitoring Changes and Soil Characterization in Mangrove Forests of the United Arab Emirates Using the Canonical Correlation Forest Model by Multitemporal of Landsat Data," *Frontiers in Remote Sensing*, vol. 3, Mar. 2022, doi: 10.3389/frsen.2022.782869.

[120] G. Friis and M. E. Killilea, "Mangrove Ecosystems of the United Arab Emirates," in *A Natural History of the Emirates*, Cham: Springer Nature Switzerland, 2024, pp. 217–240. doi: 10.1007/978-3-031-37397-8_7.

[121] I. Cybulska, G. Brudecki, A. Alassali, M. Thomsen, and J. Brown, "Phytochemical composition of some common coastal halophytes of the United Arab Emirates," *Emir. J. Food Agric.*, vol. 26, no. 12, p. 1046, 2014, doi: 10.9755/ejfa.v26i12.19104.

[122] A. Garg and S. K. Mittal, "Review on Prosopis cineraria: A potential herb of Thar desert," *Drug Invention Today*, vol. 5, no. 1, pp. 60–65, Mar. 2013, doi: 10.1016/j.dit.2013.03.002.

[123] G. Brown and G. R. Feulner, "The Vascular Flora of the United Arab Emirates," in *A Natural History of the Emirates*, Cham: Springer Nature Switzerland, 2024, pp. 387–425. doi: 10.1007/978-3-031-37397-8_13.

[124] H. Shanableh *et al.*, "A Comparative Analysis of Deep Learning Methods for Ghaf Tree Detection and Segmentation from UAV-based Images," *ISPRS Annals of the Photogrammetry, Remote Sensing and Spatial Information Sciences*, vol. X-G-2025, pp. 805–811, Jul. 2025, doi: 10.5194/isprs-annals-X-G-2025-805-2025.

[125] M. Giustra *et al.*, "Eco-luxury: Making sustainable drugs and cosmetics with Prosopis cineraria natural extracts," *Frontiers in Sustainability*, vol. 3, Nov. 2022, doi: 10.3389/frsus.2022.1047218.

[126] S. S. Anand, S. Thakur, M. Gargi, S. Choudhary, and P. Bhardwaj, "Development and characterization of genomic microsatellite markers in Prosopis cineraria," *Curr. Plant Biol.*, vol. 9–10, pp. 37–42, Jun. 2017, doi: 10.1016/j.cpb.2017.03.001.

[127] U. Purohit, S. K. Mehar, and S. Sundaramoorthy, "Role of Prosopis cineraria on the ecology of soil fungi in Indian desert," *J. Arid Environ.*, vol. 52, no. 1, pp. 17–27, Sep. 2002, doi: 10.1006/jare.2002.0977.

[128] J. Sharifi-Rad *et al.*, "Prosopis Plant Chemical Composition and Pharmacological Attributes: Targeting Clinical Studies from Preclinical Evidence," *Biomolecules*, vol. 9, no. 12, p. 777, Nov. 2019, doi: 10.3390/biom9120777.

[129] V. Pandey, S. Patel, P. Danai, G. Yadav, and A. Kumar, "Phyto-constituents profiling of Prosopis cineraria and in vitro assessment of antioxidant and anti-ulcerogenicity activities," *Phytomedicine Plus*, vol. 3, no. 3, p. 100452, Aug. 2023, doi: 10.1016/j.phyplu.2023.100452.

[130] H. Alhindaassi *et al.*, "Ghaf microgreen: A novel functional food with enhanced nutritional content via nanoparticle-seed priming," *Future Foods*, vol. 12, p. 100774, Dec. 2025, doi: 10.1016/j.fufo.2025.100774.

[131] V. Yadav and V. Gupta, "Green Synthesis Of Titanium Nanoparticle From Leaf Extract Of Prosopis Cineraria And Cytotoxicity Analysis," *Int. J. Environ. Sci.*, vol. 11, no. 10s, pp. 232–247, Jun. 2025, doi: 10.64252/nv5ta656.

[132] I. S. , K. H. M. S. , A. A. I. , I. H. , B. P. , K. A. U. , et al. Mohammad, "In vitro characterization and assessment of cosmetic potentials of W/O emulsion cream containing 2% Prosopis cineraria extract. ," Acta Poloniae Pharmaceutica - Drug Research, vol. 72, pp. 1233–1238, 2015.

[133] I. S. Mohammad *et al.*, "Phytocosmeceutical formulation development, characterization and its in-vivo investigations," *Biomedicine & Pharmacotherapy*, vol. 107, pp. 806–817, Nov. 2018, doi: 10.1016/j.biopha.2018.08.024.

[134] L. M. ElDohaji, A. M. Hamoda, R. Hamdy, and S. S. M. Soliman, "Avicennia marina a natural reservoir of phytopharmaceuticals: Curative power and platform of medicines," Dec. 05, 2020, *Elsevier Ireland Ltd*. doi: 10.1016/j.jep.2020.113179.

[135] G. E. Moore, R. E. Grizzle, K. M. Ward, and R. M. Alshihi, "Distribution, Pore-Water Chemistry, and Stand Characteristics of the Mangroves of the United Arab Emirates," *J. Coast. Res.*, vol. 314, pp. 957–963, Jul. 2015, doi: 10.2112/JCOASTRES-D-14-00142.1.

[136] F. Cerri *et al.*, "Natural Products from Mangroves: An Overview of the Anticancer Potential of Avicennia marina," *Pharmaceutics*, vol. 14, no. 12, p. 2793, Dec. 2022, doi: 10.3390/pharmaceutics14122793.

[137] S. K. Das, J. K. Patra, and H. Thatoi, "Antioxidative response to abiotic and biotic stresses in mangrove plants: A review," *Int. Rev. Hydrobiol.*, vol. 101, no. 1–2, pp. 3–19, Apr. 2016, doi: 10.1002/iroh.201401744.

[138] Z. Guo *et al.*, "Leaf sodium homeostasis controlled by salt gland is associated with salt tolerance in mangrove plant *Avicennia marina*," *Tree Physiol.*, vol. 43, no. 5, pp. 817–831, May 2023, doi: 10.1093/treephys/tpad002.

[139] J. Zhou *et al.*, "Comparative transcriptome and metabolome analysis reveals the differential roles of aboveground and belowground pneumatophores in carbon, nitrogen, and sulfur metabolisms in the adaptation of *Avicennia marina* to coastal intertidal habitat," *The Plant Journal*, vol. 121, no. 6, Mar. 2025, doi: 10.1111/tpj.70092.

[140] H. Thatoi, D. Samantaray, and S. K. Das, "The genus *Avicennia* , a pioneer group of dominant mangrove plant species with potential medicinal values: a review," *Front. Life Sci.*, vol. 9, no. 4, pp. 267–291, Oct. 2016, doi: 10.1080/21553769.2016.1235619.

[141] D. Mateos-Molina *et al.*, "Synthesis and evaluation of coastal and marine biodiversity spatial information in the United Arab Emirates for ecosystem-based management," *Mar. Pollut. Bull.*, vol. 167, p. 112319, Jun. 2021, doi: 10.1016/j.marpolbul.2021.112319.

[142] S. Machana, B. Vongsak, C. Chonanan, and B. Nuengsean, "Anti-elastase, anti-tyrosinase and anti-oxidant activity of Thai Mangrove Plants (Connarus semidecandrus, Bruguiera sexangula and Intsia bijuga)," 2017.

[143] D. B. Putri, D. Pringgenies, and A. Trianto, "Antibacterial, Antifungal, Antioxidant, and Photoprotective Analysis of Mangrove Extracts as Additives Ingredients in a Cosmetic Cream," *Hayati*, vol. 32, no. 3, pp. 571–580, Jan. 2025, doi: 10.4308/hjb.32.3.571-580.

[144] M.-C. Kouassi, M. Grisel, and E. Gore, "Multifunctional active ingredient-based delivery systems for skincare formulations: A review," *Colloids Surf. B Biointerfaces*, vol. 217, p. 112676, Sep. 2022, doi: 10.1016/j.colsurfb.2022.112676.

[145] T. Xiao *et al.*, "Advances in emulsion stability: A review on mechanisms, role of emulsifiers, and applications in food," *Food Chem. X*, vol. 29, p. 102792, Jul. 2025, doi: 10.1016/j.fochx.2025.102792.

[146] S. Fujisawa, E. Togawa, and K. Kuroda, "Nanocellulose-stabilized Pickering emulsions and their applications," *Sci. Technol. Adv. Mater.*, vol. 18, no. 1, pp. 959–971, Dec. 2017, doi: 10.1080/14686996.2017.1401423.

[147] F. Menaa, "Emulsions Systems for Skin Care: From Macro to Nano-Formulations," *Journal of Pharmaceutical Care & Health Systems*, vol. 01, no. 02, 2014, doi: 10.4172/jpchs.1000e104.

[148] M. Franceschini, F. Pizzetti, and F. Rossi, "On the Key Role of Polymeric Rheology Modifiers in Emulsion-Based Cosmetics," *Cosmetics*, vol. 12, no. 2, p. 76, Apr. 2025, doi: 10.3390/cosmetics12020076.

[149] E. Guzmán, L. Fernández-Peña, L. Rossi, M. Bouvier, F. Ortega, and R. G. Rubio, "Nanoemulsions for the Encapsulation of Hydrophobic Actives," *Cosmetics*, vol. 8, no. 2, p. 45, Jun. 2021, doi: 10.3390/cosmetics8020045.

[150] R. Zumpano *et al.*, "Sodium lauryl ether sulfates, pivotal surfactants for formulations: Rationalization of their assembly properties," *Colloids Surf. A Physicochem. Eng. Asp.*, vol. 686, p. 133375, Apr. 2024, doi: 10.1016/j.colsurfa.2024.133375.

[151] A. Casiraghi, F. Selmin, P. Minghetti, F. Cilurzo, and L. Montanari, "Nonionic Surfactants: Polyethylene Glycol (PEG) Ethers and Fatty Acid Esters as Penetration Enhancers," in *Percutaneous Penetration Enhancers Chemical Methods in Penetration Enhancement*, Berlin, Heidelberg: Springer Berlin Heidelberg, 2015, pp. 251–271. doi: 10.1007/978-3-662-47039-8_15.

[152] E. Lémery *et al.*, "Skin toxicity of surfactants: Structure/toxicity relationships," *Colloids Surf. A Physicochem. Eng. Asp.*, vol. 469, pp. 166–179, Mar. 2015, doi: 10.1016/j.colsurfa.2015.01.019.

[153] D. Venkataramani, A. Tsulaia, and S. Amin, "Fundamentals and applications of particle stabilized emulsions in cosmetic formulations," *Adv. Colloid Interface Sci.*, vol. 283, p. 102234, Sep. 2020, doi: 10.1016/j.cis.2020.102234.

[154] L. Chen, F. Ao, X. Ge, and W. Shen, "Food-Grade Pickering Emulsions: Preparation, Stabilization and Applications," *Molecules*, vol. 25, no. 14, p. 3202, Jul. 2020, doi: 10.3390/molecules25143202.

[155] W. DENG, Y. LI, L. WU, and S. CHEN, "Pickering emulsions stabilized by polysaccharides particles and their applications: a review," *Food Science and Technology*, vol. 42, 2022, doi: 10.1590/fst.24722.

[156] A. Ribeiro, J. C. B. Lopes, M. M. Dias, and M. F. Barreiro, "Pickering Emulsions Based in Inorganic Solid Particles: From Product Development to Food Applications," *Molecules*, vol. 28, no. 6, p. 2504, Mar. 2023, doi: 10.3390/molecules28062504.

[157] F. Cui *et al.*, "Polysaccharide-based Pickering emulsions: Formation, stabilization and applications," *Food Hydrocoll.*, vol. 119, p. 106812, Oct. 2021, doi: 10.1016/j.foodhyd.2021.106812.

[158] C. Hollestelle, C. Michon, N. Fayolle, and D. Huc-Mathis, "Co-stabilization mechanisms of solid particles and soluble compounds in hybrid Pickering emulsions stabilized by unrefined apple pomace powder," *Food Hydrocoll.*, vol. 146, p. 109184, Jan. 2024, doi: 10.1016/j.foodhyd.2023.109184.

[159] K. M. Z. Hossain, L. Deeming, and K. J. Edler, "Recent progress in Pickering emulsions stabilised by bioderived particles," *RSC Adv.*, vol. 11, no. 62, pp. 39027–39044, 2021, doi: 10.1039/D1RA08086E.

[160] M. Ioelovich, "Adjustment of Hydrophobic Properties of Cellulose Materials," *Polymers (Basel).*, vol. 13, no. 8, p. 1241, Apr. 2021, doi: 10.3390/polym13081241.

[161] C. Hollestelle, D. Huc-Mathis, C. Michon, and D. Blumenthal, "Quantitative effects of formulation and process parameters on the structure of food emulsions stabilized with an unrefined by-product powder: A statistical approach," *Food Research International*, vol. 182, p. 114150, Apr. 2024, doi: 10.1016/j.foodres.2024.114150.

[162] D. Huc-Mathis, G. Almeida, and C. Michon, "Pickering emulsions based on food byproducts: A comprehensive study of soluble and insoluble contents," *J. Colloid Interface Sci.*, vol. 581, pp. 226–237, Jan. 2021, doi: 10.1016/j.jcis.2020.07.078.

[163] D. Huc-Mathis, C. Journet, N. Fayolle, and V. Bosc, "Emulsifying properties of food by-products: Valorizing apple pomace and oat bran," *Colloids Surf. A Physicochem. Eng. Asp.*, vol. 568, pp. 84–91, May 2019, doi: 10.1016/j.colsurfa.2019.02.001.

[164] X. Shi, D. Qi, C. Lin, and J. Li, "A technical review on characterization methods for structures and properties of emulsion," *APL Mater.*, vol. 12, no. 11, Nov. 2024, doi: 10.1063/5.0241903.

[165] E. Guzmán, F. Ortega, and R. G. Rubio, "Pickering Emulsions: A Novel Tool for Cosmetic Formulators," *Cosmetics*, vol. 9, no. 4, p. 68, Jun. 2022, doi: 10.3390/cosmetics9040068.

[166] S. H. Teo, C. Y. Chee, M. Z. Fahmi, S. C. Wibawa Sakti, and H. V. Lee, "Review of Functional Aspects of Nanocellulose-Based Pickering Emulsifier for Non-Toxic Application and Its Colloid Stabilization Mechanism," *Molecules*, vol. 27, no. 21, p. 7170, Oct. 2022, doi: 10.3390/molecules27217170.

[167] F. Ravera, K. Dziza, E. Santini, L. Cristofolini, and L. Liggieri, "Emulsification and emulsion stability: The role of the interfacial properties," *Adv. Colloid Interface Sci.*, vol. 288, p. 102344, Feb. 2021, doi: 10.1016/j.cis.2020.102344.

[168] O. Mengual, "TURBISCAN MA 2000: multiple light scattering measurement for concentrated emulsion and suspension instability analysis," *Talanta*, vol. 50, no. 2, pp. 445–456, Sep. 1999, doi: 10.1016/S0039-9140(99)00129-0.

[169] M. P. L. Sentis, G. Lemahieu, E. Hemsley, M. Bouzaid, and G. Brambilla, "Size distribution of migrating particles and droplets under gravity in concentrated dispersions measured with static multiple light scattering," *J. Colloid Interface Sci.*, vol. 653, pp. 1358–1368, Jan. 2024, doi: 10.1016/j.jcis.2023.09.163.

[170] Microtrac, a Verder Company. Available online: https://www.microtrac.com/it/prodotti/static-multiple-light-scattering (Accessed on 12 January 2026).

[171] D. D. Kaombe, M. Lenes, K. Toven, and W. R. Glomm, "Turbiscan as a Tool for Studying the Phase Separation Tendency of Pyrolysis Oil," *Energy & Fuels*, vol. 27, no. 3, pp. 1446–1452, Mar. 2013, doi: 10.1021/ef302121r.

[172] B. Kupikowska-Stobba, J. Domagała, and M. M. Kasprzak, "Critical Review of Techniques for Food Emulsion Characterization," *Applied Sciences*, vol. 14, no. 3, p. 1069, Jan. 2024, doi: 10.3390/app14031069.

[173] D. Lerche and T. Sobisch, "Direct and Accelerated Characterization of Formulation Stability," *J. Dispers. Sci. Technol.*, vol. 32, no. 12, pp. 1799–1811, Dec. 2011, doi: 10.1080/01932691.2011.616365.

[174] S. Bjerregaard, C. Vermehren, I. Söderberg, and S. Frokjaer, "Accelerated Stability Testing of a Water-in-Oil Emulsion," *J. Dispers. Sci. Technol.*, vol. 22, no. 1, pp. 23–31, Feb. 2001, doi: 10.1081/DIS-100102677.

[175] A. Viton, R. Coatmeur, B. Anthouard, M. Claeys-Bruno, and P. Piccerelle, "Anticipating cosmetic emulsion stability using a novel multi-analytical approach," *Int. J. Cosmet. Sci.*, Dec. 2025, doi: 10.1111/ics.70047.

[176] B. V. S. Jyoti, M. Varma, and S. W. Baek, "Comparative Study of Rheological Properties of Ethanol and UDMH based Gel Propellants," EUCASS.

[177] S. Guido, "Shear-induced droplet deformation: Effects of confined geometry and viscoelasticity," *Curr. Opin. Colloid Interface Sci.*, vol. 16, no. 1, pp. 61–70, Feb. 2011, doi: 10.1016/j.cocis.2010.12.001.

[178] J. M. Zuidema, C. J. Rivet, R. J. Gilbert, and F. A. Morrison, "A protocol for rheological characterization of hydrogels for tissue engineering strategies," *J. Biomed. Mater. Res. B Appl. Biomater.*, vol. 102, no. 5, pp. 1063–1073, Jul. 2014, doi: 10.1002/jbm.b.33088.

[179] L. M. C. Sagis and P. Fischer, "Nonlinear rheology of complex fluid–fluid interfaces," *Curr. Opin. Colloid Interface Sci.*, vol. 19, no. 6, pp. 520–529, Dec. 2014, doi: 10.1016/j.cocis.2014.09.003.

[180] M. A. Hesarinejad, A. Koocheki, and S. M. A. Razavi, "Dynamic rheological properties of Lepidium perfoliatum seed gum: Effect of concentration, temperature and heating/cooling rate," *Food Hydrocoll.*, vol. 35, pp. 583–589, Mar. 2014, doi: 10.1016/j.foodhyd.2013.07.017.

[181] M. C. T. R. Vidigal and A. A. Simiqueli, "Rheology Measurements for Characterization of Molecular Interactions," 2025, pp. 113–123. doi: 10.1007/978-1-0716-4294-8_9.

[182] H. Li, J. Li, J. Bodycomb, and G. S. Patience, "Experimental Methods in Chemical Engineering: Particle Size Distribution by Laser Diffraction—PSD," *Can. J. Chem. Eng.*, vol. 97, no. 7, pp. 1974–1981, Jul. 2019, doi: 10.1002/cjce.23480.

[183] F. Storti and F. Balsamo, "Particle size distributions by laser diffraction: sensitivity of granular matter strength to analytical operating procedures," *Solid Earth*, vol. 1, no. 1, pp. 25–48, Apr. 2010, doi: 10.5194/se-1-25-2010.

[184] S. Meyer, S. Berrut, T. I. J. Goodenough, V. S. Rajendram, V. J. Pinfield, and M. J. W. Povey, "A comparative study of ultrasound and laser light diffraction techniques for particle size determination in dairy beverages," *Meas. Sci. Technol.*, vol. 17, no. 2, pp. 289–297, Feb. 2006, doi: 10.1088/0957-0233/17/2/009.

[185] A. Afolabi, O. Akinlabi, and E. Bilgili, "Impact of process parameters on the breakage kinetics of poorly water-soluble drugs during wet stirred media milling: A microhydrodynamic view," *European Journal of Pharmaceutical Sciences*, vol. 51, pp. 75–86, Jan. 2014, doi: 10.1016/j.ejps.2013.09.002.

[186] B.-M. Kwak, J. E. Lee, J.-H. Ahn, and T.-H. Jeon, "Laser diffraction particle sizing by wet dispersion method for spray-dried infant formula," *J. Food Eng.*, vol. 92, no. 3, pp. 324–330, Jun. 2009, doi: 10.1016/j.jfoodeng.2008.12.005.

2 Aim

The cosmetic industry is currently experiencing significant growth, driven by the increasing demand for skincare products, particularly anti-aging formulations aimed at mitigating visible signs of skin aging in a progressively aging population[1]. At the same time, this sector is facing major challenges related to the ongoing climate crisis, which has led to heightened consumer awareness regarding sustainability issues and a growing preference for natural, environmentally friendly, and low-impact products[2]. In response to these evolving expectations, the cosmetic industry is increasingly committed to the development of sustainable formulations, integrating responsible raw material selection, environmentally friendly extraction and production processes, and the design of final products[3][4].

Within this context, the main objective of this PhD project was the development of an innovative and sustainable semi-solid anti-aging cosmetic formulation. The project followed an integrated approach, starting from the bioprospecting and selection of new plant-based active ingredients, through low-impact extraction processes, and culminating in the formulation of a functional cosmetic product. In parallel, considering the possibility that the selected plant extracts might not be suitable for cosmetic anti-aging applications, the project also aimed to explore alternative biological uses to ensure their scientific and functional valorization.

To achieve these goals, the PhD project was structured into three main steps:

1) Evaluation of the potential anti-aging properties of Prosopis cineraria and Avicennia marina extracts

Prosopis cineraria (commonly known as Ghaf) and *Avicennia marina*, respectively the national tree of UAE [5]and the dominant mangrove species along the Arabian Gulf coastline[6], were selected due to their remarkable adaptive capacity to extreme environmental stresses, which is often reflected in the biosynthesis of specific secondary metabolites[7]. Although both species are well known in traditional medicine and cultural practices and have been reported to contain antioxidant compounds associated with relevant pharmacological activities, their cosmetic applications remain largely unexplored, making them promising candidates as natural anti-aging actives[8][9].

The first phase of the study aimed to prepare extracts from different plant portions of both species using a green extraction technique, followed by the screening of their potential anti-aging properties.

This evaluation was conducted through the assessment of antioxidant activity and the inhibitory capacity against key enzymes involved in extracellular matrix (ECM) remodeling. In addition, the secondary objective of this step was the optimization of specific *in vitro* assay protocols, which was necessary due to the limited consistency and methodological clarity found in the existing literature.

2) Study of Ghaf extract as an anti-aging active ingredient and its incorporation into cosmetic emulsions

After confirming the anti-aging potential of Ghaf extracts, the second step focused on process optimization and sustainability by selecting a single Ghaf extract representative of the whole plant. The aim was to further characterize its anti-aging properties and to evaluate its incorporation into a cosmetic formulation. Specifically, after the preparation and validation of the bioactivity of the Ghaf extract, a sustainable base cosmetic emulsion was developed, followed by the inclusion of the extract as an active ingredient. This step was intended to bridge the gap between bioactivity screening and practical cosmetic application, assessing the feasibility of Ghaf extract as anti-age ingredient in semi-solid formulations.

3) Phytochemical characterization of A. marina extracts and investigation of their antioxidant and in vitro cytotoxic potential

Finally, since *A. marina* extracts did not prove suitable for cosmetic anti-aging applications, a parallel investigation was conducted to characterize their phytochemical composition and explore alternative biological applications. In particular, the antioxidant properties and *in vitro* cytotoxic effects of the extracts were evaluated against cancer cell lines, with healthy cell lines used as comparative control. Although the chemical composition and anticancer activity of *A. marina* have been widely reported in the literature[10], studies specifically focused on *A. marina* populations growing in the UAE are extremely limited. Given that this species is the only mangrove naturally occurring in the UAE and is exposed to particularly harsh environmental conditions, it is plausible that these populations may produce unique secondary metabolites with distinct biological activities[11]. This aspect further supports the relevance of investigating *A. marina* extracts beyond cosmetic applications.

2.1 References

[1] G. Daniels and S. Gupta, "Responsible and Sustainable Beauty Consumption for Wellbeing of Older Adults," *Journal of Macromarketing*, vol. 45, no. 4, pp. 747–761, Dec. 2025, doi: 10.1177/02761467251331440.

[2] R. Dhillon, B. Agarwal, and N. Rajput, "Experiential marketing strategies used by luxury cosmetics companies," *Innovative Marketing*, vol. 18, no. 1, pp. 49–62, Feb. 2022, doi: 10.21511/im.18(1).2022.05.

[3] M. Usman, M. Nakagawa, and S. Cheng, "Emerging Trends in Green Extraction Techniques for Bioactive Natural Products," *Processes*, vol. 11, no. 12, p. 3444, Dec. 2023, doi: 10.3390/pr11123444.

[4] H. Plainfossé, P. Burger, S. Azoulay, A. Landreau, G. Verger-Dubois, and X. Fernandez, "Development of a Natural Anti-Age Ingredient Based on Quercus pubescens Willd. Leaves Extract—A Case Study," *Cosmetics*, vol. 5, no. 1, p. 15, Jan. 2018, doi: 10.3390/cosmetics5010015.

[5] H. Shanableh *et al.*, "A Comparative Analysis of Deep Learning Methods for Ghaf Tree Detection and Segmentation from UAV-based Images," *ISPRS Annals of the Photogrammetry, Remote Sensing and Spatial Information Sciences*, vol. X-G-2025, pp. 805–811, Jul. 2025, doi: 10.5194/isprs-annals-X-G-2025-805-2025.

[6] G. E. Moore, R. E. Grizzle, K. M. Ward, and R. M. Alshihi, "Distribution, Pore-Water Chemistry, and Stand Characteristics of the Mangroves of the United Arab Emirates," *J. Coast. Res.*, vol. 314, pp. 957–963, Jul. 2015, doi: 10.2112/JCOASTRES-D-14-00142.1.

[7] "Antioxidant Activity, Total Phenolic, Phytochemical Content, and HPLC Profile of Selected Mangrove Species from Tanjung Api-Api Port Area, South Sumatra, Indonesia," *Tropical Journal of Natural Product Research*, vol. 7, no. 7, Jul. 2023, doi: 10.26538/tjnpr/v7i7.29.

[8] M. Giustra *et al.*, "Eco-luxury: Making sustainable drugs and cosmetics with Prosopis cineraria natural extracts," *Frontiers in Sustainability*, vol. 3, Nov. 2022, doi: 10.3389/frsus.2022.1047218.

[9] F. Cerri *et al.*, "Natural Products from Mangroves: An Overview of the Anticancer Potential of Avicennia marina," *Pharmaceutics*, vol. 14, no. 12, p. 2793, Dec. 2022, doi: 10.3390/pharmaceutics14122793.

[10] H. Thatoi, D. Samantaray, and S. K. Das, "The genus *Avicennia* , a pioneer group of dominant mangrove plant species with potential medicinal values: a review," *Front. Life Sci.*, vol. 9, no. 4, pp. 267–291, Oct. 2016, doi: 10.1080/21553769.2016.1235619.

[11] S. K. Das, J. K. Patra, and H. Thatoi, "Antioxidative response to abiotic and biotic stresses in mangrove plants: A review," *Int. Rev. Hydrobiol.*, vol. 101, no. 1–2, pp. 3–19, Apr. 2016, doi: 10.1002/iroh.201401744.

3 Evaluation of the potential anti-aging properties of Ghaf and *A.marina* extracts

3.1 Abstract

The ecological transition of the cosmetics industry emphasizes the need for sustainable formulations based on natural raw materials without compromising efficacy. Anti-aging skincare is a major cosmetic application, as skin aging can be accelerated by oxidative stress and ECM degradation mediated by enzymes. In this context, identifying natural ingredients with antioxidant and enzyme-modulating properties is of increasing interest.

Ghaf, the national tree of UAE, and *A. marina*, the only mangrove species naturally occurring in the UAE, thrive in arid and saline environments and are hypothesized to produce bioactive secondary metabolites as adaptive responses to environmental stress. Despite their recognized relevance in traditional medicine and local culture, their cosmetic applications remain poorly explored. Therefore, this chapter focused on the investigation of the antioxidant and enzyme-modulating properties relevant to skin aging of hydroalcoholic extracts obtained from different plant portions of Ghaf (twigs, roots, leaves, and bark) and *A. marina* (roots, leaves, propagules, pericarps, and cotyledons) collected in the UAE.

Following the optimization of *in vitro* enzymatic assay protocols, necessary due to the limited consistency and methodological clarity found in the existing literature, a comprehensive screening of the extracts was performed. Ghaf extracts exhibited remarkable radical scavenging activity in the DPPH assay, significantly outperforming ascorbic acid used as the positive control. Moreover, all Ghaf extracts demonstrated biologically relevant inhibitory activity against elastase, collagenase, and hyaluronidase without substantial differences among plant portions. This suggests the feasibility of using a single extract representative of the whole plant, potentially enhancing synergistic effects among bioactive compounds while improving process efficiency. In contrast, *A. marina* extracts showed only moderate antioxidant activity, comparable to the positive control, which did not translate into a comparable inhibitory capacity against elastase, collagenase, or hyaluronidase. Only minor and tissue-specific effects were observed for propagules and cotyledons, which were insufficient to support their use as primary anti-aging cosmetic ingredients.

Overall, these results highlight Ghaf as a promising multifunctional natural source for anti-aging cosmetic applications, providing a strong foundation for subsequent formulation studies.

3.2 Results and Discussion

3.2.1 Plants extraction

To comprehensively capture a broad spectrum of phytochemical classes across a wide polarity range while adhering to principles of sustainability, the selected portions of Ghaf and *A. marina* were subjected to conventional maceration using a green hydro-alcoholic solvent system (50% v/v Milli-Q water and ethanol). Hydro-alcoholic mixtures are widely recognized for their ability to solubilize both polar and moderately non-polar secondary metabolites more effectively than pure solvents, thereby maximizing extraction yields and phytochemical diversity in plant matrices. This improved extraction efficiency with mixed polar solvents has been documented across multiple species and is attributed to the intermediate solvent polarity enhancing diffusion and solubilization of diverse compound classes including polyphenols, flavonoids, glycosides, and saponins[1][2].

The extraction yields, expressed as the weight percentage of lyophilized extract relative to the initial dry plant material, are summarized in **Table 3.1**. For Ghaf, the highest yield was observed in bark (44.00% w/w), followed by twigs (29.48% w/w) and leaves (22.11% w/w), whereas roots exhibited the lowest yield (11.23% w/w). The pronounced variability in yield across plant tissues likely reflects differences in anatomical structure and secondary metabolite distribution[3]. Bark tissues often contain high concentrations of cell-wall bound polyphenolic polymers and other hydrophilic compounds that are readily solubilized in hydro-alcoholic media, leading to higher extractable content[4]. Conversely, root tissues may harbor a greater proportion of hydrophobic lipids, waxes, or tightly bound metabolites, resulting in reduced extract recovery under the chosen solvent conditions[5]. Intermediate yields in leaves and twigs are consistent with these tissues being enriched in moderately polar flavonoids, glycosides, and related compounds that are efficiently extracted by hydro-alcoholic systems[6].

Table 3.1. Percentage yields of hydroalcoholic extraction of the different portions of Ghaf and *A. marina* expressed as a w/w percentage of freeze-dried extract on the dry weight of the initial plant matrix.

Plant species	Plant portion	Extraction yield (% w/w)
Ghaf	Twigs	29.48
	Roots	11.23
	Leaves	22.11
	Bark	44.00
A. marina	Roots	31.98
	Cotyledons	64.73
	Pericarp	41.10
	Propagule	39.33
	Leaves	34.30

Similarly, extraction of different parts of *A. marina* revealed substantial inter-tissue differences. Cotyledons exhibited the highest extraction yield (64.73% w/w), which may be associated with the intense metabolic activity and storage of reserves (e.g., carbohydrates, glycosylated metabolites, and osmoprotectants) in embryonic tissues that are highly amenable to dissolution in polar solvent mixtures[7]. The pericarp (41.10% w/w) and propagule (39.33% w/w) showed comparable yields, likely reflecting the compositional similarity between these developmentally related structures and their shared roles in seed protection and nutrient provisioning[8]. Roots (31.98% w/w) and leaves (34.30% w/w) displayed moderately lower yields, indicating a relatively lower abundance or accessibility of soluble phytochemicals under the applied extraction conditions. These patterns suggest that embryonic and storage tissues yield more extractable material than mature vegetative organs, consistent with observations in other plant systems where seed and cotyledon extracts often present high levels of soluble metabolites [2].

The overall higher extraction yields observed in *A. marina* compared to Ghaf may also reflect intrinsic biochemical and ecological differences between the two species. Mangrove plants are exposed to high salinity and osmotic stress and therefore tend to accumulate large amounts of water-soluble osmoprotective metabolites such as sugars, polyols, glycosides, and other polar compounds that contribute to osmotic balance and stress tolerance[9], [10]. These metabolites are readily extracted with hydro-alcoholic solvent systems, which may partially explain the higher extractable fraction observed in several *A. marina* tissues compared with Ghaf organs grown in arid terrestrial environments.

It is also noteworthy that the extraction yields reported here were obtained using a conventional maceration approach designed to balance extraction efficiency with simplicity and sustainability. Although this method is widely used for preliminary phytochemical investigations, further optimization of the extraction process could potentially enhance the recovery of bioactive compounds from both species.

3.2.2 Evaluation of antioxidant capacity of plants extracts

Given the increasing interest in the cosmetic market for natural resources with anti-aging applications [11]and considering that oxidative stress is a primary driver of skin aging and age-associated dermal degradation[12], the antioxidant activity of Ghaf and *A. marina* extracts was first evaluated.

3.2.2.1 DPPH Radical Scavenging Activity

The antioxidant capacity of Ghaf and *A. marina* extracts was assessed using the DPPH radical scavenging assay. This method evaluates the ability of samples to reduce the stable radical DPPH by monitoring spectrophotometrically its color transition from violet (oxidized form) to yellow (reduced form). All extracts were tested at increasing concentrations, and the decrease in absorbance was converted into percentage scavenging activity normalized on the control (lacking antioxidant).

As shown in **Figure 3.1 (a),** Ghaf extracts exhibited a concentration-dependent increase in radical scavenging capacity within the range 0–10 µg/mL, reaching approximately 30–40% inhibition at the highest tested concentration. Notably, the scavenging profiles of bark, twigs, leaves, and roots were almost superimposable, indicating the absence of significant differences in antioxidant potential

among the various plant portions. This behavior suggests a rather homogeneous distribution of redox-active constituents across Ghaf tissues and is likely attributable to the presence of abundant phenolic compounds, flavonoids, and other electron- or hydrogen-donating metabolites that efficiently neutralize free radicals[13]. Recent studies have similarly reported that Ghaf contains high levels of polyphenols and flavonoids with marked free-radical scavenging potential[14], and that hydroalcoholic extraction effectively recovers these constituents from different anatomical tissues[15], often yielding comparable antioxidant responses across plant parts when phenolic enrichment is widespread rather than tissue-restricted.

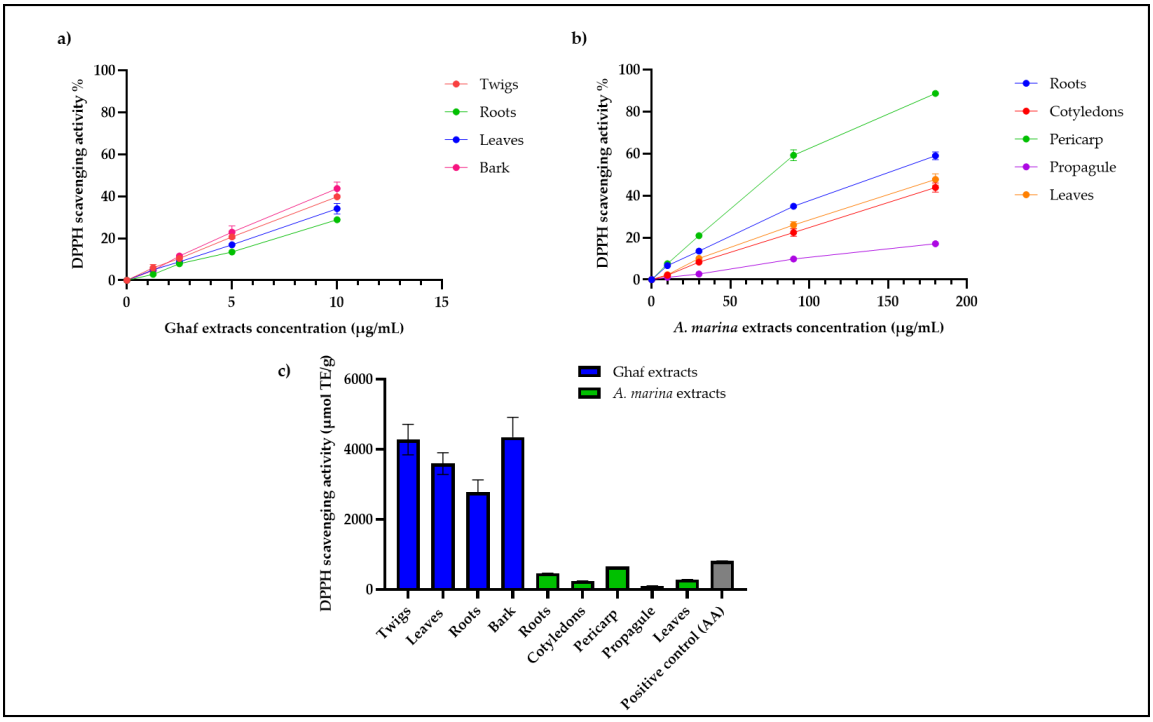

Figure 3.1. Concentration-dependent DPPH radical scavenging activity of Ghaf (a) and *A. marina* (b) extracts. The plots show the percentage of DPPH radical scavenging activity as a function of extracts concentrations. (c) DPPH radical scavenging activity of Ghaf and *A. marina* extracts, and ascorbic acid expressed as Trolox equivalents (µmol TE/g). Bar graph shows the antioxidant capacity of the extracts compared with ascorbic acid included as positive control. Values are expressed as mean ± standard deviation of two independent experiments, each in technical triplicate.

The same analysis performed on *A. marina* required extension of the concentration range due to the absence of measurable activity in the lower Ghaf-equivalent concentrations. Therefore, *A. marina* extracts were evaluated between 0 and 180 µg/mL. As illustrated in **Figure 3.1. (b),** a concentration-

dependent increase in DPPH scavenging activity was also observed, although the response appeared less linear than in Ghaf, which may reflect the higher chemical heterogeneity typically associated with halophytic species[16]. Halophytes often accumulate structurally diverse osmoprotectants, phenolics, and secondary metabolites in response to salinity and oxidative stress[17]; such compositional diversity frequently translates into nonlinear radical-scavenging profiles because different antioxidant families contribute at different concentration thresholds. At the highest concentration tested, maximum inhibition reached approximately 88%, although this value was achieved only at substantially higher extract doses than those required for Ghaf.

Within *A. marina* extracts, cotyledons and leaves displayed almost overlapping profiles, while the pericarp exhibited the highest scavenging capacity and the propagule the lowest. This observation is particularly interesting considering that pericarp and propagule are developmentally associated structures[18]. Their distinct antioxidant performance may therefore be attributed not to qualitative chemical differences, but to variations in the relative abundance, extractability, or matrix accessibility of phenolic and other redox-active compounds. Root extracts showed an antioxidant behavior comparable to cotyledons and leaves, suggesting that soluble antioxidant metabolites are distributed across multiple tissues, although generally at lower efficiency than in Ghaf. These findings align with recent literature describing *A. marina* extracts as possessing measurable antioxidant activity but often requiring higher concentrations to achieve strong radical scavenging[19], likely due to a lower proportion of readily available phenolics relative to other metabolite classes.

To further quantify and standardize these activities, the results were expressed as µmol Trolox equivalents per gram of extract (µmol TE/g) (**Figure 3.1 (c)**) with ascorbic acid included as a positive control. Ghaf extracts demonstrated remarkably high DPPH scavenging capacity, reaching values of approximately 4300 µmol TE/g for bark and twigs and slightly lower but still elevated values for leaves and roots. These values were substantially higher than those of ascorbic acid (~800 µmol TE/g under identical conditions) and far superior to those obtained for *A. marina*. The latter displayed much lower overall antioxidant capacity, with most portions yielding around 300 µmol TE/g and only the pericarp reaching ~650 µmol TE/g.

Collectively, these results clearly demonstrate that Ghaf extracts possess outstanding radical scavenging properties, significantly exceeding a standard reference antioxidant and performing consistently across plant tissues. Such pronounced antioxidant behavior can be potentially attributed to a complex phytochemical composition of Ghaf, like polyphenols, flavonoids, and other redox-active secondary metabolites acting additively or synergistically. The absence of major differences among Ghaf plant portions further supports the decision, later adopted in this project thesis, to focus on a single whole-plant representative extract to streamline subsequent development. Conversely, although *A. marina* extracts did display antioxidant capacity, their activity was markedly lower than Ghaf and required much higher concentrations to achieve comparable effects. This suggests that *A. marina* may be less attractive as a cosmetic anti-aging source, while still retaining potential interest for other biological applications explored in the parallel bioprospecting study described in *Chapter 5*.

3.2.3 In vitro enzymatic inhibition assays

In addition to antioxidant activity, the anti-aging potential of the extracts was further assessed by evaluating their ability to inhibit key enzymes involved in extracellular matrix (ECM) degradation, namely elastase, collagenase, and hyaluronidase. Inhibition of these enzymes contributes to the preservation of elastin, collagen, and hyaluronic acid, respectively, thereby counteracting the loss of skin elasticity and firmness associated with cutaneous aging[20]. Accordingly, the next step of the study focused on determining the inhibitory effects of the plant extracts against these enzymes as an additional indicator of their anti-aging potential.

3.2.3.1 Protocols optimization

A preliminary survey of the literature on these enzyme inhibition assays revealed the absence of fully standardized protocols for the evaluation of anti-aging activity, highlighting the need to establish a simple, rapid, and cost-effective preliminary screening methodology that can be readily applied to future natural active ingredient candidates. On one hand, commercially available kits offer convenience and high sensitivity, but they typically employ fluorescent substrates and proprietary reagents that may obscure basic enzymatic dynamics and may not be readily accessible in all research settings. On the other hand, numerous colorimetric protocols reported in the literature allow robust assessment of elastase, collagenase, and hyaluronidase activities; however, these

protocols varied widely in terms of enzyme and substrate loads, incubation times, and detection modalities (absorbance vs. fluorescence). Therefore, this study adapted and optimized simple spectrophotometric assays based on established literature to yield reproducible, plate-based measurements of enzyme inhibition using absorbance endpoints: a choice that facilitates rapid throughput, reduced reagent costs, and direct mechanistic insight into the enzymatic reaction. The adopted methodology aligns with the sustainability goals of this work by minimizing reliance on single-use commercial kits and emphasizing accessible, mechanistically transparent protocols.

The optimized conditions identified in this step were subsequently applied to the evaluation of the inhibitory activity of the plant extracts, as described in the following sections.

3.2.3.1.1 Elastase inhibition assay protocol optimization

A comprehensive literature survey was first conducted to identify existing *in-vitro* protocols designed to evaluate the inhibitory potential of natural extracts toward elastase. The selected assay relies on the ability of elastase to hydrolyze a chromogenic synthetic peptide substrate, releasing *p-nitroaniline* that can be quantified spectrophotometrically. The decrease in product formation in the presence of a test sample, compared to the untreated control, therefore represents its inhibitory capacity after a short reaction time.

Although this assay is widely used, the literature revealed substantial variability in its implementation, particularly in terms of enzyme units and substrate micromoles employed, final reaction volumes, substrate type, pre-incubation strategy, and incubation time (**Table 3.2**). This variability highlighted the need to establish a simple, rapid, and reproducible protocol, rationally optimized and suitable for high-throughput screening.

Table 3.2. Overview of representative literature protocols for elastase inhibition assays, highlighting enzyme source, substrate, final reaction volume, enzyme and substrate amounts, reaction time, and pre-incubation strategy. PPE: porcine pancreatic elastase; HLE: human leukocyte elastase; MAAPVN: N-methoxysuccinyl-Ala-Ala-Pro-Val-p-nitroanilide; SANA and AAAPVN: N-succinyl-Ala-Ala-Ala-p-nitroanilide; N/A: not available. Green rows indicate protocols involving pre-incubation of inhibitor/sample with the substrate, whereas blue rows indicate pre-incubation with the enzyme.

Enzyme source	Substrate used	Final reaction volume (mL)	Enzyme (U)	Substrate (µmol)	Reaction time (minutes)	Reference
PPE	MAAPVN	0.20	0.0075	0.25	15	[21]
PPE	SANA	N/A	N/A	N/A	15	[22]
PPE	AAAPVN	0.180	N/A	N/A	20	[23][24]
Elastase	AAAPVN	0.20	0.0100	0.11	15	[25]
PPE	AAAPVN	0.17	0.0500	0.02	5	[25]
PPE EnzChek™ kit	DQ™ elastin	0.20	0.0400	N/A	30	[26]
PPE	AAAPVN	0.22	0.0750	0.20	10	[27]
PPE	SANA	0.24	0.0006	0.20	10	[28]
PPE	AAAPVN	0.20	0.0100	10.00	20	[29]
PPE	AAAPVN	0.10	0.0023	0.03	30	[30]
PPE	SANA	0.24	0.0006	0.20	10	[31]
HLE	SANA	1500.00	37.500	1319.50	10	[32]

Pragmatic constraints were first defined to align the method with the objectives of this work: (i) use of reaction volumes compatible with 96-well microplate format to enable rapid parallel screening; (ii) employment of standard, accessible reagents to avoid reliance on commercial kits; (iii) short

assay times; and (iv) single end-point absorbance readings to minimize data processing while preserving robustness.

Based on literature evidence and preliminary evaluations, porcine pancreatic elastase was selected in combination with the chromogenic substrate N-Methoxysuccinyl-Ala-Ala-Pro-Val p-nitroanilide (MAAPVN). Although MAAPVN is classically associated with human neutrophil elastase[21][33], porcine elastase shares similar substrate preferences and is able to hydrolyze AAPV-based substrates efficiently[21]. The use of porcine elastase ensured assay affordability and sustainability, enabling the development of a rapid and cost-effective screening tool.

Pre-incubation of the potential inhibitor was performed with the enzyme, rather than with the substrate. This choice aimed to allow potential interactions between enzyme active/surface sites and the extract constituents before substrate introduction, which is appropriate for general inhibition screening rather than mechanistic competition studies.

Regarding enzyme and substrate loads, a preliminary kinetic study was performed to define the optimal conditions for the untreated condition (enzyme and substrate only), which would subsequently serve as the reference condition for inhibition experiments. The release of *p*-nitroaniline was monitored at 410 nm in kinetic mode over the entire reaction time (15 min) while varying enzyme and substrate amounts (**Figure 3.2**). The assay was initially set using 0.01 U elastase and 0.30 µmol substrate, corresponding to approximately twice the theoretical amount of substrate expected to be hydrolyzed under uninhibited conditions within 15 min (Condition 1). However, this configuration resulted in absorbance values exceeding 1.5, which are considered suboptimal for quantitative accuracy and linearity. To improve assay performance, the enzyme load was reduced to 0.0075 U and the enzyme-to-substrate *ratio* was adjusted accordingly, using 0.1125 µmol substrate, corresponding to the theoretical amount hydrolyzed in 15 min under uninhibited conditions (Condition 2). Under these conditions, absorbance values ranged between 0.25 and 0.75, which was considered optimal for assay sensitivity and reliability. This configuration was therefore selected as the final untreated condition, corresponding to 100% elastase activity (0% inhibition) for subsequent inhibitor screening experiments. A final reaction volume of 200 µL was selected to maintain compatibility with 96-well plates and facilitate multi-sample screening.

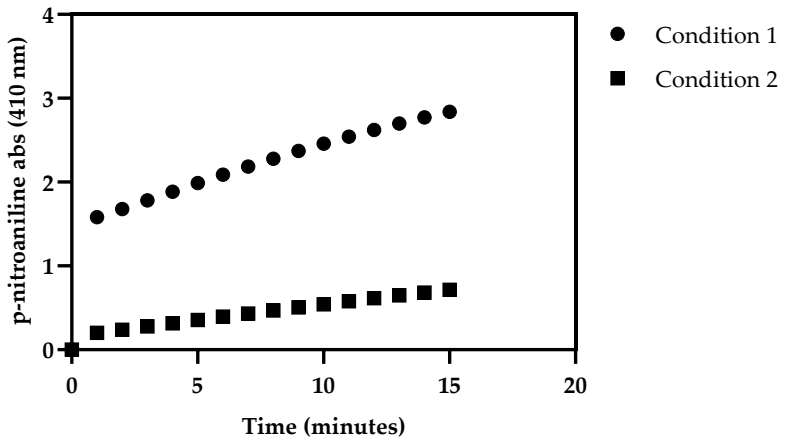

Figure 3.2. Kinetic monitoring of *p*-nitroaniline release at 410 nm during elastase-catalyzed hydrolysis of MAAPVN under two different enzyme–substrate conditions: condition 1 (0.01 U elastase, 0.30 µmol substrate) and condition 2 (0.0075 U elastase, 0.1125 µmol substrate). Absorbance was recorded every minute over a 15 min reaction time.

The finalized protocol was subsequently applied to evaluate the inhibitory activity of Ghaf and *A. marina* extracts toward elastase.

3.2.3.1.2 Collagenase inhibition assay protocol optimization

Similarly to the elastase assay, an extensive literature survey was conducted to identify existing *in vitro* protocols for evaluating the inhibitory activity of plant extracts against collagenase. The selected assay is based on the spectrophotometric monitoring of an intact chromogenic substrate, whose absorbance decreases as a result of collagenase-catalyzed cleavage in the absence of potential inhibitors. The preservation of the uncleaved substrate in the presence of a sample is therefore directly related to its inhibitory capacity.

Although less pronounced than for elastase assays, the collagenase inhibition protocols reported in the literature showed notable differences in terms of enzyme and substrate type, final reaction volumes, especially reaction times, and absolute enzyme and substrate amounts, as summarized in **Table 3.3.** This variability highlighted the need to define a simple, rapid, reproducible, and rationally optimized protocol, suitable for preliminary high-throughput screening of plant extracts.

Table 3.3. Comparison of representative literature protocols for collagenase inhibition assays, including enzyme source, substrate, final reaction volume, enzyme and substrate amounts, reaction time, and incubation strategy. MMP-1: interstitial (fibroblast) collagenase, human recombinant; FALGPA: *N*-[3-(2-furyl)acryloyl]-Leu-Gly-Pro-Ala; N/S: not specified; N/A: not available. Blue rows indicate protocols involving pre-incubation of enzyme with inhibitor/sample, whereas green rows indicate simultaneous incubation of enzyme, substrate, and inhibitor.

Enzyme source	Substrate used	Final reaction volume (mL)	Enzyme (U)	Substrate (µmol)	Reaction time (minutes)	Reference
MMP-1	Ac-Pro-Leu-Gly-S-Leu-Leu-Gly-Oet	0.10	N/A	N/A	10	[21]
ChC type IA	FALGPA	0.12	0.0110	0.02	20	[23]
MMP-1 and MMP-2 of EnzCheck™ kit	DQ™collagen 1 and DQ™gelatin	0.20	0.0400	N/A	90	[26]
ChC N/S	FALGPA	0.15	0.1000	0.12	20	[34]
ChC type I	FALGPA	0.57	N/A	0.57	60	[35]
ChC type H	FALGPA	0.12	0.0001	0.02	20	[36]

Regarding reagent selection, the synthetic peptide FALGPA was chosen as substrate due to its rapid hydrolysis, which enables a sensitive and time-efficient assay[37]. It is highly specific for collagenase activity and is not efficiently cleaved by other proteases, ensuring assay selectivity. As enzyme source, collagenase from *Clostridium histolyticum* Class II (type H) was selected, as it is function-tested and shows a strong preference for short synthetic substrates such as FALGPA. In contrast, collagenase preparations of types I and IA are crude mixtures containing multiple proteolytic activities (e.g., collagenase, clostripain, and other proteases), which may compromise assay specificity[38]. The use of recombinant human MMP-1 and its specific substrate was deliberately excluded, as it is less accessible and less suitable for large-scale screening. Similarly, commercial kits

were avoided in favor of a cost-effective and transparent assay design, allowing better control over reaction parameters and improved sustainability.

Compared to elastase assays, literature protocols for collagenase inhibition show lower variability in absolute substrate amounts, which typically range between 0.02 and 0.12 µmol, whereas enzyme units are more variable and often used in excess relative to the substrate hydrolyzed during the reaction time. Since in this assay the uncleaved substrate is detected spectrophotometrically, the first optimization step focused on identifying an appropriate substrate amount, corresponding to the maximum absorbance value and theoretically representing 100% enzyme inhibition. Starting from literature, 0.02 µmol FALGPA (most commonly reported) and a doubled amount (0.04 µmol) were tested, yielding absorbance values of approximately 0.58 and 0.75, respectively. The latter was selected as optimal, as it provided a sufficiently high absorbance while avoiding signal saturation. Subsequently, enzyme loading was optimized by fixing 0.04 µmol FALGPA and testing two collagenase amounts: 0.001 U (Condition 1) and 0.01 U (Condition 2). These conditions corresponded to enzyme amounts capable of hydrolyzing approximately half (Condition 1) or fivefold more (Condition 2) substrate than the amount theoretically convertible within the 20 min reaction time. This approach allowed evaluation of both moderate and excess enzyme conditions, the latter being frequently reported in the literature.

As shown in **Figure 3.3**, the excess-enzyme condition (Condition 2) provided a clearer and faster decrease in substrate absorbance during the initial reaction phase, whereas Condition 1 resulted in minimal absorbance changes. Moreover, the observed kinetic profile (characterized by an initial decrease in absorbance followed by stabilization at values above zero) is consistent with previously reported data, where the absorbance of the untreated control decreases within the first minutes before reaching a plateau[23]. This behavior likely reflects rapid initial substrate turnover followed by enzyme–substrate equilibrium or partial substrate depletion.

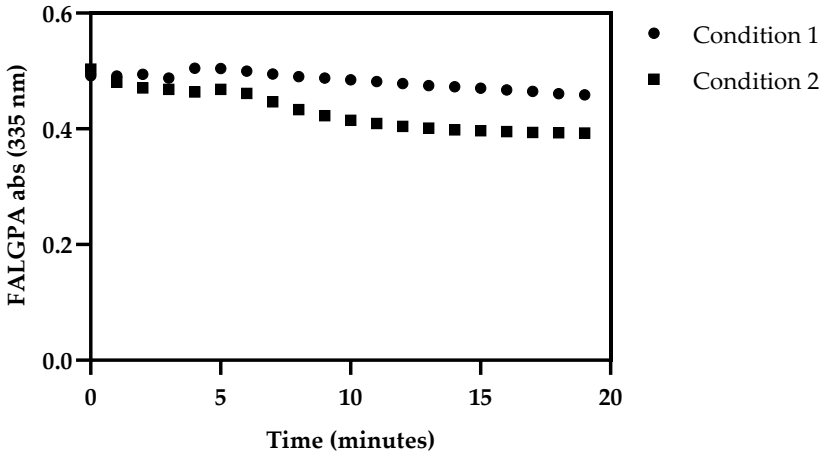

Figure 3.3. Kinetic monitoring of FALGPA absorbance decrease during collagenase-catalyzed hydrolysis under two enzyme-loading conditions: condition 1 (0.001 U collagenase, 0.04 µmol FALGPA) and condition 2 (0.01 U collagenase, 0.04 µmol FALGPA). Absorbance was recorded every minute over a 20 min reaction time.

Based on these results, 0.04 µmol FALGPA and 0.01 U collagenase were selected as optimal conditions and subsequently used for screening the collagenase inhibitory activity of *Ghaf* and *Avicennia marina* extracts.

Finally, an adaptation of the method employed for reduction of activity calculation was required for collagenase assays. In literature, the enzyme activity is often calculated using the same equation employed for elastase assays, as the following equation (1):

$$\text{Collagenase activity } \% = \left(\frac{\text{B}}{\text{A}}\right) * 100 \qquad (1)$$

where *B* is the absorbance in the presence of inhibitor and *A* is the control absorbance. However, in the collagenase assay, enzyme activity results in a decrease in absorbance, meaning that the untreated control corresponds to 100% activity (0% inhibition), while the upper absorbance limit corresponding to 0% activity (100% inhibition) is not inherently defined. To address this limitation, the protocol was modified to enable a clear definition of both reference points. Specifically, the pre-incubation step between enzyme and inhibitor commonly reported in the literature was removed and replaced by an initial dispensing of substrate and inhibitor/sample, followed by an immediate absorbance reading corresponding to 0% activity (substrate in the absence of enzyme). Collagenase was then added, and a second absorbance reading was recorded at the end of the reaction time. This

approach allowed determination, for each condition, of both the absorbance corresponding to 100% activity (untreated control) and 0% activity (substrate only).

Accordingly, collagenase activity was calculated using the following equation (2):

$$\text{Collagenase activity (\%)} = \frac{(\text{Abs}_{\text{pre}} - \text{Abs}_{\text{post}})_{\text{treated}}}{(\text{Abs}_{\text{pre}} - \text{Abs}_{\text{post}})_{\text{untreated}}} \times 100 \quad (2)$$

where Abs_{pre} is the absorbance recorded in the presence of substrate before enzyme addition (substrate-only condition), and Abs_{post} is the absorbance recorded after enzyme addition at the end of the reaction time. Treated and untreated refer to reactions carried out in the presence or absence of the tested sample, respectively.

3.2.3.1.3 Hyaluronidase inhibition assay protocol optimization

A literature survey was finally conducted to identify *in vitro* assays suitable for evaluating the potential inhibitory activity of plant extracts against hyaluronidase. Most of the available studies refer to the classical turbidimetric assay originally proposed by Kass and Seastone (1944), which exploits the turbidity generated by hyaluronic acid (HA) when mixed with acidified protein[39]. In this system, turbidity is directly proportional to the concentration of intact, non-degraded HA and can therefore be used as an indirect measure of hyaluronidase activity in the presence or absence of inhibitors.

The protocols identified in the literature were largely consistent in terms of assay principle and reaction conditions. Typically, bovine testicular hyaluronidase (15 U/mL) is incubated with HA (0.3 mg/mL) for 45 min, after which the reaction is stopped by the addition of an acidified bovine serum albumin (BSA) solution. The turbidity generated by the remaining intact HA is then measured spectrophotometrically at 600 nm after 10 min of incubation (**Table 3.4**). The main variability among published protocols concerned the final reaction volumes used for the enzyme–substrate incubation, which ranged from 0.05 to 2 mL (excluding the stopping acidified solution). In the present work, the literature protocol was maintained in terms of enzyme and substrate type, concentrations, and incubation times, while a final reaction volume of 0.205 mL was selected as a suitable compromise. This volume was considered sufficiently small to enable multiwell plate screening while avoiding excessively low volumes that could compromise pipetting accuracy and assay reproducibility.

Table 3.4. Comparison of representative literature protocols for turbidimetric assays, to evaluate hyaluronidase inhibition including the enzyme and substrate type, enzyme and substrate concentrations, final reaction volume, reaction time between enzyme and substrate, and incubation time with acidified protein solution prior to absorbance measurement. HA: hyaluronic acid; N/A: not available. Ref.: reference.

Enzyme source	Substrate used	Final reaction volume (mL)	Enzyme (U/mL)	Substrate (mg/mL)	Reaction time (minutes)	Incubation time (minutes)	Ref.
Hyaluronidase	HA	2.00	N/A	N/A	10	10	[40]
Bovine hyaluronidase	HA	0.05	N/A	0.3	45	10	[36][41] [42]
Bovine hyaluronidase	HA	0.25	15	0.3	45	10	[28]

To experimentally verify the validity of the assay principle, the proportionality between turbidity at 600 nm and increasing concentrations of HA in the presence of acidified BSA was assessed, using the maximum HA concentration reported in the literature as the upper limit. As shown in **Figure 3.4**, a direct linear relationship was observed, with a coefficient of determination (R^2) of 0.99 and a maximum absorbance value of approximately 0.55 at the highest HA concentration tested. These results confirmed the reliability and sensitivity of the turbidimetric method under the selected conditions.

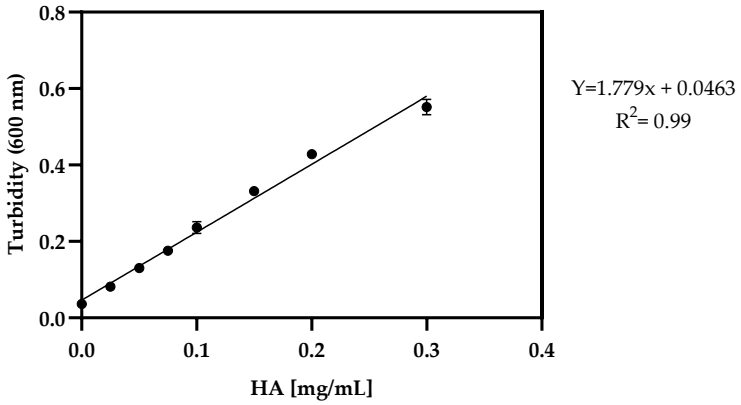

Figure 3.4. Validation of the turbidimetric hyaluronidase assay. Turbidity absorbance at 600 nm as a function of increasing hyaluronic acid (HA) concentrations in the presence of acidified BSA. Each point represents the absorbance mean ± standard deviation of two technical replicates.

The main modification introduced in this assay, similarly to the collagenase inhibition test, concerned the calculation and interpretation of absorbance values. In literature reports[28], [42], the reduction in hyaluronidase activity is calculated using equations analogous to those applied in elastase assays, like the following equation (3).

$$\text{Hyaluronidase activity (\%)} = \left(\frac{\text{B}}{\text{A}}\right) * 100 \quad (3)$$

where A represents the untreated condition absorbance, whereas B represents the treated with sample absorbance, thus without explicitly accounting for the fact that the maximum absorbance measurable in this system corresponds to the HA-only condition (substrate without enzyme), which represents the theoretical 0% of activity. Consequently, the measurable absorbance range is bounded by two well-defined limits: (i) the absorbance of HA incubated with hyaluronidase in the absence of inhibitors, corresponding to 100% activity, and (ii) the absorbance of HA alone, corresponding to 0% activity.

To properly normalize the data within this defined absorbance window, the percentage of hyaluronidase activity was calculated using the following equation (4):

$$\text{Hyaluronidase activity (\%)} = 1 - \left(\frac{A_{\text{sample}} - A_{\text{enzyme control}}}{A_{\text{substrate control}} - A_{\text{enzyme control}}}\right) \times 100 \quad (4)$$

where A_{sample} is the absorbance measured in the presence of enzyme, substrate, and tested extract; $A_{enzyme\ control}$ is the absorbance of HA incubated with hyaluronidase in the absence of inhibitors (100% activity); and $A_{substrate\ control}$ is the absorbance of HA alone without enzyme (0% activity).

These optimized conditions and the revised data processing approach were subsequently applied to investigate the potential hyaluronidase inhibitory activity of Ghaf and *A. marina* extracts.

3.2.3.2 Elastase inhibition assay

The inhibitory activity of the extracts against elastase was evaluated by quantifying enzyme activity in the presence of increasing concentrations of Ghaf and *A. marina* extracts (0–270 µg/mL), or oleanolic acid as a positive control, by measuring the amount of substrate converted by the enzyme relative to the untreated control. As shown in **Figure 3.5 (a)**, all Ghaf extracts exhibited elastase inhibitory activity starting from 50 µg/mL, with a slight dose-dependent trend as extract concentration increased. At the highest tested concentration, enzyme activity was reduced by approximately 50%, with a maximum inhibition of 46% observed for the bark extract. Although the inhibitory effect of all Ghaf extracts was evident, no single plant part displayed a markedly stronger activity than the others, suggesting a relatively homogeneous distribution of the metabolites responsible for elastase inhibition across the different tissues of the plant.

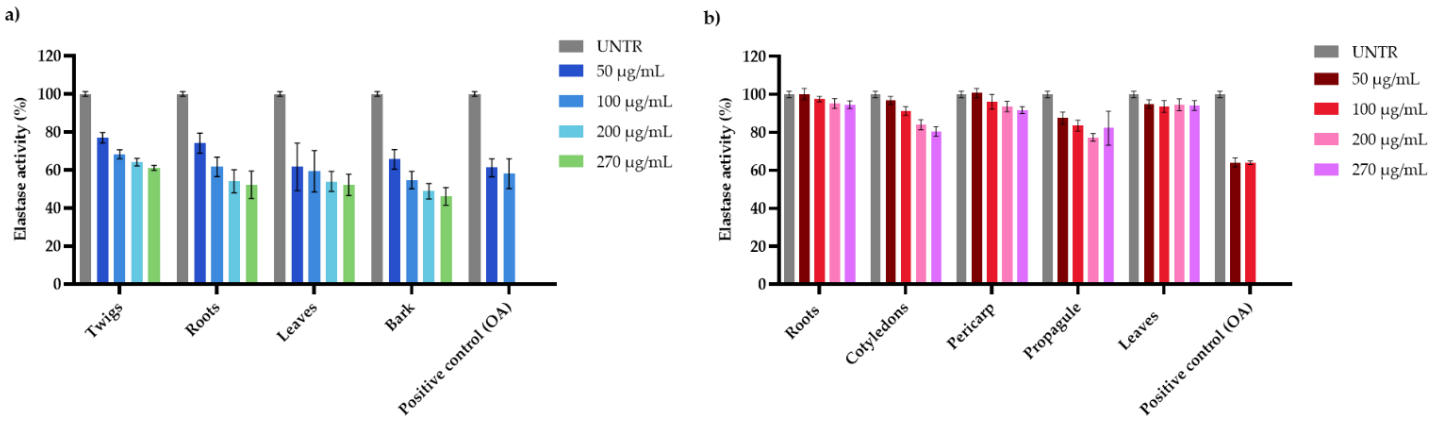

Figure 3.5. Elastase activity in presence of Ghaf (a) and *A.marina* (b) extracts compared to oleanolic acid used as positive control. Each bar represents the mean percentage activity ± standard deviation of two independent experiments, each in technical triplicate.

In contrast, *A.marina* extracts showed a very limited inhibitory effect on elastase activity (**Figure 3.5 (b)**). Enzyme activity remained close to the untreated control for most extracts, with values around 80% observed only for cotyledon and propagule extracts at the highest tested concentration. As observed for Ghaf extracts, a weak dose-dependent trend was detected, possibly due to a fraction of the enzyme population that remains catalytically active even in the presence of excess inhibitor.

Oleanolic acid reproducibly reduced elastase activity to approximately 60% (**Figures 3.5 (a) and (b)**), confirming the reliability of the assay. Notably, while the positive control was more effective than *A. marina* extracts, a comparable inhibitory effect was observed between oleanolic acid and Ghaf extracts at equivalent concentrations, despite the latter being crude extracts. This observation suggests a higher abundance of active constituents and/or synergistic interactions within Ghaf extracts.

3.2.3.3 Collagenase inhibition assay

The ability of Ghaf and *A. marina* extracts to inhibit collagenase activity was also investigated, given the central role of collagen degradation in skin aging. Collagenase activity was quantified in the presence of increasing concentrations of plant extracts (0–270 μg/mL), using epigallocatechin gallate (EGCG, 270 μg/mL) as a reference inhibitor. The reduction in absorbance of the uncleaved substrate was monitored and expressed as percentage enzyme activity normalized to the control. As shown in **Figure 3.6**, all Ghaf extracts induced a marked reduction in collagenase activity, already detectable at low concentrations and becoming more pronounced from 200 μg/mL forward. At the highest tested concentration, enzyme activity was reduced to below 30% for root and bark extracts, reaching a minimum of 16% residual activity for the leaf extract. Overall, all four Ghaf extracts displayed a similar inhibition profile, with slightly stronger effects observed for roots, leaves, and bark compared to twigs. EGCG exhibited a comparable, and in some cases weaker, inhibitory effect than Ghaf root, leaf, and bark extracts at the same concentration, further supporting the hypothesis of synergistic interactions among the bioactive components of Ghaf. Conversely, among *A. marina* extracts, only the cotyledon extract showed any effect on collagenase activity, although very modest, with enzyme activity remaining around 90% at all tested concentrations (**Figure 3.6**). Root, pericarp, propagule, and leaf extracts displayed 100% enzyme activity across the entire concentration range and were therefore excluded from the graphical representation.

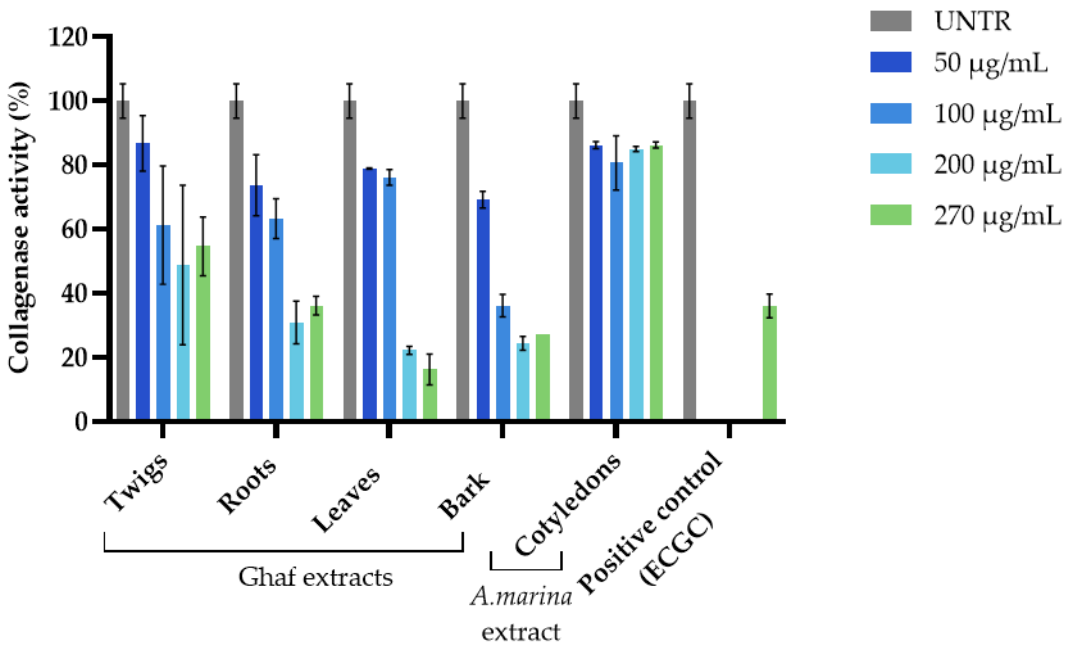

Figure 3.6. Collagenase activity in presence of increasing concentration of Ghaf extracts and *A.marina* cotyledons extract, with ECGC included as positive control. Each bar represents the mean percentage activity ± standard deviation of two independent experiments, each in technical triplicate.

3.2.3.4 Hyaluronidase inhibition assay

Finally, the inhibitory activity of Ghaf and *A. marina* extracts against hyaluronidase was evaluated. This enzyme contributes, together with collagenase and elastase, to the loss of skin structural integrity and elasticity during aging by accelerating hyaluronic acid (HA) degradation. Enzyme activity was assessed by measuring the turbidity generated by undigested HA in the presence of acidified BSA and increasing extract concentrations. When initially tested at the same concentrations as *A. marina* extracts (33–66–132 µg/mL), all Ghaf extracts resulted in complete inhibition of hyaluronidase activity (0% residual activity). To investigate a possible dose-dependent effect, the extracts were subsequently tested at lower concentrations. As shown in **Figure 3.7 (a)**, Ghaf extracts induced a strong concentration-dependent inhibition of hyaluronidase, reaching complete inhibition already at 11 µg/mL for the twig extract and at 33 µg/mL for root and bark extracts. These results indicate extremely low IC_{50} values and highlight the remarkable efficacy of Ghaf extracts against hyaluronidase. Notably, the inhibitory effect exerted by Ghaf extracts exceeded that of the positive control (oleanolic acid), even though the latter was tested at a higher concentration (100 µg/mL).

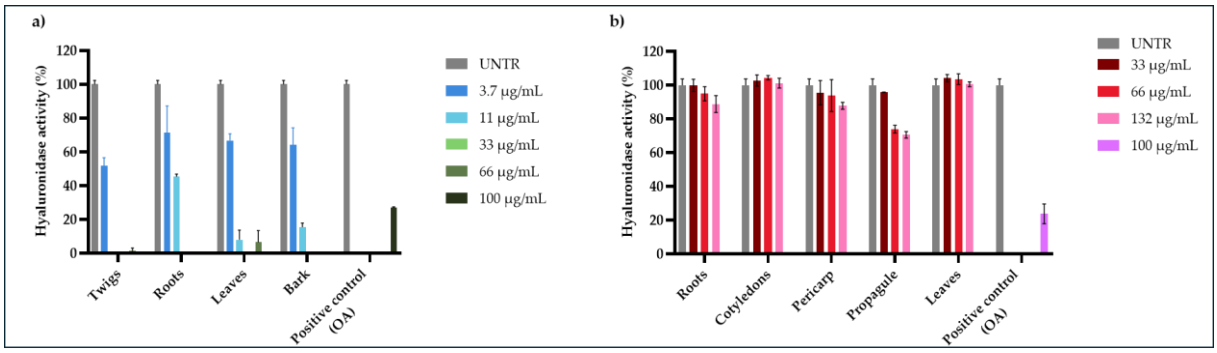

Figure 3.7. Hyaluronidase activity in presence of increasing concentration of Ghaf (a) and *A. marina* (b) extracts, compared to oleanolic acid used as positive control. Each bar represents the mean percentage activity ± standard deviation of two independent experiments, each in technical triplicate.

In contrast, *A. marina* cotyledon and leaf extracts showed no inhibitory activity, with enzyme activity remaining close to 100% at all tested concentrations (**Figure 3.7 (b)**). A slight reduction to approximately 90% activity was observed only for root and pericarp extracts at the highest concentration, while the propagule extract displayed the strongest effect, reducing enzyme activity to approximately 70% from 66 µg/mL onwards. This reduction was nevertheless modest compared to the pronounced inhibition observed for Ghaf extracts. Overall, these results clearly demonstrate that Ghaf extracts are highly effective hyaluronidase inhibitors at substantially lower concentrations than *A. marina* extracts, which appear largely ineffective.

3.3 Conclusions

This chapter provides a comprehensive preliminary evaluation of the anti-aging potential of Ghaf and *A. marina* extracts through an integrated assessment of antioxidant capacity and inhibition of key enzymes involved in extracellular matrix (ECM) remodeling.

Overall, the results clearly identify Ghaf extracts as particularly promising multifunctional anti-aging candidates. All Ghaf tissue-specific extracts exhibited consistent antioxidant activity and a robust inhibitory profile against ECM-degrading enzymes. Specifically, moderate elastase inhibition was observed at low concentrations, a more pronounced inhibition of collagenase activity was achieved at higher concentrations (with residual enzyme activity dropping below 50%), and an outstanding efficacy against hyaluronidase was recorded, with complete enzyme inhibition reached at remarkably low extract doses. When combined with the strong antioxidant activity observed in

the DPPH assay, these findings position *Ghaf* extracts as highly promising natural anti-aging actives and fully aligned with the objectives of this doctoral project. Furthermore, the enzymatic screening revealed that individual *Ghaf* extracts exhibited largely comparable and overlapping inhibition profiles, with no single plant portion consistently outperforming the others. This homogeneity suggests a widespread distribution of bioactive constituents throughout the plant and provided a strong scientific rationale for the subsequent development of a whole-plant representative Ghaf extract. This strategic choice, aimed at simplifying processing while maintaining bioactivity, supports the study presented in *Chapter 4*.

In contrast, *A. marina* extracts did not demonstrate a comparable inhibitory capacity against elastase, collagenase, or hyaluronidase. Only minor and isolated effects were observed for specific tissues (propagules and cotyledons), which were insufficient to justify further development of these extracts as primary anti-aging cosmetic ingredients. Nevertheless, several *A. marina* extracts exhibited measurable antioxidant activity, in some cases approaching that of ascorbic acid. Although this activity was moderate and required higher concentrations than Ghaf, it suggested that *A. marina* extracts may possess alternative biological potential beyond cosmetic anti-aging applications. Consequently, to fully valorize these extracts, a parallel bioprospecting-oriented study was initiated to explore their phytochemical composition and potential therapeutic relevance, with particular focus on antioxidant and in *vitro* cytotoxic properties, as will be presented in *Chapter 5*.

Beyond the biological findings, this chapter also provided an important methodological contribution. Through critical analysis and rational adaptation of existing literature protocols, optimized spectrophotometric assays for elastase, collagenase, and hyaluronidase inhibition were established. Combined with antioxidant assays, these methods form a rapid, reliable, cost-effective, and resource-efficient screening workflow for the preliminary evaluation of the anti-age properties of plant extracts. This integrated assay platform proved essential for the decision-making process within this project and represents a valuable, broadly applicable tool for future research aimed at identifying and prioritizing novel botanical ingredients for cosmetic applications.

3.4 Materials and methods

3.4.1 Chemicals and materials

2,2-Diphenyl-1-picrylhydrazyl (DPPH), (±)-6-Hydroxy-2,5,7,8-tetramethylchromane-2-carboxylic acid (Trolox), ascorbic acid, elastase from porcine pancreas (Type IV), N-Methoxysuccinyl-Ala-Ala-Pro-Val p-nitroanilide (MAAPVN), Trizma®base, oleanolic acid, N,N-Dimethylformamide (DMF) anydrous, collagenase from *Clostridium histolyticum* Sigma Blend Type H, N-[3-(2 Furyl)acryloyl]-Leu-Gly-Pro-Ala (FALGPA), tricine, calcium chloride dihydrate, sodium chloride, epigallocatechin gallate (ECGC), hyaluronidase type I-S, hyaluronic acid sodium salt from rooster comb, albumin from bovin serum (BSA), sodium phosphate monobasic, sodium phosphate dibasic, sodium acetate anhydrous and acetic acid were all purchased from Sigma-Aldrich (St. Louis, MO, USA). Ultrapure water (18 MΩ) was prepared by a Milli-Q purification system (Millipore, Bedford, MA, USA), while ethanol and methanol were purchased from CARLO ERBA Reagents s.r.l. (Milan, Italy). 96-well and 48-well plates were purchased from EuroClone (Pero, Italy).

3.4.2 Plant collection

Samples of different portions of *Prosopis cineraria*, including twigs, roots, leaves, and bark were harvested in September 2022 from multiple individuals in the UAE. Flowers and fruits were not collected, as these tissues were not available at the time of sampling. During the same period, samples from different parts of *A. marina*, including leaves, roots, propagules, and cotyledons were collected from multiple individual plants within the mangrove forest of Ajman Emirate, UAE. The cotyledons were obtained from seedlings at an early growth stage, when the propagules had already opened and developed roots. For more precise investigation, propagules were separated into the pericarp, representing the external protective tissue, and the internal tissues. Thus, in this thesis, the term pericarp (and pericarp extract) refers exclusively to the external part, while the generic term propagule (and propagule extract) refers to the internal tissues.

Each type of plants material was pooled by type and immediately freeze-dried after collection. The dried samples were homogenized using a Grindomix GM 200 knife mill (Retsch, Haan, Germany) and then sieved through a test sieve (Retsch AS 200, Haan, Germany) with a mesh size range of 300–600 µm to obtain powders with uniform particle size distribution.

3.4.3 Sample preparation and extraction

Each sample of Ghaf and *A. marina* thus obtained was subjected to exhaustive ultrasound-assisted extraction using a thermostatically controlled ultrasonic bath (ElmaSonic S 30H; Elma Schmidbauer GmbH, Singen, Germany). A 50% (v/v) aqueous ethanol solution was selected as extraction solvent due to its balanced polarity and established suitability for recovering a wide spectrum of bioactive metabolites, including phenolics (which are well known for their antioxidant properties) [29] [30], while maintaining low toxicity for subsequent biological assays [31] [32]. For the extraction, 1 g of powder sample was mixed with 40 mL of solvent (solid-to-solvent ratio 1:40, w/v) in a 50-mL polypropylene tube, which is commonly applied in metabolite profiling studies [33]. Ultrasonic extraction was performed at 25 °C for 15 min. To ensure exhaustive recovery of soluble compounds, the process was repeated several times with fresh solvent until colorless supernatants were obtained. After each cycle, samples were centrifuged at 3112 × g for 5 min using a ROTINA 380R centrifuge (Hettich Zentrifugen, Germany), and the resulting supernatants underwent filtration through Whatman No. 1 filter paper (pore size 7–12 µm). The combined filtrates obtained from each sample were then concentrated under reduced pressure at 40 °C using a Hei-VAP Core rotary evaporator (Heidolph, Germany) to remove ethanol. The aqueous residues were reconstituted in Milli-Q water and subjected to a second clarification step by centrifugation at 2375 × g for 10 min to isolate the water-soluble fractions. The resulting extracts were subsequently lyophilized using an Alpha 1-4 LSCplus freeze dryer (Christ, Germany) to obtain dry extracts. The extraction yields were determined by calculating the ratio of the weight of dried extract obtained to the initial weight of dried plant material powder and expressed as a percentage.

3.4.4 DPPH Radical Scavenging activity

The antioxidant capacity (AOC) of the Ghaf and *A. marina* extracts were quantified using the 1,1-diphenyl-2-picrylhydrazyl (DPPH•) radical scavenging assay. The extracts were dissolved in ultrapure water and tested over a concentration range of 0 –10 µg/mL for Ghaf extracts and of 0 -180 µg/mL for *A. marina* extracts, while Trolox (0–75 µM) was used as calibration standard starting from a 5 mM stock solution in methanol, subsequently diluted to generate working standards. Ascorbic acid solution in ultrapure water was included as a positive control. A fresh 150 µM DPPH• solution was prepared in ethanol immediately before each experiment and protected from light due to the

reagent's photosensitivity. All reactions were carried out in 96-well plates. For each measurement, 10 µL of sample, Trolox standard, or ultrapure water (blank) were added to 190 µL of the operative DPPH solution, reaching a final reaction volume of 200 µL. Plates were then incubated for 30 min at room temperature, under gentle orbital shaking (70 rpm) and protected from light. After incubation, absorbance was recorded at 517 nm using EnSight Multimode Microplate Reader (PerkinElmer, Waltham, MA,USA).

DPPH scavenging activity (%) was calculated after blank correction using the following equation (5):

$$DPPH\ scavengig\ activity\ \% = \left(1 - \frac{A_{sample}}{A_0}\right) * 100 \qquad (5)$$

where A_0 corresponds to the absorbance of the zero-Trolox standard (0 µM), and A_{sample} corresponds to the absorbance of the tested sample or Trolox concentration. The antioxidant activity of each extract was then converted into Trolox Equivalent Antioxidant Capacity (TEAC), by interpolating the scavenging activity of samples on the Trolox standard curve according to the following equation (6):

$$TEAC\ (\mu M\ TX) = \frac{(DPPH\ scavenging\ activity\ \%_{sample} - intercept)}{slope} \qquad (6)$$

where slope and intercept correspond to the linear regression parameter of the Trolox calibration curve. To normalize the antioxidant activity to the amount of tested material, TEAC values were further expressed as µmol Trolox equivalents per gram of extract (TE/g), by dividing the interpolated TEAC values by the corresponding extract concentration tested (g/L). This normalization allows direct comparison of antioxidant capacity independently of the tested concentration.

3.4.5 *In vitro* enzymatic inhibition assays

3.4.5.1 Elastase inhibition assay

The inhibitory activity of the Ghaf and *A.marina* extracts against elastase was evaluated using a spectrophotometric assay adapted and optimized from literature protocols. Elastase is a serine protease involved in the degradation of elastin, a key component of the ECM. The method is based

on the ability of pancreatic porcine elastase to hydrolyze the synthetic chromogenic substrate N-Methoxysuccinyl-Ala-Ala-Pro-Val p-nitroanilide (MAAPVN), resulting in the release of *p*-nitroaniline (pNA), which can be quantified by measuring absorbance at 410 nm.

Preliminary experiments were conducted to optimize the assay conditions by testing different combinations of substrate and enzyme concentrations. Specifically, MAAPVN was evaluated at working concentrations of 3.5 mg/mL and 1.328 mg/mL, while elastase was tested at 0.5 U/mL and 0.375 U/mL. Enzymatic reactions were monitored kinetically over 15 min to identify conditions that ensured a linear reaction rate and adequate sensitivity. Based on these optimization studies, MAAPVN at 1.328 mg/mL and elastase at 0.375 U/mL were selected as the optimal working concentrations and subsequently used for the inhibition assays.

For the final protocol, a stock solution of MAAPVN (25 mg/mL) was prepared in dimethylformamide (DMF) and diluted with Tris–HCl buffer (50 mM, pH 8.0) to obtain the working substrate solution (1.328 mg/mL). Porcine pancreatic elastase was prepared at a concentration of 0.375 U/mL in the same buffer. The assays were carried out in 96-well microplates by mixing 10 µL of Ghaf or *A. marina* extracts aqueous solution with 20 µL of the enzyme solution and 120 µL of Tris–HCl buffer, resulting in final extract concentrations ranging from 50 to 270 µg/mL. The mixtures were pre-incubated for 15 min at room temperature to allow interaction between the enzyme and the tested extracts. The reaction was initiated by adding 50 µL of the working substrate solution and allowed to proceed for 15 min, after which the absorbance was measured at 410 nm using a microplate reader. Oleanolic acid (OA) was included as positive control under the same experimental conditions.

Elastase activity was expressed as a percentage relative to the control (enzyme without inhibitor) and calculated according to the following equation (7):

$$Elastase\ activity\ \% = \left(\frac{B}{A}\right) * 100 \qquad (7)$$

where *B* represents the absorbance in the presence of the inhibitor and *A* corresponds to the control absorbance.

3.4.5.2 Collagenase inhibition assay

The inhibitory activity of the Ghaf and *A.marina* extracts against collagenase was assessed using a microplate-based assay adapted and optimized from literature protocols. The assay quantifies the ability of an extract to inhibit *Clostridium histolyticum* collagenase (ChC), which catalyzes the cleavage of the synthetic peptide N-[3-(2-furyl)acryloyl]-Leu-Gly-Pro-Ala (FALGPA). Hydrolysis of FALGPA results in a decrease in absorbance at 335 nm, enabling spectrophotometric monitoring of residual non-cleaved substrate. Preliminary optimization experiments were carried out to identify suitable enzyme and substrate concentrations ensuring a measurable and linear reaction rate. Different combinations of collagenase (0.1 and 1 U/mL) and FALGPA (1 and 2 mM) solutions were tested by monitoring the decrease in absorbance at 335 nm over a 20 min kinetic assay. Based on these experiments, collagenase at 1 U/mL and FALGPA at 2 mM were selected as the optimal working concentrations and used for subsequent inhibition assays. For the final protocol, assays were performed in 96-well microplates. Briefly, 30 µL of Ghaf or *A. marina* extract aqueous solutions were mixed with 20 µL of FALGPA working solution (2 mM), previously diluted in methanol from a 4.1971 mM stock solution, and 60 µL of assay buffer (50 mM tricine, 10 mM $CaCl_2$, 400 mM NaCl, pH 7.5), yielding final extract concentrations ranging from 50 to 270 µg/mL. The plate was immediately placed in a microplate reader pre-equilibrated at 37 °C, and the absorbance at 335 nm was recorded to determine the initial value corresponding to the substrate-only condition (0% activity). The enzymatic reaction was then initiated by adding 10 µL of collagenase solution (1 U/mL in cold water, freshly prepared immediately before use) to each well. After incubation for 20 min at 37 °C, the absorbance at 335 nm was measured again. Epigallocatechin gallate (EGCG) was used as a positive control inhibitor under the same experimental conditions.

Enzymatic activity (%) was calculated by comparing the decrease in absorbance in extract-treated wells with that observed in enzyme-only control wells according to the following equation (8):

$$\text{Collagenase activity (\%)} = \frac{(\text{Abs}_{\text{pre}} - \text{Abs}_{\text{post}})_{\text{treated}}}{(\text{Abs}_{\text{pre}} - \text{Abs}_{\text{post}})_{\text{untreated}}} \times 100 \quad (8)$$

where Abs_{pre} is the absorbance recorded in the presence of substrate before enzyme addition (substrate-only condition), and Abs_{post} is the absorbance recorded after enzyme addition at the end

of the reaction time. Treated and untreated refer to reactions carried out in the presence or absence of the tested sample, respectively.

3.4.5.3 Hyaluronidase inhibition assay

The inhibitory effect of the Ghaf and *A.marina* extracts on hyaluronidase activity was evaluated using a turbidimetric assay adapted and optimized from literature methods. Hyaluronidase catalyzes the hydrolytic degradation of hyaluronic acid (HA), a key glycosaminoglycan responsible for maintaining skin hydration, viscoelasticity, and structural integrity. In this assay, the remaining non-degraded HA reacts with an acidic bovine serum albumin (BSA) solution to form an insoluble precipitate whose turbidity is proportional to the amount of intact HA and can be quantified at 600 nm. Prior to testing the extracts, a calibration curve was generated to confirm the linear relationship between HA concentration and turbidity by analyzing HA solutions ranging from 0 to 0.03% (w/v). Subsequently, the extracts were tested as following: 5 µL of Ghaf or *A. marina* extract aqueous solutions were added to the wells of a 48-well microplate and mixed with 100 µL of hyaluronidase type I-S solution (15 U/mL) prepared in 20 mM sodium phosphate buffer containing 77 mM NaCl and 0.01% BSA (pH 7.0), yielding final Ghaf extracts concentrations ranging from 3.7 to 66 µg/mL and *A. marina* extracts from 33 to 132 µg/mL. After a 10 min pre-incubation at 37 °C to allow interaction between the enzyme and the extracts, 100 µL of HA substrate solution (0.03% w/v dissolved in 300 mM sodium phosphate buffer, pH 5.35) were added to each well, followed by incubation for 45 min at 37 °C. The enzymatic reaction was terminated by adding 1 mL of acidic albumin reagent (0.1% BSA, 24 mM sodium acetate, 79 mM acetic acid, pH 3.75). After a further 10 min incubation at room temperature, turbidity was measured at 600 nm using a microplate reader. Higher absorbance values correspond to higher amounts of intact HA and therefore greater inhibition of hyaluronidase activity. Oleanolic acid was used as a positive control inhibitor under the same experimental conditions.

Hyaluronidase activity (%) was calculated according to the following optimized equation (9):

$$\text{Hyaluronidase activity (\%)} = 1 - \left(\frac{A_{\text{sample}} - A_{\text{enzyme control}}}{A_{\text{substrate control}} - A_{\text{enzyme control}}}\right) \times 100 \qquad (9)$$

where A_{sample} is the absorbance measured in the presence of enzyme, substrate, and tested extract; $A_{\text{enzyme control}}$ is the absorbance of HA incubated with hyaluronidase in the absence of inhibitors (100% activity); and $A_{\text{substrate control}}$ is the absorbance of HA alone without enzyme (0% activity).

3.5 References

[1] M. Tourabi *et al.*, "Efficacy of various extracting solvents on phytochemical composition, and biological properties of Mentha longifolia L. leaf extracts," *Sci. Rep.*, vol. 13, no. 1, p. 18028, Oct. 2023, doi: 10.1038/s41598-023-45030-5.

[2] S. Sun *et al.*, "Impact of extraction techniques on phytochemical composition and bioactivity of natural product mixtures," *Front. Pharmacol.*, vol. 16, Jul. 2025, doi: 10.3389/fphar.2025.1615338.

[3] R. Zhang, L. Dan, L. Su, and X. Wei, "Tissue-specific partitioning of flavonoids and phenolic acids coordinates bioactivities in Ormosia henryi Prain," *BMC Plant Biol.*, vol. 25, no. 1, p. 1309, Oct. 2025, doi: 10.1186/s12870-025-07390-0.

[4] A. Nisca and C. Tanase, "Approaches to Extracting Bioactive Compounds from Bark of Various Plants: A Brief Review," *Plants*, vol. 14, no. 18, p. 2929, Sep. 2025, doi: 10.3390/plants14182929.

[5] D. T. Ayele, M. L. Akele, and A. T. Melese, "Analysis of total phenolic contents, flavonoids, antioxidant and antibacterial activities of Croton macrostachyus root extracts," *BMC Chem.*, vol. 16, no. 1, p. 30, Dec. 2022, doi: 10.1186/s13065-022-00822-0.

[6] M. Tourabi *et al.*, "Efficacy of various extracting solvents on phytochemical composition, and biological properties of Mentha longifolia L. leaf extracts," *Sci. Rep.*, vol. 13, no. 1, p. 18028, Oct. 2023, doi: 10.1038/s41598-023-45030-5.

[7] Z. Z. Yan, L. Ke, and N. F. Y. Tam, "Lead stress in seedlings of Avicennia marina, a common mangrove species in South China, with and without cotyledons," *Aquat. Bot.*, vol. 92, no. 2, pp. 112–118, Feb. 2010, doi: 10.1016/j.aquabot.2009.10.014.

[8] N. Nadzrin, N. W. Mazlan, M. N. I. Kassim, R. Lakshminarayanan, and S. Vigneswari, "Phytochemicals from mangrove species: prospective saviour in battle against cancer?," *Nat. Prod. Res.*, pp. 1–25, Jan. 2026, doi: 10.1080/14786419.2026.2615745.

[9] S. Sudhir, A. Arunprasath, and V. Sankara Vel, "A critical review on adaptations, and biological activities of the mangroves," *Journal of Natural Pesticide Research*, vol. 1, p. 100006, Jun. 2022, doi: 10.1016/j.napere.2022.100006.

[10] D. Mehta, S. Gamit, D. Dudhagara, V. Parmar, A. Patel, and S. Vyas, "Carbohydrate accumulation patterns in mangrove and halophytic plant species under seasonal variation," *Sci. Rep.*, vol. 14, no. 1, p. 21512, Sep. 2024, doi: 10.1038/s41598-024-72627-1.

[11] R. Dhillon, B. Agarwal, and N. Rajput, "Experiential marketing strategies used by luxury cosmetics companies," *Innovative Marketing*, vol. 18, no. 1, pp. 49–62, Feb. 2022, doi: 10.21511/im.18(1).2022.05.

[12] V. Francois-Newton *et al.*, "Antioxidant and Anti-Aging Potential of Indian Sandalwood Oil against Environmental Stressors In Vitro and Ex Vivo," *Cosmetics*, vol. 8, no. 2, p. 53, Jun. 2021, doi: 10.3390/cosmetics8020053.

[13] S. Burda and W. Oleszek, "Antioxidant and Antiradical Activities of Flavonoids," *J. Agric. Food Chem.*, vol. 49, no. 6, pp. 2774–2779, Jun. 2001, doi: 10.1021/jf001413m.

[14] V. Pandey, S. Patel, P. Danai, G. Yadav, and A. Kumar, "Phyto-constituents profiling of Prosopis cineraria and in vitro assessment of antioxidant and anti-ulcerogenicity activities," *Phytomedicine Plus*, vol. 3, no. 3, p. 100452, Aug. 2023, doi: 10.1016/j.phyplu.2023.100452.

[15] J. SHARIFI-RAD *et al.*, "Bioactive compounds from Prosopis species as potential oxidative stress and inflammation modulators: an update on mechanisms," *Minerva Biotechnology and Biomolecular Research*, vol. 35, no. 2, Jun. 2023, doi: 10.23736/S2724-542X.23.02977-2.

[16] Z. D. Stevanović, M. S. Stanković, J. Stanković, P. Janaćković, and M. Stanković, "Use of halophytes as medicinal plants: phytochemical diversity and biological activity.," in *Halophytes and climate change: adaptive mechanisms and potential uses*, UK: CABI, 2019, pp. 343–358. doi: 10.1079/9781786394330.0343.

[17] F. Ahmed, A.-B. El-Saied, R. Salah El Din, and Z. El swaify, "Phytochemical Screening and Anticancer Activities of Some Terrestrial and Aquatic Plants Growing in Saline Habitats.," *Al-Azhar Journal of Agricultural Research*, vol. 0, no. 0, pp. 0–0, Jan. 2024, doi: 10.21608/ajar.2024.220188.1184.

[18] T. Van der Stocken *et al.*, "A general framework for propagule dispersal in mangroves," *Biological Reviews*, vol. 94, no. 4, pp. 1547–1575, Aug. 2019, doi: 10.1111/brv.12514.

[19] P. S. T. Lakshme, A. Roy, P. Sivaperumal, and T. Lakshmi, "Exploration of Antioxidant Effects of Crude Extract of Mangrove Plant - Avicennia marina," *J. Pharm. Res. Int.*, pp. 321–329, Dec. 2021, doi: 10.9734/jpri/2021/v33i62B35586.

[20] S. Davinelli, J. C. Bertoglio, A. Polimeni, and G. Scapagnini, "Cytoprotective Polyphenols Against Chronological Skin Aging and Cutaneous Photodamage," *Curr. Pharm. Des.*, vol. 24, no. 2, pp. 99–105, Apr. 2018, doi: 10.2174/1381612823666171109102426.

[21] N. Azmi, P. Hashim, D. M. Hashim, N. Halimoon, and N. M. N. Majid, "Anti–elastase, anti–tyrosinase and matrix metalloproteinase–1 inhibitory activity of earthworm extracts as potential new anti–aging agent," *Asian Pac. J. Trop. Biomed.*, vol. 4, pp. S348–S352, May 2014, doi: 10.12980/APJTB.4.2014C1166.

[22] J. H. Kim, J. Chul Byun, A. Kumar, R. Bandi, C.-G. Hyun, and N. H. Lee, "Compounds with elastase inhibition and free radical scavenging activities from Callistemon lanceolatus," 2009. [Online]. Available: http://www.academicjournals.org/jmpr

[23] J. Wittenauer, S. Mäckle, D. Sußmann, U. Schweiggert-Weisz, and R. Carle, "Inhibitory effects of polyphenols from grape pomace extract on collagenase and elastase activity," *Fitoterapia*, vol. 101, pp. 179–187, Mar. 2015, doi: 10.1016/j.fitote.2015.01.005.

[24] S. Drouet *et al.*, "A Green Ultrasound-Assisted Extraction Optimization of the Natural Antioxidant and Anti-Aging Flavonolignans from Milk Thistle Silybum marianum (L.) Gaertn. Fruits for Cosmetic Applications," *Antioxidants*, vol. 8, no. 8, p. 304, Aug. 2019, doi: 10.3390/antiox8080304.

[25] C. Liu *et al.*, "Inhibitory effects of skin permeable glucitol-core containing gallotannins from red maple leaves on elastase and their protective effects on human keratinocytes," *J. Funct. Foods*, vol. 75, p. 104208, Dec. 2020, doi: 10.1016/j.jff.2020.104208.

[26] S. Pientaweeratch, V. Panapisal, and A. Tansirikongkol, "Antioxidant, anti-collagenase and anti-elastase activities of *Phyllanthus emblica* , *Manilkara zapota* and silymarin: an *in vitro* comparative study for anti-aging applications," *Pharm. Biol.*, vol. 54, no. 9, pp. 1865–1872, Sep. 2016, doi: 10.3109/13880209.2015.1133658.

[27] C. Jiratchayamaethasakul *et al.*, "In vitro screening of elastase, collagenase, hyaluronidase, and tyrosinase inhibitory and antioxidant activities of 22 halophyte plant extracts for novel cosmeceuticals," *Fish. Aquatic Sci.*, vol. 23, no. 1, p. 6, Dec. 2020, doi: 10.1186/s41240-020-00149-8.

[28] P. Tu and S. Tawata, "Anti-Oxidant, Anti-Aging, and Anti-Melanogenic Properties of the Essential Oils from Two Varieties of Alpinia zerumbet," *Molecules*, vol. 20, no. 9, pp. 16723–16740, Sep. 2015, doi: 10.3390/molecules200916723.

[29] B. P. Pandey, S. Prakash Pradhan, P. Joshi, and K. Adhikari, "Antioxidant and Enzymes Inhibitory Activities of Leaf Extracts of Plant Species Traditionally Used for Medicinal and Spiritual Purposes in Nepal," *J. Herbs Spices Med. Plants*, vol. 28, no. 3, pp. 265–280, Jul. 2022, doi: 10.1080/10496475.2022.2053026.

[30] A. Angelis, P. Mavros, P. E. Nikolaou, S. Mitakou, M. Halabalaki, and L. Skaltsounis, "Phytochemical analysis of olive flowers' hydroalcoholic extract and in vitro evaluation of tyrosinase, elastase and collagenase inhibition activity," *Fitoterapia*, vol. 143, p. 104602, Jun. 2020, doi: 10.1016/j.fitote.2020.104602.

[31] J. Chompoo, A. Upadhyay, M. Fukuta, and S. Tawata, "Effect of Alpinia zerumbet components on antioxidant and skin diseases-related enzymes," *BMC Complement. Altern. Med.*, vol. 12, no. 1, p. 106, Dec. 2012, doi: 10.1186/1472-6882-12-106.

[32] N. Maity, N. Nema, B. Sarkar, and P. Mukherjee, "Standardized Clitoria ternatea leaf extract as hyaluronidase, elastase and matrix-metalloproteinase-1 inhibitor," *Indian J. Pharmacol.*, vol. 44, no. 5, p. 584, 2012, doi: 10.4103/0253-7613.100381.

[33] Y.-J. Kim, H. Uyama, and S. Kobayashi, "Inhibition effects of (+)-catechin–aldehyde polycondensates on proteinases causing proteolytic degradation of extracellular matrix," *Biochem. Biophys. Res. Commun.*, vol. 320, no. 1, pp. 256–261, Jul. 2004, doi: 10.1016/j.bbrc.2004.05.163.

[34] P. Tu and S. Tawata, "Anti-Oxidant, Anti-Aging, and Anti-Melanogenic Properties of the Essential Oils from Two Varieties of Alpinia zerumbet," *Molecules*, vol. 20, no. 9, pp. 16723–16740, Sep. 2015, doi: 10.3390/molecules200916723.

[35] L. Cui *et al.*, "Anti-skin Aging Potential of Sargassum thunbergii Ethanolic Extract: Antioxidant, Anti-inflammatory, and Antiwrinkle Effects on L929 Fibroblast Cells," *J. Food Process. Preserv.*, vol. 2023, pp. 1–16, Sep. 2023, doi: 10.1155/2023/2230456.

[36] W. Widowati *et al.*, "Antioxidant and Anti Aging Assays of <I>Oryza sativa</I> Extracts, Vanillin and Coumaric Acid," *Journal of Natural Remedies*, vol. 16, no. 3, p. 88, Nov. 2016, doi: 10.18311/jnr/2016/7220.

[37] H. E. Van Wart and D. R. Steinbrink, "A continuous spectrophotometric assay for Clostridium histolyticum collagenase," *Anal. Biochem.*, vol. 113, no. 2, pp. 356–365, May 1981, doi: 10.1016/0003-2697(81)90089-0.

[38] K. K. Yang and N. Bennett, "The History of Collagenase Clostridium Histolyticum," *Sex. Med. Rev.*, vol. 3, no. 4, pp. 289–297, Oct. 2015, doi: 10.1002/smrj.54.

[39] E. H. Kass and C. V. Seastone, "THE RÔLE OF THE MUCOID POLYSACCHARIDE (HYALURONIC ACID) IN THE VIRULENCE OF GROUP A HEMOLYTIC STREPTOCOCCI," *Journal of Experimental Medicine*, vol. 79, no. 3, pp. 319–330, Mar. 1944, doi: 10.1084/jem.79.3.319.

[40] K. Madan and S. Nanda, "In-vitro evaluation of antioxidant, anti-elastase, anti-collagenase, anti-hyaluronidase activities of safranal and determination of its sun protection factor in skin photoaging," *Bioorg. Chem.*, vol. 77, pp. 159–167, Apr. 2018, doi: 10.1016/j.bioorg.2017.12.030.

[41] L. Liana *et al.*, "Antioxidant and Anti-Hyaluronidase Activities of Dragon Fruit Peel Extract and Kaempferol-3-O-Rutinoside," *Jurnal Kedokteran Brawijaya*, vol. 30, no. 4, pp. 247–252, Aug. 2019, doi: 10.21776/ub.jkb.2019.030.04.3.

[42] W. Widowati *et al.*, "Antioxidant and antiaging activities of Jasminum Sambac extract, and its compounds," *Journal of Reports in Pharmaceutical Sciences*, vol. 7, no. 3, p. 270, 2018, doi: 10.4103/2322-1232.254804.

4 Study on Ghaf extract as anti-age active ingredient and its inclusion in cosmetic emulsions

4.1 Abstract

The ecological transition of the cosmetics industry is driving the development of sustainable formulations, from ingredient selection to the final product. In this context, the identification of plant-based anti-aging active ingredients combined with the design of minimal but efficient delivery systems represents an actual challenge[1]. Building on the promising bioactivities previously observed, this chapter aimed to investigate Ghaf extract as a multifunctional anti-aging active and to develop a sustainable cosmetic formulation suitable for its incorporation, thereby bridging the gap between bioactivity screening and practical cosmetic application.

A representative whole-plant Ghaf extract was prepared and comprehensively characterized to evaluate potential synergistic effects while optimizing the overall process. Chemical profiling by UHPLC–DAD–HRMS/MS revealed a polyphenol-rich composition dominated by catechins and flavonoid derivatives. The extract confirmed exceptionally high radical scavenging activity in the DPPH assay, strongly correlated with its elevated total phenolic content. Beyond antioxidant properties, Ghaf extract exhibited biologically relevant inhibitory activity against elastase, hyaluronidase, tyrosinase, and collagenase, key enzymes involved in extracellular matrix degradation and skin pigmentation[2].

In parallel, a formulative study was conducted to develop a sustainable oil-in-water Pickering emulsion. Several natural powders were screened as potential Pickering stabilizers, and a Design of Experiments (DoE) approach enabled the identification of a stable and cosmetically appealing base emulsion with a minimal INCI list, produced without heating and prioritizing natural ingredients. The incorporation of Ghaf extract did not induce significant changes in physical stability, pH, rheological behavior, or microstructural integrity of the formulation.

Overall, these results position Ghaf as a multifunctional natural ingredient for dermocosmetic applications and demonstrate the value of an integrated approach combining bioactivity assessment with formulation development. Further studies using cellular and *ex vivo* models are required to confirm efficacy, safety, and long-term formulation compatibility.

4.2 Results and Discussion

4.2.1 Plant extraction

Given the lack of significant activity differences among the individual Ghaf extracts observed in *Chapter 3* and considering sustainability and time efficiency, a decision was made to develop a composite extract representative of the whole Ghaf plant. To this end, dried powders of each plant portion were homogenized and combined based on their relative abundance in the sampled biomass, creating a unified plant matrix and the representative matrix thus obtained was then subjected to hydro-alcoholic extraction. The aggregated Ghaf extract yielded an average extraction efficiency of 25% w/w ± 0.8, with high reproducibility observed across seven independent replicates. A violin plot (**Figure 4.1**) displays a narrow, symmetric distribution of extraction yields, indicative of excellent process robustness and consistent phytochemical recovery.

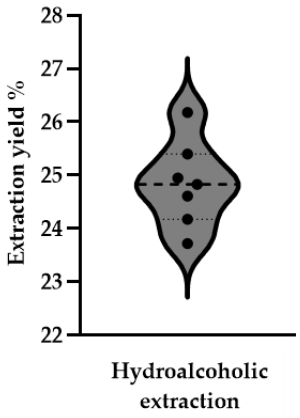

Figure 4.1. Violin plot showing the percentage yields of seven independent hydroalcoholic extractions of the combined Ghaf matrix. The plot depicts the distribution and variability of extraction yields with n=7.

Furthermore, this extraction yield obtained for the Ghaf extract closely corresponds to the average yield expected from the individual plant portions when considered collectively. In particular, the yield of the composite extract falls within the range defined by the lower-yielding roots fraction (11.23%) and the higher-yielding bark fraction (44%), and approximates the mean contribution of twigs (29.48%) and leaves (22.11%). This outcome is consistent with the preparation strategy adopted, in which the different plant tissues were combined according to their relative abundance in the starting biomass. As a result, the overall extraction efficiency reflects the intrinsic extractability of each tissue rather than being dominated by a single high-yield component. This confirms that the

hydroalcoholic extraction process behaves in an additive and predictable manner when applied to a heterogeneous plant matrix. From a methodological perspective, this finding further supports the robustness of the extraction approach, indicating that no preferential or biased extraction occurred upon matrix aggregation. From a practical point of view, this approach not only aligns with green extraction principles but also streamlines workflow by reducing redundancy in extraction steps without compromising extract quality, facilitating scalable formulation development.

4.2.2 Ghaf extract characterization

This characterization was kindly performed in collaboration with the FoodNutraLab Research Group of the University of Milano-Bicocca

Accordingly, phytochemical characterization was deliberately performed at this stage of the study, after the identification of the extract of greatest interest, rather than at an earlier exploratory phase. This strategy allowed analytical efforts to be focused on a biologically validated extract, ensuring that the chemical profiling would be directly relevant to the observed anti-aging activities and to the subsequent stages of the project.

The Ghaf extract thus obtained was subjected to phytochemical profiling using ultra-high performance liquid chromatography coupled with diode array detection and high-resolution tandem mass spectrometry (UHPLC–DAD–HRMS/MS), in order to comprehensively characterize its metabolite composition and to gain insights into the chemical constituents potentially responsible for the observed biological effects.

The chromatographic profile of the extract is reported in **Figure 4.2** and the compounds tentatively identified are shown in **Table 4.1**, with their corresponding identification level (IL), which reflects the confidence of compound annotation based on MSI guidelines (see *Section 4.4.4*). For compounds assigned to IL2, the identification relied on comparisons of MS/MS fragmentation data with published spectra from the literature or spectral databases included directly in the table.

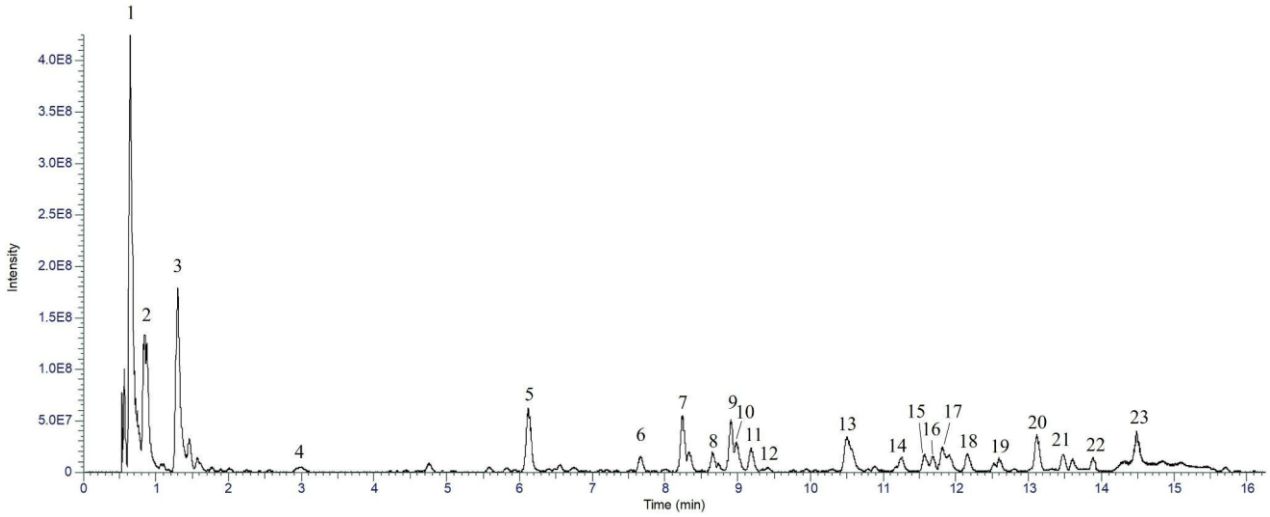

Figure 4.2. Representative chromatogram of the Ghaf extract.

Table 4.1. HPLC-HRMS data of compounds detected in Ghaf extract.

N°	RT (min)	$[M-H]^-$	Formula	Error (ppm)	Diagnostic products ion (m/z)	Name	Class	IL	Ref.
1	0.56	209.0305	$C_6H_{10}O_8$	1.40	115.0039, 89.0246, 85.0297, 71.0140	Galactaric acid[b]	Dicarboxylic Acid	4	[3]
2	0.85	191.0216	$C_6H_8O_7$	2.24	111.0089, 87.0089, 85.0296,	Citric acid	Tricarboxylic acids	2	[4]
3	1.33	169.0145	$C_7H_6O_5$	1.47	125.0247, 97.0297, 81.0343, 79.0192, 69.0347	Gallic acid	Phenolic acids and derivatives	1	std*
4	2.82	305.0650	$C_{15}H_{14}O_7$	-3.6	179.0334, 167.0376, 139.0372, 137.0254,125.0244, 109.0281	(Epi)gallocatechin	Catechins	2	[5]
5	6.12	451.2191	-	-	405.2136, 389.1100, 287.0162, 179.0567, 161.0463	Unknown	-	4	-
6	7.67	325.0936	$C_{15}H_{18}O_8$	2.49	163.0405, 119.0505	Cumaric acid O-glucoside	Hydroxycinnamic acid derivative	2	[6]
7	8.33	289.0724	$C_{15}H_{14}O_6$	2.16	245.0825, 221.0826, 205.0511, 203.0719, 161.0611, 151.0389, 125.0245, 123.0454, 109.0297, 97.0296	(Epi)catechin	Catechins	1	std*
8	8.72	457.0773	$C_{22}H_{18}O_{11}$	0.44	305.0654, 169.0128, 125.0230	(Epi)gallocatechin gallate	Catechins	2	[7]

9	8.90	431.1928[a]	$C_{19}H_{30}O_8$	1.92	385.1875, 223.1343, 205.1241, 153,0926	Drovomifoliol-O-glucoside (roseoside)	Sesquiterpenoid glycoside	2	[6]
10	9.01	197.0459	$C_9H_{10}O_5$	2.70	169.0148, 125.0247, 124.0169	Ethyl gallate	Ellagitannins	2	[8]
11	9.21	557.2253	$C_{26}H_{38}O_{13}$	3.23	-	Unknown	-	4	-
12	9.41	163.0405	$C_9H_8O_3$	3.18	119.0505	p-cumaric acid	Hydroxycinnamic acids	2	[9]
13	10.50	479.0841	$C_{21}H_{20}O_{13}$	1.38	316.0230, 271.0252	myricetin 3-O-beta-D-galactopyranoside	Flavonoid-glycosides	2	[10]
14	11.26	463.0891	$C_{21}H_{20}O_{12}$	1.71	316.0232, 271.0256, 179.0565	Myricitrin	Flavonoid-glycosides	2	[11]
15	11.65	577.1574	$C_{27}H_{30}O_{14}$	2.77	457.1149, 413.0885, 293.0463	2″-O-rhamnosylvitexin	Flavonoid-glycosides	2	[7]
16	11.68	609.1479	$C_{27}H_{30}O_{16}$	2.72	300.0282	Rutin	Flavonoid-glycosides	1	std*
17	11.80	463.0889	$C_{21}H_{20}O_{12}$	1.65	301.0335, 300.0256	Quercetin-3-*O*-galactoside (hyperoside)	Flavonoid-glycosides	2	[10]
18	12.15	493.0998	$C_{22}H_{22}O_{13}$	2.15	330.0389, 315.0155	Patuletin-7-O-glucoside	Flavonoid-glycosides	2	[10]
19	12.53	567.2099	$C_{27}H_{36}O_{13}$	3.52	457.1146, 383,0775, 353,0668, 341,0668, 293,0461	Dimethoxylflavanone derivate	Flavonoid derivates	3	[12]
20	13.31	415.1979	-	-	255.4785, 240.5105, 137.0976	Unknown	-	4	-
21	13.61	547.1471	$C_{26}H_{28}O_{13}$	2.64	383.0777	Unknown	-	4	-
22	13.97	577.1577	$C_{27}H_{30}O_{14}$	-	559.1448, 457.1127, 395.0760, 293.0451, 269.0450	Apigenin-di-C-glucoside isomer	Flavonoid-glycosides	2	[13] [14]
23	14.51	577.1578	$C_{27}H_{30}O_{14}$	-	559.1445, 457.1126, 395.0762, 293.0457, 269.0444	Apigenin-di-C-glucoside isomer	Flavonoid-glycosides	2	[13] [14]

*std: standard compound, a [M + HCOOH − H]− , b Annotations based on accurate mass and molecular formula only (no MS/MS) MSI level 4.

The analysis revealed that the Ghaf extract contains 23 compounds, which mainly belong to the phenolic compound class. Flavonoids are a heterogeneous group of polyphenols with high antioxidant activity that are widely distributed in the plant kingdom and are the most representative of the phenols compounds in the Ghaf extract. In plants, flavonoids can be either aglycones or glycosides containing hexose, deoxyhexose or pentose sugar moieties. Flavonoid glycosides can be classified as O-glycosides or C-glycosides according to their sugar linkage[15]. These can be clearly distinguished by their characteristic MS/MS fragmentation behaviour in negative ion mode. C-glycosides typically exhibit neutral losses of 30, 90 and 120 Da for hexose sugars, 74 and 104 Da for deoxyhexose sugars and 60 Da for pentose sugars. Based on this diagnostic fragmentation pattern, compound 15 was tentatively identified as a C-glycoside. Specifically, the deprotonated molecular ion $[M–H]^-$ at m/z 577.1574, which corresponds to the molecular formula $C_{27}H_{30}O_{14}$, was assigned to 2′-O-rhamnosylvitexin. The fragment ion at m/z 457.1146 resulted from the characteristic neutral loss of 120 Da, confirming the presence of a C-linked hexose moiety. Following this fragmentation pattern the compounds 22, 23 were identified as C-glycosides. In contrast, O-glycosides exhibit neutral losses of 162 Da (hexose sugars), 176 Da (glucuronic acid), 146 Da (deoxyhexose sugars) and 132 Da (pentose sugar). Based on this information, the compound 17 with m/z 463.0889 and molecular formula $C_{21}H_{20}O_{12}$ was tentatively identified as quercetin-3-O-galactoside as indicated by the fragment ion at m/z 301.0335 corresponded to the loss of hexose sugar (162 Da) with O-linked. Following this fragmentation pattern the compounds 13, 14, 16 and 18 were identified as O-glycosides.

A group of flavonoids is represented by flavan-3-ols, to which catechins belong. Peak 4, with an m/z of 305.0650 ($C_{15}H_{14}O_7$) [M-H-], was identified as epigallocatechin, based on its fragmentation pattern[16]. The main ions produced during fragmentation were 179.0329 ([M-H-C6H6O3]-), 167.0331 ([M-H-C7H6O3]-), and 125.0230. The latter corresponds to ring A of the flavonoid. Meanwhile, peak 8 (m/z 457.0773 ($C_{27}H_{18}O_{11}$)) [M-H-], was identified as epigallocatechin gallate, exhibiting characteristic fragments at m/z 305.0654 and 169.0128 corresponding to epigallocatechin and gallic acid, respectively.

Flavonoids and phenolic acids are known for their antioxidant activity and their ability to modulate enzymes involved in the degradation of the extracellular matrix, such as metalloproteinases

(MMPs). Among the compounds present in the extract, gallic acid shows a marked inhibition of collagenase, due to the number and arrangement of hydroxyl groups on the benzene ring, which facilitate interaction with the catalytic site and chelation of the Zn^{2+} ion[17], [18]. Similarly, flavan-3-ols such as catechin, epicatechin, and epicatechin gallate inhibit collagenase and elastase, with the galloyl group enhancing their activity. Glycosidic flavonoids, such as quercetin glycosides, also modulate these proteases; although aglycones are generally more active, glycosylation improves solubility and stability[18]. Furthermore, this class of molecules is also known for its important anti-inflammatory and immunostimulatory activity, contributing to a protective and beneficial effect[19]. Overall, the composition of the hydroalcoholic extract of Ghaf suggests the presence of bioactive molecules with anti-aging potential, justifying its selection for further functional studies.

4.2.3 Evaluation of antioxidant capacity of Ghaf extract

4.2.3.1 DPPH Radical Scavenging Activity

The antioxidant activity of the newly prepared Ghaf extract was first assessed using the DPPH radical scavenging assay, expanding the range of tested concentrations in order to better characterize the dose–response relationship and to directly compare the results with those previously obtained for extracts derived from individual plant tissues. As shown in **Figure 4.3. (a),** a clear concentration-dependent scavenging trend was maintained also for the whole-plant extract, with DPPH scavenging activity values reaching approximately 60% at the highest newly tested concentration, exceeding the 30–40% scavenging activity previously observed and confirmed at the former maximum tested concentration (10 µg/mL). This behavior suggests a relatively homogeneous distribution of redox-active compounds across the different tissues of the Ghaf plant and is consistent with the high abundance of phenolic compounds, flavonoids, and other electron- or hydrogen-donating metabolites identified during the phytochemical characterization of the extract, which are known to efficiently neutralize free radicals[20].

To further quantify and standardize the observed antioxidant activity, the results were expressed as micromoles of Trolox equivalents per gram of extract (µmol TE/g) and compared with the previously obtained values. As reported in **Figure 4.3 (b),** Ghaf extract exhibited a remarkably high DPPH scavenging capacity, with a mean value of 3092.48 ± 233 µmol TE/g, corresponding to an activity almost fourfold higher than that of the positive control, ascorbic acid.

Although the antioxidant capacity of the whole-plant extract was slightly lower than that previously measured for the twigs and bark extracts, it was comparable to the values obtained for leaves and roots extracts. These differences can reasonably be attributed to a dilution effect resulting from the combination of multiple plant tissues, each contributing distinct but complementary phytochemical profiles. Importantly, despite these minor variations, all extracts (including the Ghaf extract) consistently displayed very high antioxidant activities, supporting the robustness of the result. Overall, the preservation of strong radical scavenging capacity in the representative whole-plant extract further supports its selection as a biologically relevant and functionally effective material for subsequent anti-aging and formulation-oriented studies.

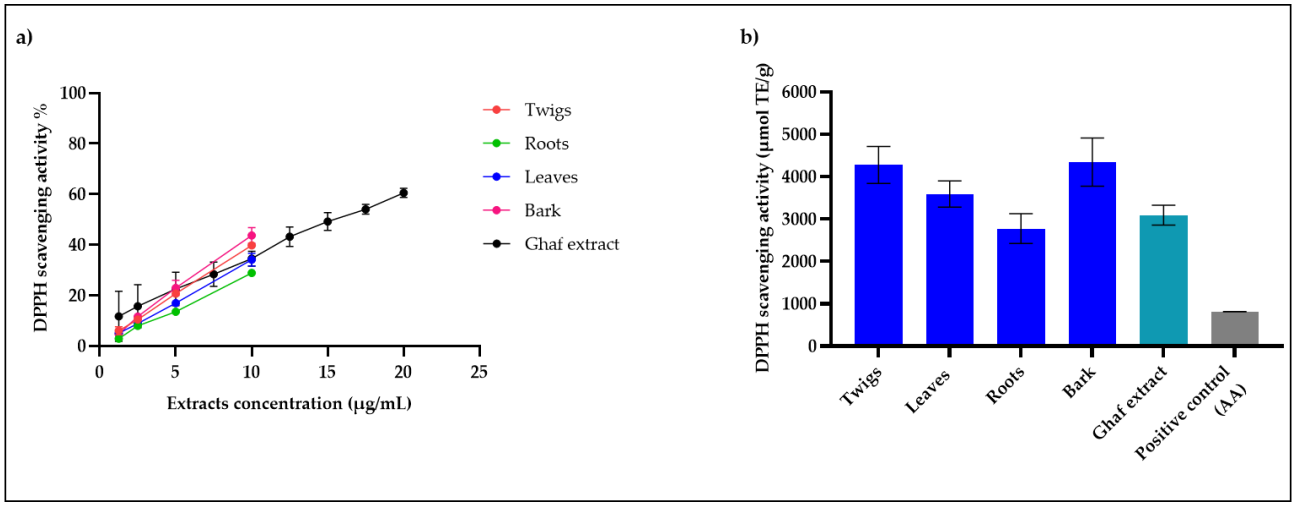

Figure 4.3. (a) Concentration-dependent DPPH radical scavenging activity of the Ghaf extracts obtained from different plant portions (Twigs, Roots, Leaves and Bark) and the Ghaf extract. The plot shows the percentage of DPPH radical scavenging activity as a function of extract concentration. (b) DPPH radical scavenging activity of the same extracts and ascorbic acid expressed as Trolox equivalents (µmol TE/g). Values are expressed as mean ± standard deviation of two independent experiments, each in technical triplicate.

4.2.3.2 Total phenolic content (TPC)

Phenolic compounds, including flavonoids and phenolic acids, are known to be the major contributors to the antioxidant capacity of plants [21] [22]. Accordingly, the total phenolic content of Ghaf extract was also evaluated by using the Folin–Ciocalteu colorimetric assay. This assay relies on the reagent reduction by phenolic compounds under alkaline conditions, leading to the production of a blue coloration detectable in absorbance at 760 nm, proportional to the phenolic content in the samples. The total phenol content of extract was expressed in terms of gallic acid

equivalent (µg GAE/mg extract) as described in *Section 4.4.5.2*. The Ghaf extract exhibited remarkably high TPC, with a mean value of 281.82 ± 14.63 µg GAE/mg of extract, indicative of a rich presence of secondary metabolites with known redox potential. This finding aligns well with the strong antioxidant capacity previously observed in the DPPH radical scavenging assay, suggesting a close relationship between chemical composition and biological activity. Such correlation between total polyphenol content and antioxidant efficacy is consistently reported in literature, where polyphenolic compounds (especially flavonoids, tannins, and catechins) are recognized as major contributors to the antioxidant potential of plant extracts [23].

The UHPLC–DAD–HRMS/MS analysis further confirmed the presence of abundant catechins and flavonoid derivatives, both known for their ability to donate hydrogen atoms or electrons to neutralize free radicals, as well as to chelate metal ions involved in oxidative reactions[24]. These results provide strong evidence that the antioxidant activity of the Ghaf extract can be primarily attributed to its polyphenolic fraction, although synergistic effects among different compound classes cannot be excluded.

4.2.4 In vitro enzymatic inhibition assays

After confirming the strong antioxidant activity of the Ghaf extract and more robustly linking this effect to the high abundance of phenolic compounds identified through phytochemical characterization and TPC assay, the next step consisted in validating the anti-aging properties previously observed in enzymatic inhibition assays performed on tissue-specific extracts *(Chapter 3)*.

4.2.4.1 Elastase inhibition assay

For the elastase inhibition assay, the representative Ghaf extract was tested over an expanded concentration range in order to investigate whether a stronger reduction in enzymatic activity could be achieved compared with previous experiments. Increasing concentrations of Ghaf extract (12.5–400 µg/mL) were therefore evaluated, with oleanolic acid included once again as a positive control. As shown in **Figure 4.4**, elastase activity was reduced in a weakly concentration-dependent manner, becoming statistically significant from 25 µg/mL and reaching a plateau at approximately 50% residual activity at concentrations ≥100 µg/mL.

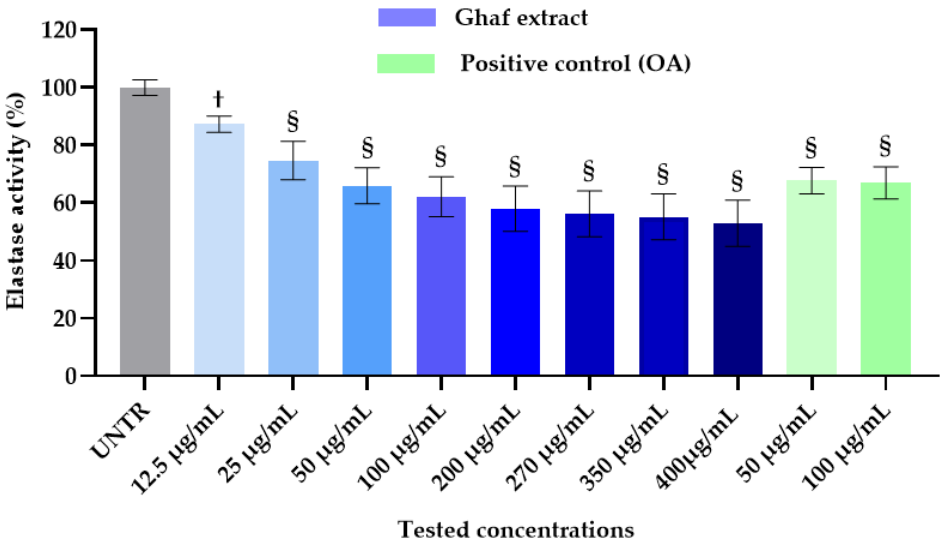

Figure 4.4. Elastase activity in presence of Ghaf extract compared to oleanolic acid used as positive control. Each bar represents the mean percentage activity ± standard deviation of two independent experiments, each in technical triplicate. Each enzyme activity reduction was significant compared to untreated condition with $p < 0.0001$ (§), except for Ghaf at 12.5 µg/mL with $p < 0.01$ (†).

These results confirm the mild elastase inhibitory activity previously observed for extracts obtained from individual Ghaf plant tissues, while also highlighting the reproducibility and robustness of the assay. Indeed, the comparable inhibitory effect of oleanolic acid in this experiment (approximately 67% residual activity) relative to the previous assay (around 60%) further supports the reliability of the test. Moreover, the similar inhibition profile observed for the Ghaf extract reinforces the hypothesis that elastase inhibition is not attributable to a single specific tissue, but rather to a relatively uniform distribution of the bioactive constituents across Ghaf plant tissues.

The persistence of a plateau in elastase inhibition, already observed for tissue-specific extracts up to 270 µg/mL and here extending to the highest tested concentration, further supports the hypothesis that a fraction of the enzyme population remains catalytically active even in the presence of excess inhibitor. This behavior suggests that the Ghaf extract reaches its maximal inhibitory potential at relatively low concentrations, a feature that may represent an advantage for topical applications.

4.2.4.2 Collagenase inhibition assay

In parallel, the Ghaf extract was evaluated using the collagenase inhibition assay to verify whether the combined extract retained the ability to slow down collagen degradation, and to compare its

activity with that previously observed for Ghaf tissue-specific extracts. In this case, the concentration range was expanded not by increasing the maximum concentration, given the already pronounced inhibition observed in earlier experiments, but by introducing lower concentrations and increasing the number of intermediate points, allowing a more detailed assessment of dose-dependent variations in enzymatic activity. The resulting data are shown in **Figure 4.5**. The inhibition profile revealed a gradual reduction in collagenase activity, becoming significant relative to the untreated control from 100 μg/mL, followed by a clear dose-dependent trend, reaching a maximal reduction of approximately 34% at the highest tested concentration. This behavior closely mirrors that previously observed for Ghaf roots and bark extracts. Overall, the common inhibitory trend observed across all Ghaf tissue-derived extracts is confirmed for the Ghaf extract, although maximal inhibition values were occasionally slightly lower than those observed for twigs and leaves extracts. This difference can reasonably be attributed to a dilution effect arising from the combination of multiple portions, each contributing active compounds that are not sufficiently heterogeneously distributed to markedly reduce the overall inhibitory efficacy. These findings therefore further support the choice of a whole-plant extract as a favorable and pragmatic option. Furthermore, EGCG reduced collagenase activity to a lesser extent than the Ghaf extract at the same concentration tested, further underscoring its inhibitory potential in this context.

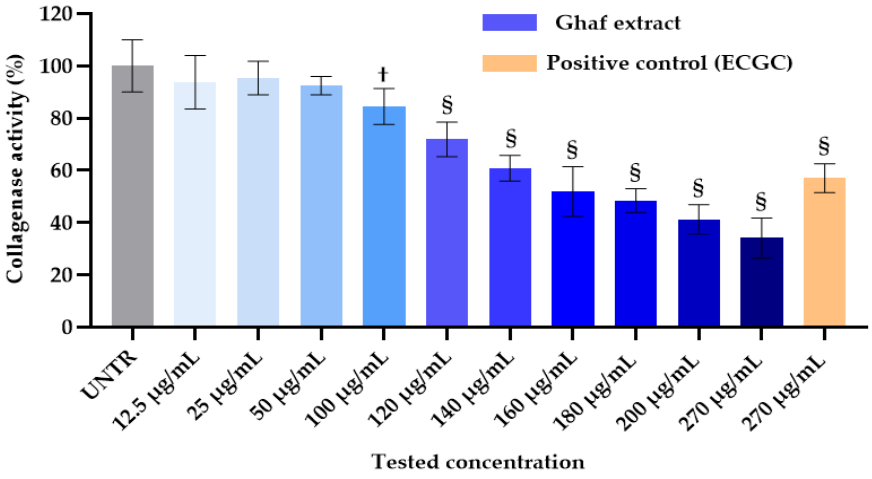

Figure 4.5. Collagenase activity in presence of increasing concentration of Ghaf extract and of ECGC as positive control. Each bar represents the mean percentage activity ± standard deviation of two independent experiments, each in technical triplicate. Each enzyme activity % was significant compared to untreated condition with $p < 0.0001$ (§) or $p < 0.01$ (†), except for Ghaf at 12.5, 25 and 50 μg/mL.

4.2.4.3 Hyaluronidase inhibition assay

Finally, the anti-aging activity of the Ghaf extract was also evaluated in terms of hyaluronidase inhibition. The same concentration range previously used for tissue-specific Ghaf extracts was applied, as complete inhibition had already been observed under these conditions. As shown in **Figure 4.6**, the Ghaf extract displayed a pronounced inhibitory activity, reducing hyaluronidase activity almost completely at 66 µg/mL, thereby surpassing the efficacy of oleanolic acid at considerably lower concentrations. This behavior is consistent with that previously observed for individual Ghaf portion extracts, with percentage enzyme activity values comparable to the average inhibition recorded for tissue-specific extracts at the same concentrations. This again can be attributed to a dilution effect resulting from the combination of different plant components. Overall, these results confirm the strong inhibitory potential of the Ghaf extract against hyaluronidase, indicating a robust capacity to counteract ECM degradation and preserve dermal moisture, thereby contributing to the maintenance of skin hydration and elasticity even at very low concentrations.

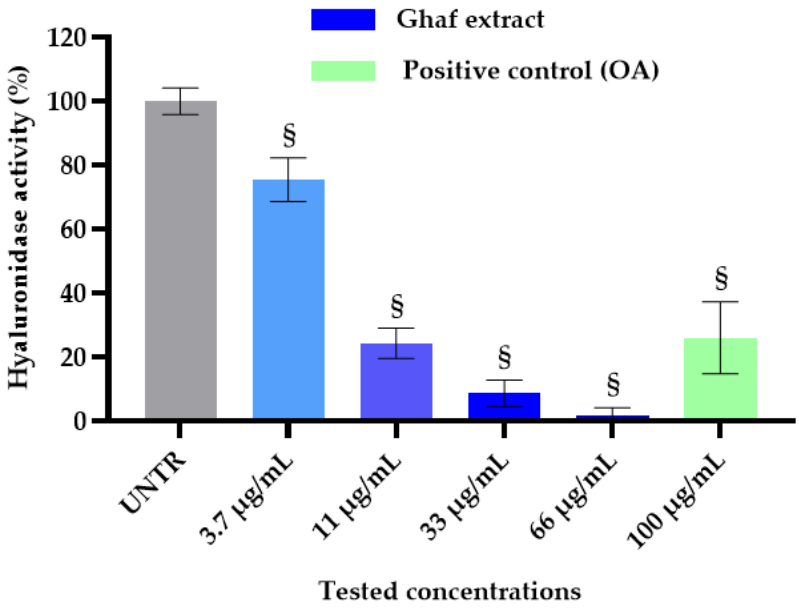

Figure 4.6. Hyaluronidase activity in presence of increasing concentration of Ghaf extract compared to oleanolic acid used as positive control. Each bar represents the mean percentage activity ± standard deviation of two independent experiments, each in technical triplicate. All enzyme activities reported were significant compared to untreated condition with $p < 0.0001$ (§).

4.2.4.4 Human tyrosinase inhibition assay

Given the strong anti-aging potential demonstrated by the Ghaf extract through antioxidant and extracellular matrix–related enzymatic inhibition assays, its multifunctionality was further explored by evaluating its ability to inhibit human tyrosinase. Tyrosinase is the crucial, rate-limiting enzyme in melanogenesis. It first hydroxylates L-tyrosine to L-DOPA and subsequently oxidizes L-DOPA to o-dopaquinone, which is further converted into melanin (the pigment responsible for skin, hair, and eye coloration[25]). Although melanin plays an essential photoprotective role, its excessive accumulation within the epidermis is associated with several pigmentary disorders, including lentigo, melasma, and age-related hyperpigmentation[26]. Accordingly, tyrosinase inhibitors represent valuable candidates for skin-brightening and whitening applications. Ghaf extract was therefore investigated for human cellular tyrosinase inhibiting abilities in MNT-1 cell lysate. In this assay the TYR-mediated dopachrome and eumelanin formation was monitored at 478 nm and 600 nm respectively, in the presence or absence of Ghaf extract, with kojic acid included as a positive control. The resulting typical kinetic profiles were subsequently converted into slope values normalized on the untreated condition, yielding the percentage of human tyrosinase activity. As shown in **Figure 4.7**, kojic acid produced a characteristic sigmoidal dose–response with strong inhibition, validating the sensitivity and robustness of the assay. Ghaf extract similarly reduced tyrosinase activity in a concentration-dependent manner, although with lower potency, reaching an estimated IC_{50} below 100 μg/mL. Despite being less active than kojic acid, this inhibitory effect is remarkable given the crude, heterogeneous nature of the botanical extract.

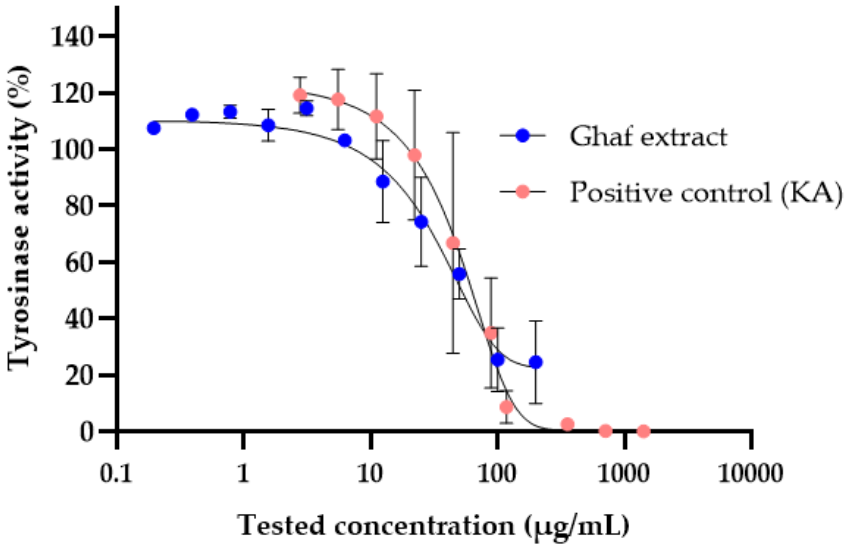

Figure 4.7. Tyrosinase inhibition by kojic acid and Ghaf extract. (a) Dose–response inhibition curve of human tyrosinase in the presence of kojic acid (positive control), and (b) exposed to increasing concentrations of Ghaf extract. Data represent mean ± SD of three independent experiments (n=3), each in technical triplicate.

Taken together, these findings suggest that the Ghaf extract contains bioactive molecules capable of modulating melanogenic enzymes, supporting its potential use as a multifunctional cosmetic ingredient with mild skin-brightening or tone-evening effects. The observed activity, together with previously demonstrated antioxidant and hyaluronidase-inhibitory properties at low concentrations, indicates that the extract's dermo-cosmetic potential likely arises from complementary mechanisms.

4.2.5 Cell viability assay of Ghaf extract on HaCaT cell line

Before proceeding with formulation development, it was essential to evaluate the biocompatibility of the selected Ghaf extract on skin-relevant cells. Human immortalized keratinocytes (HaCaT) were therefore used as an *in vitro* model to assess the effect of the extract on epidermal cell viability and to define a non-cytotoxic concentration range suitable for cosmetic applications.

To this end, HaCaT cells were treated with increasing concentrations of the Ghaf extract and incubated for 48 hours. Cell viability was subsequently assessed using the MTS assay, and results were expressed as the percentage of viable cells relative to the untreated control (**Figure 4.8**). The obtained data revealed that the extract maintained high cell viability (>70%) up to concentrations of

200 µg/mL, followed by a slow decrease reaching 47% of cell viability at the highest tested concentration. Althought a cytotoxic effect is observed at higher doses, the profile suggests that the Ghaf extract does not negatively affect HaCaT cell viability within the concentration range relevant to the enzymatic and antioxidant activities observed in the aforementioned assays. These findings confirm that the extract can exert meaningful bioactivity without compromising cell viability, supporting its safe integration into topical formulations. Furthermore, cytotoxicity in monolayer cultures should be interpreted cautiously, as formulated systems typically reduce the effective bioavailable concentration of active ingredients[27], [28].

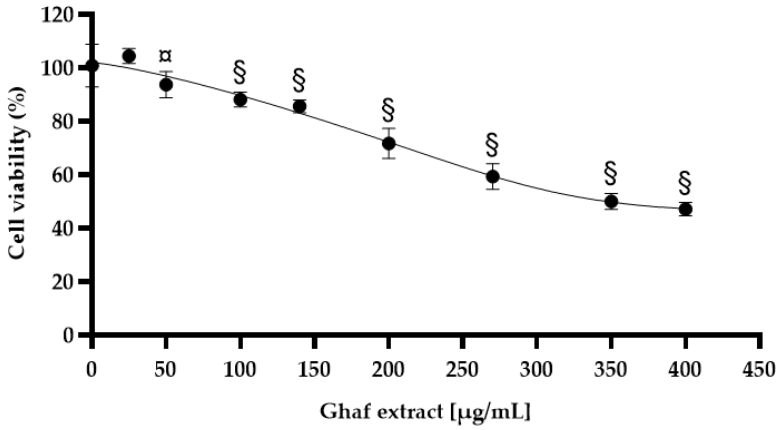

Figure 4.8. Cell viability (%) of HaCaT cell line treated with Ghaf extract (25–400 µg/mL) for 48 h compared to untreated condition. Bars represent mean percentage ± standard deviation of two independent experiments, each in technical quadruplicate. § ($p < 0.0001$) and ¤ ($p < 0.05$) vs untreated condition.

4.2.6 Formulation study with Ghaf extract as anti-age active ingredient

The following results related to the formulation study were conducted during a research period abroad at AgroParisTech, Chaire de Cosmétologie (Orléans, France) under the supervision of Professor Delphine Huc-Mathis and Professor Richard Daniellou.

Based on the biological findings presented above, which identified the Ghaf extract as a highly promising anti-aging active, the next step of this study focused on the development and evaluation of a cosmetic formulation incorporating the Ghaf extract. A facial cream was selected as the delivery system, as nowadays creams together with serums, represent the most widely attractive and commercially relevant cosmetic formats for facial skincare applications [29].

4.2.6.1 Development of base emulsion

4.2.6.1.1 Selection of formulation ingredients

In the framework of developing a base emulsion suitable for the subsequent incorporation of the Ghaf extract, the initial step focused on the careful selection of raw materials. In line with current trends in sustainable and eco-conscious skincare, the formulation was designed according to strict sustainability-driven criteria, including a minimal INCI list, avoidance of heating steps, and the exclusive use of biodegradable and naturally derived ingredients. To further enhance sustainability and skin compatibility, a Pickering emulsification strategy was adopted. This approach enables emulsion stabilization through solid particles rather than conventional surfactants, thereby reducing the need for synthetic emulsifiers. Pickering emulsions are increasingly recognized as an innovative and environmentally friendly alternative, offering improved physical stability, enhanced biocompatibility, and favorable biodegradability profiles [30] [31].

Based on these criteria, the formulation was intentionally designed to include only the essential components required to obtain a stable emulsion. Water was selected as the water phase solvent, while the oil phase consisted of a blend of vegetable oils, namely sunflower oil and plum oil. Sunflower oil was chosen as a widely used, cost-effective lipid base with good emollient properties[32], whereas plum oil, although more refined, provides a naturally pleasant fragrance, allowing the formulation to be sensorially appealing without the addition of external fragrance ingredients[33]. Together, these oils provide a simple yet effective emollient, nourishing, and sensorially balanced oil phase. Glycerin (5% w/w) and potassium sorbate (0.2% w/w) were included as humectant and preservative, respectively. The most critical formulation step concerned the selection of a suitable stabilizing system. For this reason, a preliminary screening was performed to identify biodegradable natural powders capable of producing physically stable Pickering emulsions.

Three candidate stabilizers were initially evaluated: VITACEL® CF312 Citrus powder, VITACEL® CS5 Apple powder, and VIVAPUR® CS TEX EASY. The citrus powder is a plant-based dietary fiber sustainably obtained from citrus peel, characterized by a high water-binding capacity and amphiphilic behavior, which enhances viscosity, structural integrity, and overall emulsion stability[34]. The apple powder is an upcycled material derived from food industry by-products and contains both hydrophilic and hydrophobic domains, facilitating its adsorption at the oil–water

interface. In addition, the presence of soluble proteins and surface charge contributes to droplet stabilization[35]. VIVAPUR® CS TEX EASY is a co-processed blend of microcrystalline cellulose, xanthan gum, and cellulose gum, functioning as a natural, biodegradable, universal thickener and stabilizer[36].

Four emulsions containing different combinations of these powders were prepared and evaluated for physical stability using Turbiscan analysis (**Figure 4.9 (a)**), as well as for visual appearance and color (**Figure 4.9 (b)**). Turbiscan is an analytical technique used to assess the physical stability of dispersions such as emulsions by measuring transmitted and backscattered light along the height of the sample over time[37]. Among the measured parameters, the backscattering (BS) signal is particularly informative, as it reflects droplet size distribution and emulsion homogeneity[38].

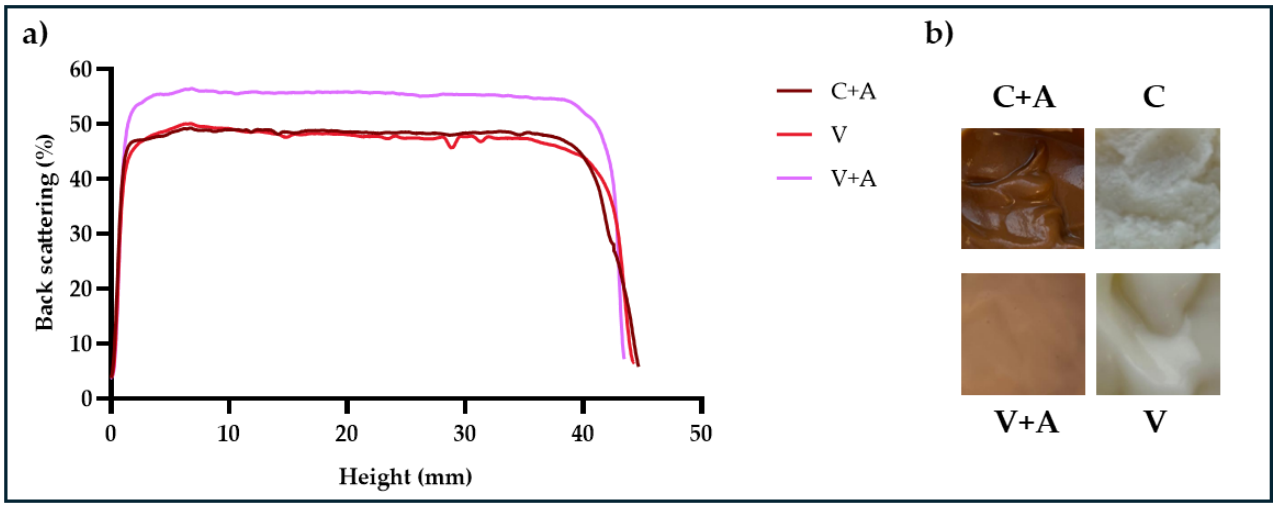

Figure 4.9. (a) Physical stability of C+A, V, and V+A emulsions expressed as backscattering (%) profiles along the sample height, as measured by Turbiscan analysis and (b) the corresponding visual appearance of the emulsions. C: VITACEL® CF312 Citrus powder, A: VITACEL® CS5 Apple powder, V: VIVAPUR® CS TEX EASY and their corresponding combinations.

The combination of citrus and apple powders resulted in a physically stable emulsion, characterized by BS values around 48% and a satisfactory texture, likely thanks to the presence of pectins contributing to network reinforcement and viscosity enhancement[39]. However, this formulation exhibited a pronounced brown coloration due to the apple fiber, causing it to be aesthetically unsuitable for a facial cosmetic product. Consequently, this configuration was excluded from further studies. When citrus powder was employed as the sole stabilizing agent, the resulting formulation

displayed a pasty and highly irregular consistency, which prevented Turbiscan analysis (data not shown), confirming its inadequacy as a standalone emulsifier.

VIVAPUR® CS TEX EASY was subsequently evaluated both in combination with apple powder and as a single stabilizing agent. The latter condition yielded the most promising results, producing a white, homogeneous, and physically stable emulsion. Although the BS values were slightly lower than those observed for apple-containing formulations, this behavior can be reasonably attributed to differences in particle packing and network architecture. Apple fibers, rich in pectins and proteins, may generate denser interfacial networks and smaller droplets, leading to higher BS values[39]. In contrast, the cellulose-based VIVAPUR® system forms a more uniform but less optically dense network[40], resulting in slightly lower BS values while still ensuring excellent physical stability. Importantly, the use of VIVAPUR® CS TEX EASY alone allowed the formulation of a stable emulsion with a minimal ingredient list, without the need for additional stabilizers or thickeners. For these reasons, the formulation corresponding to condition (V) was selected as the starting point for further optimization.

4.2.6.1.2 Emulsion optimization with Design of Experiment (DoE)

After selecting the ingredients, a Design of Experiments (DoE) approach was employed to optimize ingredient concentrations and explore the formulation space. Specifically, glycerin (5% w/w) and potassium sorbate (0.2% w/w) were fixed, while the concentrations of oil phase and VIVAPUR® CS TEX EASY were defined as continuous variables, representing the most critical formulation parameters governing the structure and stability of Pickering emulsions: the oil fraction directly determines the dispersed phase volume and droplet packing, whereas the concentration of solid particles controls interfacial coverage and the formation of a stabilizing particulate network around the droplets. The investigated ranges were selected based on a combination of literature data, preliminary screening trials, and manufacturer recommendations for the particle stabilizer. The oil phase was varied between 10–40% (w/w), a range commonly explored for oil-in-water cosmetic emulsions that allows evaluation of systems from relatively dilute dispersions to highly packed emulsions while maintaining processability and spreadability. The concentration of VIVAPUR® CS TEX EASY was varied between 3–8% (w/w). The lower bound of this range corresponds to the typical usage levels recommended for this microcrystalline cellulose-based stabilizer in cosmetic

formulations, while the upper limit was intentionally extended to explore the formulation space more comprehensively. The water content was adjusted accordingly to reach 100% w/w.

Using a response surface model, ten combinations were generated by JMP software (**Table 4.2**), where "–" and "+" represent the lower and upper limits of the defined ranges, "a" and "A" correspond to axial points outside the range, and "0" indicates the central value. Each formulation was prepared and analyzed by Turbiscan, and the mean backscattering value at time zero (BS_0) from three independent measurements was used as the response variable to build a predictive linear regression model (**Figure 4.10**).

Table 4.2. Ten formulation configurations generated by JMP software through DoE, characterized by different combinations of oil and VIVAPUR® CS TEX EASY content (% w/w).

Configuration	Oil	VIVAPUR® CS TEX EASY
+ +	40.00	8.00
− +	10.00	8.00
0 A	25.00	9.04
0 0 (1)	25.00	5.50
− −	10.00	3.00
a 0	3.79	5.50
A 0	46.21	5.50
0 a	25.00	1.96
+ −	40.00	3.00
0 0 (2)	25.00	5.50

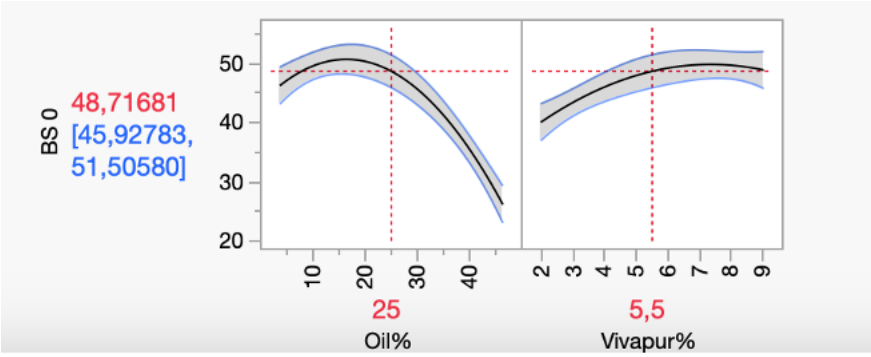

Figure 4.10. Linear regression model predicting the BS_0 value as function of two continuous variables: oil and VIVAPUR® CS TEX EASY content (% w/w). The model was generated by JMP software, with BS_0 values expressed as the mean of three independent measurements.

The model revealed that oil content exerted a more pronounced influence on BS_0 values than the concentration of VIVAPUR® CS TEX EASY. This finding indicates that the internal structure and droplet organization of the emulsions can be effectively modulated by adjusting the oil fraction. Higher BS_0 values are typically associated with emulsions characterized by a high number of small droplets and a dense internal network, whereas lower BS_0 values generally reflect systems with larger droplets and a less compact structure[38].

Although this tunability represents an interesting opportunity for tailoring emulsions to specific active ingredients, such as reducing droplet surface area for oxidation-prone oils or enhancing incorporation efficiency for actives requiring deeper matrix integration, this aspect was not further explored in the present work, as the primary objective at this stage was the identification of a robust and versatile base formulation suitable for active inclusion.

Turbiscan analysis also provided BS profiles along the entire sample height at time zero for all ten formulations (**Figure 4.11 (a)**). Stable plateau profiles were observed for all formulations except A0, ++, and 0A, which exhibited highly irregular BS profiles indicative of emulsion heterogeneity. These irregularities correspond to localized variations in droplet distribution, leading to increased light transmission and reduced backscattering signals. The heterogeneity detected by Turbiscan was consistent with the visual appearance of these samples (**Figure 4.11 (b)**).

Further insight can be gained from the comparison of BS_0 values among the different formulations shown in **Figure 4.11. (a)**. Specifically, formulations 0a and +- exhibited similar BS values of approximately 35%, whereas a0 and − − showed intermediate values around 45%. Both replicates of

the central point ($00_{(1)}$ and $00_{(2)}$) yielded BS values close to 50%, while the −+ formulation displayed the highest BS value, reaching approximately 53%. The lower BS values observed for 0a and +- can be reasonably attributed to their reduced content of VIVAPUR® CS TEX EASY. Although these emulsions appeared homogeneous, the lower stabilizer concentration likely resulted in a less compact internal network, characterized by larger droplet sizes and lower droplet density. In contrast, formulations a0 and − − are both characterized by reduced oil content, which favors the formation of a more structured network even in the presence of variable stabilizer levels, likely leading to smaller droplets and higher packing density. The close agreement between the two central-point formulations (00) further confirms the reproducibility and reliability of the formulation process. Finally, the − + formulation exhibited the highest BS value, which can be attributed to the combined effect of low oil content and high stabilizer concentration, resulting in the most compact and densely structured emulsion network. As expected, variations in oil and VIVAPUR® CS TEX EASY content were also reflected in the visual appearance of the emulsions, with higher oil fractions imparting a more yellowish hue and increased stabilizer content yielding whiter, more opaque systems (**Figure 4.11. (b)**).

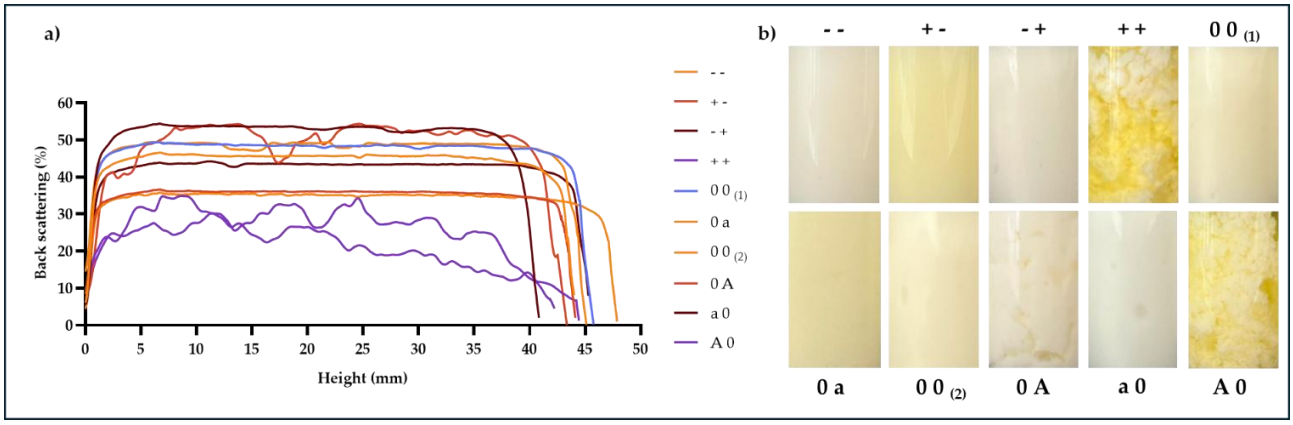

Figure 4.11. (a) Back scattering (%) profiles of the ten emulsions configuration obtained through DoE at time 0, and (b) the corresponding visual appearance.

To further assess stability, the six formulations initially classified as stable (--, +-, -+, 00, 0a, a0) were subjected to a centrifugation test to simulate accelerated mechanical stress. Under these conditions, only formulations a0 and -+ remained completely stable. Formulations 00 and - - exhibited a thin aqueous layer at the surface, while +- and 0a showed clear phase separation with the formation of an oil-rich upper layer.

Based on these results, formulation a0 was selected as the base emulsion, as it provided stability comparable to -+ while requiring lower amounts of both oil and VIVAPUR® CS TEX EASY. This composition represents a more sustainable and minimalist option, without compromising physical robustness. The final composition of this formulation is reported in **Table 4.3.** From this point onward, this formulation is referred to as the base emulsion (BE) and was used for subsequent studies on the inclusion of the Ghaf extract as an active ingredient.

Table 4.3. Base emulsion (BE) composition. Each quantity is expressed as % w/w relative to the emulsion total weight.

Ingredient	Phase	Quantity
Demineralized water	Water	85.52
Glycerin	Water	5
Potassium sorbate	Water	0.2
VIVAPUR® CS TEX EASY	Water	5.5
Sunflower oil	Oil	2.53
Plum oil	Oil	1.26

Overall, the systematic formulation approach described above led to the identification of a physically stable, minimalist, and fully biodegradable base emulsion. The selected formulation (BE) combines robustness under mechanical stress with a reduced number of ingredients, and mild processing conditions, making it particularly suitable as a carrier system for bioactive compounds. Importantly, the Pickering-based stabilization strategy and the absence of conventional surfactants minimize the risk of undesired interactions with sensitive phytochemicals. On this basis, the BE was considered an appropriate and versatile platform for the subsequent inclusion of the Ghaf extract, enabling the investigation of its physical chemical behavior and stability.

4.2.6.2 Ghaf extract formulations

After defining and formulating the base emulsion, the Ghaf extract was incorporated as an aqueous solution (2 mg/mL, based on its solubility in water) at three different concentrations: 3%, 5%, and 10% (w/w), corresponding to final extract concentrations in the formulation of 60, 100, and 200 μg/mL, respectively. The lowest inclusion level (3% w/w) was selected as a rational compromise between extract concentration range commonly reported in the literature [41] for cosmetic actives and the favorable safety profile observed in preliminary cell viability assays. Given that the biological activity and tolerability of an active ingredient may change within a complex formulation matrix[27], higher extract loadings (5% and 10% w/w) were also evaluated to explore potential concentration-dependent effects. All Ghaf-containing emulsions were subsequently characterized and compared with the base formulation in order to evaluate their physicochemical stability and organoleptic properties.

4.2.6.2.1 Characterization of Ghaf extract formulations

4.2.6.2.1.1 Organoleptic Characteristics

First, the organoleptic properties of the Ghaf-loaded emulsions were evaluated in comparison with the base emulsion. All formulations were stored for seven days at three different temperatures (4°C, 25 °C, and 45 °C), and the results are summarized in **Table 4.4.**

Table 4.4. Physical study of base emulsion and emulsion with Ghaf extract at different percentages for one week. Ghaf-containing emulsions correspond to the incorporation of a 2 mg/mL aqueous Ghaf extract solution at 3, 5, and 10% (w/w), yielding final extract concentrations of 60, 100, and 200 µg/mL, respectively.

Duration	7 days						
	Storage condition						
Parameter	4°C	25°C	45°C	Parameter	4°C	25°C	45°C
Appearance				Odour			
Base emulsion	Semisolid	Semisolid	Semisolid	Base emulsion	Characteristics	Characteristics	Characteristics
BE + Ghaf 3%	Semisolid	Semisolid	Semisolid	BE + Ghaf 3%	Characteristics, mild herbal	Characteristics, mild herbal	Characteristics, mild herbal
BE + Ghaf 5%	Semisolid	Semisolid	Semisolid	BE + Ghaf 5%	Characteristics, strong herbal	Characteristics, strong herbal	Characteristics, strong herbal
BE + Ghaf 10%	Semisolid	Semisolid	Semisolid	BE + Ghaf 10%	Characteristics, strong herbal	Characteristics, strong herbal	Characteristics, strong herbal
Colour							
Base emulsion	Off white	Off white	Off white				
BE + Ghaf 3%	Off white	Off white	Off white				
BE + Ghaf 5%	Off white	Off white	Off white				
BE + Ghaf 10%	Off white	Light greyish	Light beige				

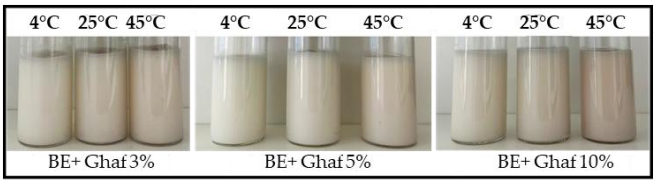

In detail, both the base emulsion and the formulations containing the *Ghaf* extract retained a semi-solid, homogeneous appearance over 7 days, regardless of temperature conditions (4°C, 25°C, or 45°C). A slight color shift from the off white of the base emulsion to a light beige/gray tone was observed at higher extract concentrations, with further intensification at elevated storage temperatures. Such behavior is consistent with natural pigment oxidation (e.g., polyphenols and flavonoids that may undergo mild oxidation or color deepening upon heat exposure[42]). Odor evaluation revealed an enhancement of the characteristic plum oil scent, complemented by a subtle vegetal note that increased proportionally with extract content. The odor profile remained stable at all three storage temperatures, indicating the absence of extract degradation or rancidity phenomena during the observation period.

4.2.6.2.1.2 Physical stability

Emulsion stability was further monitored by Turbiscan analysis after seven days of storage at 4 °C, 25 °C, and 45 °C (**Figure 4.12**). The backscattering (BS%) profiles revealed no significant variations as a function of storage temperature for either the base emulsion or the Ghaf-containing formulations. Moreover, the BS% values of the emulsions loaded with Ghaf extract were consistently close to 40%, comparable to those of the base emulsion. These results indicate that the

incorporation of the aqueous Ghaf extract solution does not adversely affect the internal structure or physical stability of the Pickering emulsion, confirming that the strength and integrity of the particulate network remain preserved.

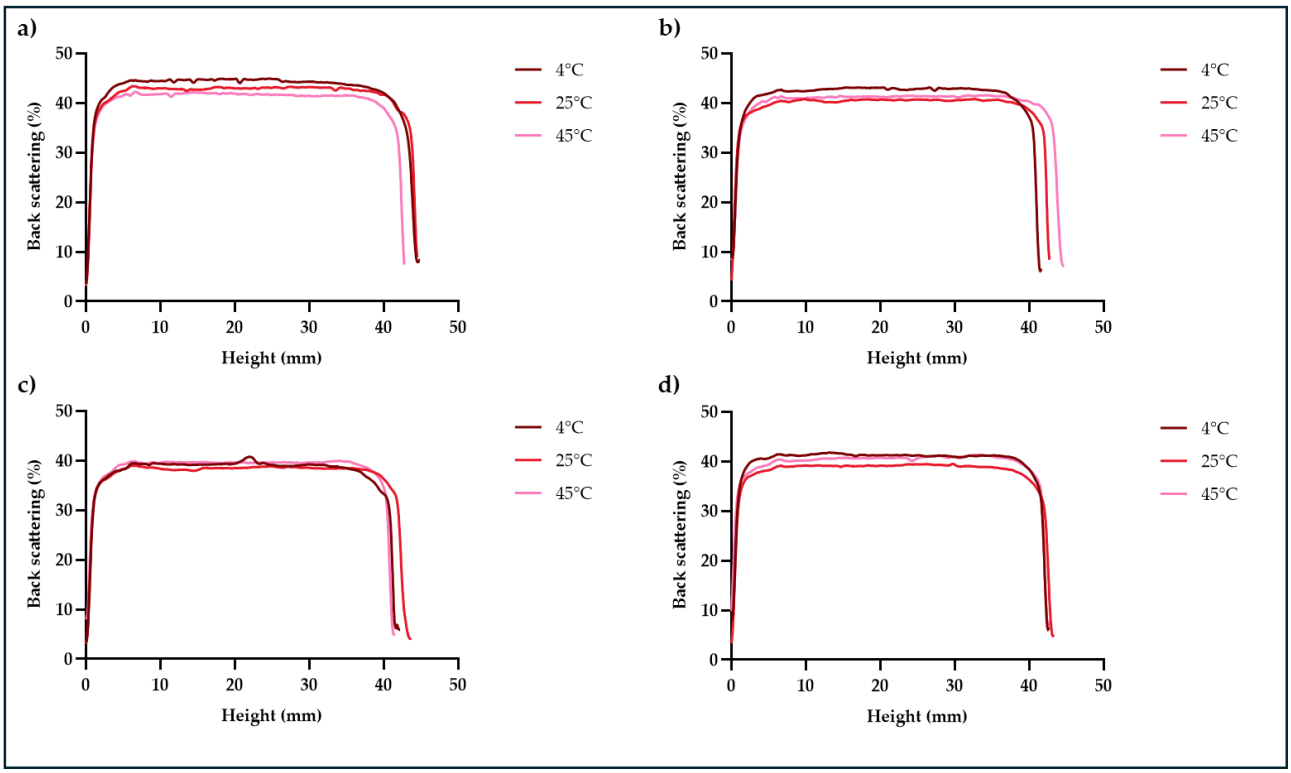

Figure 4.12. Physical stability of a) base emulsion, and emulsions with Ghaf solution (2 mg/mL) at b) 3, c) 5 and d) 10% w/w, yielding final extract concentrations of 60, 100, and 200 µg/mL, respectively. Results are expressed as backscattering (%) profiles along the sample height, as measured by Turbiscan analysis after 7-day storage at 4°C, 25°C and 45°C.

4.2.6.2.1.3 pH determination

The pH values of formulations were 5.6 for the base emulsion and 5.9, 5.8, 5.9 for the emulsions containing 3%, 5%, and 10% (w/w) of Ghaf extract solution, respectively. Thus, all samples remained within the dermo compatible acidic range typically recommended for topical applications [43]. Importantly, *Ghaf* extract solution therefore does not perturb acid–base equilibria within the emulsion, a desirable feature in cosmetic emulsions, as it prevents irritation potential and ensures formulation stability and preservative efficacy [44] .

4.2.6.2.1.4 Centrifugation (accelerated stability) test

The centrifugation test was performed on both the base emulsion and the *Ghaf*-containing formulations after 24 h. No phase separation or signs of creaming or sedimentation were observed in any sample. This result demonstrates that all emulsions were physically stable even under strong mechanical stress, confirming the excellent interfacial stabilization capacity of VIVAPUR® CS TEX EASY. The findings suggest that the formulations possess high kinetic stability, which is a strong predictor of long-term shelf stability and robustness under real storage conditions.

4.2.6.2.1.5 Rheological behavior

The rheological behavior of the base emulsion and of formulations containing increasing concentrations of *Ghaf* extract solution at 2 mg/mL (3%, 5%, and 10% w/w) was evaluated to investigate the effect of extract incorporation on the structural integrity and viscoelastic properties of the system. Flow and oscillatory measurements were performed at 25 °C using a Discovery HR-10 rheometer, following the procedure described in *Section 4.4.10.4.5.*

The flow sweep analysis (**Figure 4.13. (a)**) revealed a shear-thinning behavior for all samples, characterized by a marked decrease in viscosity with increasing shear rate, from approximately 10^4 Pa·s at 0.01 s^{-1} down to below 1 Pa·s at 1000 s^{-1}. This pseudoplastic profile is typical of Pickering-type emulsions and indicates a stable, structured network that can recover its internal organization after shear removal[45]. Importantly, the viscosity curves of the *Ghaf*-containing formulations perfectly overlapped with that of the base emulsion, confirming that extract solution incorporation did not significantly alter the microstructure and flow properties of the system. The consistency and slope of the viscosity profiles remained nearly identical across all tested concentrations, suggesting that the polysaccharide–cellulose interfacial network provided by VIVAPUR® CS TEX EASY dominates the rheological response, even in the presence of bioactive solutes.

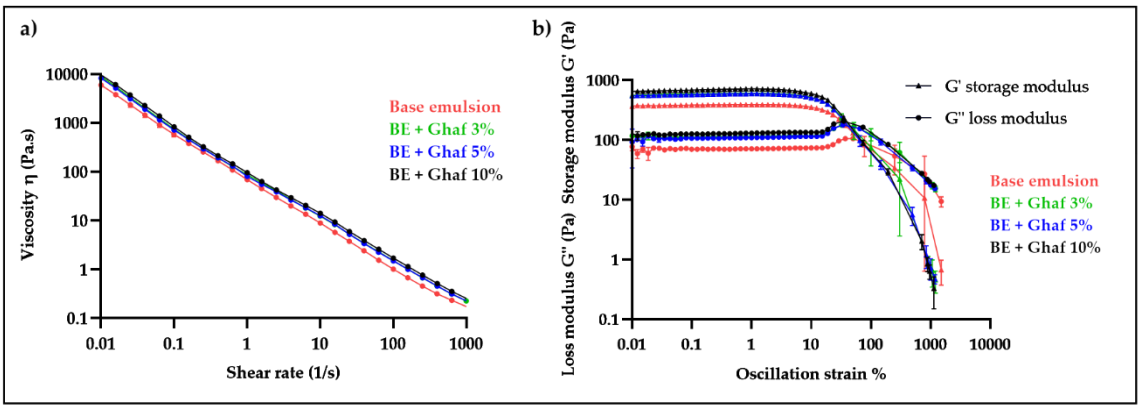

Figure 4.13. (a) Viscosity (η) vs. shear rate for all formulations (base emulsion in red; Ghaf solution at 3% (w/w) in green; Ghaf solution at 5% (w/w) in blue; Ghaf solution at 10% (w/w) in black). (b) Oscillatory strain sweep curves of storage (G′) and loss (G″) moduli as a function of oscillation strain (%). Each value represents the mean ± standard deviation of three independent measurements (n=3).

Oscillatory strain sweep tests (**Figure 4.13. (b)**) further supported these findings. All formulations exhibited a linear viscoelastic region (LVR) extending up to approximately 63% strain, within which the storage modulus (G′) exceeded the loss modulus (G″), indicating predominantly elastic solid-like behavior. Beyond this point, both moduli decreased as the structure progressively broke down under increasing deformation. The near superimposition of G′ and G″ curves across all samples confirmed that the addition of the *Ghaf* extract solution at concentrations up to 10% (w/w) did not compromise the internal microstructure or viscoelastic balance of the emulsion.

Overall, these results demonstrate that the incorporation of *Ghaf* extract as aqueous solution does not negatively impact the mechanical stability or rheological integrity of the Pickering emulsion. The formulations maintain consistent shear-thinning and viscoelastic properties, essential for good spreadability, sensory performance, and storage stability in topical cosmetic applications.

4.2.6.2.1.6 Droplet size distribution analysis

The droplet size distribution of the base emulsion and of formulations containing the Ghaf extract solution at 3%, 5%, and 10% (w/w) was assessed by laser diffraction granulometry. As shown in **Figure 4.14**, the measured parameters indicate a consistent micrometric size distribution across all formulations, with median values ranging between 11.05 and 15.78 μm.

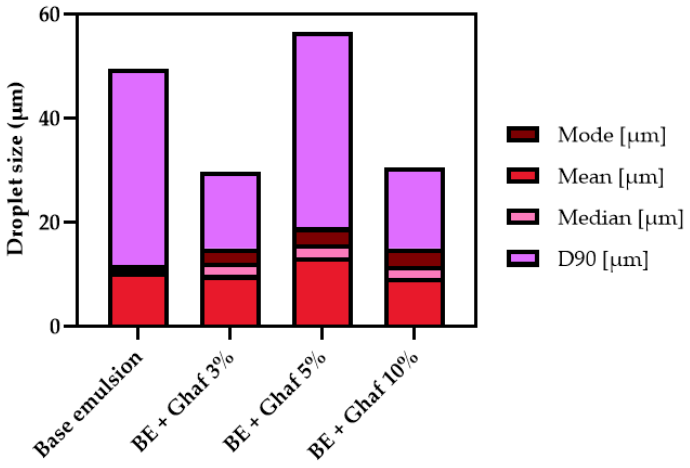

Figure 4.14. Droplet size distribution parameters of base emulsion and Ghaf-containing emulsions correspond to the incorporation of a 2 mg/mL aqueous Ghaf extract solution at 3, 5, and 10% (w/w), yielding final extract concentrations of 60, 100, and 200 µg/mL, respectively. Median, mode, mean droplet diameter, and D90 values were determined by laser diffraction granulometry and expressed as the mean of three independent measurements.

Although slight numerical variations were observed, especially an increase in the median and mode values in the emulsion containing Ghaf solution at 5% (w/w) formulation, the differences remain within the expected experimental variability and do not indicate a systematic or concentration-dependent shift in droplet size. Importantly, neither the mean diameter nor the variability among independent measurements exhibited a progressive trend with increasing extract concentration. The reported standard deviation values in **Table 4.5** (remaining within the narrow interval 0.44–0.52 µm) refer to the variability between replicate measurements, highlighting the high reproducibility of the droplet diameters across all samples. This observation suggests that the particulate stabilization mechanism provided by VIVAPUR® CS TEX EASY control droplet formation and stabilization and is not disrupted by extract loading.

Table 4.5. Droplet size mean ± standard deviation of three measurements of base emulsion and Ghaf-containing emulsions correspond to the incorporation of a 2 mg/mL aqueous Ghaf extract solution at 3, 5, and 10% (w/w), yielding final extract concentrations of 60, 100, and 200 µg/mL, respectively.

	Mean (µm)	Std Dev
Base emulsion	10.43	0.50
BE + Ghaf 3%	9.81	0.44
BE + Ghaf 5%	13.24	0.51
BE + Ghaf 10%	9.29	0.46

From a formulation perspective, this structural stability together with the consistent rheological behavior and physical stability described above, is a desirable feature for consistent texture, stability, and sensorial performance in cosmetic applications.

4.3 Conclusions

Taken together, the results obtained from the antioxidant and enzymatic inhibition assays clearly identify the Ghaf extract as a highly promising candidate for cosmetic anti-aging applications within the scope of this project. The extract consistently demonstrated a multifunctional anti-age profile, characterized by strong radical-scavenging activity, marked inhibition of hyaluronidase at very low concentrations, in addition to moderate and reproducible inhibitory effects against elastase, collagenase, and human tyrosinase. This combination of activities is particularly relevant in the context of skin aging, as it addresses both oxidative stress and key enzymatic pathways involved in extracellular matrix degradation and pigmentation processes. Importantly, the biological performance of the whole-Ghaf plant extract (Ghaf extract) closely mirrored the inhibitory profiles previously observed (*Chapter 3*) for extracts obtained from individual Ghaf tissues, confirming that the combination of different plant parts does not compromise bioactivity. On the contrary, this approach offers practical and conceptual advantages, including reduced processing time and costs, improved sustainability, and the potential contribution of synergistic interactions among phytochemicals naturally co-occurring in different tissues. From an industrial and formulation-oriented perspective, the use of a representative Ghaf extract further aligns with scalability requirements and regulatory considerations relevant to cosmetic ingredient development.

Furthermore, the strong and broad-spectrum anti-aging potential demonstrated by the Ghaf extract provided a clear rationale for advancing the project toward an application-driven stage. This

enabled the subsequent development of a cosmetic base formulation designed to accommodate the extract as an active ingredient. Through careful ingredient selection and systematic formulation exploration, a sustainable and innovative Pickering emulsion was successfully developed. The selected base formulation proved to be a robust and versatile carrier, capable of incorporating increasing amounts of the aqueous Ghaf extract without compromising physical stability, pH, rheological behavior, or microstructural integrity.

Overall, the formulation study confirmed that the Ghaf extract can be incorporated at relevant concentrations while maintaining the key physicochemical attributes required for topical cosmetic applications. This represents a crucial prerequisite for further development, as it demonstrates formulation compatibility and stability prior to more advanced biological efficacy and safety evaluations. Within this framework, a stable and innovative semi-solid cosmetic prototype containing Ghaf extract as an anti-aging active was successfully obtained. Although the project covered most of the essential steps involved in the development of a cosmetic active ingredient (from extraction and biological screening to formulation) the biological evaluation of the final formulation could not be performed within the timeframe of this study. Nevertheless, the comprehensive physicochemical characterization achieved represents a solid and necessary foundation for future investigations aimed at assessing biological efficacy, skin compatibility, and long-term safety of the formulated product.

4.4 Materials and methods

4.4.1 Chemicals and materials

2,2-Diphenyl-1-picrylhydrazyl (DPPH), (±)-6-Hydroxy-2,5,7,8-tetramethylchromane-2-carboxylic acid (Trolox), ascorbic acid, elastase from porcine pancreas (Type IV), N-Methoxysuccinyl-Ala-Ala-Pro-Val p-nitroanilide (MAAPVN), Trizma®base, oleanolic acid, N,N-Dimethylformamide (DMF) anydrous, Folin & Ciocalteu's phenol reagent, 3,4,5- Trihydroxybenzoic acid (gallic acid), sodium carbonate, collagenase from *Clostridium histolyticum* Sigma Blend Type H, N-[3-(2 Furyl)acryloyl]-Leu-Gly-Pro-Ala (FALGPA), tricine, calcium chloride dihydrate, sodium chloride, epigallocatechin gallate (ECGC), hyaluronidase type I-S, hyaluronic acid sodium salt from rooster comb, albumin from bovin serum (BSA), sodium phosphate monobasic, sodium phosphate dibasic, sodium acetate anhydrous, acetic acid, phosphate buffered saline (PBS), kojic acid, dimethyl sulfoxide (DMSO), 3,4-

Dihydroxy-L-phenylalanine (L-DOPA), potassium sorbate, citric acid/sodium hydroxide/hydrogen chloride (buffer solutions for pH calibration curve), Sodium Dodecyl Sulfate (SDS) were all purchased from Sigma-Aldrich (St. Louis, MO, USA). Ultrapure water (18 MΩ) was prepared by a Milli-Q purification system (Millipore, Bedford, MA, USA), while ethanol and methanol were purchased from CARLO ERBA Reagents s.r.l. (Milan, Italy). Acetonitrile and formic acid were purchased from Romil Chemicals (Cambridge, UK). High-glucose Dulbecco's Modified Eagle Medium (DMEM) with and without L-glutamine, fetal bovine serum (FBS), 1% penicillin–streptomycin (P/S), L-glutamine, 96-well and 48-well plates were purchased from EuroClone (Pero, Italy). Sunflower oil (commercial food grade Fruit d'Or) was acquired from a local retail market (Orléans, France) and used without further purification, whereas plum oil and glycerin were acquired from AromaZone (Paris, France). VIVAPUR® CS TEX EASY, VITACEL® CS5 Apple powder and VITACEL® CF312 Citrus powder were kindly provided by JRS Retteinmaier (Rosenberg, Germany).

4.4.2 Plant material

Samples of different portions of Ghaf, including twigs, roots, leaves, and bark were harvested in September 2022 from multiple individuals in the United Arab Emirates. Flower and fruits were not collected, as these tissues were not available at the time of sampling. Each type of plant material was pooled by type and immediately freeze-dried after collection. The dried samples were homogenized using a Grindomix GM 200 knife mill (Retsch, Haan, Germany) and sieved (300–600 μm; Retsch AS 200) to obtain powders with uniform particle size distribution. However, a unified extraction approach was adopted to streamline the workflow and support future scale-up. Accordingly, after lyophilization, mechanical homogenization, and maceration of each plant component, the powders were combined into a single matrix representative of the whole plant. A final mass of 1 g was prepared (**Table 4.6**) by mixing the individual fractions in proportions reflecting their relative abundance in the sampled plant material (based on the dry weight obtained for each part). This whole-plant matrix was subsequently used for all extraction procedures reported in this study.

Table 4.6. Percentage and weight of final Ghaf unified powder.

Plant portion	Total weight (g) of obtained powders	Percentage of each portion on total (%)	Weight of each portion (g) used
Twigs	3.77	8.2	0.082
Roots	7.43	16.2	0.162
Leaves	32.01	70.0	0.700
Bark	2.53	5.5	0.055
Total	45.74	100	1

4.4.3 Sample preparation and extraction

The whole-Ghaf plant matrix (comprehensive of twigs, roots, leaves, and bark) thus obtained was subjected to ultrasound-assisted extraction using an ElmaSonic S 30H ultrasonic bath (Elma Schmidbauer GmbH, Singen, Germany). A 50% aqueous ethanol solution (v/v) was selected as extraction solvent due to its balanced polarity and established suitability for recovering a wide spectrum of bioactive metabolites, including phenolics (which are well known for their antioxidant properties) [28] [29], while maintaining low toxicity for subsequent biological assays [30] [31]. For the extraction, 1 g of plant powder was mixed with 40 mL of solvent (solid-to-solvent ratio 1:40, w/v) in a 50-mL polypropylene tube, which is commonly applied in metabolite profiling studies [32]. Ultrasonic extraction was performed at 25 °C for 15 min. To ensure exhaustive recovery of soluble compounds, the process was repeated several times with fresh solvent until colorless supernatant was obtained. After each cycle, the sample was centrifuged at 3112 × g for 5 min using a ROTINA 380R centrifuge (Hettich Zentrifugen, Germany), and the resulting supernatant was clarified by filtration through Whatman No. 1 filter paper (pore size 7–12 μm). The combined filtrates were then concentrated under reduced pressure at 40 °C using a Hei-VAP Core rotary evaporator (Heidolph, Germany) to remove ethanol. The aqueous residue was reconstituted in Milli-Q water and subjected to a second clarification step by centrifugation at 2375 × g for 10 min to isolate the water-soluble fraction. The resulting supernatant was subsequently lyophilized using an Alpha 1-4 LSCplus freeze dryer (Christ, Germany) to obtain dry extract for further characterization. The extraction yield was

determined by calculating the ratio of the weight of dried extract obtained to the initial weight of dried plant material powder and expressed as a percentage.

4.4.4 Extract characterization

The chemical characterization of Ghaf extract was performed in negative mode using a Thermo Scientific Vanquish UPLC system coupled with an Orbitrap Exploris 120 mass spectrometer (Thermo Scientific, Waltham, Massachusetts, USA). The compounds were separated using a 100 × 2.1 mm, 2.6 µm biphenyl column (Phenomenex, Torrance, California, USA). The mobile phase consisted of 0.1% (v/v) formic acid in water (A) and 0.1% (v/v) formic acid in acetonitrile (B) at a flow rate of 0.4 mL min−1. The following gradient was used: 5% B (0-1 min), 5-30% B (1-7 min), 30-60% B (7-15 min), 60% B (15-18 min), 60-95% B (18-28 min) with 5 minutes of washing (95% B) and 5 minutes of equilibration (5% B) after each run. The injection volume was 5 µL for each analysis and the column was set to 30°C. For positive ion mode, the spray voltage was set to 3400 V, while for negative ion mode it was set to −2500 V. The flow rates of the sheet gas and the auxiliary gas were set to 40 and 10 arb, respectively. The flow rate of the sweep gas was set to 2 arb. The ion transfer temperature was set to 325 °C and the vaporizer temperature to 350 °C. The full scan resolution was set to 60,000 with a scan range of m/z 100–1200 and the ddMS² resolution to 45,000. The dynamic exclusion duration was set to 8 seconds, with an intensity threshold of 4×10^5, and the collision energy was normalized to 30%. Metabolite identification followed the Metabolomics Standards Initiative (MSI) guidelines, which define three confidence levels indicated in the "IL" column of Table 4: Level 1 (IL1): compounds were unequivocally identified by comparison with authentic reference standards (retention time, MS/MS spectrum, and exact mass); Level 2 (IL2): tentative identifications were assigned based on matches between experimental MS/MS spectra and literature data or spectral libraries (e.g., GNPS, MassBank); Level 3 (IL3): compounds were classified by spectral similarity to known chemical families and supported by taxonomic evidence. Level 4 (IL4): unknown compounds.

4.4.5 Antioxidant capacity and Phytochemical content

4.4.5.1 DPPH Radical Scavenging Assay

The antioxidant capacity (AOC) of the Ghaf extract was quantified using the 1,1-diphenyl-2-picrylhydrazyl (DPPH•) radical scavenging assay. The extract was dissolved in ultrapure water and

tested over a concentration range of 1.25–20 µg/mL, while Trolox (0–75 µM) was used as calibration standard starting from a 5 mM stock solution in methanol, subsequently diluted to generate working standards. Ascorbic acid solution in ultrapure water was included as a positive control. A fresh 150 µM DPPH• solution was prepared in ethanol immediately before each experiment and protected from light due to the reagent's photosensitivity. All reactions were carried out in 96-well plates. For each measurement, 10 µL of sample, Trolox standard, or ultrapure water (blank) were added to 190 µL of the operative DPPH solution, reaching a final reaction volume of 200 µL. Plates were then incubated for 30 min at room temperature, under gentle orbital shaking (70 rpm) and protected from light. After incubation, absorbance was recorded at 517 nm using EnSight Multimode Microplate Reader (PerkinElmer, Waltham, MA,USA).

DPPH scavenging activity (%) was calculated after blank correction using the following equation (10):

$$DPPH\ scavengig\ activity\% = \left(1 - \frac{A_{sample}}{A_0}\right) * 100 \qquad (10)$$

where A_0 corresponds to the absorbance of the zero-Trolox standard (0 µM), and A_{sample} corresponds to the absorbance of the tested sample or Trolox concentration. A Trolox calibration curve was constructed by plotting the overmentioned activity % versus Trolox concentration (µM), yielding the equation (11):

$$Y = 0.979x + 3.0218\ (R^2 - 0.9791) \quad (11)$$

The antioxidant activity of the Ghaf extract was then converted into Trolox Equivalent Antioxidant Capacity (TEAC), by interpolating the scavenging activity of sample on the Trolox standard curve according to the following equation (12):

$$TEAC\ (\mu M\ TX) = \frac{(DPPH\ scavenging\ activity\ \%_{sample} - intercept)}{slope} \qquad (12)$$

where slope and intercept correspond to the linear regression parameter of the Trolox calibration curve. To normalize the antioxidant activity to the amount of tested material, TEAC values were further expressed as µmol Trolox equivalents per gram of extract (TE/g), by dividing the interpolated TEAC values by the corresponding extract concentration tested (g/L). This

normalization allows direct comparison of antioxidant capacity independently of the tested concentration.

4.4.5.2 Total phenolic content (TPC)

The total phenolic content of the Ghaf extract was quantified using the Folin–Ciocalteu method described by Dewanto et al. [33] in 48-well microplate-adapted, with minor modifications. The extract was solubilized in 80% methanol with sonication, and 62.5 µL of the resulting solution were added to each well, together with 250 µL of ultrapure water, yielding final extract concentrations ranging from 7.8 to 62.5 µg/mL. Wells containing water instead of extract served as negative controls. Subsequently, 62.5 µL of Folin–Ciocalteu reagent (2 N) were added, and the mixture was incubated for 5 min at room temperature. Then, 62.5 µL of 7% (w/v) sodium carbonate were added to initiate color development. Plates were incubated 90 min at room temperature in the dark, after which absorbance was measured at 760 nm using a microplate reader. A standard calibration curve was generated using gallic acid dissolved in 80% methanol at final concentrations of 0.24, 0.49, 0.98, 1.95, 3.91, 7.81, and 15.63 µg/mL, yielding the equation (13):

$$Y = 0.1071X + 0.0991 \ (R^2 = 0.9998) \quad (13)$$

Total phenol content was expressed as micrograms of gallic acid equivalents per milligram of extract (µg GAE/mg). Values are expressed as mean ± standard deviation of two independent experiments, each in technical triplicate. The assay relies on the reduction of the Folin–Ciocalteu reagent by phenolic compounds under alkaline conditions, producing a blue molybdenum–tungsten complex quantifiable spectrophotometrically.

4.4.6 *In vitro* enzymatic inhibition assays

4.4.6.1 Elastase inhibition assay

The inhibitory activity of the Ghaf extract against elastase (a serine protease involved in the degradation of elastin, a key component of the extracellular matrix) was evaluated using the following optimized spectrophotometric assay. The method is based on the ability of pancreatic porcine elastase to hydrolyze the synthetic chromogenic substrate N-Methoxysuccinyl-Ala-Ala-Pro-Val p-nitroanilide (MAAPVN), releasing *p*-nitroaniline (pNA), which can be quantified by measuring absorbance at 410 nm. A stock solution of MAAPVN (25 mg/mL) was prepared in

dimethylformamide (DMF) and subsequently diluted in Tris-HCl buffer (50 mM, pH 8.0) to obtain the working substrate solution (1.328 mg/mL). Porcine pancreatic elastase was prepared at a concentration of 0.375 U/mL in the same buffer. Assays were performed in 96-well microplates by mixing 10 µL of Ghaf extract aqueous solution with 20 µL of enzyme solution and 120 µL of buffer, resulting in final extract concentrations ranging from 12.5 to 400 µg/mL. The mixture was pre-incubated for 15 min at room temperature to allow interaction between the enzyme and the extract. Subsequently, 50 µL of the working substrate solution were added to initiate the reaction. After 15 min, absorbance at 410 nm was recorded using a microplate reader. Elastase activity (%) was calculated by comparing the absorbance of extract-treated wells with that of enzyme controls (without inhibitor). Oleanolic acid (OA) was included as a positive control.

4.4.6.2 Collagenase inhibition assay

The inhibitory activity of the Ghaf extract against collagenase was assessed using the following optimized microplate-based assay. The assay quantifies the ability of the extract to inhibit *Clostridium histolyticum* collagenase (ChC), which catalyzes the cleavage of the synthetic peptide N-[3-(2-furyl)acryloyl]-Leu-Gly-Pro-Ala (FALGPA). Hydrolysis of FALGPA results in a decrease in absorbance at 335 nm, enabling spectrophotometric monitoring of residual non-cleaved substrate. In a 96-well microplate, 30 µL of Ghaf extract aqueous solutions at concentrations ranging from 0.05 to 1.08 mg/mL were mixed with 20 µL of FALGPA 2mM, previously diluted in methanol from a 4.1971 mM stock, in 60 µL of assay buffer (50 mM tricine, 10 mM $CaCl_2$, 400 mM NaCl, pH 7.5). The plate was immediately placed in the microplate reader pre-equilibrated at 37°C, and the absorbance at 335 nm was recorded to determine the value corresponding to 0% activity (substrate in the absence of enzyme). Collagenase was then added by dispensing 10 µL of enzyme solution (1 U/mL in cold water, freshly prepared immediately before use) into each well. Following a 20 min incubation at 37°C, the absorbance at 335 nm was measured again. Enzymatic activity (%) was calculated by comparing the decrease in absorbance in extract-treated wells with that observed in enzyme-only control wells. Epigallocatechin gallate (EGCG) was used as positive control.

4.4.6.3 Hyaluronidase inhibition assay

The inhibitory effect of the Ghaf extract on hyaluronidase activity was evaluated using the following optimized turbidimetric assay. Hyaluronidase catalyzes the hydrolytic degradation of hyaluronic

acid (HA), a key glycosaminoglycan responsible for maintaining skin hydration, viscoelasticity, and structural integrity. In this assay, the remaining non-degraded HA reacts with an acidic bovine serum albumin (BSA) solution to form an insoluble precipitate whose turbidity is proportional to the amount of intact HA and can be quantified at 600 nm. 5 µL of Ghaf extract aqueous solutions were added to wells of a 48-well microplate and mixed with 100 µL of hyaluronidase type I-S (15 U/mL prepared in 20 mM sodium phosphate buffer containing 77 mM NaCl and 0.01% BSA, pH 7.0), yielding to Ghaf extract final concentrations ranging from 3.7 to 66 µg/mL. After a 10 min pre-incubation at 37 °C to allow interaction between the enzyme and the extracts, 100 µL of HA substrate solution (0.03% w/v dissolved in 300 mM sodium phosphate buffer, pH 5.35) were added to each well, followed by a 45 min incubation at 37°C. The reaction was terminated by adding 1 mL of acid albumin reagent (0.1% BSA, 24 mM sodium acetate, 79 mM acetic acid, pH 3.75). After a further 10 min incubation at RT, turbidity was measured at 600 nm using a spectrophotometric microplate reader. Increased absorbance reflects higher levels of remaining HA and therefore higher inhibition of hyaluronidase activity. Hyaluronidase activity (%) was calculated by comparing sample turbidity with that of the control conditions, where 0% activity corresponds to the turbidity of HA incubated in the absence of enzyme, and 100% activity corresponds to HA fully hydrolyzed by the enzyme (untreated condition). Oleanolic acid was used as positive control.

4.4.6.4 Human tyrosinase inhibition assay

Lyophilized Ghaf extract was dissolved in PBS and serially diluted to obtain concentrations ranging from 400 µg/mL to 0 µg/mL. Kojic acid (1.4 mg/mL to 0 mg/mL) was used as a positive control. Then, 20 µL of each Ghaf extract dilution (in PBS) and positive control (in DMSO) were dispensed in triplicate into a 96-well plate. The MNT-1 human melanoma cell line (highly pigmented) was lysed with PBS containing 0.1% Triton X-100. Subsequently, 90 µL of the MNT-1 lysate, diluted to 5×10^5 cells/mL in PBS, was added to each well. For blank controls (no-enzyme condition), 90 µL of PBS was added instead of lysate. Finally, 100 µL of L-DOPA substrate solution (4 mM in PBS) was added to each well. Absorbance was recorded in kinetic mode every 30 min for 18h at 478 nm (DOPAchrome formation) and 600 nm (eumelanin formation) by using Multiskan SkyHigh Microplate Spectrophotometer (ThermoFischerScientific, MA,USA). Enzyme activity was expressed as the percentage slope normalized to the untreated condition (no extract or positive control).

4.4.7 Cell lines and Culture Conditions

The immortalized human keratinocyte cell line HaCaT was purchased from AddexBio Technologies (San Diego, CA, USA), and the highly pigmented human melanoma cell line MNT-1 was kindly provided by AgroParisTech, Chaire de Cosmétologie (Orléans, France). HaCaT cells were cultured in high-glucose Dulbecco's Modified Eagle Medium (DMEM, ECB7501, Euroclone, Pero, Italy) supplemented with 10% heat-inactivated fetal bovine serum (FBS), 1% penicillin–streptomycin (P/S), and 2 mM L-glutamine. MNT-1 cells were maintained under the same conditions using DMEM (Gibco, 42430-025), which contains L-glutamine as supplied by the manufacturer. All cell lines were grown at 37 °C in a humidified incubator with 5% CO_2 and 95% air.

4.4.8 Cell viability assay

The cytotoxicity of Ghaf extract was investigated using the *in vitro* colorimetric MTS assay (CellTiter 96® AQ_{ueous} One Solution Cell Proliferation Assay, Promega, Madison, WI, USA) on an immortalized human keratinocyte cell line (HaCaT) following the manufacturer's protocol. This assay detects the mitochondrial cell activity, measuring the conversion of MTS by NADPH and NADH produced by dehydrogenase enzymes in soluble formazan product, whose absorbance can be recorded at 490 nm. Briefly, $5x10^3$ cells in 100 µL of growth medium were seeded in a 96-well microplate. After an incubation of 24 hours at 37°C in 5 % CO_2, the medium was removed and cells were treated with 9 extracts concentrations (0, 25, 50, 100, 140, 200, 270, 350 and 400 µg/mL). After 48 hours of incubation, the treated medium was replaced and 20 µL of MTS solution were added. After 2 hours at 37°C in 5 % CO_2, formazan product was detected by using a microplate reader at 490 nm. Cell viability was expressed as a mean percentage compared with the untreated cells and medium with MilliQ water at the same concentration (10% v/v) of extract-treated wells was used as blank.

4.4.9 Statistical analysis

Statistical analyses were conducted using one-way analysis of variance (ANOVA) followed by Tukey's honest significant difference (HSD) *post hoc* test. Data are presented as mean values ± standard deviation (SD). All tests assumed normal distribution and the statistical significance was considered when $p < 0.05$. Statistical analyses were performed by using GraphPad Prism (version 10.4.1).

4.4.10 Development and characterization of cosmetic emulsions

4.4.10.1 Cream formulation

Oil-in-water (O/W) Pickering emulsions (semisolid formulations) were formulated. The continuous water phase, together with potassium sorbate used as preservative and glycerin as humectant was prepared by mixing with a mechanical stirrer. A combination of vegetable oils (sunflower oil and plum oil) was employed as the dispersed phase (oil phase). Specific natural Pickering stabilizers were added in suitable phases according to their solubility. No heating step was applied during formulation. The water phase was gradually added to the oil phase, and emulsification was performed for 3 minutes at 10,000 rpm using the high-shear homogenizer POLYTRON® PT 10-35GT (Kinematica, AG, Switzerland). This procedure was followed for each emulsion, except for the ones involving VIVAPUR® CS TEX EASY that required a little adjustment. Specifically, this powder was pre-activated in water at 2000 rpm by using Hei-TORQUE Core mechanical stirrer (Heidolf, Schwabach, Germany). After a resting period of 15 minutes, the water phase was completed by adding the humectant and the preservative.

4.4.10.2 Development of base emulsion

4.4.10.2.1 Selection of ingredients

For the preliminary trials, water, glycerin, and potassium sorbate were selected as the water phase, while sunflower oil and plum oil were used as the oil phase. This formulation framework was adopted to explore different natural powders as potential Pickering stabilizers. Each emulsion was prepared following the procedure described in the section above, with VITACEL® CS5 Apple powder and VITACEL® CF312 Citrus powder added to the oil phase, and VIVAPUR® CS TEX EASY added to the water phase. The specific emulsions composition is summarized in **Table 4.7.**

Table 4.7 Composition (% w/w) of emulsions containing different powders as possible Pickering stabilizers; C: VITACEL® CF312 Citrus powder, A: VITACEL® CS5 Apple powder, V: VIVAPUR® CS TEX EASY and their corresponding combinations.

Ingredient	Phase	C+A	C	V+A	V
Demineralized water	Water	73.88	73.88	74.88	74.88
Glycerin	Water	5	5	5	5
Potassium sorbate	Water	0.2	0.2	0.2	0.2
VIVAPUR® CS TEX EASY	Water	-	-	3	4
Sunflower oil	Oil	8.17	10	10.5	10.5
Plum oil	Oil	4.08	5	5.5	5.5
VITACEL® CF312 Citrus powder	Oil	2.67	6	-	-
VITACEL® CS5 Apple powder	Oil	6	-	1	-

4.4.10.2.2 Design of experiment (DoE)

A response surface model, specifically a Central Composite Rotatable Design (CCRD), with two central points was generated using JMP statistical software (SAS Institute Inc., Cary, NC, USA). The concentration of VIVAPUR® CS TEX EASY (3–8% w/w) and the oil concentration (10–40% w/w) were selected as continuous factors (x variables). The response variable (y) was emulsion stability, assessed by physical stability measurements performed with Turbiscan analyzer. The software generated ten different combinations of the two independent variables (**Figure 4.15**). Each formulation was prepared and analyzed, and the resulting stability values of backscattering value at time zero (BS_0) were used to build a predictive linear regression model.

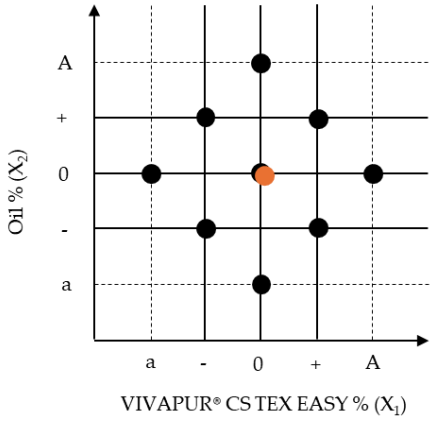

Figure 4.15. Graphical representation of the ten combinations VIVAPUR® CS TEX EASY % (X_1) and Oil % (X_2) generated by JMP statistical software according to Central Composite Rotatable Design (CCRD). "–" and "+" represent the lower and upper limits of the defined ranges, "a" and "A" correspond to axial points outside the range, and "0" indicates the central value.

4.4.10.3 Ghaf extract formulations

A formulation study was conducted to evaluate the physicochemical stability of the selected base emulsion containing the Ghaf extract obtained from hydroalcoholic extraction (50% EtOH/water). An aqueous solution of Ghaf extract was prepared at a concentration of 2 mg/mL and used as active ingredient. The extract solution was incorporated into the water phase at inclusion levels of 3%, 5%, and 10% (w/w), corresponding to final extract concentrations in the formulation of 60, 100, and 200 µg/mL, respectively (**Table 4.8**) prior to emulsification with the oil phase.

Table 4.8. Base emulsions (BE) percentage composition (% w/w) containing Ghaf extract as aqueous solution (2 mg/mL) at 3, 5, and 10% (w/w), yielding final extract concentrations of 60, 100, and 200 µg/mL, respectively.

Ingredient	Phase	BE + Ghaf 3%	BE + Ghaf 5%	BE + Ghaf 10%
Demineralized water	Water	82.52	80.52	75.52
Glycerin	Water	5.00	5.00	5.00
Potassium sorbate	Water	0.20	0.20	0.20
VIVAPUR® CS TEX EASY	Water	5.50	5.50	5.50
Ghaf solution 2mg/mL	Water	3.00	5.00	10.00
Sunflower oil	Oil	2.53	2.53	2.53
Plum oil	Oil	1.26	1.26	1.26

Each emulsion was then characterized in terms of organoleptic properties, physical stability, pH, accelerated stability, rheological behavior and droplet size distribution analysis.

4.4.10.4 Emulsions characterization

4.4.10.4.1 Organoleptic characteristics

Organoleptic properties of the emulsions, including appearance, odor, and color, were assessed under standardized conditions (fixed lighting, location, and black background). Evaluations were performed from immediately after preparation (t_0) up to 7 days of storage at room temperature. In addition, BE and emulsions containing Ghaf extract solution as active were stored at 4 °C, 25 °C, or 45 °C, and visual inspections were conducted at predefined time points to monitor possible changes in homogeneity, phase separation and color over time. Odor was evaluated by direct smelling, and color was recorded for each sample.

4.4.10.4.2 Physical stability

Physical stability was evaluated using a Turbiscan analyzer (Turbiscan™ LAB, Formulaction, France). A fixed volume of each emulsion was transferred into transparent glass vials and analyzed by static multiple light scattering. For the base emulsion (BE) and for emulsions containing the Ghaf extract solution as active ingredient, Turbiscan measurements were performed immediately after preparation (t_0) and after 1 h, 2 h, 24 h, 48 h, and 7 days. In addition, these samples were stored at 4 °C, 25 °C, and 45 °C, and analyzed at the same time intervals to evaluate their stability under different temperature conditions. In contrast, emulsions C+A, V+A, V, and those prepared according to the design of experiment (DoE) were analyzed only at room temperature immediately after preparation (t_0), in order to assess their initial dispersion state and phase homogeneity. Stability was assessed through the backscattering (BS%) profiles, plotted as backscattering intensity (%) as a function of sample height (mm) along the vial.

4.4.10.4.3 pH determination

The pH was measured after 24h of preparation at RT using a pH meter 1100L (VWR Phenomenal, Germany) calibrated with standard buffers at pH 4.0, 7.0, and 9.0. The electrode probe was directly immersed in the emulsion.

4.4.10.4.4 Centrifugation (accelerated stability) test

The accelerated stability of the ten emulsions prepared according to the design of experiment (DoE), BE and emulsions containing Ghaf extract solution as active was assessed by centrifugation. Around each 10 g of each emulsion was transferred into a Falcon tube and centrifugated at 4000 rpm for 30 minutes at 25°C. Phase separation or the appearance of distinct layers was evaluated visually after centrifugation.

4.4.10.4.5 Rheological behavior

Rheological properties of BE and emulsions containing Ghaf extract solution were studied using a Discovery HR-10 rheometer (TA Instruments, DE, USA) by placing each sample between a 40 mm diameter sandblasted plate. Two types of measurements were performed at 25°C: flow sweep analysis by setting shear rate ranging from 0.01 to 1000 s^{-1} to measure the viscosity profile and strain sweep oscillatory test performed at a fixed frequency of 1 Hz, with strain ranging from 0.01% to

1000% to investigate linear viscoelastic region (LVR) limits. For both analyses, samples were allowed to equilibrate for 3 minutes prior to measurement.

4.4.10.4.6 Droplet size distribution analysis

Droplet size distribution was measured for BE and emulsions containing Ghaf extract solution by using a SALD-2300 laser diffraction granulometer equipped with the SALD-MS23 Flow Cell with Sampler mode (Shimadzu, Japan). For each test, 2 g of emulsion were dispersed in either 18 g of water or 1% (w/v) SDS solution under magnetic stirring at room temperature for ~30 minutes until homogeneous dispersion was achieved. The suspension was then introduced dropwise into the flow cell. Measurements were conducted using the Fraunhofer optical model, suitable for micron-sized samples with unknown refractive indices (set to 3.00 – 0.20i). Each sample was analyzed in triplicate, at a light intensity corresponding to an absorbance of ~0.07. The software returned normalized droplet size distributions (µm), along with mean, mode, median, standard deviation, and D90 percentiles.

4.5 References

[1] S. Bom, J. Jorge, H. M. Ribeiro, and J. Marto, "A step forward on sustainability in the cosmetics industry: A review," Jul. 10, 2019, *Elsevier Ltd*. doi: 10.1016/j.jclepro.2019.03.255.

[2] S. Davinelli, J. C. Bertoglio, A. Polimeni, and G. Scapagnini, "Cytoprotective Polyphenols Against Chronological Skin Aging and Cutaneous Photodamage," *Curr. Pharm. Des.*, vol. 24, no. 2, pp. 99–105, Apr. 2018, doi: 10.2174/1381612823666171109102426.

[3] C. B. Steingass, M. P. Glock, R. M. Schweiggert, and R. Carle, "Studies into the phenolic patterns of different tissues of pineapple (Ananas comosus [L.] Merr.) infructescence by HPLC-DAD-ESI-MS n and GC-MS analysis," *Anal. Bioanal. Chem.*, vol. 407, no. 21, pp. 6463–6479, Aug. 2015, doi: 10.1007/s00216-015-8811-2.

[4] D. Bylund, S. H. Norström, S. A. Essén, and U. S. Lundström, "Analysis of low molecular mass organic acids in natural waters by ion exclusion chromatography tandem mass spectrometry," *J. Chromatogr. A*, vol. 1176, no. 1–2, pp. 89–93, Dec. 2007, doi: 10.1016/j.chroma.2007.10.064.

[5] T. Hofmann, E. Nebehaj, and L. Albert, "Antioxidant properties and detailed polyphenol profiling of European hornbeam (Carpinus betulus L.) leaves by multiple antioxidant capacity assays and high-performance liquid chromatography/multistage electrospray mass spectrometry," *Ind. Crops Prod.*, vol. 87, pp. 340–349, Sep. 2016, doi: 10.1016/j.indcrop.2016.04.037.

[6] V. Spínola and P. C. Castilho, "Phytochemical Profile, Chemotaxonomic Studies, and *In Vitro* Antioxidant Activities of Two Endemisms from Madeira Archipelago: *Melanoselinum decipiens* and *Monizia edulis* (Apiaceae)," *Chem. Biodivers.*, vol. 13, no. 10, pp. 1290–1306, Oct. 2016, doi: 10.1002/cbdv.201600039.

[7] J. Dou, V. S. Y. Lee, J. T. C. Tzen, and M.-R. Lee, "Identification and Comparison of Phenolic Compounds in the Preparation of Oolong Tea Manufactured by Semifermentation and Drying Processes," *J. Agric. Food Chem.*, vol. 55, no. 18, pp. 7462–7468, Sep. 2007, doi: 10.1021/jf0718603.

[8] J. Sun, F. Liang, Y. Bin, P. Li, and C. Duan, "Screening Non-colored Phenolics in Red Wines using Liquid Chromatography/Ultraviolet and Mass Spectrometry/Mass Spectrometry Libraries," *Molecules*, vol. 12, no. 3, pp. 679–693, Mar. 2007, doi: 10.3390/12030679.

[9] M. N. Clifford, S. Marks, S. Knight, and N. Kuhnert, "Characterization by LC-MS ^{n} of Four New Classes of *p* -Coumaric Acid-Containing Diacyl Chlorogenic Acids in Green Coffee Beans," *J. Agric. Food Chem.*, vol. 54, no. 12, pp. 4095–4101, Jun. 2006, doi: 10.1021/jf060536p.

[10] I. Parejo, O. Jáuregui, F. Viladomat, J. Bastida, and C. Codina, "Characterization of acylated flavonoid-*O* -glycosides and methoxylated flavonoids from *Tagetes maxima* by liquid chromatography coupled to electrospray ionization tandem mass spectrometry," *Rapid Communications in Mass Spectrometry*, vol. 18, no. 23, pp. 2801–2810, Dec. 2004, doi: 10.1002/rcm.1697.

[11] C. Dos Santos *et al.*, "Antioxidative, Antiproliferative and Antimicrobial Activities of Phenolic Compounds from Three Myrcia Species," *Molecules*, vol. 23, no. 5, p. 986, Apr. 2018, doi: 10.3390/molecules23050986.

[12] S. Gouveia and P. C. Castilho, "Characterisation of phenolic acid derivatives and flavonoids from different morphological parts of Helichrysum obconicum by a RP-HPLC–DAD-(−)–ESI-MSn method," *Food Chem.*, vol. 129, no. 2, pp. 333–344, Nov. 2011, doi: 10.1016/j.foodchem.2011.04.078.

[13] N. I. Tahir, K. Shaari, F. Abas, G. K. A. Parveez, Z. Ishak, and U. S. Ramli, "Characterization of Apigenin and Luteolin Derivatives from Oil Palm (*Elaeis guineensis* Jacq.) Leaf Using LC–ESI-MS/MS," *J. Agric. Food Chem.*, vol. 60, no. 45, pp. 11201–11210, Nov. 2012, doi: 10.1021/jf303267e.

[14] M. M. , E. A. , L. R. R. A. , A.-H. E. S. S. , K. S. A. , & H. S. R. Marzouk, "C-glycosyl flavonoids-rich extract of Dipcadi erythraeum Webb & Berthel. bulbs: Phytochemical and anticancer evaluations," *J. Appl. Pharm. Sci.*, vol. 9, no. 6, pp. 94–98, Jul. 2019, doi: 10.7324/JAPS.2019.90613.

[15] S. Pagliari *et al.*, "A comparative metabolomic investigation of different sections of Sicilian *Citrus x limon* (L.) Osbeck, characterization of bioactive metabolites, and evaluation of in vivo toxicity on zebrafish embryo," *J. Food Sci.*, vol. 89, no. 6, pp. 3729–3744, Jun. 2024, doi: 10.1111/1750-3841.17079.

[16] T. Hofmann, E. Nebehaj, and L. Albert, "Antioxidant properties and detailed polyphenol profiling of European hornbeam (Carpinus betulus L.) leaves by multiple antioxidant capacity assays and high-performance liquid chromatography/multistage electrospray mass spectrometry," *Ind. Crops Prod.*, vol. 87, pp. 340–349, Sep. 2016, doi: 10.1016/j.indcrop.2016.04.037.

[17] S. Pientaweeratch, V. Panapisal, and A. Tansirikongkol, "Antioxidant, anti-collagenase and anti-elastase activities of *Phyllanthus emblica* , *Manilkara zapota* and silymarin: an *in vitro* comparative study for anti-aging applications," *Pharm. Biol.*, vol. 54, no. 9, pp. 1865–1872, Sep. 2016, doi: 10.3109/13880209.2015.1133658.

[18] J. Wittenauer, S. Mäckle, D. Sußmann, U. Schweiggert-Weisz, and R. Carle, "Inhibitory effects of polyphenols from grape pomace extract on collagenase and elastase activity," *Fitoterapia*, vol. 101, pp. 179–187, Mar. 2015, doi: 10.1016/j.fitote.2015.01.005.

[19] A. Kumar, S. Kaur, P. L. Sangwan, and S. A. Tasduq, "Therapeutic and cosmeceutical role of glycosylated natural products in dermatology," *Phytotherapy Research*, vol. 37, no. 4, pp. 1574–1589, Apr. 2023, doi: 10.1002/ptr.7752.

[20] S. Burda and W. Oleszek, "Antioxidant and Antiradical Activities of Flavonoids," *J. Agric. Food Chem.*, vol. 49, no. 6, pp. 2774–2779, Jun. 2001, doi: 10.1021/jf001413m.

[21] H. LI, K. CHENG, C. WONG, K. FAN, F. CHEN, and Y. JIANG, "Evaluation of antioxidant capacity and total phenolic content of different fractions of selected microalgae," *Food Chem.*, vol. 102, no. 3, pp. 771–776, 2007, doi: 10.1016/j.foodchem.2006.06.022.

[22] S. Kumar, R. Sandhir, and S. Ojha, "Evaluation of antioxidant activity and total phenol in different varieties of Lantana camara leaves," *BMC Res. Notes*, vol. 7, no. 1, p. 560, Dec. 2014, doi: 10.1186/1756-0500-7-560.

[23] Y. Zhang, P. Cai, G. Cheng, and Y. Zhang, "A Brief Review of Phenolic Compounds Identified from Plants: Their Extraction, Analysis, and Biological Activity," *Nat. Prod. Commun.*, vol. 17, no. 1, Jan. 2022, doi: 10.1177/1934578X211069721.

[24] L. Mira, M. Tereza Fernandez, M. Santos, R. Rocha, M. Helena Florêncio, and K. R. Jennings, "Interactions of Flavonoids with Iron and Copper Ions: A Mechanism for their Antioxidant Activity," *Free Radic. Res.*, vol. 36, no. 11, pp. 1199–1208, Jan. 2002, doi: 10.1080/1071576021000016463.

[25] C. D. Papaemmanouil *et al.*, "ANTIAGE-DB: A Database and Server for the Prediction of Anti-Aging Compounds Targeting Elastase, Hyaluronidase, and Tyrosinase," *Antioxidants*, vol. 11, no. 11, p. 2268, Nov. 2022, doi: 10.3390/antiox11112268.

[26] E. Ersoy, E. Eroglu Ozkan, M. Boga, M. A. Yilmaz, and A. Mat, "Anti-aging potential and anti-tyrosinase activity of three Hypericum species with focus on phytochemical composition by LC–MS/MS," *Ind. Crops Prod.*, vol. 141, p. 111735, Dec. 2019, doi: 10.1016/j.indcrop.2019.111735.

[27] S. Yang, L. Liu, J. Han, and Y. Tang, "Encapsulating plant ingredients for dermocosmetic application: an updated review of delivery systems and characterization techniques," *Int. J. Cosmet. Sci.*, vol. 42, no. 1, pp. 16–28, Feb. 2020, doi: 10.1111/ics.12592.

[28] A. L. S. Oliveira, D. Valente, H. R. Moreira, M. Pintado, and P. Costa, "Effect of squalane-based emulsion on polyphenols skin penetration: Ex vivo skin study," *Colloids Surf. B Biointerfaces*, vol. 218, p. 112779, Oct. 2022, doi: 10.1016/j.colsurfb.2022.112779.

[29] A. M. Juncan, C. Morgovan, L.-L. Rus, and F. Loghin, "Development and Evaluation of a Novel Anti-Ageing Cream Based on Hyaluronic Acid and Other Innovative Cosmetic Actives," *Polymers (Basel).*, vol. 15, no. 20, p. 4134, Oct. 2023, doi: 10.3390/polym15204134.

[30] F. B. de Carvalho-Guimarães, K. L. Correa, T. P. de Souza, J. R. Rodríguez Amado, R. M. Ribeiro-Costa, and J. O. C. Silva-Júnior, "A Review of Pickering Emulsions: Perspectives and Applications," *Pharmaceuticals*, vol. 15, no. 11, p. 1413, Nov. 2022, doi: 10.3390/ph15111413.

[31] B. Hazt *et al.*, "Unconventional and conventional Pickering emulsions: Perspectives and challenges in skin applications," *Int. J. Pharm.*, vol. 636, p. 122817, Apr. 2023, doi: 10.1016/j.ijpharm.2023.122817.

[32] H. C. Lim *et al.*, "Mechanistic insights and clinical evidence of Helianthus annuus Linn. (Sunflower) seed oil for dermatological applications: A narrative review," *Drug Deliv. Transl. Res.*, vol. 15, no. 11, pp. 4260–4276, Nov. 2025, doi: 10.1007/s13346-025-01939-0.

[33] I. Savić-Gajić, I. Savić, N. Cekić, D. Đorđević, and M. Bogićević, "The valorization of plum seed oil for the development of topical formulation," *Advanced Technologies*, vol. 11, no. 1, pp. 22–31, 2022, doi: 10.5937/savteh2201022S.

[34] J. Qi, L. Song, W. Zeng, and J. Liao, "Citrus fiber for the stabilization of O/W emulsion through combination of Pickering effect and fiber-based network," *Food Chem.*, vol. 343, p. 128523, May 2021, doi: 10.1016/j.foodchem.2020.128523.

[35] C. Hollestelle, C. Michon, N. Fayolle, and D. Huc-Mathis, "Co-stabilization mechanisms of solid particles and soluble compounds in hybrid Pickering emulsions stabilized by unrefined apple pomace powder," *Food Hydrocoll.*, vol. 146, p. 109184, Jan. 2024, doi: 10.1016/j.foodhyd.2023.109184.

[36] M. Kowalska, M. Wozniak, A. Zbikowska, J. Okolus, and A. Molik, "Xanthan Gum and Microcrystalline Cellulose as Stabilizers in Emulsions Containing Catalytically Modified Animal and Vegetable Fat," *Catalysts*, vol. 15, no. 1, p. 41, Jan. 2025, doi: 10.3390/catal15010041.

[37] M. P. L. Sentis, G. Lemahieu, E. Hemsley, M. Bouzaid, and G. Brambilla, "Size distribution of migrating particles and droplets under gravity in concentrated dispersions measured with static multiple light scattering," *J. Colloid Interface Sci.*, vol. 653, pp. 1358–1368, Jan. 2024, doi: 10.1016/j.jcis.2023.09.163.

[38] D. D. Kaombe, M. Lenes, K. Toven, and W. R. Glomm, "Turbiscan as a Tool for Studying the Phase Separation Tendency of Pyrolysis Oil," *Energy & Fuels*, vol. 27, no. 3, pp. 1446–1452, Mar. 2013, doi: 10.1021/ef302121r.

[39] D. Huc-Mathis, G. Almeida, and C. Michon, "Pickering emulsions based on food byproducts: A comprehensive study of soluble and insoluble contents," *J. Colloid Interface Sci.*, vol. 581, pp. 226–237, Jan. 2021, doi: 10.1016/j.jcis.2020.07.078.

[40] C. Costa *et al.*, "Emulsion Formation and Stabilization by Biomolecules: The Leading Role of Cellulose," *Polymers (Basel).*, vol. 11, no. 10, p. 1570, Sep. 2019, doi: 10.3390/polym11101570.

[41] A. P. Goh, S. Goh, W. Tow, K. Toh, U. D. Palanisamy, and U. Sundralingam, "Exploring the Role of Herbal Compounds in Skin Aging: A Systematic Review of Topical Approaches," *Phytotherapy Research*, vol. 39, no. 1, pp. 315–363, Jan. 2025, doi: 10.1002/ptr.8375.

[42] R. Pandiselvam *et al.*, "The influence of non-thermal technologies on color pigments of food materials: An updated review," *Curr. Res. Food Sci.*, vol. 6, p. 100529, 2023, doi: 10.1016/j.crfs.2023.100529.

[43] M. Lukić, I. Pantelić, and S. D. Savić, "Towards Optimal pH of the Skin and Topical Formulations: From the Current State of the Art to Tailored Products," *Cosmetics*, vol. 8, no. 3, p. 69, Aug. 2021, doi: 10.3390/cosmetics8030069.

[44] C. Janssens-Böcker, C. Doberenz, M. Monteiro, and M. de Oliveira Ferreira, "Influence of Cosmetic Skincare Products with pH < 5 on the Skin Microbiome: A Randomized Clinical Evaluation," *Dermatol. Ther. (Heidelb).*, vol. 15, no. 1, pp. 141–159, Jan. 2025, doi: 10.1007/s13555-024-01321-x.

[45] E. Lee, D. Kim, and K. Kim, "Distinctive rheological properties of Pickering emulsions: from their origin to the applications," *Korea-Australia Rheology Journal*, vol. 34, no. 2, pp. 91–103, May 2022, doi: 10.1007/s13367-022-00018-x.

5 Phytochemical composition of *A. marina* extracts and investigation of antioxidant and *in vitro* cytotoxic potential

This chapter was adapted and modified from the following published work:

Cerri, F.†, De Santes, B.†, Spena, F.†, Salvioni, L., Forcella, M., Fusi, P., Pagliari, S., Stahl, H., Galli, P., Colombo, M., Giustra, M., Campone, L. (2025). Phytochemical profiling, antioxidant activity, and *in vitro* cytotoxic potential of Mangrove *Avicennia marina*. *Pharmaceuticals, 18(9), 1308,* †equal contribution**.**

5.1 Abstract

Avicennia marina (Forsk.) Vierh., a widely distributed mangrove species, is known for its diverse secondary metabolites with potential pharmacological applications[1]. Despite its dominance in the Arabian Gulf, where *A. marina* may have adapted to extreme environmental conditions with a distinct set of bioactive molecules, research in this region remains limited. Even though *A. marina* was initially selected together with Ghaf as potential natural anti-aging ingredients for this PhD project, the results obtained from preliminary screening did not justify pursuing the same formulation-driven development pathway adopted for Ghaf. Consequently, a parallel bioprospecting-oriented strategy was undertaken to further valorize *A. marina* by exploring alternative biological applications.

Therefore, this chapter is focused on the investigation of the phytochemical composition, antioxidant activity, and *in vitro* cytotoxicity of extracts from different plant parts, including roots, leaves, propagules, pericarps, and cotyledons, collected in the United Arab Emirates. Extracts were analyzed using ultra-pressure liquid chromatography coupled with high-resolution mass spectrometry (UPLC-HRMS). Antioxidant activity was assessed using DPPH and ABTS assays, while cytotoxicity was evaluated against human cancer and normal cell lines. Analysis revealed 49 compounds, including iridoid glycosides, hydroxycinnamic acids, phenylethanoid glycosides, flavonoid glycosides, and triterpene saponins, several reported for the first time in *A. marina* and mangroves. The pericarp and root extracts exhibited the highest scavenging activity (DPPH: 187.14 ± 2.87 and 128.25 ± 1.12; ABTS: 217.16 ± 2.67 and 147.21 ± 2.42 μmol TE/g, respectively), correlating with phenylethanoid content. The root extract also displayed the highest cytotoxicity, with IC_{50} values of 58.46, 81.98, and 108.10 μg/mL against MDA-MB-231, SW480, and E705, respectively. *In silico* analysis identified triterpene saponins as potential contributors. Overall, these findings

highlight *A. marina*, and particularly its root extract, as a promising source of bioactive compounds with antioxidant and anticancer potential, supporting its further investigation as a reservoir of novel therapeutic candidates beyond cosmetic applications.

5.2 Results

5.2.1 Characterization of *Avicennia marina* extracts

This characterization was kindly performed in collaboration with the FoodNutraLab Research Group of the University of Milano-Bicocca.

To investigate the bioprospecting potential of *A. marina* from the Arabian Gulf, a comprehensive UHPLC–ESI–HRMS analysis was performed on hydroalcoholic extracts obtained from different plant portions. Roots, leaves, cotyledons, pericarps, and propagules of *A. marina* displayed distinct metabolite profiles. The chromatographic profiles of the extracts are provided in *Supplementary informations* (**Figure S1.1-S1.5**), and the list of tentatively identified compounds is shown in **Table 5.1**, along with their corresponding identification level (IL), which reflects the confidence of compound annotation based on MSI guidelines (*Section 5.5.4*). For compounds assigned to IL2, the identification relied on comparisons of MS/MS fragmentation data with published spectra from the literature or spectral databases. The specific references used to support each IL2 assignment are included directly in the table.

Table 5.1. UHPLC-ESI/HRMS data of compounds detected in *Avicennia marina* extracts. The main fragmention for each compound is indicated in bold.

No.	RT (min)	$[M-H]^-$	Formula	Δ ppm	MS/MS	Name	Class	Part	IL	Ref.
1	0.58	701.1893 $[M+Cl]^-$	$C_{24}H_{42}O_{21}$	−2.1677	665.2134, 485.1499, 443.1393, **383.1182**, 341.1075, 179.0549	Stachyose	Tetrasaccharides	Cotyledons/pericarps /propagules/roots	IL2	[2]
2	0.99	191.0188	$C_6H_8O_7$	6.3850	111.0073	Citric acid	Tricarboxylic acids	Cotyledons/pericarps	IL2	[3]
3	3.87	373.1139	$C_{16}H_{22}O_{10}$	0.3221	211.0605, 167.0700, 149.0597, **123.0440**, 105.0333	Geniposidic acid	Iridoid glycosides	Leaves/cotyledons/pericarps/propagules/roots	IL2	[4]

4	4.03	353.0875	$C_{16}H_{18}O_9$	0.8633	**191.0551**, 179.0339, 161.0233, 135.0439	Caffeoylquinic acid isomer	Hydroxycinnamic acids and derivatives	Roots	IL2	[5]
5	4.05	375.1291	$C_{16}H_{24}O_{10}$	1.5167	213.0756, 169.0857, **151.0753**, 133.0644, 125.0595, 107.0490	Mussaenosidic acid	Iridoid glycosides	Leaves/cotyledons/pericarps/propagules	IL2	[6]
6	4.33	375.1285	$C_{16}H_{24}O_{10}$	3.1119	213.0747, 169.0854, **151.0748**, 133.0644, 125.0591, 113.0230, 107.0484	(Epi)loganic acid	Iridoid glycosides	Leaves	IL2	[6]
7	4.53	487.1451	$C_{21}H_{28}O_{13}$	1.2588	**179.0334**, 161.0228, 135.0435	Cistanoside F	Phenylethanoid glycosides	Pericarps	IL2	[7]
8	4.80	327.0715	$C_{14}H_{16}O_9$	1.9983	179.0335, 165.0389, 147.0283, **135.0434**, 105.0178	Unidentified	-	Leaves		
9	5.09	353.0871	$C_{16}H_{18}O_9$	−3.0904	**191.0550**, 179.0337, 173.0442, 161.0232, 135.0439**,**	Caffeoylquinic acid isomer	Hydroxycinnamic acids and derivatives	Leaves/cotyledons/pericarps/propagules/roots	IL2	[5]
10	5.47	371.0982	$C_{15}H_{16}O_{11}$	−8.7858	**209.0635**, 179.0337, 161.0228, 135.0435, 129.0178	Caffeoyl hexaric acid	Hydroxycinnamic acids and derivatives	Leaves	IL2	[47][8]
11	5.60	443.0655	$C_{18}H_{20}O_{11}S$	−0.3243	275.0218, **167.0338**, **152.0105**, 123.0440, 108.0204	Unidentified	-	Roots		
12	5.65	415.1603	$C_{19}H_{28}O_{10}$	1.6114	235.0963, **191.1062**, 173.0958, 149.0953, 137.0590, 101.0226	Icariside D1	Flavonoid glycosides	Leaves	IL2	[48][9]
13	5.93	639.1964	$C_{29}H_{36}O_{16}$	−5.2193	621.1807, 529.1554, 459.1488, 251.0549, 179.0337, **161.0232**, 151.0387	Suspensaside isomer	Phenylethanoid glycosides	Pericarps/roots	IL2	[10][11]
14	5.95	639.1964	$C_{29}H_{36}O_{16}$	−5.2193	621.1807, 529.1554, 459.1488, 251.0549, 179.0337, **161.0232**, 151.0387	Suspensaside isomer	Phenylethanoid glycosides	Pericarps/roots	IL2	[10][11]

15	6.14	537.1628	$C_{25}H_{30}O_{13}$	−2.6672	493.1708, 375.1275, 323.0758, 213.0752, 179.0334, 169.0854, **161.0230**, 151.0750, 135.0435, 125.0593, 107.0486	Grandifloroside	Hydroxycinnamic acid and derivatives	Leaves	IL2	[12]
16	6.33	619.1644	$C_{29}H_{32}O_{15}$	3.9407	383.0758, **311.0549**, 267.0646	Unidentified	-	Pericarps/roots		
17	6.41	639.1929	$C_{29}H_{36}O_{16}$	0.2477	**621.1817**, 529.1554, 459.1493, 251.0549 **179.0338**, 161.0236, 151.0385	Suspensaside isomer	Phenylethanoid glycosides	Roots	IL2	[10][11]
18	6.65	521.1658	$C_{25}H_{30}O_{12}$	1.2446	357.1176, 169.0854, 163.0385, 151.0749, 145.0280, 125.0591, 119.0486, 117.0329, 107.0486	Marinoid C	Iridoid glycosides	Leaves/cotyledons/pericarps	IL3	[13]
19	6.65	653.2091	$C_{29}H_{34}O_{17}$	9.55333	621.1822, 459.1499, 179.0338, **161.0234**, 151.0388, 135.0437	Suspensaside methyl ether	Phenylethanoid glycosides	Roots	IL2	[10][11]
20	6.79	623.1981	$C_{29}H_{36}O_{15}$	0.0705	461.1657, **161.0233**, 113.0283	Verbascoside (acteoside) isomer	Phenylethanoid glycosides	Leaves/pericarps/roots	IL2	[14]
21	6.9	463.0874	$C_{21}H_{20}O_{12}$	1.7229	301.0324, **300.0264,** 271.0235, 255.0285	Quercetin 3-*O*-hexoside	Flavonoid glycosides	Roots	IL2	[15][16] [17]
22	7.02	667.2239	$C_{31}H_{40}O_{16}$	0.6864	621.1824, 459.1499, **179.0338**, **161.0235**, 151.0386, 135.0436	β-ethyl-OH-verbascoside	Phenylethanoid glycosides	Pericarps	IL2	[18][19]
23	7.11	623.2001	$C_{29}H_{36}O_{15}$	−3.1336	461.1661, **161.0235**,	Verbascoside (acteoside) isomer	Phenylethanoid glycosides	Leaves/pericarps/roots	IL2	[25]
24	7.21	621.1838	$C_{29}H_{34}O_{15}$	−2.0992	461.1652, 179.0337, **161.0233**, 151.0387	Suspensaside A	Phenylethanoid glycosides	Roots	IL2	[49,50][10][11]
25	7.21	461.0718	$C_{21}H_{18}O_{12}$	1.6222	**285.0391**	Kaempferol-3-*O*-glucuronide	Flavonoid glycosides	Leaves	IL2	[20]

26	7.21	681.2063	$C_{31}H_{38}O_{17}$	−3.9236	519.1708, 490.1321, 181.0129, 179.0334, **161.0230**	Unidentified	-	Pericarps		
27	7.3	447.0926	$C_{21}H_{20}O_{11}$	1.5287	327.0494, 285.0648, **284.0315**, 255.0288, 227.0338, 151.0013	Kaempferol 3-*O*-glucoside	Flavonoid glycosides	Roots	IL2	[16][21] [22][23]
28	7.40	623.1658	$C_{28}H_{32}O_{16}$	−6.4750	**315.0494**, 314.0421, 300.0258, 299.0187, 271.0234	Isorhamnetin-3-*O*-rutinoside	Flavonoid glycosides	Leaves/pericarps	IL2	[24]
29	7.40	491.0828	$C_{22}H_{20}O_{13}$	0.6385	**315.0499**, 300.0264	Isorhamnetin glucuronide	Flavonoid glycosides	Leaves	IL2	[25]
30	7.51	535.1477	$C_{25}H_{28}O_{13}$	−3.7032	329.1021, **179.0338**, 161.0232, 149.0595, 135.0438	Unidentified	-	Leaves/Pericarps		
31	7.51	477.1036	$C_{22}H_{22}O_{12}$	−5.1250	315.0467, **314.0420**, 285.0392, 271.0236, 257.0441, 243.0286,	Isorhamnetin 7-glucoside	Flavonoid glycosides	Leaves	IL2	[25]
32	7.61	471.1874	$C_{22}H_{32}O_{11}$	−0.4545	287.1273, **263.1278**, 219.1379, 201.1273, 186.1036, 147.1166	Unidentified	-	Pericarps		
33	7.86	519.1143	$C_{24}H_{24}O_{13}$	0.2199	315.0472, **314.0423**, 299.0186, 285.0383, 271.0236, 257.0443, 243.0286	Unidentified	-	Leaves		
34	7.90	553.1556	$C_{25}H_{30}O_{14}$	1.2256	329.1021, **197.0445**, 182.0206, 153.0454, 149.0596, 131.0489,	Marinoid D	Iridoid glycosides	Cotyledons/pericarps /propagules/roots	IL3	[13]
35	7.95	505.1757	$C_{25}H_{29}O_{11}$	0.2000	357.1184, 213.0757, 195.0650, 169.0857, 151.0753, **147.0439**, 125.0596, 113.0230, 107.0487, 103.0539	Marinoid A	Iridoid glycosides	Leaves	IL3	[13]
36	8.03	519.1505	$C_{25}H_{28}O_{12}$	0.5766	313.1072, 295.0961, **163.0388**, 149.0596, 145.0282, 131.0490, 119.0487	Unidentified	-	Leaves/cotyledons/pericarps/roots		

37	8.03	475.0887	$C_{22}H_{20}O_{12}$	−1.0510	300.0589, **299.0554**, 285.0358, **284.0318.**	Diosmetin 7-glucuronide	Flavonoid glycosides	Leaves	IL2	[26]
38	8.24	549.1616	$C_{26}H_{30}O_{13}$	−0.4279	343.1176, 325.1064, **193.0495**, 175.0387, 149.0595, 134.0360, 131.0489	Unidentified	-	Leaves/cotyledons/pericarps/roots		
39	8.36	591.2119	$C_{29}H_{36}O_{13}$	−6.0539	179.0333, **161.0234**, 133.0282, 113.0228	Jionoside C	Phenylethanoid glycosides	Pericarps	IL2	[27]
40	8.62	825.4276	$C_{44}H_{66}O_{16}$	0.2536	**663.3744**, 601.3735	Unknown triterpene saponin	Triterpene saponins	Roots	IL3	[28][29]
41	8.70	539.2152	$C_{26}H_{36}O_{12}$	−3.3318	193.0485, 183.1010, 175.0382, 149.0591, 131.0485, 121.0642	Unidentified	-	Leaves		
42	8.80	541.2285	$C_{26}H_{38}O_{12}$	1.0147	193.0485, 185.1166, 175.0382, 149.0591, 131.0485, 121.0642	Unidentified	-	Leaves		
43	8.88	825.4285	$C_{42}H_{66}O_{16}$	−0.8354	**663.3744**, 601.3735, 487.3421	Unknown triterpene saponin	Triterpene saponins	Roots	IL3	[28][29]
44	8.97	299.0546	$C_{16}H_{12}O_6$	5.0379	285.0345, **284.0313**, 256.0363, 227.0334	Trihydroxy-methoxyflavone	Flavones	Leaves	IL2	[30]
45	8.99	825.4273	$C_{42}H_{66}O_{16}$	0.6166	**663.3744**, 601.3735,	Medicoside G (medicagenic acid 3,28-di-glucoside)	Triterpene saponins	Roots	IL2	[28][29]
46	9.08	809.4316	$C_{42}H_{66}O_{15}$	1.5979	689.3884, **647.3788**, 629.3680, 585.3786	Esculentoside C (phycolaccoside D)	Triterpene saponins	Cotyledons/pericarps/propagules/roots	IL2	[31][32]
47	9.30	505.1711	$C_{25}H_{30}O_{11}$	0.8600	281.1170, 195.0649, 151.0750, **147.0438**, 133.0645, 107.0486	Unidentified	-	Leaves		
48	9.38	503.1572	$C_{25}H_{28}O_{11}$	−2.6077	279.1010, 253,0854, 209.0954, 195.0647,	Unidentified	-	Leaves/pericarps		

					147.0437, 131.0486, 103.0536					
49	9.54	809.4342	$C_{42}H_{66}O_{15}$	−1.6102	**647.3797**, 471.3469	Azukisaponin III	Triterpene saponins	Roots	IL2	[33]

Analysis detected a total of 49 compounds across all plant parts. Triterpene saponins are a heterogeneous secondary metabolite consisting of a terpene-based aglycone linked to one or more sugar chains, commonly glucose (−162 Da), glucuronic acid (−176 Da), and pentoses (−146 Da) [34]. For example, compound 49, which has an m/z of 809.4342 and a molecular formula of C42H66O15, displayed characteristic MS/MS fragments at m/z 647.3797 [M-H-162] and 471.3469 [M-H-162-176], corresponding to sequential losses of sugar moieties. Based on this fragmentation and the molecular formula, it was identified as Azukisaponin III. Using similar fragmentation patterns, compounds 40, 43, 45, and 46 were also assigned as triterpene saponins[28], [29], [31], [32], [33]. Phenylethanoid glycosides are often based on β-D-glucosides of 2-phenylethanol, often with α-L-rhamnose (Rha) substitution at C-3′ of the glucose, resembling variants of verbascoside [35]. Simple phenylethanoid glycosides such as acteoside, isoacteoside, and plantamajoside exhibit similar fragmentation patterns in MS/MS experiments. These are characterized by neutral losses of 162, 152, or 146 m/z, which are associated with the presence of caffeic acid, glucose, rhamnose, and the phenethanol aglycone. Diagnostic fragment ions at m/z 179, 161, and 135 indicate the presence of caffeoyl, anhydroglucose, and anhydrophenethanol. Additionally, losses of water (−18 Da) or CO2 (−44 Da) are frequently observed [36]. Based on this information, the compounds 7, 13, 14, 17, 20, 22, 23, 24, and 39 belonged to the phenylethanoid glycosides group. Flavonoid glycosides are a group of secondary metabolites that are widely distributed throughout the plant kingdom. Depending on the bond of the sugar portion, they are divided into O-glycosides or C-glycosides and can be distinguished by their unique MS/MS fragmentation spectra, which depend on the nature of the sugar fraction. Generally, C glycosides exhibit neutral losses of 30, 90, and 120 Da for hexose sugars; 74 and 104 Da for deoxyhexose sugars; and 60 Da for pentose sugars. In contrast, O-glycosides exhibit neutral losses of 162 Da (hexose sugars), 176 Da (glucuronic acid), 146 Da (deoxyhexose sugars), and 132 Da (pentose sugars) [37]. Based on this information, compounds 12, 21, 25, 27, 28, 29, 31, and 37 were identified as O-glycosides. Iridoid glycosides exhibit distinct fragmentation

patterns that depend on the structure of the aglycone ring, the presence of functional groups, and the degree of unsaturation. Typically, a neutral loss of 162 Da is observed, corresponding to the breakage of the bond with the glucoside fraction. Subsequently, the formation of fragments due to the loss of water (18 Da) and the carboxyl group (44 Da) is also observed, together with characteristic fragments resulting from aglycone ring cleavage. Peak 3 with m/z 373.1139 and molecular formula C16H22O10 was identified as geniposidic acid based on its MS/MS spectrum. Fragment m/z 211.0605 corresponded to the loss of hexose sugar (162 Da), followed by the presence of fragments m/z 167.0700 and 149.0597, reflecting subsequent losses of H2O (−18 Da) and CO2 (−44 Da), respectively [38]. Furthermore, fragment 123.0440 is characteristic of the genistein ring. Based on the different fragmentation patterns, compounds 5, 6, 18, 34, and 35 were identified as iridoid glycosides. Tissue-specific profiling revealed clear metabolic differentiation among parts, with the leaves containing the highest number of secondary metabolites (26), followed by the pericarps (23), roots (23), cotyledons (10), and propagules (6). Notably distinct distribution patterns were observed for specific classes of compounds across the different *A. marina* extracts. The results show that triterpene saponins occur almost exclusively in the root extract (five in roots and only one each in cotyledons, pericarps, and propagules; none in leaves). Phenylethanoid glycosides were predominantly found in root and pericarp extracts (seven in each), with only two detected in leaves and none in cotyledons and propagules. Flavonoid glycosides were mainly associated with leaf extract (six in leaves, two in roots, one in pericarps, and absent in cotyledons and propagules). In contrast, iridoid glycosides and hydroxycinnamic acid and derivatives showed a more uniform distribution across all the extracts. Analysis confirmed several compounds previously reported in *A. marina*, including caffeoylquinic acid, geniposidic acid, marinoid A, C, and D, acteoside, quercetin 3-O-hexoside, kaempferol 3-O-glucuronide, isorhamnetin-3-O-rutinoside, diosmetin 7-glucuronide, and jionoside C [13], [39], [40], [41], [42] Additionally, cistanoside F and kaempferol 3-O-glucoside were also detected, previously reported in other mangrove species but not in *A. marina* [43], [44]. To our knowledge, several compounds such as mussaenosidic acid, (epi)loganic acid, caffeoylglucaric acid, icariside D1, suspensaside, grandifloroside, suspensaside methyl ether, suspensaside A, isorhamnetin glucuronide, isorhamnetin 7-glucoside, medicoside G, esculentoside C, and azukisaponin III have been newly reported in mangrove species.

5.2.2 Antioxidant activity

5.2.2.1 DPPH and ABTS assays

The antioxidant activity of *A. marina* extracts was evaluated using DPPH and ABTS assays, two spectrophotometric assays widely used to assess the free radical scavenging activity of natural compounds. The results are shown in **Figure 5.1**.

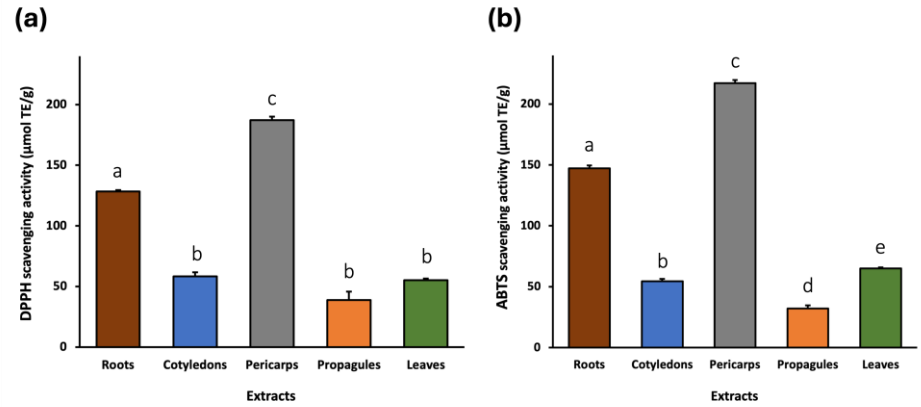

Figure 5.1. DPPH (a) and ABTS (b) radical scavenging activity of *A. marina* extracts expressed as µmol Trolox equivalents per gram of sample matrix (µmol TE/g). The bars represent the mean ± standard deviation (SD) from n = 3 independent experiments. Different lowercase letters indicate statistically significant differences between extracts ($p < 0.05$).

The DPPH assay showed that the pericarp extract exhibited the highest radical scavenging activity, with a Trolox equivalent antioxidant capacity (TEAC) value of 187.14 ± 2.87 µmol TE/g. This was followed by the extracts of root (128.25 ± 1.12 µmol TE/g), cotyledon (58.23 ± 3.49 µmol TE/g), leaf (55.12 ± 1.52 µmol TE/g), and propagule (38.72 ± 6.96 µmol TE/g). Similarly, the ABTS assay (Figure 22.b) confirmed that the root and pericarp extracts exhibit high antioxidant activity compared to the other parts of the plant. In fact, the pericarp extracts again displayed the highest TEAC value (217.16 ± 2.67 µmol TE/g), followed by the root (147.21 ± 2.42 µmol TE/g), leaf (64.98 ± 0.84 µmol TE/g), cotyledon (54.46 ± 1.95 µmol TE/g), and propagule (32.23 ± 2.53 µmol TE/g) extracts.

5.2.2.2 Correlation Between Compound Classes and Antioxidant Activity

The pericarp and root extracts, which exhibited the highest antioxidant activity, are also the ones that contain a high number of phenylethanoid glycosides, compared to the other extracts, which may explain their higher activity. To explore the potential associations between the phytochemical

composition of each extract and their antioxidant capacity, a Spearman correlation analysis was performed between the number of compounds in each major chemical class and the measured antioxidant activities (DPPH and ABTS assay) across the five plant-part extracts (n = 5) (**Table 5.2**). The analysis revealed a significant positive correlation between the number of phenylethanoid glycosides in the extracts and DPPH activity ($\varrho = 0.949$; $p = 0.014$). ABTS activity showed a similar trend, though the correlation did not reach statistical significance ($\varrho = 0.791$; $p = 0.111$). Antioxidant activity showed no statistically significant correlations with the number of other classes of compounds, including flavonoid glycosides, iridoid glycosides, hydroxycinnamic acids and derivatives, and triterpene saponins (all $p > 0.05$). Given the small sample size and the use of compound counts (not concentrations), these associations should be considered exploratory.

Table 5.2. Spearman correlation coefficients (ϱ) between the number of compounds per chemical class and the antioxidant activity (DPPH and ABTS assays). Statistically significant correlations are indicated in bold (*p* value < 0.05).

Compound Class	DPPH		ABTS	
	ϱ-Value	***p*-Value**	***p*-Value**	***p*-Value**
Iridoid glycosides	−0.103	0.870	0.510	0.935
Hydroxycinnamic acid and derivatives	−0.112	0.858	0.224	0.718
Phenylethanoid glycosides	0.791	0.111	0.949	**0.014**
Flavonoid glycosides	0.205	0.741	0.574	0.322
Triterpene saponins	0.447	0.450	0.224	0.718

5.2.3 *In Vitro* Cytotoxic Activity

The cytotoxic effects of *A. marina* extracts (leaf, cotyledon, pericarp, propagule, and root) were evaluated against a panel of human cancer cell lines using the MTT assay. Four concentrations (20, 60, 180, and 540 μg/mL) were tested on two colorectal cancer cell lines (SW480 and E705) (**Figure 5.2**) and three additional cancer cell lines: MDA-MB-231 (triple-negative breast cancer), U-87 (glioblastoma), and HeLa (cervical cancer) (**Figure 5.3**). Furthermore, two non-cancerous cell lines,

MRC-5 (normal human fibroblasts) and CCD 841 (healthy human mucosa), served as controls to assess extract selectivity (**Figure 5.4**). The complete data for all concentrations and cell lines are reported in **Table S1.**

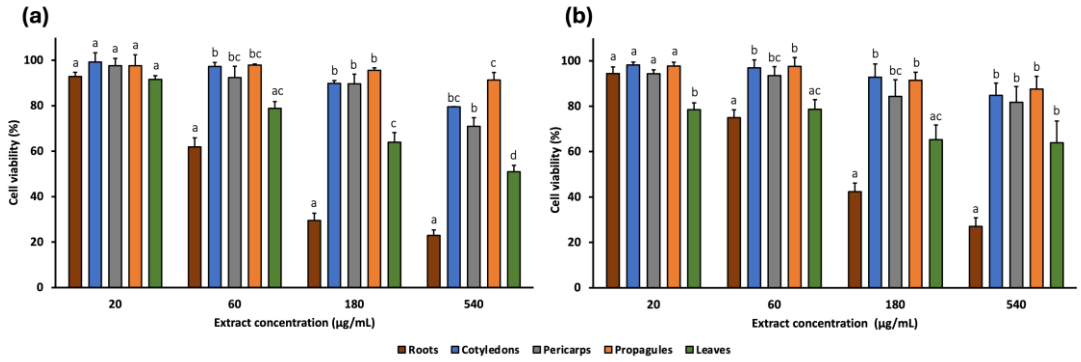

Figure 5.2. Cell viability (%) of SW480 (a) and E705 (b) human colorectal cancer cell lines treated with *A. marina* extracts (20–540 µg/mL) for 48 h. Bars represent mean ± standard error of the mean (SEM) from n = 3 independent experiments. Different lowercase letters indicate statistically significant differences between extracts ($p < 0.05$) and were assigned independently for each concentration.

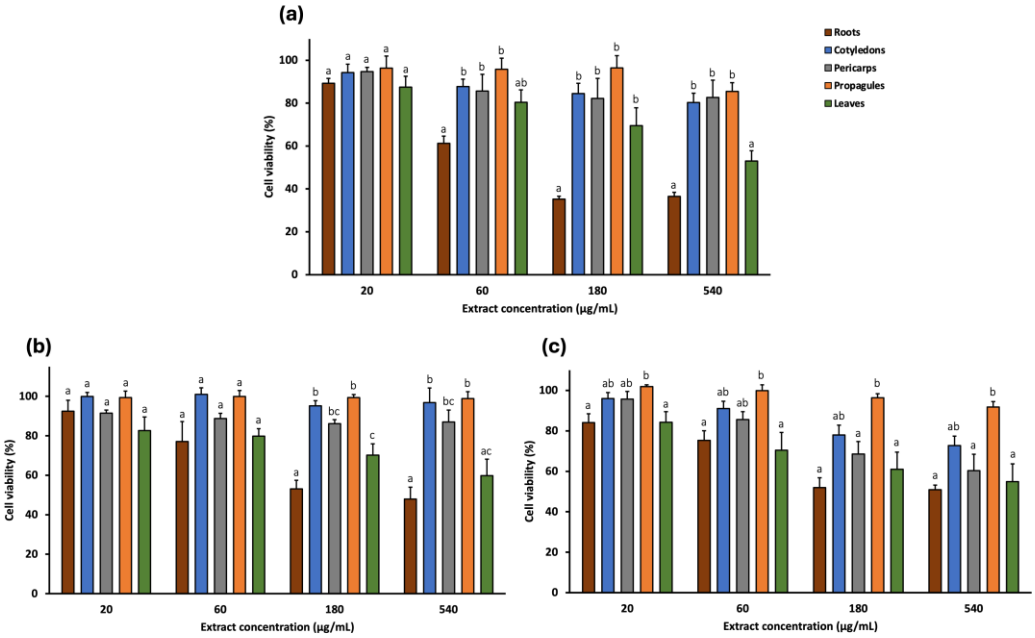

Figure 5.3. Cell viability (%) of MDA-MB-231 (a), U-87 (b), and HeLa (c) human cancer cell lines treated with *A. marina* extracts (20–540 µg/mL) for 48 h. Bars represent mean ± standard error of the mean (SEM)fromn=3independentexperiments. Different lowercase letters indicate statistically significant differences between extracts ($p < 0.05$) and were assigned independently for each concentration.

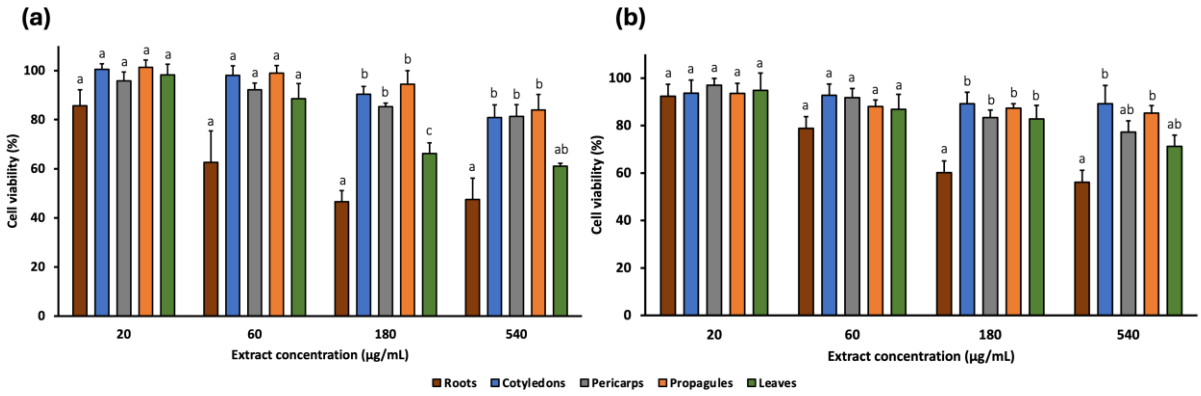

Figure 5.4. Cell viability (%) of CCD 841 (**a**) and MRC-5 (**b**) healthy human cell lines treated with *A. marina* extracts (20–540 µg/mL) for 48 h. Bars represent mean ± standard error of the mean (SEM) from n = 3 independent experiments. Different lowercase letters indicate statistically significant differences between extracts ($p < 0.05$) and were assigned independently for each concentration.

Among the extracts, cotyledon, pericarp, and propagule generally exhibited the lowest cytotoxic activity, reducing cell viability by no more than 70% at the highest concentration (540 µg/mL) across all cell lines. The exception was the pericarp extract, which reduced viability of HeLa cells to 60.30%. The leaf extract showed low cytotoxicity at lower concentrations. At 60 µg/mL, cell viability remains near 80% for SW480, E705, and MDA-MB-231 and was 70.44% for HeLa. In the non-cancerous cell lines, viability was even higher: 88.59% and 86.86% for CCD 841 and MRC-5, respectively. However, at 540 µg/mL, the extract reduced viability to 50–60% in most cell lines, particularly 50.98% for SW480, 63.91% for E705, 53.00% for MDA-MB-231, 59.77% for U-87, 54.96% for HeLa, and 61.01% for CCD 841, while the least reduction occurred in MRC-5 (71.26%). Among all extracts, the root extract exhibited the highest cytotoxic activity. At 180 µg/mL, it reduced cell viability to 29.47% (SW480), 42.40% (E705), 35.26% (MDA MB-231), 53.06% (U87), 52.00% (HeLa), 46.60% (CCD 841), and 60.15% (MRC-5). These reductions were statistically significant compared to all other extracts, except for E705, where differences with the leaf extract were not significant, and for HeLa. At 540 µg/mL, cytotoxicity remained similar across most lines, although viability dropped further in SW480 and E705 (22.93% and 27.03%, respectively). These findings highlight the notable activity of the root extract, particularly at the highest concentrations, against SW480, E705, and MDA-MB-231 cell lines (**Figure 5.5**). Notably, at 180 µg/mL, the cytotoxic activity of the root extract in these cell lines was significantly greater than in non-cancerous MRC-5 cells, while no significant difference was

observed compared to the healthy mucosa cell line CCD 841. Additionally, at 540 µg/mL, viability of SW480 cells was significantly lower than that of CCD 841.

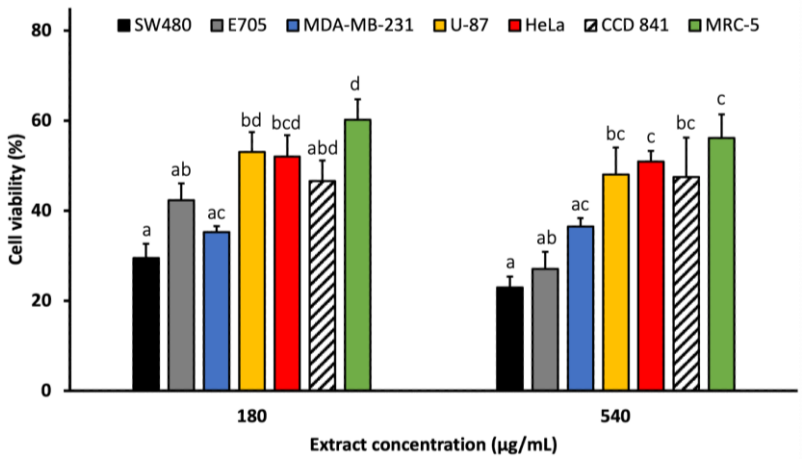

Figure 5.5. Cell viability (%) of the cancer cell lines treated with *A. marina* root extract (180 and 540 µg/mL) for 48h. Bars represent mean ± standard error of the mean (SEM) from n=3independent experiments. Different lowercase letters indicate statistically significant differences between extracts ($p < 0.05$) and were assigned independently for each concentration.

Given this pronounced response, the analysis focused on dose–response effects in SW480, E705, and MDA-MB-231. Each cell line was treated with ten increasing concentrations of root extract (2 to 540 µg/mL; **Figure S6**), and the IC_{50} values were 81.98 µg/mL for SW480, 108.10 µg/mL for E705, and 57.93 µg/mL for MDA-MB-231

5.2.4 *In Silico* Analysis

Given the strong cytotoxic activity observed for the *A. marina* root extract *in vitro*, an *in silico* analysis was conducted to evaluate the predicted biological activities of the compounds found exclusively or predominantly in this extract. PASS Online predicted potential cytotoxicity-related effects, including antineoplastic activity, apoptosis induction (caspase 3/8 stimulation and apoptosis agonism), TP53 expression enhancement, NF κB stimulation, cytostatic activity, lipid peroxidase inhibition, and inhibition of ICAM-1 expression [45], [46]. The complete list of predicted biological activities for compounds exclusive of the root extract is provided in **Table S2** in *Supplementary informations*.

Among the primary peaks detected in the root extract, the triterpene saponins medico side G and azukisaponin III were found exclusively in the root extract, while esculentoside C was detected at high levels in the roots and in trace amounts in other extracts. These compounds showed high

predicted probabilities (Pa) for antineoplastic activity (0.870, 0.905, and 0.908 for medicoside G, esculentoside C, and azukisaponin III, respectively), caspase 3/8 stimulation (0.994/0.984, 0.989/0.986, and 0.964/0.934), apoptosis agonism (0.901, 0.862, and 0.883), and NF-κB stimulation (0.965, 0.917, and 0.904). They were also predicted to inhibit ICAM-1 expression (0.908, 0.961, and 0.987) and lipid peroxidase activity (0.927, 0.952, and 0.991). Additional compounds found exclusively in the root extract, including I, suspensaside A, kaempferol 3-O-glucoside, and quercetin 3-O-hexoside, were also predicted to exhibit antineoplastic activity with Pa values of 0.804, 0.863, 0.834, and 0.833, respectively. Kaempferol 3-O-glucoside and quercetin 3-O-hexoside also showed cytostatic activity (Pa: 0.811 and 0.825), enhancement of TP53 expression (Pa: 0.952 and 0.959) and lipid peroxidase inhibition (0.960 and 0.976, resp.).

5.3 Discussion

UHPLC-ESI/HRMS analyses enabled the characterization of *A. marina* extracts, revealing a total of 49 compounds, unevenly distributed across plant parts. The leaf extract contained the highest number of secondary metabolites, followed by pericarps, roots, cotyledons, and propagules. Notably, this study distinguishes between the external tissue of the propagule (here consistently called pericarp) and the internal tissues of the propagule (here consistently called simply propagule) which are often analyzed as a single fruit unit in other studies. The propagule, which consists mainly of the embryo, contained few compounds, likely due to the focus on primary metabolites essential for germination [47]. In contrast, the pericarp, which serves a protective function, was significantly richer in secondary metabolites [48], particularly phenylethanoid glycosides. Similarly, cotyledons had low metabolite diversity and a profile similar to propagules but showed some additional peaks. These may reflect early biosynthesis of stress-related compounds in developing seedlings.

The compounds identified, including phenylethanoid glycosides, flavonoid glycosides, iridoid glycosides, hydroxycinnamic acid and derivatives, and triterpene saponins, are well known for their ecological roles in protecting plants from abiotic stressors such as drought, high salinity, intense sunlight, and elevated temperatures [49], [50], [51]. These classes are widely reported in *A. marina* from other regions, and some metabolites identified here have been documented previously, suggesting a shared core phytochemical profile with global populations [52].

However, differences from previous studies were observed. Firstly, a distinctive feature of *A. marina* elsewhere is the presence of naphthalene derivatives [52], which were not detected in our samples. This absence may reflect tissue specificity, as most of these compounds were extracted from branches, or differences in extraction methods [53]. More importantly, several compounds detected in this study have never been reported before in *A. marina*. These include one kaempferol-glycosides and two isorhamnetin glycosides. Notably, monohydroxy B-ring-substituted flavonoid glycosides (e.g., kaempferol-, diosmetin-, and isorhamnetin-glycosides) were more abundant than dihydroxy types, a pattern opposite to that expected under UV stress, where dihydroxy forms typically dominate due to their antioxidant potential [54]. This shift may reflect Gulf-specific regulation of flavonoid biosynthesis rather than species-specific traits, as it is not evident in previous reports [52]. The study identified novel compounds among the iridoid glycosides and hydroxycinnamic acids, but the most notable findings were within phenylethanoid glycosides and triterpene saponins, the latter all newly reported in *A. marina*. The high abundance of phenylethanoid glycosides in roots is consistent with their reported accumulation under water stress [50], while the accumulation of triterpene saponins is associated with osmotic stress response [51], [55]. These trends suggest that UAE-grown *A. marina* may possess a distinctive phytochemical profile shaped by the extreme environmental conditions of the Arabian Gulf [56], [57]. Nonetheless, inter-regional comparisons are limited due to methodological differences. Future comparative studies using standardized LC-MS protocols would enhance our understanding of mangrove chemical ecology and support bioprospecting efforts.

The identified metabolite classes are associated with various biological activities, including antioxidant, anticancer, antimicrobial, and anti-inflammatory [50], [56]. In particular, phenylethanoid glycosides are well-documented antioxidants, showing both DPPH and ABTS radical scavenging activity [58]. In this study, extracts of the pericarp and root were rich in these compounds and showed the highest antioxidant activity (187.14 ± 2.87 and 217.16 ± 2.67 μmol TE/g for the pericarps; 128.25 ± 1.12 and 147.21 ± 2.42 μmol TE/g for the roots). The strong positive Spearman correlation between the number of phenylethanoid glycosides and DPPH activity (ρ = 0.949; p = 0.014) supports the hypothesis that these compounds contribute to radical scavenging in the extracts. Key phenylethanoid glycosides identified in this study, such as cistanoside F, acteoside, and jionoside C, are known for their potent antioxidant activity [59], [60], while less-studied

molecules such as suspensaside and suspensaside A warrant further exploration. Our correlation findings are exploratory and do not prove causation. Definitive attribution will require targeted quantification of candidate phenylethanoid glycosides and subsequent activity testing.

In terms of cytotoxic activity, the cotyledon, pericarp, and propagule extracts showed negligible effects on cancer cell lines, even at the highest concentrations. In contrast, the leaf and root extracts displayed cytotoxicity at higher doses. The leaf extract showed limited cytotoxicity at lower concentrations but reduced viability (50–60%) at 540 μg/mL in several cancer cell lines. This agrees with Momtazi-Borojeni et al. [61], who reported no toxicity at low concentrations but moderate effects at higher doses (250 μg/mL). The root extract had the most promising cytotoxic profile, particularly against SW480, E705, and MDA-MB-231 cancer cell lines. At 540 μg/mL, it reduced cell viability below 40% but showed lower toxicity against normal cell lines (MRC-5 and CCD 841). These findings agree with previous studies showing selective cytotoxicity of root extracts towards cancer cell lines [62]. IC_{50} values for SW480, E705, and MDA-MB-231 were 81.98, 108.10, and 57.93 μg/mL, respectively. Based on the criteria established by the National Cancer Institute (NCI, USA) and the Geran protocol, which classified cytotoxicity as high when IC_{50} values are ≤ 20μg/mL, moderate between 21 and 200 μg/mL, weak between 201 and500 μg/mL, and absent above 500 μg/mL ,[63] this corresponds to moderate cytotoxic activity. While these IC_{50} values were not compared with a standard drug, they suggest the presence of active compounds. The values reported here are for crude extracts; further fractionation and isolation of active constituents are expected to yield more potent compounds, for which *in vivo* and clinical potential could be more realistically assessed through comparison with standard anticancer drugs. These are potentially triterpene saponins, which were only detected in the roots.

Triterpene saponins are gaining attention in cancer research due to their ability to target tumor-related pathways while maintaining low toxicity [64]. Although widespread in medicinal plants [65], their occurrence in mangroves is less documented, with only a few studies published on this topic [66]. *In silico* prediction using PASS software indicated a strong cytotoxic potential for several saponins identified in the root extract, including medicoside G, esculentoside C, and azukisaponin III. Additionally, two unidentified saponins suggest the presence of a potentially novel structure that merits further isolation and structural characterization. Other compounds specific to the root

extract, such as suspensaside A and kaempferol 3-O-glucoside, showed high predicted probabilities for antineoplastic effects.

Given that the root extract exhibited the highest cytotoxicity, further work will focus on bioactivity-guided fractionation of this extract, with particular emphasis on isolating the triterpene saponin-rich fraction. These purified fractions will be tested for cytotoxicity alongside a standard anticancer drug (e.g., doxorubicin) to identify the compounds responsible for the observed activity. Mechanistic studies, including apoptosis assays, cell cycle analysis, and molecular pathway investigations, will be conducted to elucidate the modes of action. Such comprehensive analyses, together with the targeted quantification of candidate constituents, will clarify structure–activity correlations and enhance both therapeutic efficacy and selectivity. Importantly, these efforts, combined with further purification and structural elucidation, could identify promising novel lead compounds suitable for subsequent *in vivo* evaluation and development as potential anticancer agents.

5.4 Conclusions

The findings of this study highlight *A. marina* as a valuable source of bioactive compounds with promising therapeutic applications. The pericarp and root extracts exhibited the highest antioxidant activity, possibly due to the presence of phenylethanoid glycosides, which are known for their antioxidant activities. Among all extracts tested, the root extract displayed the strongest cytotoxicity, in particular against the triple-negative breast cancer cell line MDA-MB-231 and two colorectal cancer cell lines, SW480 and E705, with IC_{50} values of 58.46, 81.98, and 108.10 µg/mL, respectively. *In silico* predictions identified triterpene saponins, including medicoside G, esculentoside C, and azukisaponin III, as likely contributors to these effects. The detection of triterpene saponins not previously reported from mangroves, together with several phenylethanoid glycosides and other compounds not earlier described in *A. marina*, is noteworthy. Plants adapted to extreme environments can accumulate distinctive secondary metabolites, and our plant-part-specific UPLC-HRMS analysis of UAE-grown *A. marina* provides region-specific evidence that complements existing phytochemical surveys. Moreover, combining this untargeted phytochemical investigation with biological activity screening and *in silico* analysis/statistical correlation offers a practicable approach to rapidly link observed activities to plant-part-specific compounds. To advance these observations towards pharmacological relevance, future work should focus on bioactivity-guided

fractionation of the extracts, structural elucidation, and targeted quantification of key compounds, along with mechanistic *in vitro* assays. These efforts will help clarify structure–activity correlations and potentially lead to the identification of a novel therapeutic candidate from this stress-adapted mangrove species.

Within the framework of this doctoral project, these findings provide a clear scientific rationale for the strategic redirection of *A. marina* away from cosmetic anti-aging applications toward a bioprospecting-oriented investigation of its therapeutic potential. While the preliminary anti-aging screening did not support the inclusion of *A. marina* extracts in a formulation-driven cosmetic development pathway, the comprehensive phytochemical and biological profiling presented in this chapter unequivocally demonstrates that this species represents a rich and underexplored source of bioactive compounds with relevant antioxidant and cytotoxic properties.

In this context, the present work exemplifies an adaptive and evidence-based research strategy, in which plant extracts were not evaluated according to a single predefined application, but rather valorized based on their most promising biological activities. The identification of portion-specific cytotoxic effects, together with the detection of previously unreported triterpene saponins and phenylethanoid glycosides in UAE-grown *A. marina*, highlights the importance of geographic origin and environmental adaptation in shaping phytochemical diversity and bioactivity profiles.

5.5 Materials and methods

5.5.1 Chemicals

Ethanol absolute, analytical-grade methanol, 1,1-diphenyl-2-picrylhydrazyl (DPPH$^{\bullet}$), and 2,2-azinobis-(3-ethylbenzothiazoline-6-sulfonate) (ABTS$^{\bullet+}$) reagents were obtained from Sigma-Aldrich (Milan, Italy), while methanol and formic acid of LC-MS grade were sourced from Romil (Cambridge, UK). Ultrapure water (18 MΩ) was prepared by a Milli-Q purification system (Millipore, Bedford, MA, USA).

5.5.2 Plant material

Samples were collected from different parts of *A. marina*, including leaves, roots, propagules, and cotyledons. The cotyledons were obtained from seedlings at an early growth stage, when the propagules had already opened and developed roots. All samples were harvested in September 2022

from multiple individual plants within the mangrove forest of Ajman Emirate, UAE. Although no herbarium voucher specimen was deposited, the plant material was identified based on morphological characteristics following established taxonomic keys [67]. This identification is supported by the fact that *A. marina* is the only mangrove species forming the evergreen coastal forests of the UAE [68], and its presence in the region has been validated by previous molecular analyses [69], [70].

For more precise phytochemical characterization, propagules were separated into the pericarp, representing the external protective tissue, and the internal tissues. Thus, in the manuscript, the term pericarp (and pericarp extract) refers exclusively to the external part, while the generic term propagule (and propagule extract) refers to the internal tissues. Each type of plant material (e.g., all collected leaves, roots, pericarps, propagules, and cotyledons) was pooled by type and immediately freeze-dried after collection. The dried samples were homogenized using a Grindomix GM 200 knife mill (Retsch, Haan, Germany) and then sieved through a test sieve (Retsch AS 200, Haan, Germany) with a mesh size range of 300–600 μm to obtain powders with uniform particle size distribution.

5.5.3 Sample preparation and extraction

Root, leaf, cotyledon, pericarp, and propagule samples of *A. marina* underwent exhaustive ultrasound-assisted extraction using a thermostatically controlled ultrasonic bath (Sonorex TK 52; Bandelin electronic, Berlin, Germany). Each sample was extracted under controlled conditions (25 °C, 15 min) with 50% aqueous ethanol (*v*/*v*) at a solid-to-solvent ratio of 1:10 (*w*/*v*), which is commonly applied in metabolite profiling studies [71]; specifically, 1 g of powdered sample was mixed with 10 mL of solvent in a 50-mL polypropylene tube. A 50% aqueous ethanol solution was selected as the extraction solvent due to its effectiveness as a green, low-toxicity system, making it well-suited for bioactivity screening [72]. Ethanol–water mixtures offer a balanced polarity and are widely recognized for their ability to efficiently extract a broad range of bioactive compounds, particularly polyphenolic metabolites, which are well known for their antioxidant properties [73][74]. Moreover, this solvent was selected to ensure low toxicity in downstream biological assays, in case traces of solvent remain after evaporation, and because non-polar solvents or higher ethanol concentrations could reduce solubility in aqueous assay media, potentially compromising the suitability of the extracts for biological testing.

To ensure complete extraction, the process was repeated three times with fresh solvent. Following each extraction, the mixtures were centrifuged (13,000× *g*, 10 min), and the supernatants underwent filtration through Whatman No. 1 filter paper. The combined extracts were concentrated under pressure at 40 °C using a rotary evaporator to remove ethanol and subsequently lyophilized (Alpha 1-2 LD freeze dryer, Christ, Germany) to obtain dry residues for further analysis.

The extraction yields of *A. marina* were determined by calculating the ratio of the weight of dried extract obtained to the initial weight of dried plant material powder and expressed as a percentage. The yields were 34.23% for roots, 65.02% for cotyledons, 61.76% for pericarps, 38.55% for propagules, and 33.72% for leaves.

5.5.4 Extracts characterization

The chemical characterization of extracts was performed in negative mode using liquid chromatography coupled with electrospray ionization (ESI) and high-resolution mass spectrometry (UPLC-ESI/HRMS). A Waters ACQUITY UPLC system coupled with a Waters Xevo G2-XS QTof Mass Spectrometer (Waters Corp., Milford, MA, USA) was used. The extracts were dissolved in ultrapure water at a concentration of 100 µg/mL, and then 5 µL of each sample was injected into a Biphenyl column (100 mm × 2.1 mm, 2.6 µm; Phenomenex, Torrance, CA, USA). The chromatographic gradient was conducted with solvent A (0.1% formic acid in water) and solvent B (0.1% formic acid in methanol), starting with 95% A for 1 min, followed by a linear gradient to 95% B over 10 min, and 4 min of column washing at 95% B. The flow rate was maintained at 0.4 mL/min. The ESI source was operated under the following conditions: electrospray capillary voltage of 1.5 kV, source temperature of 140 °C, and desolvation temperature of 600 °C. MS spectra were acquired in full range mode, covering a mass range of 100–1000 m/z. MS/HRMS analysis was performed using data-dependent scan (DDA), selecting the two most intense ions from the HRMS scan for collision-induced dissociation (CID) with the following conditions: a minimum signal threshold of 500,000, isolation width at 2.0, and normalized collision energy of 30%. Metabolite identification followed the Metabolomics Standards Initiative (MSI) guidelines, which define three confidence levels indicated in the "IL" column of Table 1: Level 1 (IL1): compounds were unequivocally identified by comparison with authentic reference standards (retention time, MS/MS spectrum, and exact mass); Level 2 (IL2): tentative identifications were assigned based on matches between experimental

MS/MS spectra and literature data or spectral libraries (e.g., GNPS, MassBank); Level 3 (IL3): compounds were classified by spectral similarity to known chemical families and supported by taxonomic evidence.

Novelty verification was performed using general literature databases (e.g., Google Scholar) and the chemical database SciFinder^{n}. In SciFinder^{n}, each tentatively identified compound was queried by chemical name, and all related references were investigated using keywords such as "*Avicennia marina*", "*Avicennia*", and "mangroves". This process allowed determination of whether a compound had been previously reported in *A. marina*, other species within the genus *Avicennia*, or other mangrove species, or if it represents a first identification in mangroves.

5.5.5 Antioxidant activity assessment

The antioxidant capacities (AOCs) of the exhaustive extracts of *A. marina* (leaves, roots, pericarps, propagules, and cotyledons) were evaluated using 1,1-diphenyl-2-picrylhydrazyl (DPPH•) and 2,2-azinobis-3-ethylbenzothiazoline-6-sulfonate (ABTS•+) assays according to Cannavacciuolo et al. [75]. The extracts were dissolved in ultrapure water and analyzed at a concentration of 0.5 mg/mL, with Trolox (0–500 µM) serving as a standard. The antioxidant activity was expressed as µmol Trolox equivalents per gram of sample matrix (TE/g MTX), representing the µmol of a standard Trolox solution exerting the same antioxidant capacity as 1 mg/mL of the tested extracts.

In the DPPH assay the stock solution of DPPH (5 mM) was prepared by dissolving 3.9 mg of DPPH in 100 mL of methanol and subsequently diluted to 100 µM to obtain the operating solution. This solution was prepared just before use and protected from light due to the photosensitivity of the reagent. The assay was set up in an Eppendorf by mixing 50 µL of sample with 950 µL of operative DPPH, and the mixture was incubated in the dark for 30 min. Subsequently, 200 µL of the solution was transferred to an absorbance reading plate at the 515 nm wavelength.

For the ABTS assay, the stock solution of ABTS (7 mM) was diluted with phosphate-buffered saline (PBS; 5 mM, pH 7.4) to achieve working concentrations. The assay was performed by combining 5 µL of diluted sample (or PBS control) and 500 µL of ABTS radical cation solution (0.1 mM in PBS). The reaction mixtures were protected from light and incubated at 30 °C for 60 min to allow complete radical scavenging. Absorbance measurements were then recorded at 734 nm using a microplate reader.

5.5.6 Cytotoxicity evaluation

5.5.6.1 Cell lines and culture conditions

Normal human fibroblasts (MRC-5), human glioblastoma (U-87), human triple-negative breast cancer (MDA-MB-231), human colorectal cancer (SW480), and human healthy mucosa (CCD841) cell lines were purchased from the American Type Culture Collection (Manassas, VA, USA). The human cervical cancer cell line (HeLa) was acquired from System Biosciences, and the human colon cancer cell line (E705) was provided by the Fondazione IRCCS Istituto Nazionale dei Tumori (Milan, Italy). The E705 cell line represents epithelial tissue cells of colorectal adenocarcinoma derived from a patient at the National Cancer Institute in Milan.

MRC-5, U-87, and HeLa cells were cultured in Dulbecco's Modified Eagle Medium (DMEM) high glucose medium supplemented with 10% heat-inactivated fetal bovine serum (FBS), 1% penicillin/streptomycin (P/S), and 2 mM L-glutamine. MDA-MB-231 cells were maintained in Minimum Essential Medium (MEM) with Earl's Salts supplemented with 10% heat-inactivated FBS, 1% P/S, 2 mM L-glutamine, and 0.1 mM MEM Non-Essential Amino Acids (MEM NEAA). E705 and SW480 cell lines were cultured in RPMI 1640 medium supplemented with 10% heat-inactivated FBS, 100 U/mL penicillin, 100 µg/mL streptomycin, and 2 mM L-glutamine. The CCD 841 cell line was grown in EMEM medium supplemented with 10% heat-inactivated FBS, 1% P/S, 2 mM L-glutamine, and 0.1 mM non-essential amino acids. All cell lines were incubated at 37 °C in a humidified atmosphere containing 5% CO_2 and 95% air. Cell culture media and reagents were purchased from EuroClone (Pero, Italy).

5.5.6.2 Cell viability assay

The cytotoxicity of *A. marina* extracts was evaluated using the MTT assay (CellTiter96®Non-Radioactive Cell Proliferation Assay, Promega, Madison, WI, USA) following the manufacturer's protocol. The extract powders were solubilized in Milli-Q water, and four extract concentrations (20, 60, 180, and 540 µg/mL) were tested on all cell lines. Additionally, for the root extract, an extended dose-response analysis using ten concentrations (2, 10, 20, 40, 60, 100, 140, 180, 360, and 540 µg/mL) was performed on selected cell lines to enable IC_{50} determination. IC_{50} values were calculated only for extract–cell line combinations tested with this ten-point dilution series.

No positive control drugs were included in this preliminary screening, as the primary objective was to assess and compare the relative cytotoxicity of different *A. marina* extracts. Comparative analysis with standard anticancer agents will be incorporated in subsequent studies on purified fractions or isolated compounds.

Briefly, HeLa, MRC-5, U-87, and MDA-MB-231 cells were seeded into 96-well plates (from Euroclone, Pero, Italy) at a density of 5×10^3 cells/well in 100 µL of growth medium, while E-705 and SW-480 cells were seeded at a density of 8×10^3 cells/well. After 24 h of incubation at 37 °C in 5% CO_2, the medium was replaced, and cells were treated with various concentrations of *A. marina* extracts. Following 48 h of treatment, the medium was replaced, and 15 µL of MTT solution was added to each well. After 3 h of incubation at 37 °C, formazan crystals were solubilized using 100 µL of stop solution and incubated under stirring for 1 h. Reduced MTT was quantified using a UV–vis plate reader (EnSight Multimode Microplate Reader, PerkinElmer, Waltham, MA, USA) at 570 nm with a reference wavelength of 630 nm.

Cell viability was expressed as a percentage relative to untreated cells (negative control), and medium with MilliQ water at equivalent concentrations (10% *v*/*v*) was used as a blank. Dose-response curves and the IC_{50} values, representing the extract concentration required to inhibit 50% of cell viability relative to untreated control cells, were generated using GraphPad Prism v10.5.0 software.

5.5.7 *In Silico* Analysis

To identify potential bioactive compounds responsible for the cytotoxic effect, an *in silico* prediction of biological activity was performed using PASS Online software (https://www.way2drug.com/PASSOnline/index.php; accessed on July 15, 2025), a predictive tool from Way2Drug Services. The reliability of PASS for predicting *in vitro* cytotoxic activity has been demonstrated in previous studies [76], [77], including those focusing on triterpene saponins [78].

The canonical Simplified Molecular Input Line Entry System (SMILES) of each compound was gathered from SciFinder$_n$ and was used to run the software. The program independently calculates the estimated predictive biological activities based on structure–activity relationships, providing Pa (probability of activity) and Pi (probability of inactivity) values for each activity. Only activities with $Pa > 0.7$ were considered, as this threshold indicates a high likelihood that the substance will exhibit

the predicted activity in experimental settings, although the probability of the compound being an analogue of a known pharmaceutical agent remains high [79]. Notably, when Pa > 0.9, as frequently observed in our study, the likelihood of false-positive predictions is insignificant [76].

The predicted anticancer-related activities included antineoplastic activity, apoptosis-related effects (apoptosis agonist, caspase 3/8 stimulation), TP53 expression enhancement, NF-kB modulation, cytostatic activity, lipid peroxidase inhibition, and ICAM-1 expression inhibition. These results were analyzed in relation to the cytotoxicity data of the MTT assay to establish potential correlations between the phytochemical composition and the observed cytotoxicity against cancer cells.

5.5.8 Statistical Analysis

Statistical analyses were conducted on data generated from three replicates. Cytotoxic activity results are presented as mean ± standard error of the mean (SEM). Antioxidant activity results are reported as mean ± standard deviation (SD). Before statistical analysis, the assumption of normality was assessed using the Shapiro–Wilk test. The homogeneity of the variances was evaluated using Levene's test. When normality and homogeneity assumptions were met, a one-way analysis of variance (ANOVA) was performed, followed by Tukey's honest significant difference (HSD) post hoc test to assess pairwise differences between the means of the group. In cases where the assumption of homogeneity of the variances was not met, Welch's ANOVA was applied, followed by the Games–Howell post hoc test. Statistical significance was considered when $p < 0.05$.

The correlation between phytochemical composition and antioxidant activity was assessed using Spearman's rank correlation coefficient (two-tailed). For each plant-part extract (n = 5), the number of tentatively identified compounds in each major chemical class (phenylethanoid glycosides, flavonoid glycosides, iridoid glycosides, hydroxycinnamic acids and derivatives, and triterpene saponins) was correlated with antioxidant activity (DPPH and ABTS, mean values). Statistical significance was set at $p < 0.05$. All analyses were conducted with IBM SPSS Statistics v29.0.2.0.

5.6 Supplementary informations

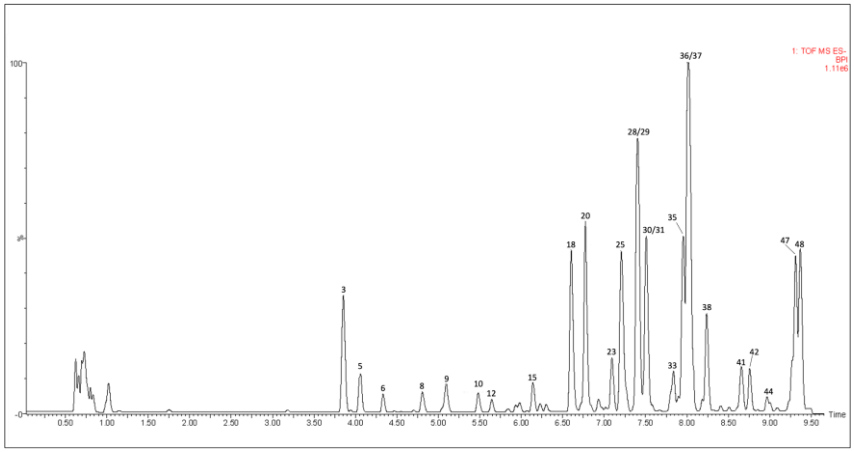

Figure S1. Representative chromatogram of the leaf extract of *A.marina.*

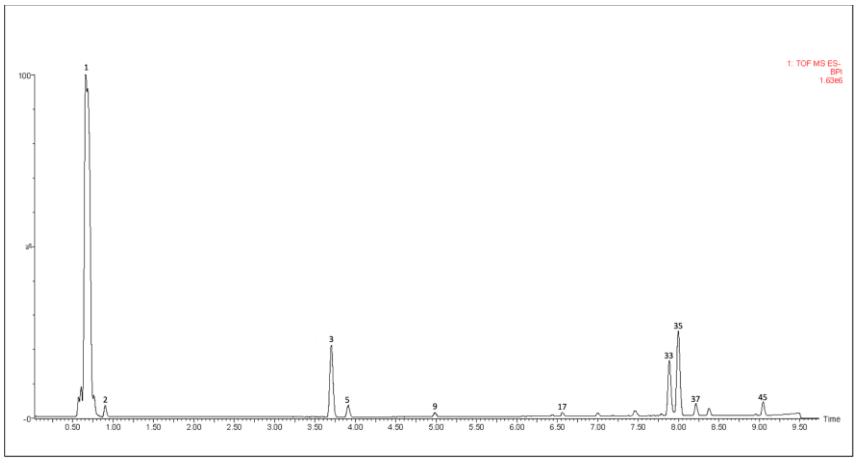

Figure S2. Representative chromatogram of the cotyledon extract of *A.marina.*

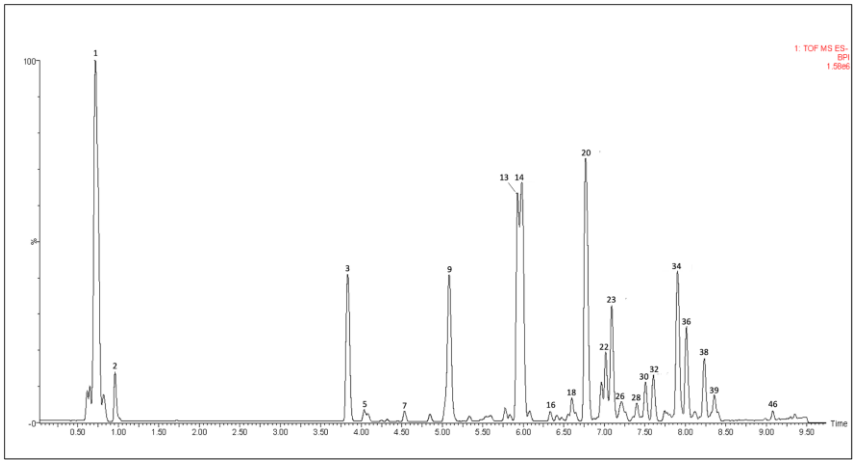

Figure S3. Representative chromatogram of the pericarp extract of *A.marina.*

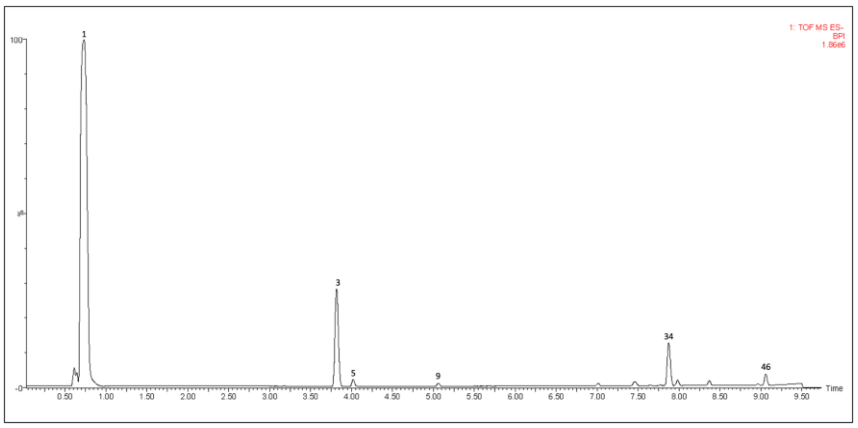

Figure S4. Representative chromatogram of the propagule extract of *A.marina.*

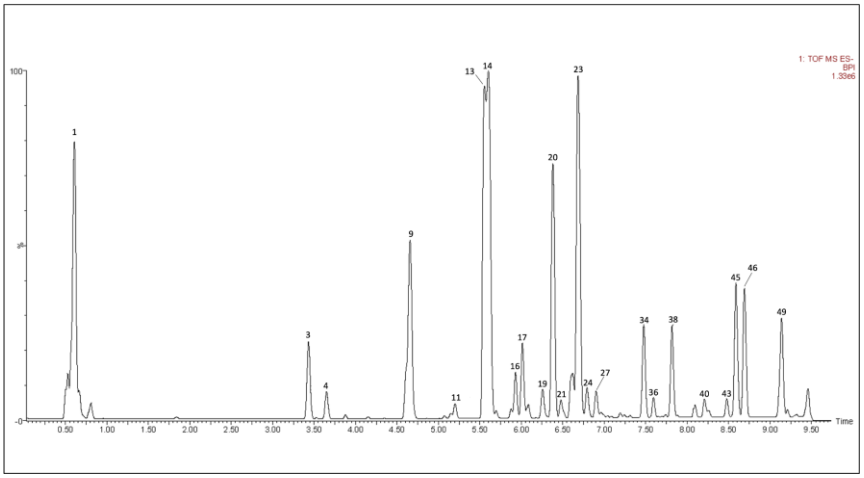

Figure S5. Representative chromatogram of the root extracts of *A.marina.*

Table S1. Cytotoxicity of *Avicennia marina* extracts on the tested cell lines at four concentrations (20–540µg/mL). Cell viability is expressed as a percentage relative to untreated cells (negative control). Standard error of the mean (SEM) is also reported.

Cell line	Extract conc. (µg/mL)	Roots		Cotyledons		Pericarps		Propagules		Leaves	
		Cell viability (%)	SEM	Cell viability (%)	SEM	Cell viability (%)	SEM	Cell viability (%)	SEM	Cell viability (%)	SEM
SW480	**20**	92,84	1,83	99,21	4,09	97,64	3,19	97,62	4,84	91,61	1,55
	60	61,92	4,00	97,25	1,85	92,42	4,93	97,89	0,49	78,80	3,02
	180	29,47	3,20	89,80	1,27	89,63	4,27	95,61	1,07	63,95	4,28
	540	22,93	2,42	79,51	0,15	70,95	3,80	91,30	3,32	50,98	2,82
E705	**20**	94,40	2,85	98,20	1,24	94,33	1,71	97,74	1,64	78,50	2,93
	60	74,94	3,42	96,94	3,50	93,48	4,00	97,59	3,86	78,67	4,26
	180	42,30	3,77	92,77	5,92	84,34	7,33	91,45	3,48	65,22	6,57
	540	27,03	3,81	84,76	5,44	81,71	6,96	87,57	5,58	63,91	9,56
	20	89,26	2,25	94,24	3,95	94,68	2,07	96,37	5,59	87,46	5,05

MDA-MB-231	**60**	61,27	3,37	87,76	3,46	85,62	7,82	95,83	5,16	80,37	5,79
	180	35,26	1,30	84,44	4,81	82,19	9,32	96,41	5,75	69,46	8,36
	540	36,47	1,90	80,29	4,39	82,62	8,10	85,50	4,03	53,00	4,84
U-87	**20**	92,49	5,55	99,97	2,02	91,47	1,55	99,38	3,26	82,61	6,94
	60	77,08	10,16	101,03	3,29	88,72	2,65	99,89	3,09	79,86	3,78
	180	53,06	4,39	95,16	2,69	86,18	2,02	99,32	1,63	70,18	5,75
	540	47,99	6,03	96,81	7,42	86,97	6,13	98,85	3,52	59,77	8,42
HeLa	**20**	84,11	4,33	95,98	2,94	95,72	3,81	101,93	0,85	84,28	5,20
	60	75,36	4,73	91,05	3,59	85,63	3,88	99,86	2,90	70,44	8,82
	180	52,00	4,79	77,94	4,91	68,55	6,14	96,37	1,97	61,00	8,50
	540	50,91	2,31	72,71	4,68	60,30	8,12	91,82	2,64	54,96	8,68
CCD 841	**20**	85,66	6,48	100,50	2,29	95,77	3,68	101,34	2,95	98,25	4,32
	60	62,58	12,88	98,06	3,92	92,16	2,76	98,97	3,07	88,59	6,13
	180	46,60	4,54	90,40	3,16	85,26	1,53	94,45	5,48	66,22	4,37
	540	47,50	8,69	80,90	5,14	81,34	4,76	83,91	6,35	61,01	1,22
MRC-5	**20**	92,36	1,25	93,64	5,58	96,99	2,88	93,50	4,33	94,79	7,38
	60	78,79	5,45	92,72	4,79	91,75	3,82	88,01	2,78	86,86	6,28
	180	60,15	4,56	89,19	4,81	83,34	3,16	87,30	1,93	82,82	5,68
	540	56,13	5,27	89,19	7,67	77,21	4,81	85,23	3,21	71,26	4,66

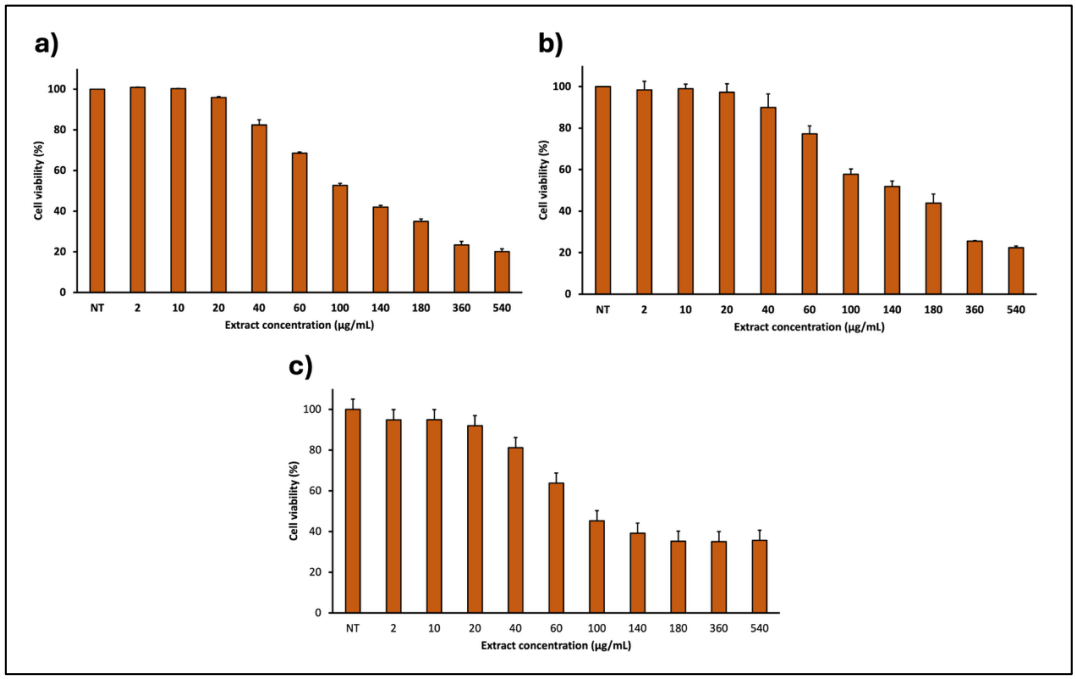

Figure S6. Cell viability of three human cancer cell lines treated with root extracts (2–540 µg/mL) for 48 h. Average values ± SE are shown.

Table S2. Probable cytotoxicity-related biological activities of 7 compounds tentatively identified in the root extract of A. marina by PASS (Prediction of Activity Spectra for Substances). Pa = probable biological activity of compound; only activities with Pa > 0.7 are shown.

Compound	Class	Cytotoxicity-related activities (Pa)
Campneoside I	Hydroxycinnamic acid and derivatives	Caspase 3 stimulant (0.814) Antineoplastic (0.804) Caspase 8 stimulant (0.727) Lipid peroxidase inhibitor (0.701)
Quercetin 3-O-hexoside	Flavonoid glycosides	Lipid peroxidase inhibitor (0.976) TP53 expression enhancer (0.959) Antineoplastic (0.833) Cytostatic (0.825)

		Caspase 3 stimulant (0.801) Apotosis agonist (0.792)
Suspensaside A	Phenylethanoid glycosides	Antineoplastic (0.863) Caspase 8 stimulant (0.743)
Kaempferol 3-O-glucoside	Flavonoid glycosides	Lipid peroxidase inhibitor (0.960) TP53 expression enhancer (0.952) Antineoplastic (0.834) Cytostatic (0.811) Caspase 3 stimulant (0.772) Apoptosis agonist (0.772)
Medicoside G	Triterpene saponins	Caspase 3 stimulant (0.994) Caspase 8 stimulant (0.984) Trascription factor NF-kB stimulant (0.965) Lipid peroxidase inhibitor (0.927) ICAM1 expression inhibitor (0.908) Apoptosis agonist (0.901) Antineoplastic (0.870)
Esculentoside C	Triterpene saponins	Caspase 3 stimulant (0.989) Caspase 8 stimulant (0.986) ICAM1 expression inhibitor (0.961) Lipid peroxidase inhibitor (0.952) Trascription factor NF-kB stimulant (0.917)

		Antineoplastic (0.905) Apoptosis agonist (0.862) Antineoplastic (lung cancer) (0.807)
Azukisaponin III	Triterpene saponins	Lipid peroxidase inhibitor (0.991) ICAM1 expression inhibitor (0.987) Caspase 3 stimulant (0.964) Caspase 8 stimulant (0.934) Antineoplastic (0.908) Trascription factor NF-kB stimulant (0.904) Apoptosis agonist (0.883) Antineoplastic (lung cancer) (0.791)

5.7 References

[1] H. Thatoi, D. Samantaray, and S. K. Das, "The genus *Avicennia* , a pioneer group of dominant mangrove plant species with potential medicinal values: a review," *Front. Life Sci.*, vol. 9, no. 4, pp. 267–291, Oct. 2016, doi: 10.1080/21553769.2016.1235619.

[2] S. Galasso *et al.*, "Influence of seasonal variation on Thymus longicaulis C. Presl chemical composition and its antioxidant and anti-inflammatory properties," *Phytochemistry*, vol. 107, pp. 80–90, Nov. 2014, doi: 10.1016/j.phytochem.2014.08.015.

[3] J. Fiori, E. Amadesi, F. Fanelli, C. V. Tropeano, M. Rugolo, and R. Gotti, "Cellular and mitochondrial determination of low molecular mass organic acids by LC–MS/MS," *J. Pharm. Biomed. Anal.*, vol. 150, pp. 33–38, Feb. 2018, doi: 10.1016/j.jpba.2017.11.071.

[4] D. Wang *et al.*, "HPLC/qTOF-MS-oriented characteristic components data set and chemometric analysis for the holistic quality control of complex TCM preparations: Niuhuang Shangqing pill as an example," *J. Pharm. Biomed. Anal.*, vol. 89, pp. 130–141, Feb. 2014, doi: 10.1016/j.jpba.2013.10.042.

[5] O. N. Seo *et al.*, "Determination of polyphenol components of Lonicera japonica Thunb. using liquid chromatography–tandem mass spectrometry: Contribution to the overall antioxidant activity," *Food Chem.*, vol. 134, no. 1, pp. 572–577, Sep. 2012, doi: 10.1016/j.foodchem.2012.02.124.

[6] N. Amessis-Ouchemoukh *et al.*, "Tentative Characterisation of Iridoids, Phenylethanoid Glycosides and Flavonoid Derivatives from *Globularia alypum* L. (Globulariaceae) Leaves by LC-ESI-QTOF-MS," *Phytochemical Analysis*, vol. 25, no. 5, pp. 389–398, Sep. 2014, doi: 10.1002/pca.2506.

[7] G. Xie *et al.*, "Chemical profiles and quality evaluation of Buddleja officinalis flowers by HPLC-DAD and HPLC-Q-TOF-MS/MS," *J. Pharm. Biomed. Anal.*, vol. 164, pp. 283–295, Feb. 2019, doi: 10.1016/j.jpba.2018.10.030.

[8] A. K. Kiss, B. Michalak, A. Patyra, and M. Majdan, "UHPLC-DAD-ESI-MS/MS and HPTLC profiling of ash leaf samples from different commercial and natural sources and their *in vitro* effects on mediators of inflammation," *Phytochemical Analysis*, vol. 31, no. 1, pp. 57–67, Jan. 2020, doi: 10.1002/pca.2866.

[9] A. García-Villegas *et al.*, "Bioactive Compounds and Potential Health Benefits through Cosmetic Applications of Cherry Stem Extract," *Int. J. Mol. Sci.*, vol. 25, no. 7, p. 3723, Mar. 2024, doi: 10.3390/ijms25073723.

[10] J. Han, M. Ye, H. Guo, M. Yang, B. Wang, and D. Guo, "Analysis of multiple constituents in a Chinese herbal preparation Shuang-Huang-Lian oral liquid by HPLC-DAD-ESI-MSn," *J. Pharm. Biomed. Anal.*, vol. 44, no. 2, pp. 430–438, Jun. 2007, doi: 10.1016/j.jpba.2007.02.023.

[11] F. Zhou *et al.*, "Varietal classification and antioxidant activity prediction of Osmanthus fragrans Lour. flowers using UPLC–PDA/QTOF–MS and multivariable analysis," *Food Chem.*, vol. 217, pp. 490–497, Feb. 2017, doi: 10.1016/j.foodchem.2016.08.125.

[12] Y.-D. Zhang, X. Huang, F.-L. Zhao, Y.-L. Tang, and L. Yin, "Study on the chemical markers of Caulis Lonicerae japonicae for quality control by HPLC-QTOF/MS/MS and chromatographic fingerprints combined with chemometrics methods," *Analytical Methods*, vol. 7, no. 5, pp. 2064–2076, 2015, doi: 10.1039/C4AY02744B.

[13] Y. Sun, J. Ouyang, Z. Deng, Q. Li, and W. Lin, "Structure elucidation of five new iridoid glucosides from the leaves of *Avicennia marina*," *Magnetic Resonance in Chemistry*, vol. 46, no. 7, pp. 638–642, Jul. 2008, doi: 10.1002/mrc.2224.

[14] J. Petreska *et al.*, "Potential bioactive phenolics of Macedonian Sideritis species used for medicinal 'Mountain Tea,'" *Food Chem.*, vol. 125, no. 1, pp. 13–20, Mar. 2011, doi: 10.1016/j.foodchem.2010.08.019.

[15] E. Hvattum, "Determination of phenolic compounds in rose hip (*Rosa canina*) using liquid chromatography coupled to electrospray ionisation tandem mass spectrometry and diode-array detection," *Rapid Communications in Mass Spectrometry*, vol. 16, no. 7, pp. 655–662, Apr. 2002, doi: 10.1002/rcm.622.

[16] D. Kammerer, R. Carle, and A. Schieber, "Characterization of phenolic acids in black carrots (*Daucus carota* ssp. *sativus* var. *atrorubens* Alef.) by high-performance liquid chromatography/electrospray ionization mass spectrometry," *Rapid Communications in Mass Spectrometry*, vol. 18, no. 12, pp. 1331–1340, Jun. 2004, doi: 10.1002/rcm.1496.

[17] D. Gu, Y. Yang, M. Bakri, Q. Chen, X. Xin, and H. A. Aisa, "A LC/QTOF–MS/MS Application to Investigate Chemical Compositions in a Fraction with Protein Tyrosine Phosphatase 1B Inhibitory Activity from *Rosa Rugosa* Flowers," *Phytochemical Analysis*, vol. 24, no. 6, pp. 661–670, Nov. 2013, doi: 10.1002/pca.2451.

[18] S. Bin Bae, H. C. Nam, and W. H. Park, "Electrospraying of environmentally sustainable alginate microbeads for cosmetic additives," *Int. J. Biol. Macromol.*, vol. 133, pp. 278–283, Jul. 2019, doi: 10.1016/j.ijbiomac.2019.04.058.

[19] P. Matos *et al.*, "Bioactivity of Acanthus mollis – Contribution of benzoxazinoids and phenylpropanoids," *J. Ethnopharmacol.*, vol. 227, pp. 198–205, Dec. 2018, doi: 10.1016/j.jep.2018.09.013.

[20] N. P. Seeram, R. Lee, H. S. Scheuller, and D. Heber, "Identification of phenolic compounds in strawberries by liquid chromatography electrospray ionization mass spectroscopy," *Food Chem.*, vol. 97, no. 1, pp. 1–11, Jul. 2006, doi: 10.1016/j.foodchem.2005.02.047.

[21] Y. Zhang, P. Shi, H. Qu, and Y. Cheng, "Characterization of phenolic compounds in *Erigeron breviscapus* by liquid chromatography coupled to electrospray ionization mass spectrometry," *Rapid Communications in Mass Spectrometry*, vol. 21, no. 18, pp. 2971–2984, Sep. 2007, doi: 10.1002/rcm.3166.

[22] Y. Zhang, C. Liu, Z. Zhang, J. Wang, G. Wu, and S. Li, "Comprehensive separation and identification of chemical constituents from Apocynum venetum leaves by high-performance counter-current chromatography and high performance liquid chromatography coupled with mass spectrometry," *Journal of Chromatography B*, vol. 878, no. 30, pp. 3149–3155, Nov. 2010, doi: 10.1016/j.jchromb.2010.09.027.

[23] D. Nijat, R. Abdulla, G. Liu, Y. Luo, and H. A. Aisa, "Identification and quantification of Meiguihua oral solution using liquid chromatography combined with hybrid quadrupole-orbitrap and triple quadrupole mass spectrometers," *Journal of Chromatography B*, vol. 1139, p. 121992, Feb. 2020, doi: 10.1016/j.jchromb.2020.121992.

[24] I. Parejo, O. Jauregui, F. Sánchez-Rabaneda, F. Viladomat, J. Bastida, and C. Codina, "Separation and Characterization of Phenolic Compounds in Fennel (*Foeniculum vulgare*) Using Liquid Chromatography−Negative Electrospray Ionization Tandem Mass Spectrometry," *J. Agric. Food Chem.*, vol. 52, no. 12, pp. 3679–3687, Jun. 2004, doi: 10.1021/jf030813h.

[25] R. M. Ibrahim *et al.*, "Agro-byproduct valorization of radish and turnip leaves and roots as new sources of antibacterial and antivirulence agents through metabolomics and molecular networking," *Sci. Hortic.*, vol. 328, p. 112924, Mar. 2024, doi: 10.1016/j.scienta.2024.112924.

[26] Z. Wang *et al.*, "Characterization of chemical constituents and metabolites in rat plasma after oral administration of Ainsliaea fragrans Champ by using UHPLC-QTOF-MS/MS," *Journal of Chromatography B*, vol. 1244, p. 124259, Aug. 2024, doi: 10.1016/j.jchromb.2024.124259.

[27] H. Lei *et al.*, "Effects of processing on the efficacy and metabolites of *Cistanche tubulosa* using ultra-performance liquid chromatography coupled with quadrupole time-of-flight mass spectrometry," *Biomedical Chromatography*, vol. 37, no. 6, Jun. 2023, doi: 10.1002/bmc.5621.

[28] W. Schliemann, C. Ammer, and D. Strack, "Metabolite profiling of mycorrhizal roots of Medicago truncatula," *Phytochemistry*, vol. 69, no. 1, pp. 112–146, Jan. 2008, doi: 10.1016/j.phytochem.2007.06.032.

[29] D. V Huhman and L. W. Sumner, "Metabolic profiling of saponins in Medicago sativa and Medicago truncatula using HPLC coupled to an electrospray ion-trap mass spectrometer," *Phytochemistry*, vol. 59, no. 3, pp. 347–360, Feb. 2002, doi: 10.1016/S0031-9422(01)00432-0.

[30] D. Zhao, X. Chen, R. Wang, H. Pang, J. Wang, and L. Liu, "Determining the chemical profile of Caragana jubata (Pall.) Poir. by UPLC–QTOF–MS analysis and evaluating its anti-ischemic stroke effects," *J. Ethnopharmacol.*, vol. 309, p. 116275, Jun. 2023, doi: 10.1016/j.jep.2023.116275.

[31] F. Saleri, G. Chen, X. Li, and M. Guo, "Comparative Analysis of Saponins from Different Phytolaccaceae Species and Their Antiproliferative Activities," *Molecules*, vol. 22, no. 7, p. 1077, Jun. 2017, doi: 10.3390/molecules22071077.

[32] C. Tavares-Silva *et al.*, "Homeopathic medicine of Melissa officinalis combined or not with Phytolacca decandra in the treatment of possible sleep bruxism in children: A crossover randomized triple-blinded controlled clinical trial," *Phytomedicine*, vol. 58, p. 152869, May 2019, doi: 10.1016/j.phymed.2019.152869.

[33] R. Liu, Z. Cai, and B. Xu, "Characterization and quantification of flavonoids and saponins in adzuki bean (Vigna angularis L.) by HPLC–DAD–ESI–MSn analysis," *Chem. Cent. J.*, vol. 11, no. 1, p. 93, Dec. 2017, doi: 10.1186/s13065-017-0317-x.

[34] H. N. Pham *et al.*, "UHPLC-Q-TOF-MS/MS Dereplication to Identify Chemical Constituents of *Hedera helix* Leaves in Vietnam," *J. Anal. Methods Chem.*, vol. 2022, no. 1, Jan. 2022, doi: 10.1155/2022/1167265.

[35] G. C. Kite, "Characterisation of phenylethanoid glycosides by multiple-stage mass spectrometry," *Rapid Communications in Mass Spectrometry*, vol. 34, no. S4, Sep. 2020, doi: 10.1002/rcm.8563.

[36] M. Qi, A. Xiong, F. Geng, L. Yang, and Z. Wang, "A novel strategy for target profiling analysis of bioactive phenylethanoid glycosides in <scp>P</scp> *lantago* medicinal plants using ultra-performance liquid chromatography coupled with tandem quadrupole mass spectrometry," *J. Sep. Sci.*, vol. 35, no. 12, pp. 1470–1478, Jun. 2012, doi: 10.1002/jssc.201200010.

[37] S. Pagliari *et al.*, "A comparative metabolomic investigation of different sections of Sicilian *Citrus x limon* (L.) Osbeck, characterization of bioactive metabolites, and evaluation of in vivo toxicity on zebrafish embryo," *J. Food Sci.*, vol. 89, no. 6, pp. 3729–3744, Jun. 2024, doi: 10.1111/1750-3841.17079.

[38] Z. Fu *et al.*, "Fragmentation patterns study of iridoid glycosides in Fructus Gardeniae by HPLC-Q/TOF-MS/MS," *Biomedical Chromatography*, vol. 28, no. 12, pp. 1795–1807, Dec. 2014, doi: 10.1002/bmc.3223.

[39] M. Sharaf, M. A. El-Ansari, and N. A. M. Saleh, "New flavonoids from Avicennia marina," *Fitoterapia*, vol. 71, no. 3, pp. 274–277, Jun. 2000, doi: 10.1016/S0367-326X(99)00169-0.

[40] A. S. Mohamed *et al.*, "*In vitro* and *in silico* analysis for elucidation of antioxidant potential of Djiboutian Avicennia Marina (Forsk.) Vierh. phytochemicals," *J. Biomol. Struct. Dyn.*, vol. 42, no. 7, pp. 3410–3425, May 2024, doi: 10.1080/07391102.2023.2213338.

[41] Y.-C. Zhang *et al.*, "Combined metabolome and transcriptome analysis reveals a critical role of lignin biosynthesis and lignification in stem-like pneumatophore development of the mangrove Avicennia marina," *Planta*, vol. 259, no. 1, p. 12, Jan. 2024, doi: 10.1007/s00425-023-04291-0.

[42] H.Kartikaningsih, H. Djamaludin, J. N. Fauziyah, N. Audina, L. Noviyanti, and D. Saputra, "GREEN EXTRACTION OF Avicennia marina LEAVES BY NATURAL DEEP EUTECTIC SOLVENTS: PHYTOCHEMICAL PROFILE, ANTIOXIDANT ACTIVITY, MOLECULAR DOCKING AND ADMET ANALYSIS," *RASAYAN Journal of Chemistry*, vol. 17, no. 03, pp. 1123–1133, 2024, doi: 10.31788/RJC.2024.1738923.

[43] J. Wu *et al.*, "Complete assignments of ^{1}H and ^{13}C NMR data for 10 phenylethanoid glycosides," *Magnetic Resonance in Chemistry*, vol. 42, no. 7, pp. 659–662, Jul. 2004, doi: 10.1002/mrc.1393.

[44] L. B. Vinh *et al.*, "Cytotoxic triterpene saponins from the mangrove *Aegiceras corniculatum*," *Nat. Prod. Res.*, vol. 33, no. 5, pp. 628–634, Mar. 2019, doi: 10.1080/14786419.2017.1402320.

[45] S. M. Clemente, O. H. Martínez-Costa, M. Monsalve, and A. K. Samhan-Arias, "Targeting Lipid Peroxidation for Cancer Treatment," *Molecules*, vol. 25, no. 21, p. 5144, Nov. 2020, doi: 10.3390/molecules25215144.

[46] J.-H. Kang *et al.*, "Tumor-intrinsic role of ICAM-1 in driving metastatic progression of triple-negative breast cancer through direct interaction with EGFR," *Mol. Cancer*, vol. 23, no. 1, p. 230, Oct. 2024, doi: 10.1186/s12943-024-02150-4.

[47] L. Rosental, H. Nonogaki, and A. Fait, "Activation and regulation of primary metabolism during seed germination," *Seed Sci. Res.*, vol. 24, no. 1, pp. 1–15, Mar. 2014, doi: 10.1017/S0960258513000391.

[48] Y. Sharif *et al.*, "Cloning and Functional Characterization of a Pericarp Abundant Expression Promoter (AhGLP17-1P) From Peanut (Arachis hypogaea L.)," *Front. Genet.*, vol. 12, Jan. 2022, doi: 10.3389/fgene.2021.821281.

[49] S. Neugart, A. Krumbein, and R. Zrenner, "Influence of Light and Temperature on Gene Expression Leading to Accumulation of Specific Flavonol Glycosides and Hydroxycinnamic Acid Derivatives in Kale (Brassica oleracea var. sabellica)," *Front. Plant Sci.*, vol. 7, Mar. 2016, doi: 10.3389/fpls.2016.00326.

[50] H. Falahi, M. Sharifi, H. Z. Maivan, and N. A. Chashmi, "Phenylethanoid glycosides accumulation in roots of Scrophularia striata as a response to water stress," *Environ. Exp. Bot.*, vol. 147, pp. 13–21, Mar. 2018, doi: 10.1016/j.envexpbot.2017.11.003.

[51] E. Sarri *et al.*, "Salinity Stress Alters the Secondary Metabolic Profile of M. sativa, M. arborea and Their Hybrid (Alborea)," *Int. J. Mol. Sci.*, vol. 22, no. 9, p. 4882, May 2021, doi: 10.3390/ijms22094882.

[52] P. Zhou *et al.*, "Botany, traditional uses, phytochemistry, pharmacological activities, and toxicity of the mangrove plant Avicennia marina: a comprehensive review," *Phytochemistry Reviews*, vol. 24, no. 6, pp. 5533–5568, Dec. 2025, doi: 10.1007/s11101-025-10080-2.

[53] L. Han *et al.*, "New Abietane Diterpenoids from the Mangrove *Avicennia marina*," *Planta Med.*, vol. 74, no. 4, pp. 432–437, Mar. 2008, doi: 10.1055/s-2008-1034318.

[54] M. Di Ferdinando, C. Brunetti, A. Fini, and M. Tattini, "Flavonoids as Antioxidants in Plants Under Abiotic Stresses," in *Abiotic Stress Responses in Plants*, New York, NY: Springer New York, 2012, pp. 159–179. doi: 10.1007/978-1-4614-0634-1_9.

[55] J. Y. Wu, K. Wong, K. P. Ho, and L. G. Zhou, "Enhancement of saponin production in Panax ginseng cell culture by osmotic stress and nutrient feeding," *Enzyme Microb. Technol.*, vol. 36, no. 1, pp. 133–138, Jan. 2005, doi: 10.1016/j.enzmictec.2004.07.010.

[56] S. K. Das, J. K. Patra, and H. Thatoi, "Antioxidative response to abiotic and biotic stresses in mangrove plants: A review," *Int. Rev. Hydrobiol.*, vol. 101, no. 1–2, pp. 3–19, Apr. 2016, doi: 10.1002/iroh.201401744.

[57] H. Oku, S. Baba, H. Koga, K. Takara, and H. Iwasaki, "Lipid composition of mangrove and its relevance to salt tolerance," *J. Plant Res.*, vol. 116, no. 1, pp. 37–45, Feb. 2003, doi: 10.1007/s10265-002-0069-z.

[58] Z. Xue and B. Yang, "Phenylethanoid Glycosides: Research Advances in Their Phytochemistry, Pharmacological Activity and Pharmacokinetics," *Molecules*, vol. 21, no. 8, p. 991, Jul. 2016, doi: 10.3390/molecules21080991.

[59] S.-H. Lu, H.-J. Zuo, J. Huang, W.-N. Li, J.-L. Huang, and X.-X. Li, "Chemical Constituents from the Leaves of Ligustrum robustum and Their Bioactivities," *Molecules*, vol. 28, no. 1, p. 362, Jan. 2023, doi: 10.3390/molecules28010362.

[60] C. Niu *et al.*, "Phenylethanoid glycosides from Callicarpa macrophylla Vahl," *Phytochem. Lett.*, vol. 38, pp. 65–69, Aug. 2020, doi: 10.1016/j.phytol.2020.05.013.

[61] A. abbas Momtazi-borojeni, M. Behbahani, H. Sadeghi-aliabadi, and S. H. Antiproliferative, "Activity and Apoptosis Induction of Crude Extract and Fractions of Avicennia marina," 2013.

[62] I. B. Tanjung, N. N. Azizah, A. Arsianti, A. S. Anisa, and K. A. Audah, "Evaluation of the Ethyl Acetate Extract of the Roots of *Avicennia marina* as Potential Anticancer Drug," 2022. doi: 10.2991/absr.k.220101.011.

[63] B. S. Addy *et al.*, "In vitro antiproliferative activities of some Ghanaian medicinal plants," *Clinical Phytoscience*, vol. 10, no. 1, p. 19, Sep. 2024, doi: 10.1186/s40816-024-00383-w.

[64] "Research Progress on Natural Triterpenoid Saponins in the Chemoprevention and Chemotherapy of Cancer," 2014, pp. 95–130. doi: 10.1016/B978-0-12-802215-3.00006-9.

[65] Y. V. da Silva Magedans, M. A. Phillips, and A. G. Fett-Neto, "Production of plant bioactive triterpenoid saponins: from metabolites to genes and back," *Phytochemistry Reviews*, vol. 20, no. 2, pp. 461–482, Apr. 2021, doi: 10.1007/s11101-020-09722-4.

[66] X.-W. Yang, Z. Dai, B. Wang, Y.-P. Liu, X.-D. Zhao, and X.-D. Luo, "Antitumor Triterpenoid Saponin from the Fruits of Avicennia marina," *Nat. Prod. Bioprospect.*, vol. 8, no. 5, pp. 347–353, Oct. 2018, doi: 10.1007/s13659-018-0167-9.

[67] N. Duke, "A systematic revision of the mangrove genus *Avicennia* (Avicenniaceae) in Australasia*," *Aust. Syst. Bot.*, vol. 4, no. 2, pp. 299–324, Jun. 1991, doi: 10.1071/SB9910299.

[68] G. Friis and M. E. Killilea, "Mangrove Ecosystems of the United Arab Emirates," in *A Natural History of the Emirates*, Cham: Springer Nature Switzerland, 2024, pp. 217–240. doi: 10.1007/978-3-031-37397-8_7.

[69] G. Friis *et al.*, "A high-quality genome assembly and annotation of the gray mangrove, *Avicennia marina*," *G3 Genes|Genomes|Genetics*, vol. 11, no. 1, Mar. 2021, doi: 10.1093/g3journal/jkaa025.

[70] G. Friis *et al.*, "Rapid diversification of grey mangroves (*Avicennia marina*) driven by geographic isolation and extreme environmental conditions in the Arabian Peninsula," *Mol. Ecol.*, vol. 33, no. 4, Feb. 2024, doi: 10.1111/mec.17260.

[71] I. S. Che Sulaiman, M. Basri, H. R. Fard Masoumi, W. J. Chee, S. E. Ashari, and M. Ismail, "Effects of temperature, time, and solvent ratio on the extraction of phenolic compounds and the anti-radical activity of Clinacanthus nutans Lindau leaves by response surface methodology," *Chem. Cent. J.*, vol. 11, no. 1, p. 54, Dec. 2017, doi: 10.1186/s13065-017-0285-1.

[72] K. J. A. Lim, A. A. Cabajar, C. F. Y. Lobarbio, E. B. Taboada, and D. J. Lacks, "Extraction of bioactive compounds from mango (Mangifera indica L. var. Carabao) seed kernel with ethanol–water binary solvent systems," *J. Food Sci. Technol.*, vol. 56, no. 5, pp. 2536–2544, May 2019, doi: 10.1007/s13197-019-03732-7.

[73] N. L. Huamán-Castilla *et al.*, "Exploring a Sustainable Process for Polyphenol Extraction from Olive Leaves," *Foods*, vol. 13, no. 2, p. 265, Jan. 2024, doi: 10.3390/foods13020265.

[74] D. Palaiogiannis, T. Chatzimitakos, V. Athanasiadis, E. Bozinou, D. P. Makris, and S. I. Lalas, "Successive Solvent Extraction of Polyphenols and Flavonoids from Cistus creticus L. Leaves," *Oxygen*, vol. 3, no. 3, pp. 274–286, Jun. 2023, doi: 10.3390/oxygen3030018.

[75] C. Cannavacciuolo *et al.*, "LC-MS and GC-MS Data Fusion Metabolomics Profiling Coupled with Multivariate Analysis for the Discrimination of Different Parts of Faustrime Fruit and Evaluation of Their Antioxidant Activity," *Antioxidants*, vol. 12, no. 3, p. 565, Feb. 2023, doi: 10.3390/antiox12030565.

[76] D. Verbanac *et al.*, "An efficient and convenient microwave-assisted chemical synthesis of (thio)xanthones with additional in vitro and in silico characterization," *Bioorg. Med. Chem.*, vol. 20, no. 10, pp. 3180–3185, May 2012, doi: 10.1016/j.bmc.2012.03.074.

[77] D. A. Filimonov *et al.*, "Prediction of the Biological Activity Spectra of Organic Compounds Using the Pass Online Web Resource," *Chem. Heterocycl. Compd. (N Y).*, vol. 50, no. 3, pp. 444–457, Jun. 2014, doi: 10.1007/s10593-014-1496-1.

[78] T. Desai and S. Joshi, "In silico evaluation of apoptogenic potential and toxicological profile of triterpenoids," *Indian J. Pharmacol.*, vol. 51, no. 3, p. 181, 2019, doi: 10.4103/ijp.IJP_90_18.

[79] A. Lagunin, A. Stepanchikova, D. Filimonov, and V. Poroikov, "PASS: prediction of activity spectra for biologically active substances," *Bioinformatics*, vol. 16, no. 8, pp. 747–748, Aug. 2000, doi: 10.1093/bioinformatics/16.8.747.

6 General conclusions and future perspectives

This PhD project was conceived and developed within the contemporary context of the cosmetic industry's dual challenge: the growing demand for effective anti-aging products and the urgent need to improve sustainability across the entire product lifecycle. By integrating bioprospecting, biological screening, phytochemical analysis, and formulation science, the work addressed these challenges through a holistic and flexible research strategy.

The initial screening phase clearly demonstrated that *Prosopis cineraria* (Ghaf) represents a highly promising natural source of anti-aging bioactivity. All Ghaf extracts exhibited strong antioxidant capacity and consistent inhibition of key enzymes involved in extracellular matrix degradation, including elastase, collagenase, and hyaluronidase. The lack of marked differences among plant parts provided a strong scientific rationale for the development of a whole-plant representative extract, enabling process simplification, improved sustainability, and potential synergistic effects among phytochemicals. In addition, the optimization of *in vitro* enzymatic assays addressed methodological gaps in the literature and resulted in a robust, cost-effective, and reproducible screening platform that can be broadly applied in future research on cosmetic actives.

Building on these results, the second part of the project successfully translated biological potential into a formulation-driven application. The Ghaf extract was shown to possess a multifunctional anti-aging profile, combining antioxidant activity with inhibition of enzymes related to ECM degradation and pigmentation. The formulation study further demonstrated that sustainability-oriented cosmetic development is achievable without compromising performance. Through careful ingredient selection and a Design of Experiments approach, a stable oil-in-water Pickering emulsion with a minimal INCI list was developed. The successful incorporation of Ghaf extract without altering stability, rheology, or microstructure represents a critical step toward practical cosmetic application and confirms formulation compatibility at relevant concentrations. Although biological testing of the final formulation could not be completed within the timeframe of this PhD, the comprehensive physicochemical characterization provides a solid foundation for future studies addressing efficacy, safety, and skin-compatibility. In addition, permeability studies should be

conducted to evaluate the capability of the bioactive constituents to cross the stratum corneum and reach the derma, where they are expected to exert their effects.

In contrast, *Avicennia marina* extracts did not meet the requirements for cosmetic anti-aging applications, as evidenced by their limited enzyme inhibitory activity. Rather than representing a limitation, this outcome underscored the importance of adopting an adaptive and evidence-based research strategy. By redirecting the investigation toward a bioprospecting-oriented approach, the project successfully revealed the therapeutic potential of *A. marina*, particularly its root and pericarp extracts. The identification of previously unreported triterpene saponins and phenylethanoid glycosides in UAE-grown populations highlights the influence of extreme environmental conditions on phytochemical diversity and bioactivity. The observed antioxidant and cytotoxic effects, supported by *in silico* analysis, position *A. marina* as a valuable and underexplored source of bioactive compounds with potential anticancer applications. In this context, future research should focus on bioactivity-guided fractionation of the most active extracts, with particular emphasis on isolating and characterizing the triterpene saponin-rich fractions that may contribute to the observed cytotoxic activity. Such studies would help clarify structure–activity relationships and could ultimately support the identification of novel therapeutic candidates derived from this stress-adapted mangrove species.

More broadly, the encouraging results obtained in this work open several additional research directions that are relevant for both cosmetic and pharmaceutical development. In particular, further efforts should focus on the quantitative phytochemical characterization of the extracts, complementing the qualitative profiling performed in this study. Targeted quantification of key bioactive compounds would represent a crucial step toward extract standardization and quality control, ensuring batch-to-batch consistency despite the intrinsic variability associated with plant-derived raw materials. In parallel, the industrial feasibility of the proposed applications should be evaluated through scalability studies of both the extraction procedures and the formulation processes. Such investigations would include optimization of extraction yield and reproducibility, assessment of long-term formulation stability, and adaptation of laboratory-scale preparation methods to industrial manufacturing conditions.

Taken together, this doctoral work exemplifies a comprehensive framework for the sustainable valorization of plant resources. Rather than pursuing a single predefined application, plant extracts were evaluated and developed according to their most promising biological activities. This flexible strategy not only maximized scientific output but also aligned with principles of sustainability, efficiency, and responsible innovation. The findings of this project contribute novel insights into the bioactivity of stress-adapted plant species from the UAE and provide practical methodologies and conceptual guidance for future research in cosmetic science, natural product chemistry, and bioprospecting-driven drug discovery.

7 List of publications

Spena, F., De Santes, B., Morelli, L., Daniellou, R., Huc-Mathis, D., Salvioni, L., Galli, P., Prosperi, D., Giustra, M., Colombo, M. (2026). From biopolymers to Pickering emulsions: a green chemistry strategy to replace microplastics in next-generation cosmetics. RSC Advances, 16(22), 20399–20410. https://doi.org/10.1039/D6RA01252C

Cerri F†, De Santes B†, Spena F†, Salvioni L, Forcella M, Fusi P, Pagliari S, Stahl H, Galli P, Colombo M, Giustra M, Campone L. Phytochemical Profiling, Antioxidant Activity, and *In Vitro* Cytotoxic Potential of Mangrove *Avicennia marina*. Pharmaceuticals (Basel). 2025 Aug 31;18(9):1308. doi: 10.3390/ph18091308. PMID: 41011179; PMCID: PMC12472679.

†equal contribution

Giustra M, Sinesi G, Spena F, De Santes B, Morelli L, Barbieri L, Garbujo S, Galli P, Prosperi D, Colombo M. Microplastics in Cosmetics: Open Questions and Sustainable Opportunities. ChemSusChem. 2024 Nov 25;17(22):e202401065. doi: 10.1002/cssc.202401065. Epub 2024 Sep 24. PMID: 39222323; PMCID: PMC11587687.

Morelli L, Ochoa E, Salvioni L, Davide Giustra M, De Santes B, Spena F, Barbieri L, Garbujo S, Tomaino G, Novati B, Bolis L, Moutaharrik S, Prosperi D, Palugan L, Colombo M. Microfluidic nanoparticle synthesis for oral solid dosage forms: A step toward clinical transition processes. Int J Pharm. 2024 Mar 5;652:123850. doi: 10.1016/j.ijpharm.2024.123850. Epub 2024 Jan 26. PMID: 38280498.

Ochoa E, Morelli L, Salvioni L, Giustra M, De Santes B, Spena F, Barbieri L, Garbujo S, Viganò M, Novati B, Tomaino G, Moutaharrik S, Prosperi D, Palugan L, Colombo M. Co-processed materials testing as excipients to produce Orally Disintegrating Tablets (ODT) using binder jet 3D-printing technology. Eur J Pharm Biopharm. 2024 Jan;194:85-94. doi: 10.1016/j.ejpb.2023.11.023. Epub 2023 Dec 2. PMID: 38048887.

Beatrice De Santes, Lucia Morelli, Francesca Spena, Stefania Pagliari, Delphine Huc-Mathis, Richard Daniellou, Marco Giustra, Luca Campone, Federico Cerri, Paolo Galli, Davide Prosperi, Lucia Salvioni, Miriam Colombo: *Prosopis cineraria* (Ghaf) Extract as a Natural Ingredient for Anti-Aging Dermocosmetic Applications (submitted)

8 Acknowledgements

I would like to express my sincere gratitude to all those who have supported me throughout this PhD journey, both professionally and personally.

First and foremost, I am deeply grateful to my tutor, Prof. Miriam Colombo, for her continuous guidance, scientific rigor, and invaluable support throughout this project. Her expertise and dedication have been fundamental to the development of this work. I also warmly thank my co-tutor, Dr. Lucia Salvioni, for her availability, insightful discussions, and practical advice during the course of my research.

I would like to extend my sincere appreciation to my supervisor, Prof. Paolo Galli, for his support and for providing me with the opportunity to carry out this research project.

I am also grateful to Prof. Davide Prosperi and the entire Nanobiolab team, where this work was developed, for providing a stimulating and collaborative research environment.

I would like to sincerely thank Prof. Richard Daniellou and Prof. Delphine Huc-Mathis for their support and for giving me the opportunity to carry out my research period abroad at AgroParisTech, Chaire de Cosmétologie. I am also grateful to their entire team for their warm welcome and for their support during this valuable experience.

A special thanks goes to Prof. Luca Campone and Dr. Stefania Pagliari for their essential contribution to the chemical characterization analyses, which were fundamental to this project.

I would also like to thank all my colleagues and fellow PhD students for their support and for sharing this journey with me. In particular, I am deeply grateful to Dr. Francesca Spena and Dr. Federico Cerri for their valuable scientific contribution and, above all, for making this experience more enjoyable and less challenging through their presence and support.

Finally, I would like to thank my friends for their encouragement, my family for their unconditional support and constant belief in me, and my partner Martino for his patience, understanding, and for always being by my side.

Tesi di dottorato realizzata nell'ambito del progetto MUSA finanziato dal PNRR Missione 4 Componente 2 Investimento 1.5, finanziato dall'Unione Europea - NextGenerationEU –

CUP H43C22000550001

pharmaceuticals

MDPI

Article

Phytochemical Profiling, Antioxidant Activity, and In Vitro Cytotoxic Potential of Mangrove *Avicennia marina*

Federico Cerri [1,2,†], Beatrice De Santes [1,3,†], Francesca Spena [1,3,†], Lucia Salvioni [3,4], Matilde Forcella [3], Paola Fusi [3], Stefania Pagliari [3,*], Henrik Stahl [5], Paolo Galli [1,2], Miriam Colombo [3,4], Marco Giustra [3,4,*] and Luca Campone [3]

[1] Department of Earth and Environmental Sciences DISAT, University of Milano-Bicocca, Piazza della Scienza 1, 20126 Milan, Italy; federico.cerri@unimib.it (F.C.); b.desantes@campus.unimib.it (B.D.S.); f.spena2@campus.unimib.it (F.S.); paolo.galli@unimib.it (P.G.)
[2] MaRHE Centre (Marine Research and Higher Education Center), Magoodhoo Island, Faafu Atoll 12030, Maldives
[3] Department of Biotechnology and Biosciences, University of Milano-Bicocca, Piazza della Scienza 2, 20126 Milan, Italy; lucia.salvioni@unimib.it (L.S.); matilde.forcella@unimib.it (M.F.); paola.fusi@unimib.it (P.F.); miriam.colombo@unimib.it (M.C.); luca.campone@unimib.it (L.C.)
[4] Nanomedicine Center NANOMIB, University of Milano-Bicocca, 20854 Vedano al Lambro, Italy
[5] College of Marine Science and Aquatic Biology, University of Khorfakkan, Sharjah 18119, United Arab Emirates; henrik.stahl@ukf.ac.ae
* Correspondence: stefania.pagliari@unimib.it (S.P.); marco.giustra@unimib.it (M.G.)
† These authors contribute equally to this work.

Abstract

Background: *Avicennia marina* (Forsk.) Vierh., a widely distributed mangrove species, is known for its diverse secondary metabolites with potential pharmacological applications. Despite its dominance in the Arabian Gulf, where *A. marina* may have adapted to extreme environmental conditions with a distinct set of bioactive molecules, research in this region remains limited. **Methods:** This study investigates the phytochemical composition, antioxidant activity, and in vitro cytotoxicity of extracts from different plant parts, including roots, leaves, propagules, pericarps, and cotyledons, collected in the United Arab Emirates (UAE). Extracts were analyzed using ultra-pressure liquid chromatography coupled with high-resolution mass spectrometry (UPLC-HRMS). Antioxidant activity was assessed using DPPH and ABTS assays, while cytotoxicity was evaluated against human cancer and normal cell lines. **Results:** Analysis revealed 49 compounds, including iridoid glycosides, hydroxycinnamic acids, phenylethanoid glycosides, flavonoid glycosides, and triterpene saponins, several reported for the first time in *A. marina* and mangroves. The pericarp and root extracts exhibited the highest scavenging activity (DPPH: 187.14 ± 2.87 and 128.25 ± 1.12; ABTS: 217.16 ± 2.67 and 147.21 ± 2.42 µmol TE/g, respectively), correlating with phenylethanoid content. The root extract also displayed the highest cytotoxicity, with IC_{50} values of 58.46, 81.98, and 108.10 µg/mL against MDA-MB-231, SW480, and E705, respectively. In silico analysis identified triterpene saponins as potential contributors. **Conclusions:** These findings highlight the root extract of *A. marina* as a promising source of bioactive compounds with potential antioxidant and anticancer applications, supporting further exploration for novel therapeutic candidates.

Keywords: mangroves; *Avicennia marina*; natural products; bioactive compounds; phytochemical analysis; UPLC-HRMS; antioxidant activity; cytotoxicity; triterpene saponins

Academic Editor: Grażyna Zgórka

Received: 21 July 2025
Revised: 21 August 2025
Accepted: 27 August 2025
Published: 31 August 2025

Citation: Cerri, F.; De Santes, B.; Spena, F.; Salvioni, L.; Forcella, M.; Fusi, P.; Pagliari, S.; Stahl, H.; Galli, P.; Colombo, M.; et al. Phytochemical Profiling, Antioxidant Activity, and In Vitro Cytotoxic Potential of Mangrove *Avicennia marina*. *Pharmaceuticals* **2025**, *18*, 1308. https://doi.org/10.3390/ph18091308

1. Introduction

Avicennia marina (Forsk.) Vierh, commonly known as the grey mangrove, is a true mangrove species [1] belonging to the Acanthaceae family. It is widely distributed across tropical and subtropical regions, including Africa; South, Southeast, and Southwest Asia; the Malay Archipelago; the North Island of New Zealand; Australia; the Southwest Pacific; and the Maldives [1–3].

The chemical profile of *A. marina* has been extensively studied, leading to the identification of diverse classes of bioactive molecules, including flavonoids, iridoid glycosides, terpenoids, alkaloids, and steroids, as well as a wide range of other metabolites [3–8].

Traditionally, *A. marina* has been utilized in folk medicine across different countries to treat several ailments and diseases [9,10]. Furthermore, its extracts and isolated compounds have demonstrated a wide range of biological activities, including antiviral, antimicrobial, anthelmintic and antimalarial, analgesic, antioxidant, antifouling, anticancer, antidiabetic, and anti-inflammatory [3,11]. In particular, extracts of this species have demonstrated promising in vitro anticancer activity [3]. However, research in this field remains relatively limited, especially in the context of the Arabian Gulf, where *A. marina* is the dominant mangrove species along the coasts of the United Arab Emirates (UAE), Saudi Arabia, Bahrain, Qatar, and Iran [12]. Ethnobotanical records for *A. marina* in the Arabian Gulf are scarce but include traditional uses in Iran for treatments of ulcers, rheumatism, and burns [9], and in the UAE for its use as an aphrodisiac, antifertility agent, and treatment for scabies and toothache [13]. *A. marina* remains largely unexplored here in terms of bioprospecting, with most studies focusing instead on its distribution, ecological significance, ecosystem services, and management and conservation [14,15]. Phytochemical investigations have only examined populations from China, India, Pakistan, Egypt, other Indo-Pacific locations, and the Red Sea coasts of Saudi Arabia [10,11,16–18].

Previous phytochemical studies on *A. marina* have generally examined only a few plant parts, typically aerial parts and primarily leaves, lacking a comprehensive analysis of plant-part-specific secondary metabolites. Biological activity also presents limitations, often focusing on few plant parts and, in the case of cytotoxicity, testing only a small number of cancer cell lines [9–11]. A major gap in existing research of *A. marina* is the absence of integrated studies combining detailed phytochemical profiling with antioxidant and cytotoxic assays across multiple parts of the plant, which is essential for linking bioactivities to tissue-specific metabolites. Such combined strategies are well established in plant research [19,20] and have been applied to mangroves [21] as they facilitate the prioritization of promising extracts and compounds, thereby enhancing efficiency in the early discovery of bioactive molecules. Moreover, the majority of chemical studies have relied on GC-MS, which biases detection towards volatile constituents [3,11,16]. Although GC-MS can also characterize phenolic compounds, abundant in mangroves [22], it requires a derivatization step that is both complex and time-consuming [23]. In contrast, ultra-high performance liquid chromatography coupled with high-resolution mass spectrometry (UPLC-HRMS) has emerged as a powerful platform for untargeted metabolomic profiling of complex plant matrices, offering superior sensitivity, selectivity, and mass accuracy, and enabling comprehensive detection and identification of secondary metabolites, especially phenolics [24–27].

In addition to these methodological gaps, the limited geographical scope of previous studies represents a crucial limitation in fully understanding the phytochemical diversity and bioactivity of *A. marina*. The Arabian Gulf is characterized by extreme environmental conditions, including elevated seawater temperatures, hypersalinity, and high turbidity, driven by its arid climate and shallow basin [28], and summer air temperatures can reach 50 °C [29], further stressing local ecosystems. Since the chemical composition of plants is

influenced by geographical, environmental, and climate factors [30–32], plants exposed to such stresses often respond by increasing the accumulation of secondary metabolites, such as flavonoids, iridoid glycosides, and phenylethanoid glycosides, which enhance their tolerance to adverse conditions and also possess bioactivities of pharmacological interest, including antioxidant and anticancer [33–39].

It is plausible that *A. marina* in the Arabian Gulf may have adapted to extreme conditions through metabolic changes and the induction of antioxidant defense systems [40], potentially resulting in a distinct set of secondary metabolites with unique biological activities. Consequently, the objective of this study is to conduct a comprehensive investigation of *A. marina* grown in the UAE by characterizing the secondary metabolite composition of multiple parts of the plant, including roots, leaves, propagules (pericarps and internal tissues), and cotyledons, and evaluating their potential health benefits through antioxidant and cytotoxic activity assays in vitro.

Unlike previous studies, this work employs UPLC-HRMS to present a detailed phytochemical profile of each tissue type, allowing for the identification of specific compounds of *A. marina* and their localization within the plant. Furthermore, while the antioxidant and anticancer potentials of *A. marina* extracts have been previously reported [3,11], this study provides a comprehensive evaluation of antioxidant and cytotoxic activities of all plant parts, along with expanded cytotoxic screening in multiple cancer cell lines. In addition, in silico predictions of biological activities were applied to compounds identified in the extracts. This multi-level approach addresses existing regional and methodological gaps and lays the groundwork for the discovery of bioactive compounds from plants adapted to extreme environmental conditions.

2. Results

2.1. Characterization of Avicennia marina Extracts

Roots, leaves, cotyledons, pericarps, and propagules of *A. marina* displayed distinct metabolite profiles. The chromatographic profiles of the extracts are provided in Supplementary Material (Figures S1–S5), and the list of tentatively identified compounds is shown in Table 1, along with their corresponding identification level (IL), which reflects the confidence of compound annotation based on MSI guidelines (see Section 4.4). For compounds assigned to IL2, the identification relied on comparisons of MS/MS fragmentation data with published spectra from the literature or spectral databases. The specific references used to support each IL2 assignment are included directly in the table.

Table 1. UHPLC-ESI/HRMS data of compounds detected in *Avicennia marina* extracts. The main fragment ion for each compound is indicated in bold.

No.	RT (min)	$[M-H]^-$	Formula	Δ ppm	MS/MS	Name	Class	Part	IL	Ref.
1	0.58	701.1893 $[M+Cl]^-$	$C_{24}H_{42}O_{21}$	−2.1677	665.2134, 485.1499, 443.1393, **383.1182**, 341.1075, 179.0549	Stachyose	Tetrasaccharides	Cotyledons/pericarps/propagules/roots	IL2	[41]
2	0.99	191.0188	$C_6H_8O_7$	6.3850	111.0073	Citric acid	Tricarboxylic acids	Cotyledons/pericarps	IL2	[42]
3	3.87	373.1139	$C_{16}H_{22}O_{10}$	0.3221	211.0605, 167.0700, 149.0597, **123.0440**, 105.0333	Geniposidic acid	Iridoid glycosides	Leaves/cotyledons/pericarps/propagules/roots	IL2	[43]
4	4.03	353.0875	$C_{16}H_{18}O_9$	0.8633	**191.0551**, 179.0339, 161.0233, 135.0439	Caffeoylquinic acid isomer	Hydroxycinnamic acids and derivatives	Roots	IL2	[44]
5	4.05	375.1291	$C_{16}H_{24}O_{10}$	1.5167	213.0756, 169.0857, **151.0753**, 133.0644, 125.0595, 107.0490	Mussaenosidic acid	Iridoid glycosides	Leaves/cotyledons/pericarps/propagules	IL2	[45]
6	4.33	375.1285	$C_{16}H_{24}O_{10}$	3.1119	213.0747, 169.0854, **151.0748**, 133.0644, 125.0591, 113.0230, 107.0484	(Epi)loganic acid	Iridoid glycosides	Leaves	IL2	[45]
7	4.53	487.1451	$C_{21}H_{28}O_{13}$	1.2588	**179.0334**, 161.0228, 135.0435	Cistanoside F	Phenylethanoid glycosides	Pericarps	IL2	[46]
8	4.80	327.0715	$C_{14}H_{16}O_9$	1.9983	179.0335, 165.0389, 147.0283, **135.0434**, 105.0178	Unidentified	-	Leaves		
9	5.09	353.0871	$C_{16}H_{18}O_9$	−3.0904	**191.0550**, 179.0337, 173.0442, 161.0232, 135.0439,	Caffeoylquinic acid isomer	Hydroxycinnamic acids and derivatives	Leaves/cotyledons/pericarps/propagules/roots	IL2	[44]
10	5.47	371.0982	$C_{15}H_{16}O_{11}$	−8.7858	**209.0635**, 179.0337, 161.0228, 135.0435, 129.0178	Caffeoyl hexaric acid	Hydroxycinnamic acids and derivatives	Leaves	IL2	[47]
11	5.60	443.0655	$C_{18}H_{20}O_{11}S$	−0.3243	275.0218, **167.0338**, **152.0105**, 123.0440, 108.0204	Unidentified	-	Roots		
12	5.65	415.1603	$C_{19}H_{28}O_{10}$	1.6114	235.0963, **191.1062**, 173.0958, 149.0953, 137.0590, 101.0226	Icariside D1	Flavonoid glycosides	Leaves	IL2	[48]
13	5.93	639.1964	$C_{29}H_{36}O_{16}$	−5.2193	621.1807, 529.1554, 459.1488, 251.0549, 179.0337, **161.0232**, 151.0387	Suspensaside isomer	Phenylethanoid glycosides	Pericarps/roots	IL2	[49,50]

Table 1. *Cont.*

No.	RT (min)	$[M-H]^-$	Formula	Δ ppm	MS/MS	Name	Class	Part	IL	Ref.
14	5.95	639.1964	$C_{29}H_{36}O_{16}$	−5.2193	621.1807, 529.1554, 459.1488, 251.0549, 179.0337, **161.0232**, 151.0387	Suspensaside isomer	Phenylethanoid glycosides	Pericarps/roots	IL2	[49,50]
15	6.14	537.1628	$C_{25}H_{30}O_{13}$	−2.6672	493.1708, 375.1275, 323.0758, 213.0752, 179.0334, 169.0854, **161.0230**, 151.0750, 135.0435, 125.0593, 107.0486	Grandifloroside	Hydroxycinnamic acid and derivatives	Leaves	IL2	[51]
16	6.33	619.1644	$C_{29}H_{32}O_{15}$	3.9407	383.0758, **311.0549**, 267.0646	Unidentified	-	Pericarps/roots		
17	6.41	639.1929	$C_{29}H_{36}O_{16}$	0.2477	**621.1817**, 529.1554, 459.1493, 251.0549 **179.0338**, 161.0236, 151.0385	Suspensaside isomer	Phenylethanoid glycosides	Roots	IL2	[49,50]
18	6.65	521.1658	$C_{25}H_{30}O_{12}$	1.2446	357.1176, 169.0854, 163.0385, 151.0749, 145.0280, 125.0591, 119.0486, 117.0329, 107.0486	Marinoid C	Iridoid glycosides	Leaves/cotyledons/pericarps	IL3	[7]
19	6.65	653.2091	$C_{29}H_{34}O_{17}$	9.55333	621.1822, 459.1499, 179.0338, **161.0234**, 151.0388, 135.0437	Suspensaside methyl ether	Phenylethanoid glycosides	Roots	IL2	[49,50]
20	6.79	623.1981	$C_{29}H_{36}O_{15}$	0.0705	461.1657, **161.0233**, 113.0283	Verbascoside (acteoside) isomer	Phenylethanoid glycosides	Leaves/pericarps/roots	IL2	[52]
21	6.9	463.0874	$C_{21}H_{20}O_{12}$	1.7229	301.0324, **300.0264,** 271.0235, 255.0285	Quercetin 3-*O*-hexoside	Flavonoid glycosides	Roots	IL2	[53–55]
22	7.02	667.2239	$C_{31}H_{40}O_{16}$	0.6864	621.1824, 459.1499, **179.0338**, **161.0235**, 151.0386, 135.0436	β-ethyl-OH-verbascoside	Phenylethanoid glycosides	Pericarps	IL2	[56,57]
23	7.11	623.2001	$C_{29}H_{36}O_{15}$	−3.1336	461.1661, **161.0235**,	Verbascoside (acteoside) isomer	Phenylethanoid glycosides	Leaves/pericarps/roots	IL2	[52]
24	7.21	621.1838	$C_{29}H_{34}O_{15}$	−2.0992	461.1652, 179.0337, **161.0233**, 151.0387	Suspensaside A	Phenylethanoid glycosides	Roots	IL2	[49,50]
25	7.21	461.0718	$C_{21}H_{18}O_{12}$	1.6222	**285.0391**	Kaempferol-3-*O*-glucuronide	Flavonoid glycosides	Leaves	IL2	[58]
26	7.21	681.2063	$C_{31}H_{38}O_{17}$	−3.9236	519.1708, 490.1321, 181.0129, 179.0334, **161.0230**	Unidentified	-	Pericarps		

Table 1. *Cont.*

No.	RT (min)	$[M-H]^-$	Formula	Δ ppm	MS/MS	Name	Class	Part	IL	Ref.
27	7.3	447.0926	$C_{21}H_{20}O_{11}$	1.5287	327.0494, 285.0648, **284.0315**, 255.0288, 227.0338, 151.0013	Kaempferol 3-*O*-glucoside	Flavonoid glycosides	Roots	IL2	[55,59–61]
28	7.40	623.1658	$C_{28}H_{32}O_{16}$	−6.4750	**315.0494**, 314.0421, 300.0258, 299.0187, 271.0234	Isorhamnetin-3-*O*-rutinoside	Flavonoid glycosides	Leaves/pericarps	IL2	[62]
29	7.40	491.0828	$C_{22}H_{20}O_{13}$	0.6385	**315.0499**, 300.0264	Isorhamnetin glucuronide	Flavonoid glycosides	Leaves	IL2	[63]
30	7.51	535.1477	$C_{25}H_{28}O_{13}$	−3.7032	329.1021, **179.0338**, 161.0232, 149.0595, 135.0438	Unidentified	-	Leaves/Pericarps		
31	7.51	477.1036	$C_{22}H_{22}O_{12}$	−5.1250	315.0467, **314.0420**, 285.0392, 271.0236, 257.0441, 243.0286,	Isorhamnetin 7-glucoside	Flavonoid glycosides	Leaves	IL2	[63]
32	7.61	471.1874	$C_{22}H_{32}O_{11}$	−0.4545	287.1273, **263.1278**, 219.1379, 201.1273, 186.1036, 147.1166	Unidentified	-	Pericarps		
33	7.86	519.1143	$C_{24}H_{24}O_{13}$	0.2199	315.0472, **314.0423**, 299.0186, 285.0383, 271.0236, 257.0443, 243.0286	Unidentified	-	Leaves		
34	7.90	553.1556	$C_{25}H_{30}O_{14}$	1.2256	329.1021, **197.0445**, 182.0206, 153.0454, 149.0596, 131.0489,	Marinoid D	Iridoid glycosides	Cotyledons/pericarps/propagules/roots	IL3	[7]
35	7.95	505.1757	$C_{25}H_{29}O_{11}$	0.2000	357.1184, 213.0757, 195.0650, 169.0857, 151.0753, **147.0439**, 125.0596, 113.0230, 107.0487, 103.0539	Marinoid A	Iridoid glycosides	Leaves	IL3	[7]
36	8.03	519.1505	$C_{25}H_{28}O_{12}$	0.5766	313.1072, 295.0961, **163.0388**, 149.0596, 145.0282, 131.0490, 119.0487	Unidentified	-	Leaves/cotyledons/pericarps/roots		
37	8.03	475.0887	$C_{22}H_{20}O_{12}$	−1.0510	300.0589, **299.0554**, 285.0358, **284.0318.**	Diosmetin 7-glucuronide	Flavonoid glycosides	Leaves	IL2	[64]
38	8.24	549.1616	$C_{26}H_{30}O_{13}$	−0.4279	343.1176, 325.1064, **193.0495**, 175.0387, 149.0595, 134.0360, 131.0489	Unidentified	-	Leaves/cotyledons/pericarps/roots		
39	8.36	591.2119	$C_{29}H_{36}O_{13}$	−6.0539	179.0333, **161.0234**, 133.0282, 113.0228	Jionoside C	Phenylethanoid glycosides	Pericarps	IL2	[65]
40	8.62	825.4276	$C_{44}H_{66}O_{16}$	0.2536	**663.3744**, 601.3735	Unknown triterpene saponin	Triterpene saponins	Roots	IL3	[66,67]

Table 1. *Cont.*

No.	RT (min)	$[M-H]^-$	Formula	Δ ppm	MS/MS	Name	Class	Part	IL	Ref.
41	8.70	539.2152	$C_{26}H_{36}O_{12}$	−3.3318	193.0485, 183.1010, 175.0382, 149.0591, 131.0485, 121.0642	Unidentified	-	Leaves		
42	8.80	541.2285	$C_{26}H_{38}O_{12}$	1.0147	193.0485, 185.1166, 175.0382, 149.0591, 131.0485, 121.0642	Unidentified	-	Leaves		
43	8.88	825.4285	$C_{42}H_{66}O_{16}$	−0.8354	**663.3744**, 601.3735, 487.3421	Unknown triterpene saponin	Triterpene saponins	Roots	IL3	[66,67]
44	8.97	299.0546	$C_{16}H_{12}O_6$	5.0379	285.0345, **284.0313**, 256.0363, 227.0334	Trihydroxy-methoxyflavone	Flavones	Leaves	IL2	[68]
45	8.99	825.4273	$C_{42}H_{66}O_{16}$	0.6166	**663.3744**, 601.3735,	Medicoside G (medicagenic acid 3,28-di-glucoside)	Triterpene saponins	Roots	IL2	[66,67]
46	9.08	809.4316	$C_{42}H_{66}O_{15}$	1.5979	689.3884, **647.3788**, 629.3680, 585.3786	Esculentoside C (phycolaccoside D)	Triterpene saponins	Cotyledons/pericarps/propagules/roots	IL2	[69,70]
47	9.30	505.1711	$C_{25}H_{30}O_{11}$	0.8600	281.1170, 195.0649, 151.0750, **147.0438**, 133.0645, 107.0486	Unidentified	-	Leaves		
48	9.38	503.1572	$C_{25}H_{28}O_{11}$	−2.6077	279.1010, 253,0854, 209.0954, 195.0647, **147.0437**, 131.0486, 103.0536	Unidentified	-	Leaves/pericarps		
49	9.54	809.4342	$C_{42}H_{66}O_{15}$	−1.6102	**647.3797**, 471.3469	Azukisaponin III	Triterpene saponins	Roots	IL2	[71]

Analysis detected a total of 49 compounds across all plant parts. Triterpene saponins are a heterogeneous secondary metabolite consisting of a terpene-based aglycone linked to one or more sugar chains, commonly glucose (−162 Da), glucuronic acid (−176 Da), and pentoses (−146 Da) [72]. For example, compound 49, which has an m/z of 809.4342 and a molecular formula of $C_{42}H_{66}O_{15}$, displayed characteristic MS/MS fragments at m/z 647.3797 [M-H-162] and 471.3469 [M-H-162-176], corresponding to sequential losses of sugar moieties. Based on this fragmentation and the molecular formula, it was identified as Azukisaponin III. Using similar fragmentation patterns, compounds 40, 43, 45, and 46 were also assigned as triterpene saponins [66,67,69–71].

Phenylethanoid glycosides are often based on β-D-glucosides of 2-phenylethanol, often with α-L-rhamnose (Rha) substitution at C-3′ of the glucose, resembling variants of verbascoside [73]. Simple phenylethanoid glycosides such as acteoside, isoacteoside, and plantamajoside exhibit similar fragmentation patterns in MS/MS experiments. These are characterized by neutral losses of 162, 152, or 146 m/z, which are associated with the presence of caffeic acid, glucose, rhamnose, and the phenethanol aglycone. Diagnostic fragment ions at m/z 179, 161, and 135 indicate the presence of caffeoyl, anhydroglucose, and anhydrophenethanol. Additionally, losses of water (−18 Da) or CO_2 (−44 Da) are frequently observed [74]. Based on this information, the compounds 7, 13, 14, 17, 20, 22, 23, 24, and 39 belonged to the phenylethanoid glycosides group.

Flavonoid glycosides are a group of secondary metabolites that are widely distributed throughout the plant kingdom. Depending on the bond of the sugar portion, they are divided into *O*-glycosides or C-glycosides and can be distinguished by their unique MS/MS fragmentation spectra, which depend on the nature of the sugar fraction. Generally, C-glycosides exhibit neutral losses of 30, 90, and 120 Da for hexose sugars; 74 and 104 Da for deoxyhexose sugars; and 60 Da for pentose sugars. In contrast, O-glycosides exhibit neutral losses of 162 Da (hexose sugars), 176 Da (glucuronic acid), 146 Da (deoxyhexose sugars), and 132 Da (pentose sugars) [75]. Based on this information, compounds 12, 21, 25, 27, 28, 29, 31, and 37 were identified as O-glycosides.

Iridoid glycosides exhibit distinct fragmentation patterns that depend on the structure of the aglycone ring, the presence of functional groups, and the degree of unsaturation. Typically, a neutral loss of 162 Da is observed, corresponding to the breakage of the bond with the glucoside fraction. Subsequently, the formation of fragments due to the loss of water (18 Da) and the carboxyl group (44 Da) is also observed, together with characteristic fragments resulting from aglycone ring cleavage. Peak 3 with m/z 373.1139 and molecular formula $C_{16}H_{22}O_{10}$ was identified as geniposidic acid based on its MS/MS spectrum. Fragment m/z 211.0605 corresponded to the loss of hexose sugar (162 Da), followed by the presence of fragments m/z 167.0700 and 149.0597, reflecting subsequent losses of H2O (−18 Da) and CO2 (−44 Da), respectively [76]. Furthermore, fragment 123.0440 is characteristic of the genistein ring. Based on the different fragmentation patterns, compounds 5, 6, 18, 34, and 35 were identified as iridoid glycosides.

Tissue-specific profiling revealed clear metabolic differentiation among parts, with the leaves containing the highest number of secondary metabolites (26), followed by the pericarps (23), roots (23), cotyledons (10), and propagules (6). Notably distinct distribution patterns were observed for specific classes of compounds across the different *A. marina* extracts. The results show that triterpene saponins occur almost exclusively in the root extract (five in roots and only one each in cotyledons, pericarps, and propagules; none in leaves). Phenylethanoid glycosides were predominantly found in root and pericarp extracts (seven in each), with only two detected in leaves and none in cotyledons and propagules. Flavonoid glycosides were mainly associated with leaf extract (six in leaves, two in roots, one in pericarps, and absent in cotyledons and propagules). In contrast, iridoid glycosides

and hydroxycinnamic acid and derivatives showed a more uniform distribution across all the extracts.

Analysis confirmed several compounds previously reported in *A. marina*, including caffeoylquinic acid, geniposidic acid, marinoid A, C, and D, acteoside, quercetin 3-*O*-hexoside, kaempferol 3-*O*-glucuronide, isorhamnetin-3-*O*-rutinoside, diosmetin 7-glucuronide, and jionoside C [5,7,77–80]. Additionally, cistanoside F and kaempferol 3-*O*-glucoside were also detected, previously reported in other mangrove species but not in *A. marina* [81,82]. To our knowledge, several compounds such as mussaenosidic acid, (epi)loganic acid, caffeoylglucaric acid, icariside D1, suspensaside, grandifloroside, suspensaside methyl ether, suspensaside A, isorhamnetin glucuronide, isorhamnetin 7-glucoside, medicoside G, esculentoside C, and azukisaponin III have been newly reported in mangrove species.

2.2. Antioxidant Activity

2.2.1. DPPH and ABTS Assays

The antioxidant potential of *A. marina* extracts was evaluated using two spectrophotometric assays, ABTS and DPPH, which are widely used to assess the free radical scavenging activity of natural compounds. The results are shown in Figure 1.

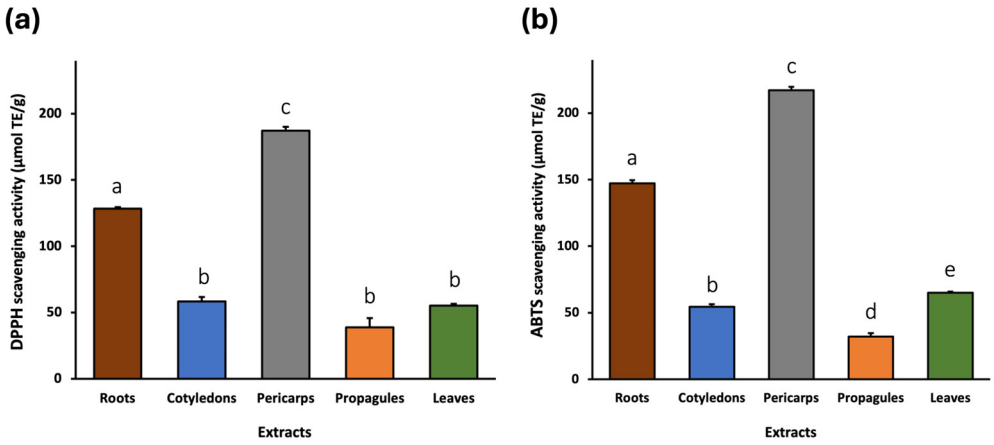

Figure 1. DPPH (**a**) and ABTS (**b**) radical scavenging activity of *A. marina* extracts expressed as µmol Trolox equivalents per gram of sample matrix (µmol TE/g). The bars represent the mean ± standard deviation (SD) from n = 3 independent experiments. Different lowercase letters indicate statistically significant differences between extracts ($p < 0.05$).

The DPPH assay showed that the pericarp extract exhibited the highest radical scavenging activity, with a Trolox equivalent antioxidant capacity (TEAC) value of 187.14 ± 2.87 µmol TE/g. This was followed by the extracts of root (128.25 ± 1.12 µmol TE/g), cotyledon (58.23 ± 3.49 µmol TE/g), leaf (55.12 ± 1.52 µmol TE/g), and propagule (38.72 ± 6.96 µmol TE/g).

Similarly, the ABTS assay confirmed that the root and pericarp extracts exhibit high antioxidant activity compared to the other parts of the plant. In fact, the pericarp extracts again displayed the highest TEAC value (217.16 ± 2.67 µmol TE/g), followed by the root (147.21 ± 2.42 µmol TE/g), leaf (64.98 ± 0.84 µmol TE/g), cotyledon (54.46 ± 1.95 µmol TE/g), and propagule (32.23 ± 2.53 µmol TE/g) extracts.

2.2.2. Correlation Between Compound Classes and Antioxidant Activity

The pericarp and root extracts, which exhibited the highest antioxidant activity, are also the ones that contain a high number of phenylethanoid glycosides, compared to the other extracts, which may explain their higher activity. To explore the potential associations between the phytochemical composition of each extract and their antioxidant capacity, a

Spearman correlation analysis was performed between the number of compounds in each major chemical class and the measured antioxidant activities (DPPH and ABTS assay) across the five plant-part extracts (n = 5) (Table 2). The analysis revealed a significant positive correlation between the number of phenylethanoid glycosides in the extracts and DPPH activity (ρ = 0.949; p = 0.014). ABTS activity showed a similar trend, though the correlation did not reach statistical significance (ρ = 0.791; p = 0.111). Antioxidant activity showed no statistically significant correlations with the number of other classes of compounds, including flavonoid glycosides, iridoid glycosides, hydroxycinnamic acids and derivatives, and triterpene saponins (all $p > 0.05$). Given the small sample size and the use of compound counts (not concentrations), these associations should be considered exploratory.

Table 2. Spearman correlation coefficients (ρ) between the number of compounds per chemical class and the antioxidant activity (DPPH and ABTS assays). Statistically significant correlations are indicated in bold (p value < 0.05).

Compound Class	DPPH		ABTS	
	ρ-Value	***p*-Value**	***p*-Value**	***p*-Value**
Iridoid glycosides	−0.103	0.870	0.510	0.935
Hydroxycinnamic acid and derivatives	−0.112	0.858	0.224	0.718
Phenylethanoid glycosides	0.791	0.111	0.949	**0.014**
Flavonoid glycosides	0.205	0.741	0.574	0.322
Triterpene saponins	0.447	0.450	0.224	0.718

2.3. In Vitro Cytotoxic Activity

The cytotoxic effects of *A. marina* extracts (leaf, cotyledon, pericarp, propagule, and root) were evaluated against a panel of human cancer cell lines using the MTT assay. Four concentrations (20, 60, 180, and 540 µg/mL) were tested on two colorectal cancer cell lines (SW480 and E705) (Figure 2) and three additional cancer cell lines: MDA-MB-231 (triple-negative breast cancer), U-87 (glioblastoma), and HeLa (cervical cancer) (Figure 3). Furthermore, two non-cancerous cell lines, MRC-5 (normal human fibroblasts) and CCD 841 (healthy human mucosa), served as controls to assess extract selectivity (Figure 4). The complete data for all concentrations and cell lines are reported in Table S1.

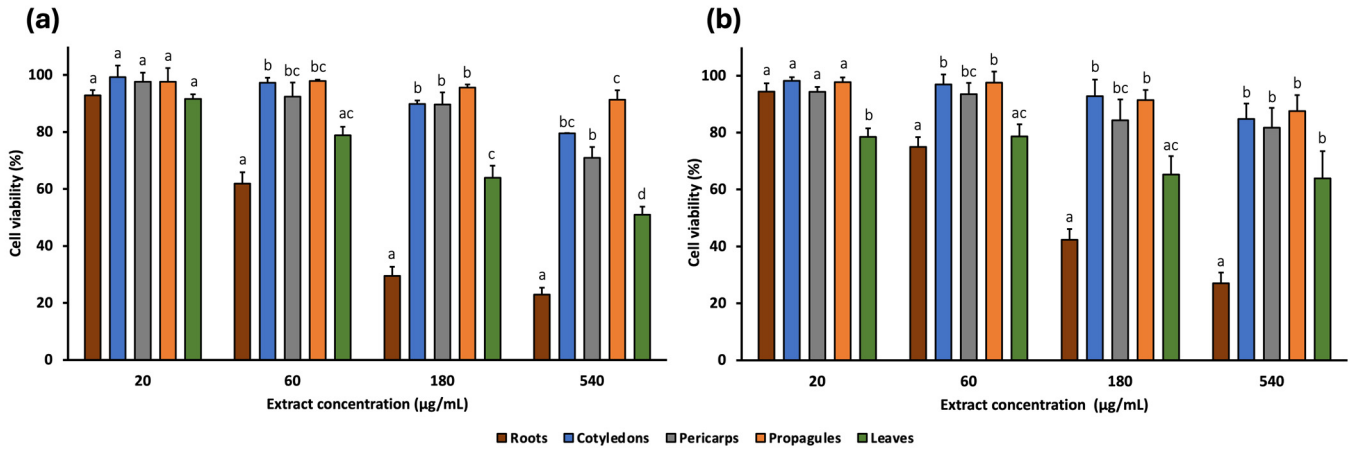

Figure 2. Cell viability (%) of SW480 (**a**) and E705 (**b**) human colorectal cancer cell lines treated with *A. marina* extracts (20–540 µg/mL) for 48 h. Bars represent mean ± standard error of the mean (SEM) from n = 3 independent experiments. Different lowercase letters indicate statistically significant differences between extracts ($p < 0.05$) and were assigned independently for each concentration.

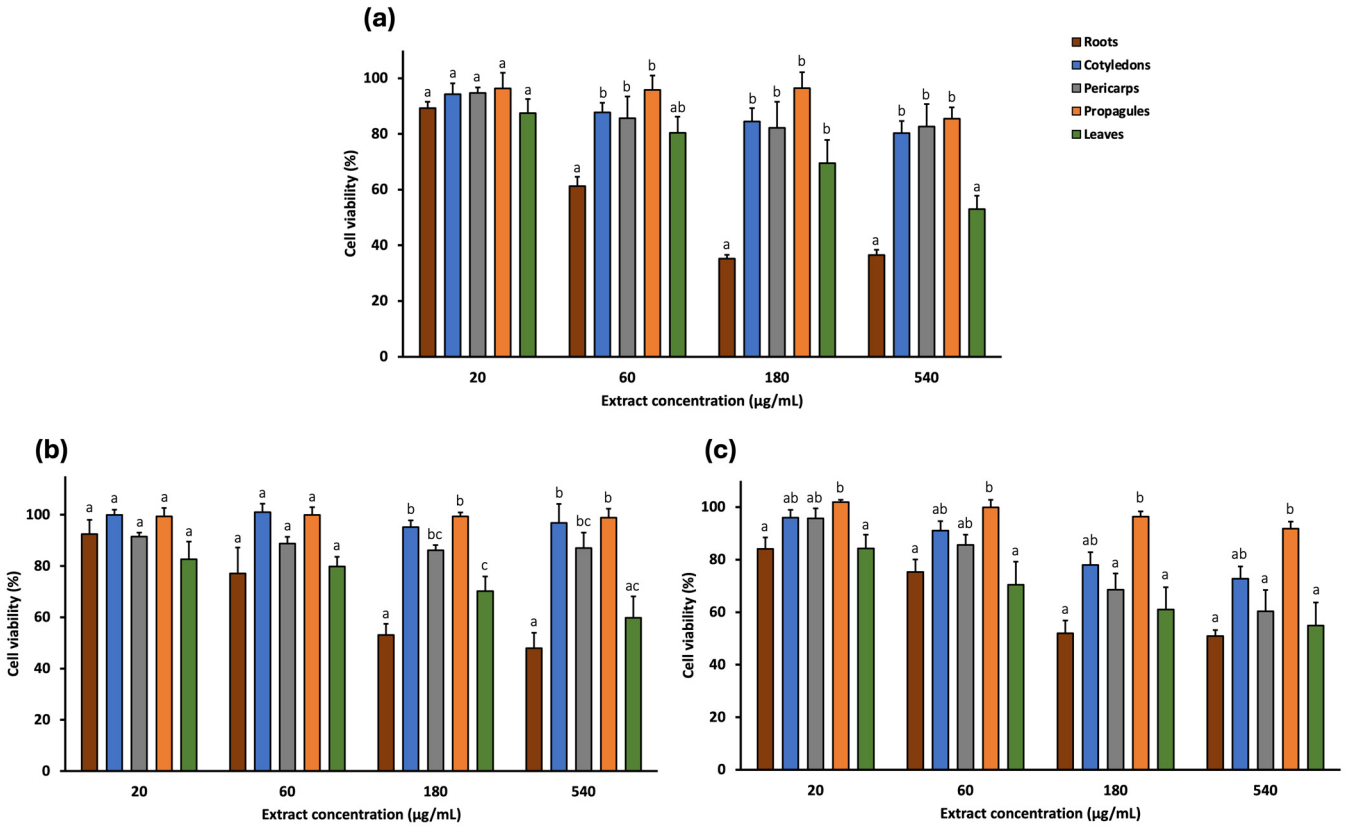

Figure 3. Cell viability (%) of MDA-MB-231 (**a**), U-87 (**b**), and HeLa (**c**) human cancer cell lines treated with *A. marina* extracts (20–540 µg/mL) for 48 h. Bars represent mean ± standard error of the mean (SEM) from n = 3 independent experiments. Different lowercase letters indicate statistically significant differences between extracts ($p < 0.05$) and were assigned independently for each concentration.

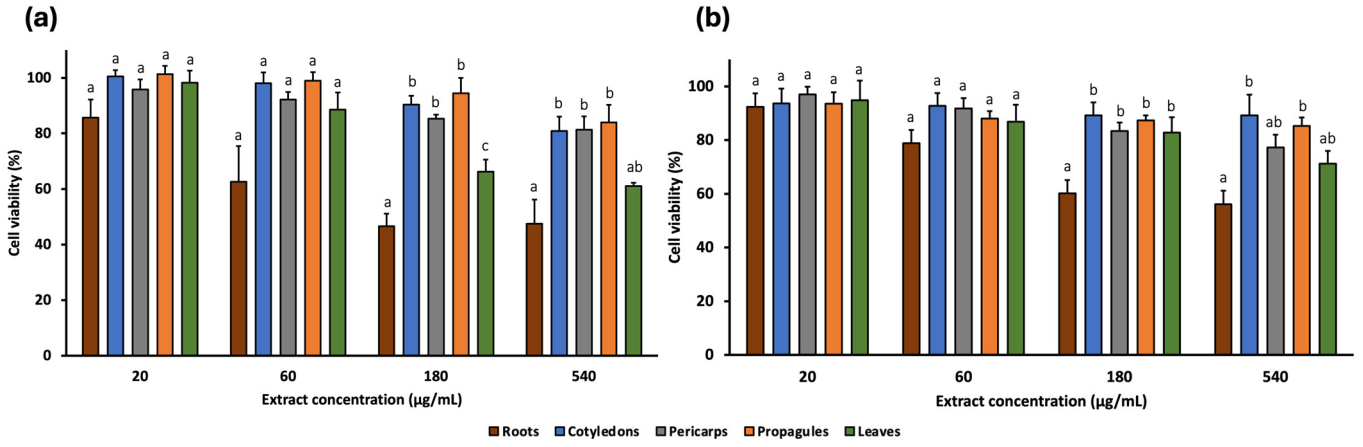

Figure 4. Cell viability (%) of CCD 841 (**a**) and MRC-5 (**b**) healthy human cell lines treated with *A. marina* extracts (20–540 µg/mL) for 48 h. Bars represent mean ± standard error of the mean (SEM) from n = 3 independent experiments. Different lowercase letters indicate statistically significant differences between extracts ($p < 0.05$) and were assigned independently for each concentration.

Among the extracts, cotyledon, pericarp, and propagule generally exhibited the lowest cytotoxic activity, reducing cell viability by no more than 70% at the highest concentration (540 µg/mL) across all cell lines. The exception was the pericarp extract, which reduced viability of HeLa cells to 60.30%.

The leaf extract showed low cytotoxicity at lower concentrations. At 60 µg/mL, cell viability remains near 80% for SW480, E705, and MDA-MB-231 and was 70.44% for HeLa.

In the non-cancerous cell lines, viability was even higher: 88.59% and 86.86% for CCD 841 and MRC-5, respectively. However, at 540 µg/mL, the extract reduced viability to 50–60% in most cell lines, particularly 50.98% for SW480, 63.91% for E705, 53.00% for MDA-MB-231, 59.77% for U-87, 54.96% for HeLa, and 61.01% for CCD 841, while the least reduction occurred in MRC-5 (71.26%).

Among all extracts, the root extract exhibited the highest cytotoxic activity. At 180 µg/mL, it reduced cell viability to 29.47% (SW480), 42.40% (E705), 35.26% (MDA-MB-231), 53.06% (U87), 52.00% (HeLa), 46.60% (CCD 841), and 60.15% (MRC-5). These reductions were statistically significant compared to all other extracts, except for E705, where differences with the leaf extract were not significant, and for HeLa. At 540 µg/mL, cytotoxicity remained similar across most lines, although viability dropped further in SW480 and E705 (22.93% and 27.03%, respectively).

These findings highlight the notable activity of the root extract, particularly at the highest concentrations, against SW480, E705, and MDA-MB-231 cell lines (Figure 5). Notably, at 180 µg/mL, the cytotoxic activity of the root extract in these cell lines was significantly greater than in non-cancerous MRC-5 cells, while no significant difference was observed compared to the healthy mucosa cell line CCD 841. Additionally, at 540 µg/mL, viability of SW480 cells was significantly lower than that of CCD 841.

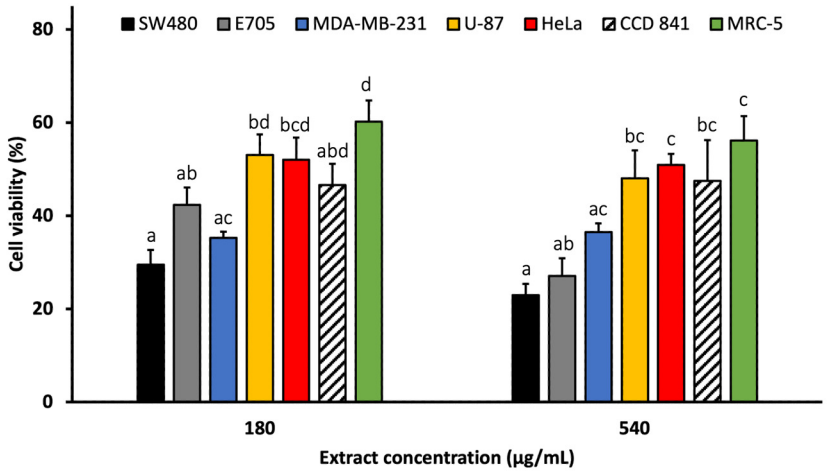

Figure 5. Cell viability (%) of the cancer cell lines treated with *A. marina* root extract (180 and 540 µg/mL) for 48 h. Bars represent mean ± standard error of the mean (SEM) from n = 3 independent experiments. Different lowercase letters indicate statistically significant differences between extracts ($p < 0.05$) and were assigned independently for each concentration.

Given this pronounced response, the analysis focused on dose–response effects in SW480, E705, and MDA-MB-231. Each cell line was treated with ten increasing concentrations of root extract (2 to 540 µg/mL; Figure S6), and the IC_{50} values were 81.98 µg/mL for SW480, 108.10 µg/mL for E705, and 57.93 µg/mL for MDA-MB-231.

2.4. In Silico Analysis

Given the strong cytotoxic activity observed for the *A. marina* root extract in vitro, an in silico analysis was conducted to evaluate the predicted biological activities of the compounds found exclusively or predominantly in this extract. PASS Online predicted potential cytotoxicity-related effects, including antineoplastic activity, apoptosis induction (caspase 3/8 stimulation and apoptosis agonism), TP53 expression enhancement, NF-κB stimulation, cytostatic activity, lipid peroxidase inhibition, and inhibition of ICAM-1 expression [83,84]. The complete list of predicted biological activities for compounds exclusive of the root extract is provided in Table S2 in the Supplementary Materials section.

Among the primary peaks detected in the root extract, the triterpene saponins medicoside G and azukisaponin III were found exclusively in the root extract, while esculentoside C was detected at high levels in the roots and in trace amounts in other extracts. These compounds showed high predicted probabilities (Pa) for antineoplastic activity (0.870, 0.905, and 0.908 for medicoside G, esculentoside C, and azukisaponin III, respectively), caspase 3/8 stimulation (0.994/0.984, 0.989/0.986, and 0.964/0.934), apoptosis agonism (0.901, 0.862, and 0.883), and NF-κB stimulation (0.965, 0.917, and 0.904). They were also predicted to inhibit ICAM-1 expression (0.908, 0.961, and 0.987) and lipid peroxidase activity (0.927, 0.952, and 0.991).

Additional compounds found exclusively in the root extract, including I, suspensaside A, kaempferol 3-O-glucoside, and quercetin 3-O-hexoside, were also predicted to exhibit antineoplastic activity with Pa values of 0.804, 0.863, 0.834, and 0.833, respectively. Kaempferol 3-O-glucoside and quercetin 3-O-hexoside also showed cytostatic activity (Pa: 0.811 and 0.825), enhancement of TP53 expression (Pa: 0.952 and 0.959) and lipid peroxidase inhibition (0.960 and 0.976, resp.).

3. Discussion

UHPLC-ESI/HRMS analyses enabled the characterization of *A. marina* extracts, revealing a total of 49 compounds, unevenly distributed across plant parts. The leaf extract contained the highest number of secondary metabolites, followed by pericarps, roots, cotyledons, and propagules. Notably, this study distinguishes between the external tissue of the propagule (here consistently called pericarp) and the internal tissues of the propagule (here consistently called simply propagule) [85], which are often analyzed as a single fruit unit in other studies. The propagule, which consists mainly of the embryo, contained few compounds, likely due to the focus on primary metabolites essential for germination [86]. In contrast, the pericarp, which serves a protective function, was significantly richer in secondary metabolites [87], particularly phenylethanoid glycosides. Similarly, cotyledons had low metabolite diversity and a profile similar to propagules but showed some additional peaks. These may reflect early biosynthesis of stress-related compounds in developing seedlings.

The compounds identified, including phenylethanoid glycosides, flavonoid glycosides, iridoid glycosides, hydroxycinnamic acid and derivatives, and triterpene saponins, are well known for their ecological roles in protecting plants from abiotic stressors such as drought, high salinity, intense sunlight, and elevated temperatures [33–36,38]. These classes are widely reported in *A. marina* from other regions, and some metabolites identified here have been documented previously, suggesting a shared core phytochemical profile with global populations [10].

However, differences from previous studies were observed. Firstly, a distinctive feature of *A. marina* elsewhere is the presence of naphthalene derivatives [10], which were not detected in our samples. This absence may reflect tissue specificity, as most of these compounds were extracted from branches, or differences in extraction methods [8]. More importantly, several compounds detected in this study have never been reported before in *A. marina*. These include one kaempferol-glycosides and two isorhamnetin glycosides. Notably, monohydroxy B-ring-substituted flavonoid glycosides (e.g., kaempferol-, diosmetin-, and isorhamnetin-glycosides) were more abundant than dihydroxy types, a pattern opposite to that expected under UV stress, where dihydroxy forms typically dominate due to their antioxidant potential [33,35,88]. This shift may reflect Gulf-specific regulation of flavonoid biosynthesis rather than species-specific traits, as it is not evident in previous reports [10]. The study identified novel compounds among the iridoid glycosides and hydroxycinnamic acids, but the most notable findings were within phenylethanoid

glycosides and triterpene saponins, the latter all newly reported in *A. marina*. The high abundance of phenylethanoid glycosides in roots is consistent with their reported accumulation under water stress [36], while the accumulation of triterpene saponins is associated with osmotic stress response [38,89]. These trends suggest that UAE-grown *A. marina* may possess a distinctive phytochemical profile shaped by the extreme environmental conditions of the Arabian Gulf [40,90] Nonetheless, inter-regional comparisons are limited due to methodological differences. Future comparative studies using standardized LC-MS protocols would enhance our understanding of mangrove chemical ecology and support bioprospecting efforts.

The identified metabolite classes are associated with various biological activities, including antioxidant, anticancer, antimicrobial, and anti-inflammatory [91–95]. In particular, phenylethanoid glycosides are well-documented antioxidants, showing both DPPH and ABTS radical scavenging activity [91,96,97]. In this study, extracts of the pericarp and root were rich in these compounds and showed the highest antioxidant activity (187.14 ± 2.87 and 217.16 ± 2.67 µmol TE/g for the pericarps; 128.25 ± 1.12 and 147.21 ± 2.42 µmol TE/g for the roots). The strong positive Spearman correlation between the number of phenylethanoid glycosides and DPPH activity ($\rho = 0.949$; $p = 0.014$) supports the hypothesis that these compounds contribute to radical scavenging in the extracts. Key phenylethanoid glycosides identified in this study, such as cistanoside F, acteoside, and jionoside C, are known for their potent antioxidant activity [98–100], while less-studied molecules such as suspensaside and suspensaside A warrant further exploration. Our correlation findings are exploratory and do not prove causation. Definitive attribution will require targeted quantification of candidate phenylethanoid glycosides and subsequent activity testing.

In terms of cytotoxic activity, the cotyledon, pericarp, and propagule extracts showed negligible effects on cancer cell lines, even at the highest concentrations. In contrast, the leaf and root extracts displayed cytotoxicity at higher doses. The leaf extract showed limited cytotoxicity at lower concentrations but reduced viability (50–60%) at 540 µg/mL in several cancer cell lines. This agrees with Momtazi-Borojeni et al. [101], who reported no toxicity at low concentrations but moderate effects at higher doses (250 µg/mL). The root extract had the most promising cytotoxic profile, particularly against SW480, E705, and MDA-MB-231 cancer cell lines. At 540 µg/mL, it reduced cell viability below 40% but showed lower toxicity against normal cell lines (MRC-5 and CCD 841). These findings agree with previous studies showing selective cytotoxicity of root extracts towards cancer cell lines [102]. IC_{50} values for SW480, E705, and MDA-MB-231 were 81.98, 108.10, and 57.93 µg/mL, respectively. Based on the criteria established by the National Cancer Institute (NCI, USA) and the Geran protocol, which classified cytotoxicity as high when IC_{50} values are $\leq$ 20 µg/mL, moderate between 21 and 200 µg/mL, weak between 201 and 500 µg/mL, and absent above 500 µg/mL [103–105], this corresponds to moderate cytotoxic activity. While these IC50 values were not compared with a standard drug, they suggest the presence of active compounds. The values reported here are for crude extracts; further fractionation and isolation of active constituents are expected to yield more potent compounds, for which in vivo and clinical potential could be more realistically assessed through comparison with standard anticancer drugs. These are potentially triterpene saponins, which were only detected in the roots.

Triterpene saponins are gaining attention in cancer research due to their ability to target tumor-related pathways while maintaining low toxicity [106]. Although widespread in medicinal plants [107,108], their occurrence in mangroves is less documented, with only a few studies published on this topic [82,108]. In silico prediction using PASS software indicated a strong cytotoxic potential for several saponins identified in the root extract, including medicoside G, esculentoside C, and azukisaponin III. Additionally, two uniden-

tified saponins suggest the presence of a potentially novel structure that merits further isolation and structural characterization. Other compounds specific to the root extract, such as suspensaside A and kaempferol 3-*O*-glucoside, showed high predicted probabilities for antineoplastic effects.

Given that the root extract exhibited the highest cytotoxicity, further work will focus on bioactivity-guided fractionation of this extract, with particular emphasis on isolating the triterpene saponin-rich fraction. These purified fractions will be tested for cytotoxicity alongside a standard anticancer drug (e.g., doxorubicin) to identify the compounds responsible for the observed activity. Mechanistic studies, including apoptosis assays, cell cycle analysis, and molecular pathway investigations, will be conducted to elucidate the modes of action. Such comprehensive analyses, together with the targeted quantification of candidate constituents, will clarify structure–activity correlations and enhance both therapeutic efficacy and selectivity. Importantly, these efforts, combined with further purification and structural elucidation, could identify promising novel lead compounds suitable for subsequent in vivo evaluation and development as potential anticancer agents.

4. Materials and Methods

4.1. Chemicals

Ethanol absolute, analytical-grade methanol, 1,1-diphenyl-2-picrylhydrazyl (DPPH$^{\bullet}$), and 2,2-azinobis-(3-ethylbenzothiazoline-6-sulfonate) (ABTS$^{\bullet+}$) reagents were obtained from Sigma-Aldrich (Milan, Italy), while methanol and formic acid of LC-MS grade were sourced from Romil (Cambridge, UK). Ultrapure water (18 MΩ) was prepared by a Milli-Q purification system (Millipore, Bedford, MA, USA).

4.2. Plant Material

Samples were collected from different parts of *A. marina*, including leaves, roots, propagules, and cotyledons. The cotyledons were obtained from seedlings at an early growth stage, when the propagules had already opened and developed roots. All samples were harvested in September 2022 from multiple individual plants within the mangrove forest of Ajman Emirate, UAE. Although no herbarium voucher specimen was deposited, the plant material was identified based on morphological characteristics following established taxonomic keys [109]. This identification is supported by the fact that *A. marina* is the only mangrove species forming the evergreen coastal forests of the UAE [14], and its presence in the region has been validated by previous molecular analyses [110,111].

For more precise phytochemical characterization, propagules were separated into the pericarp, representing the external protective tissue, and the internal tissues. Thus, in the manuscript, the term pericarp (and pericarp extract) refers exclusively to the external part, while the generic term propagule (and propagule extract) refers to the internal tissues. Each type of plant material (e.g., all collected leaves, roots, pericarps, propagules, and cotyledons) was pooled by type and immediately freeze-dried after collection. The dried samples were homogenized using a Grindomix GM 200 knife mill (Retsch, Haan, Germany) and then sieved through a test sieve (Retsch AS 200, Haan, Germany) with a mesh size range of 300–600 µm to obtain powders with uniform particle size distribution.

4.3. Sample Preparation and Extraction

Root, leaf, cotyledon, pericarp, and propagule samples of *A. marina* underwent exhaustive ultrasound-assisted extraction using a thermostatically controlled ultrasonic bath (Sonorex TK 52; Bandelin electronic, Berlin, Germany). Each sample was extracted under controlled conditions (25 °C, 15 min) with 50% aqueous ethanol (*v*/*v*) at a solid-to-solvent ratio of 1:10 (*w*/*v*), which is commonly applied in metabolite profiling studies [112]; specifi-

cally, 1 g of powdered sample was mixed with 10 mL of solvent in a 50-mL polypropylene tube. A 50% aqueous ethanol solution was selected as the extraction solvent due to its effectiveness as a green, low-toxicity system, making it well-suited for bioactivity screening [113,114]. Ethanol–water mixtures offer a balanced polarity and are widely recognized for their ability to efficiently extract a broad range of bioactive compounds, particularly polyphenolic metabolites, which are well known for their antioxidant properties [115,116]. Moreover, this solvent was selected to ensure low toxicity in downstream biological assays, in case traces of solvent remain after evaporation, and because non-polar solvents or higher ethanol concentrations could reduce solubility in aqueous assay media, potentially compromising the suitability of the extracts for biological testing.

To ensure complete extraction, the process was repeated three times with fresh solvent. Following each extraction, the mixtures were centrifuged (13,000× *g*, 10 min), and the supernatants underwent filtration through Whatman No. 1 filter paper. The combined extracts were concentrated under pressure at 40 °C using a rotary evaporator to remove ethanol and subsequently lyophilized (Alpha 1-2 LD freeze dryer, Christ, Germany) to obtain dry residues for further analysis.

The extraction yields of *A. marina* were determined by calculating the ratio of the weight of dried extract obtained to the initial weight of dried plant material powder and expressed as a percentage. The yields were 34.23% for roots, 65.02% for cotyledons, 61.76% for pericarps, 38.55% for propagules, and 33.72% for leaves.

4.4. Characterization of Extracts

The chemical characterization of extracts was performed in negative mode using liquid chromatography coupled with electrospray ionization (ESI) and high-resolution mass spectrometry (UPLC-ESI/HRMS). A Waters ACQUITY UPLC system coupled with a Waters Xevo G2-XS QTof Mass Spectrometer (Waters Corp., Milford, MA, USA) was used. The extracts were dissolved in ultrapure water at a concentration of 100 µg/mL, and then 5 µL of each sample was injected into a Biphenyl column (100 mm × 2.1 mm, 2.6 µm; Phenomenex, Torrance, CA, USA). The chromatographic gradient was conducted with solvent A (0.1% formic acid in water) and solvent B (0.1% formic acid in methanol), starting with 95% A for 1 min, followed by a linear gradient to 95% B over 10 min, and 4 min of column washing at 95% B. The flow rate was maintained at 0.4 mL/min. The ESI source was operated under the following conditions: electrospray capillary voltage of 1.5 kV, source temperature of 140 °C, and desolvation temperature of 600 °C. MS spectra were acquired in full range mode, covering a mass range of 100–1000 m/z. MS/HRMS analysis was performed using data-dependent scan (DDA), selecting the two most intense ions from the HRMS scan for collision-induced dissociation (CID) with the following conditions: a minimum signal threshold of 500,000, isolation width at 2.0, and normalized collision energy of 30%. Metabolite identification followed the Metabolomics Standards Initiative (MSI) guidelines, which define three confidence levels indicated in the "IL" column of Table 1: Level 1 (IL1): compounds were unequivocally identified by comparison with authentic reference standards (retention time, MS/MS spectrum, and exact mass); Level 2 (IL2): tentative identifications were assigned based on matches between experimental MS/MS spectra and literature data or spectral libraries (e.g., GNPS, MassBank); Level 3 (IL3): compounds were classified by spectral similarity to known chemical families and supported by taxonomic evidence.

Novelty verification was performed using general literature databases (e.g., Google Scholar) and the chemical database SciFinder^{n}. In SciFinder^{n}, each tentatively identified compound was queried by chemical name, and all related references were investigated using keywords such as "*Avicennia marina*", "*Avicennia*", and "mangroves". This process

allowed determination of whether a compound had been previously reported in *A. marina*, other species within the genus *Avicennia*, or other mangrove species, or if it represents a first identification in mangroves.

4.5. Determination of Antioxidant Activity

The antioxidant capacities (AOCs) of the exhaustive extracts of *A. marina* (leaves, roots, pericarps, propagules, and cotyledons) were evaluated using 1,1-diphenyl-2-picrylhydrazyl ($DPPH^{\bullet}$) and 2,2-azinobis-3-ethylbenzothiazoline-6-sulfonate ($ABTS^{\bullet+}$) assays according to Cannavacciuolo et al. [117]. The extracts were dissolved in ultrapure water and analyzed at a concentration of 0.5 mg/mL, with Trolox (0–500 µM) serving as a standard. The antioxidant activity was expressed as µmol Trolox equivalents per gram of sample matrix (TE/g MTX), representing the µmol of a standard Trolox solution exerting the same antioxidant capacity as 1 mg/mL of the tested extracts.

In the DPPH assay the stock solution of DPPH (5 mM) was prepared by dissolving 3.9 mg of DPPH in 100 mL of methanol and subsequently diluted to 100 µM to obtain the operating solution. This solution was prepared just before use and protected from light due to the photosensitivity of the reagent. The assay was set up in an Eppendorf by mixing 50 µL of sample with 950 µL of operative DPPH, and the mixture was incubated in the dark for 30 min. Subsequently, 200 µL of the solution was transferred to an absorbance reading plate at the 515 nm wavelength.

For the ABTS assay, the stock solution of ABTS (7 mM) was diluted with phosphate-buffered saline (PBS; 5 mM, pH 7.4) to achieve working concentrations. The assay was performed by combining 5 µL of diluted sample (or PBS control) and 500 µL of ABTS radical cation solution (0.1 mM in PBS). The reaction mixtures were protected from light and incubated at 30 °C for 60 min to allow complete radical scavenging. Absorbance measurements were then recorded at 734 nm using a microplate reader.

4.6. Cytotoxicity Evaluation

4.6.1. Cell Lines and Culture Conditions

Normal human fibroblasts (MRC-5), human glioblastoma (U-87), human triple-negative breast cancer (MDA-MB-231), human colorectal cancer (SW480), and human healthy mucosa (CCD841) cell lines were purchased from the American Type Culture Collection (Manassas, VA, USA). The human cervical cancer cell line (HeLa) was acquired from System Biosciences, and the human colon cancer cell line (E705) was provided by the Fondazione IRCCS Istituto Nazionale dei Tumori (Milan, Italy). The E705 cell line represents epithelial tissue cells of colorectal adenocarcinoma derived from a patient at the National Cancer Institute in Milan.

MRC-5, U-87, and HeLa cells were cultured in Dulbecco's Modified Eagle Medium (DMEM) high glucose medium supplemented with 10% heat-inactivated fetal bovine serum (FBS), 1% penicillin/streptomycin (P/S), and 2 mM L-glutamine. MDA-MB-231 cells were maintained in Minimum Essential Medium (MEM) with Earl's Salts supplemented with 10% heat-inactivated FBS, 1% P/S, 2 mM L-glutamine, and 0.1 mM MEM Non-Essential Amino Acids (MEM NEAA). E705 and SW480 cell lines were cultured in RPMI 1640 medium supplemented with 10% heat-inactivated FBS, 100 U/mL penicillin, 100 µg/mL streptomycin, and 2 mM L-glutamine. The CCD 841 cell line was grown in EMEM medium supplemented with 10% heat-inactivated FBS, 1% P/S, 2 mM L-glutamine, and 0.1 mM non-essential amino acids. All cell lines were incubated at 37 °C in a humidified atmosphere containing 5% CO_2 and 95% air. Cell culture media and reagents were purchased from EuroClone (Pero, Italy).

4.6.2. Viability Assay

The cytotoxicity of *A. marina* extracts was evaluated using the MTT assay (CellTiter96® Non-Radioactive Cell Proliferation Assay, Promega, Madison, WI, USA) following the manufacturer's protocol. The extract powders were solubilized in Milli-Q water, and four extract concentrations (20, 60, 180, and 540 µg/mL) were tested on all cell lines. Additionally, for the root extract, an extended dose-response analysis using ten concentrations (2, 10, 20, 40, 60, 100, 140, 180, 360, and 540 µg/mL) was performed on selected cell lines to enable IC_{50} determination. IC_{50} values were calculated only for extract–cell line combinations tested with this ten-point dilution series.

No positive control drugs were included in this preliminary screening, as the primary objective was to assess and compare the relative cytotoxicity of different *A. marina* extracts. Comparative analysis with standard anticancer agents will be incorporated in subsequent studies on purified fractions or isolated compounds.

Briefly, HeLa, MRC-5, U-87, and MDA-MB-231 cells were seeded into 96-well plates (from Euroclone, Pero, Italy) at a density of 5×10^3 cells/well in 100 µL of growth medium, while E-705 and SW-480 cells were seeded at a density of 8×10^3 cells/well. After 24 h of incubation at 37 °C in 5% CO_2, the medium was replaced, and cells were treated with various concentrations of *A. marina* extracts. Following 48 h of treatment, the medium was replaced, and 15 µL of MTT solution was added to each well. After 3 h of incubation at 37 °C, formazan crystals were solubilized using 100 µL of stop solution and incubated under stirring for 1 h. Reduced MTT was quantified using a UV–vis plate reader (EnSight Multimode Microplate Reader, PerkinElmer, Waltham, MA, USA) at 570 nm with a reference wavelength of 630 nm.

Cell viability was expressed as a percentage relative to untreated cells (negative control), and medium with MilliQ water at equivalent concentrations (10% v/v) was used as a blank. Dose-response curves and the IC_{50} values, representing the extract concentration required to inhibit 50% of cell viability relative to untreated control cells, were generated using GraphPad Prism v10.5.0 software.

4.7. In Silico Prediction for Anticancer Activity

To identify potential bioactive compounds responsible for the cytotoxic effect, an in silico prediction of biological activity was performed using PASS Online software (https://www.way2drug.com/PASSOnline/index.php; accessed on 15 July 2025), a predictive tool from Way2Drug Services. The reliability of PASS for predicting in vitro cytotoxic activity has been demonstrated in previous studies [118,119], including those focusing on triterpene saponins [120].

The canonical Simplified Molecular Input Line Entry System (SMILES) of each compound was gathered from $SciFinder_n$ and was used to run the software. The program independently calculates the estimated predictive biological activities based on structure–activity relationships, providing Pa (probability of activity) and Pi (probability of inactivity) values for each activity. Only activities with Pa > 0.7 were considered, as this threshold indicates a high likelihood that the substance will exhibit the predicted activity in experimental settings, although the probability of the compound being an analogue of a known pharmaceutical agent remains high [121]. Notably, when Pa > 0.9, as frequently observed in our study, the likelihood of false-positive predictions is insignificant [118].

The predicted anticancer-related activities included antineoplastic activity, apoptosis-related effects (apoptosis agonist, caspase 3/8 stimulation), TP53 expression enhancement, NF-kB modulation, cytostatic activity, lipid peroxidase inhibition, and ICAM-1 expression inhibition. These results were analyzed in relation to the cytotoxicity data of the MTT

assay to establish potential correlations between the phytochemical composition and the observed cytotoxicity against cancer cells.

4.8. Statistical Analysis

Statistical analyses were conducted on data generated from three replicates. Cytotoxic activity results are presented as mean ± standard error of the mean (SEM). Antioxidant activity results are reported as mean ± standard deviation (SD). Before statistical analysis, the assumption of normality was assessed using the Shapiro–Wilk test. The homogeneity of the variances was evaluated using Levene's test. When normality and homogeneity assumptions were met, a one-way analysis of variance (ANOVA) was performed, followed by Tukey's honest significant difference (HSD) post hoc test to assess pairwise differences between the means of the group. In cases where the assumption of homogeneity of the variances was not met, Welch's ANOVA was applied, followed by the Games–Howell post hoc test. Statistical significance was considered when $p < 0.05$.

The correlation between phytochemical composition and antioxidant activity was assessed using Spearman's rank correlation coefficient (two-tailed). For each plant-part extract (n = 5), the number of tentatively identified compounds in each major chemical class (phenylethanoid glycosides, flavonoid glycosides, iridoid glycosides, hydroxycinnamic acids and derivatives, and triterpene saponins) was correlated with antioxidant activity (DPPH and ABTS, mean values). Statistical significance was set at $p < 0.05$.

All analyses were conducted with IBM SPSS Statistics v29.0.2.0.

5. Conclusions

The findings of this study highlight *A. marina* as a valuable source of bioactive compounds with promising therapeutic applications. The pericarp and root extracts exhibited the highest antioxidant activity, possibly due to the presence of phenylethanoid glycosides, which are known for their antioxidant activities. Among all extracts tested, the root extract displayed the strongest cytotoxicity, in particular against the triple-negative breast cancer cell line MDA-MB-231 and two colorectal cancer cell lines, SW480 and E705, with IC_{50} values of 58.46, 81.98, and 108.10 µg/mL, respectively. In silico predictions identified triterpene saponins, including medicoside G, esculentoside C, and azukisaponin III, as likely contributors to these effects.

The detection of triterpene saponins not previously reported from mangroves, together with several phenylethanoid glycosides and other compounds not earlier described in *A. marina*, is noteworthy. Plants adapted to extreme environments can accumulate distinctive secondary metabolites, and our plant-part-specific UPLC-HRMS analysis of UAE-grown *A. marina* provides region-specific evidence that complements existing phytochemical surveys. Moreover, combining this untargeted phytochemical investigation with biological activity screening and in silico analysis/statistical correlation offers a practicable approach to rapidly link observed activities to plant-part-specific compounds.

To advance these observations towards pharmacological relevance, future work should focus on bioactivity-guided fractionation of the extracts, structural elucidation, and targeted quantification of key compounds, along with mechanistic in vitro assays. These efforts will help clarify structure–activity correlations and potentially lead to the identification of a novel therapeutic candidate from this stress-adapted mangrove species.

Supplementary Materials: The following supporting information can be downloaded at: https://www.mdpi.com/article/10.3390/ph18091308/s1, Figures S1–S5: Representative chromatograms of *A. marina* extracts; Table S1: Cytotoxicity of *Avicennia marina* extracts on the tested cell lines at four concentrations (20–540 µg/mL); Figure S6: Cell viability of SW480 (a), E705 (b), and MDA-MB-231 (c) human cancer cell lines treated with root extract (2–540 µg/mL) for 48 h; Table S2: Probable

cytotoxicity-related biological activities of 6 compounds tentatively identified in the root extract of *A. marina* by PASS (Prediction of Activity Spectra for Substances).

Author Contributions: Conceptualization, P.G., M.C. and L.C.; investigation, F.C. (cell line experiment on SW480, E705, and CCD 841 and chemical investigation), B.D.S. (cell line experiment on U-87 and MRC-5), F.S. (cell line experiment on MDA-MB-231 and HeLa), S.P. (chemical analysis); resources, P.F., P.G., M.C. and L.C.; writing—original draft preparation, F.C., B.D.S. and F.S.; writing—review and editing, F.C., S.P., M.F., M.G., L.S., P.G., M.C., L.C.; supervision, H.S., M.F., P.F., M.G., L.S., P.G., M.C. and L.C.; funding acquisition, P.G. All authors have read and agreed to the published version of the manuscript.

Funding: This research was funded under the National Recovery and Resilience Plan (NRRP), Mission 4, Component 2 Investment 1.3—Call for tender No. 3138, 16 December 2021, rectified by Decree n. 341 of 15 March 2022 of the Italian Ministry of University and Research funded by the European Union—NextGenerationEU; Project code PE0000003 ON FOODS—CUP:H43C22000820001—Spoke 6, Project title "ON Foods—Research and innovation network on food and nutrition Sustainability, Safety and Security—Working ON Foods".

Data Availability Statement: Data presented in this study is contained within the article and Supplementary Materials. Further inquiries can be directed to the corresponding author.

Acknowledgments: The authors thank the National Biodiversity Future Center (NBFC), Palermo, Italy.

Conflicts of Interest: The authors declare no conflicts of interest.

References

1. Kathiresan, K.; Bingham, B.L. Biology of Mangroves and Mangrove Ecosystems. *Adv. Mar. Biol.* **2001**, *40*, 81–251. [CrossRef]
2. Cerri, F.; Louis, Y.D.; Fallati, L.; Siena, F.; Mazumdar, A.; Nicolai, R.; Zitouni, M.S.; Adam, A.S.; Mohamed, S.; Lavorano, S.; et al. Mangroves of the Maldives: A Review of Their Distribution, Diversity, Ecological Importance and Biodiversity of Associated Flora and Fauna. *Aquat. Sci.* **2024**, *86*, 44. [CrossRef]
3. Cerri, F.; Giustra, M.; Anadol, Y.; Tomaino, G.; Galli, P.; Labra, M.; Campone, L.; Colombo, M. Natural Products from Mangroves: An Overview of the Anticancer Potential of *Avicennia marina*. *Pharmaceutics* **2022**, *14*, 2793. [CrossRef]
4. Han, L.; Huang, X.; Dahse, H.M.; Moellmann, U.; Fu, H.; Grabley, S.; Sattler, I.; Lin, W. Unusual Naphthoquinone Derivatives from the Twigs of *Avicennia marina*. *J. Nat. Prod.* **2007**, *70*, 923–927. [CrossRef]
5. Sharaf, M.; El-Ansari, M.A.; Saleh, N.A.M. New Flavonoids from *Avicennia marina*. *Fitoterapia* **2000**, *71*, 274–277. [CrossRef] [PubMed]
6. Feng, Y.; Li, X.M.; Duan, X.J.; Wang, B.G. Iridoid Glucosides and Flavones from the Aerial Parts of *Avicennia marina*. *Chem. Biodivers.* **2006**, *3*, 799–806. [CrossRef]
7. Sun, Y.; Ouyang, J.; Deng, Z.; Li, Q.; Lin, W. Structure Elucidation of Five New Iridoid Glucosides from the Leaves of *Avicennia marina*. *Magn. Reson. Chem.* **2008**, *46*, 638–642. [CrossRef]
8. Han, L.; Huang, X.; Dahse, H.-M.; Moellmann, U.; Grabley, S.; Lin, W.; Sattler, I. New Abietane Diterpenoids from the Mangrove *Avicennia marina*. *Planta Med.* **2008**, *74*, 432–437. [CrossRef]
9. Nabeelah Bibi, S.; Fawzi, M.M.; Gokhan, Z.; Rajesh, J.; Nadeem, N.; Rengasamy Kannan, R.R.; Albuquerque, R.D.D.G.; Pandian, S.K. Ethnopharmacology, Phytochemistry, and Global Distribution of Mangroves—A Comprehensive Review. *Mar. Drugs* **2019**, *17*, 231. [CrossRef]
10. Zhou, P.; Hu, H.; Wu, X.; Feng, Z.; Li, X.; Tavakoli, S.; Wu, K.; Deng, L.; Luo, H. Botany, traditional uses, phytochemistry, pharmacological activities, and toxicity of the mangrove plant *Avicennia marina*: A comprehensive review. *Phytochem. Rev.* **2025**, 1–36. [CrossRef]
11. ElDohaji, L.M.; Hamoda, A.M.; Hamdy, R.; Soliman, S.S. *Avicennia marina* a natural reservoir of phytopharmaceuticals: Curative power and platform of medicines. *J. Ethnopharmacol.* **2020**, *263*, 113179. [CrossRef]
12. El-Tarabily, K.A.; Sham, A.; Elbadawi, A.A.; Hassan, A.H.; Alhosani, B.K.K.; El-Esawi, M.A.; AlKhajeh, A.S.; AbuQamar, S.F. A Consortium of Rhizosphere-Competent Actinobacteria Exhibiting Multiple Plant Growth-Promoting Traits Improves the Growth of *Avicennia marina* in the United Arab Emirates. *Front. Mar. Sci.* **2021**, *8*, 715123. [CrossRef]
13. Department of Health—Abu Dhabi. Encyclopedia of Medicine Plant of UAE. Available online: https://www.medicinalplants.doh.gov.ae/Encyclopedia-of-medicine-plant-of-UAE (accessed on 12 August 2025).
14. Friis, G.; Killilea, M.E. Mangrove Ecosystems of the United Arab Emirates. In *A Natural History of the Emirates*; Burt, J.A., Ed.; Springer: Cham, Switzerland, 2023; pp. 217–240.

15. Haseeba, K.P.; Aboobacker, V.M.; Vethamony, P.; Al-Khayat, J.A. Significance of *Avicennia Marina* in the Arabian Gulf Environment: A Review. *Wetlands* **2025**, *45*, 16. [CrossRef]
16. Mitra, S.; Naskar, N.; Lahiri, S.; Chaudhuri, P. A study on phytochemical profiling of *Avicennia marina* mangrove leaves collected from Indian Sundarbans. *Sustain. Chem. Environ.* **2023**, *4*, 100041. [CrossRef]
17. Khattab, R.A.; Temraz, T.A. Mangrove *Avicennia marina* of Yanbu, Saudi Arabia: GC-MS constituents and mosquito repellent activities. *Egypt. J. Aquat. Biol. Fish.* **2017**, *21*, 45–54. [CrossRef]
18. Al-Mur, B.A. Biological activities of *Avicennia marina* roots and leaves regarding their chemical constituents. *Arab. J. Sci. Eng.* **2021**, *46*, 5407–5419. [CrossRef]
19. Mohammed, H.A. Phytochemical Analysis, Antioxidant Potential, and Cytotoxicity Evaluation of Traditionally Used *Artemisia Absinthium* L. (Wormwood) Growing in the Central Region of Saudi Arabia. *Plants* **2022**, *11*, 1028. [CrossRef]
20. Alzandi, A.A.; Taher, E.A.; Al-Sagheer, N.A.; Al-Khulaidi, A.W.; Azizi, M.; Naguib, D.M. Phytochemical components, antioxidant and anticancer activity of 18 major medicinal plants in Albaha region, Saudi Arabia. *Biocatal. Agric. Biotechnol.* **2021**, *34*, 102020. [CrossRef]
21. Youssef, A.M.M.; Maaty, D.A.M.; Al-Saraireh, Y.M. Phytochemistry and Anticancer Effects of Mangrove (*Rhizophora mucronata* Lam.) Leaves and Stems Extract against Different Cancer Cell Lines. *Pharmaceuticals* **2022**, *16*, 4. [CrossRef]
22. Botosoa, E.P.; Shahidi, F. Phenolics and polyphenolics in mangrove plants: Antioxidant activity and recent trends in food application—A review. *Crit. Rev. Food Sci. Nutr.* **2025**, 1–35. [CrossRef]
23. Wang, Y.; Xing, L.; Zhang, J.; Chen, Y.; Lu, S. Simultaneous Determination of 32 Polyphenolic Compounds in Berries via HPLC–MS/MS. *Molecules* **2025**, *30*, 2008. [CrossRef] [PubMed]
24. Kodikara, C.; Netticadan, T.; Bandara, N.; Wijekoon, C.; Sura, S. A new UHPLC-HRMS metabolomics approach for the rapid and comprehensive analysis of phenolic compounds in blueberry, raspberry, blackberry, cranberry and cherry fruits. *Food Chem.* **2024**, *445*, 138778. [CrossRef] [PubMed]
25. Singh, A.; Choudhary, K.K. Utilizing UHPLC-HRMS-metabolomic profiling to uncover enhanced bioactive potential and health benefits in chili (*Capsicum annum* L.) under salinity stress. *Food Chem.* **2025**, *483*, 144255. [CrossRef]
26. Lee, I.Y.; Lee, D.H.; Park, J.H.; Joo, N. UHPLC-HRMS/MS–Based Metabolic Profiling and Quantification of Phytochemicals in Different Parts of *Coccinia grandis* (L.) Voigt. *Food Sci. Nutr.* **2025**, *13*, e70004. [CrossRef]
27. Zanatta, A.C.; Vilegas, W.; Edrada-Ebel, R. UHPLC-(ESI)-HRMS and NMR-Based Metabolomics Approach to Access the Seasonality of *Byrsonima intermedia* and *Serjania marginata* From Brazilian Cerrado Flora Diversity. *Front. Chem.* **2021**, *9*, 534. [CrossRef]
28. Mateos-Molina, D.; Ben Lamine, E.; Antonopoulou, M.; Burt, J.A.; Das, H.S.; Javed, S.; Judas, J.; Khan, S.B.; Muzaffar, S.B.; Pilcher, N.; et al. Synthesis and Evaluation of Coastal and Marine Biodiversity Spatial Information in the United Arab Emirates for Ecosystem-Based Management. *Mar. Pollut. Bull.* **2021**, *167*, 112319. [CrossRef]
29. United Arab Emirates—Climatology | Climate Change Knowledge Portal. Available online: https://climateknowledgeportal.worldbank.org/country/united-arab-emirates/climate-data-historical#cckp-watershed-map (accessed on 1 April 2025).
30. Jin, J.; Koroleva, O.A.; Gibson, T.; Swanston, J.; Maganj, J.; Zhang, Y.A.N.; Rowland, I.R.; Wagstaff, C. Analysis of Phytochemical Composition and Chemoprotective Capacity of Rocket (Eruca Sativa and Diplotaxis Tenuifolia) Leafy Salad Following Cultivation in Different Environments. *J. Agric. Food Chem.* **2009**, *57*, 5227–5234. [CrossRef]
31. Abd-Elgawad, A.M.; Elshamy, A.I.; Al-Rowaily, S.L.; El-Amier, Y.A. Habitat Affects the Chemical Profile, Allelopathy, and Antioxidant Properties of Essential Oils and Phenolic Enriched Extracts of the Invasive Plant *Heliotropium curassavicum*. *Plants* **2019**, *8*, 482. [CrossRef]
32. Rozirwan; Nugroho, R.Y.; Hendri, M.; Fauziyah; Putri, W.A.E.; Agussalim, A. Phytochemical Profile and Toxicity of Extracts from the Leaf of *Avicennia marina* (Forssk.) Vierh. Collected in Mangrove Areas Affected by Port Activities. *S. Afr. J. Bot.* **2022**, *150*, 903–919. [CrossRef]
33. Neugart, S.; Krumbein, A.; Zrenner, R. Influence of Light and Temperature on Gene Expression Leading to Accumulation of Specific Flavonol Glycosides and Hydroxycinnamic Acid Derivatives in Kale (*Brassica oleracea* var. sabellica). *Front. Plant Sci.* **2016**, *7*, 181383. [CrossRef] [PubMed]
34. Wang, D.H.; Du, F.; Liu, H.Y.; Liang, Z.S. Drought stress increases iridoid glycosides biosynthesis in the roots of *Scrophularia ningpoensis* seedlings. *J. Med. Plants* **2010**, *4*, 2691–2699. [CrossRef]
35. Ferdinando, M.D.; Brunetti, C.; Fini, A.; Tattini, M. Flavonoids as antioxidants in plants under abiotic stresses. In *Abiotic Stress Responses in Plants: Metabolism, Productivity and Sustainability*; Ahmad, P., Prasad, M.N.V., Eds.; Springer: Berlin/Heidelberg, Germany, 2012.
36. Falahi, H.; Sharifi, M.; Maivan, H.Z.; Chashmi, N.A. Phenylethanoid Glycosides Accumulation in Roots of *Scrophularia Striata* as a Response to Water Stress. *Environ. Exp. Bot.* **2018**, *147*, 13–21. [CrossRef]

37. Franzoni, G.; Trivellini, A.; Bulgari, R.; Cocetta, G.; Ferrante, A. Bioactive molecules as regulatory signals in plant responses to abiotic stresses. In *Plant Signaling Molecules*; Khan, M.I.R., Reddy, P.S., Ferrante, A., Khan, N., Eds.; Woodhead Publishing: Duxford, UK, 2019; Volume 1, pp. 169–182.
38. Sarri, E.; Termentzi, A.; Abraham, E.M.; Papadopoulos, G.K.; Baira, E.; Machera, K.; Loukas, V.; Komaitis, F.; Tani, E. Salinity Stress Alters the Secondary Metabolic Profile of *M. sativa*, *M. arborea* and Their Hybrid (Alborea). *Int. J. Mol. Sci.* **2021**, *22*, 4882. [CrossRef] [PubMed]
39. Toscano, S.; Trivellini, A.; Cocetta, G.; Bulgari, R.; Francini, A.; Romano, D.; Ferrante, A. Effect of preharvest abiotic stresses on the accumulation of bioactive compounds in horticultural produce. *Front. Plant Sci.* **2019**, *10*, 1212. [CrossRef]
40. Das, S.K.; Patra, J.K.; Thatoi, H. Antioxidative response to abiotic and biotic stresses in mangrove plants: A review. *Int. Rev. Hydrobiol.* **2015**, *101*, 3–19. [CrossRef]
41. Galasso, S.; Pacifico, S.; Kretschmer, N.; Pan, S.P.; Marciano, S.; Piccolella, S.; Monaco, P.; Bauer, R. Influence of Seasonal Variation on *Thymus longicaulis* C. Presl Chemical Composition and Its Antioxidant and Anti-Inflammatory Properties. *Phytochemistry* **2014**, *107*, 80–90. [CrossRef]
42. Fiori, J.; Amadesi, E.; Fanelli, F.; Tropeano, C.V.; Rugolo, M.; Gotti, R. Cellular and Mitochondrial Determination of Low Molecular Mass Organic Acids by LC–MS/MS. *J. Pharm. Biomed. Anal.* **2018**, *150*, 33–38. [CrossRef]
43. Wang, D.-D.; Liang, J.; Yang, W.-Z.; Hou, J.j.; Yang, M.; Da, J.; Wang, Y.; Jiang, B.h.; Liu, X.; Wu, W.y.; et al. HPLC/QTOF-MS-Oriented Characteristic Components Data Set and Chemometric Analysis for the Holistic Quality Control of Complex TCM Preparations: Niuhuang Shangqing Pill as an Example. *J. Pharm. Biomed. Anal.* **2014**, *89*, 130–141. [CrossRef]
44. Seo, O.N.; Kim, G.S.; Park, S.; Lee, J.H.; Kim, Y.H.; Lee, W.S.; Lee, S.J.; Kim, C.Y.; Jin, J.S.; Choi, S.K.; et al. Determination of Polyphenol Components of *Lonicera japonica* Thunb. Using Liquid Chromatography–Tandem Mass Spectrometry: Contribution to the Overall Antioxidant Activity. *Food Chem.* **2012**, *134*, 572–577. [CrossRef]
45. Amessis-Ouchemoukh, N.; Abu-Reidah, I.M.; Quirantes-Piné, R.; Rodríguez-Pérez, C.; Madani, K.; Fernández-Gutiérrez, A.; Segura-Carretero, A. Tentative Characterisation of Iridoids, Phenylethanoid Glycosides and Flavonoid Derivatives from *Globularia alypum* L. (Globulariaceae) Leaves by LC-ESI-QTOF-MS. *Phytochem. Analy* **2014**, *25*, 389–398. [CrossRef] [PubMed]
46. Xie, G.; Xu, Q.; Li, R.; Shi, L.; Han, Y.; Zhu, Y.; Wu, G.; Qin, M. Chemical Profiles and Quality Evaluation of *Buddleja officinalis* Flowers by HPLC-DAD and HPLC-Q-TOF-MS/MS. *J. Pharm. Biomed. Anal.* **2019**, *164*, 283–295. [CrossRef] [PubMed]
47. Kiss, A.K.; Michalak, B.; Patyra, A.; Majdan, M. UHPLC-DAD-ESI-MS/MS and HPTLC Profiling of Ash Leaf Samples from Different Commercial and Natural Sources and Their in Vitro Effects on Mediators of Inflammation. *Phytochem. Anal.* **2020**, *31*, 57–67. [CrossRef]
48. García-Villegas, A.; Fernández-Ochoa, Á.; Alañón, M.E.; Rojas-García, A.; Arráez-Román, D.; De La Luz Cádiz-Gurrea, M.; Segura-Carretero, A. Bioactive Compounds and Potential Health Benefits through Cosmetic Applications of Cherry Stem Extract. *Mar. Drugs* **2024**, *25*, 3723. [CrossRef] [PubMed]
49. Han, J.; Ye, M.; Guo, H.; Yang, M.; Wang, B.-R.; Guo, D.-A. Analysis of Multiple Constituents in a Chinese Herbal Preparation Shuang-Huang-Lian Oral Liquid by HPLC-DAD-ESI-MSn. *J. Pharm. Biomed. Anal.* **2007**, *44*, 430–438. [CrossRef]
50. Zhou, F.; Peng, J.; Zhao, Y.; Huang, W.; Jiang, Y.; Li, M.; Wu, X.; Lu, B. Varietal Classification and Antioxidant Activity Prediction of *Osmanthus fragrans* Lour. Flowers Using UPLC–PDA/QTOF–MS and Multivariable Analysis. *Food Chem.* **2017**, *217*, 490–497. [CrossRef] [PubMed]
51. Zhang, Y.-D.; Huang, X.; Zhao, F.L.; Tang, Y.L.; Yin, L. Study on the Chemical Markers of Caulis *Lonicerae japonicae* for Quality Control by HPLC-QTOF/MS/MS and Chromatographic Fingerprints Combined with Chemometrics Methods. *Anal. Methods* **2015**, *7*, 2064–2076. [CrossRef]
52. Petreska, J.; Stefova, M.; Ferreres, F.; Moreno, D.A.; Tomás-Barberán, F.A.; Stefkov, G.; Kulevanova, S.; Gil-Izquierdo, A. Potential Bioactive Phenolics of *Macedonian sideritis* Species Used for Medicinal "Mountain Tea". *Food Chem.* **2011**, *125*, 13–20. [CrossRef]
53. Hvattum, E. Determination of Phenolic Compounds in Rose Hip (*Rosa canina*) Using Liquid Chromatography Coupled to Electrospray Ionisation Tandem Mass Spectrometry and Diode-Array Detection. *Rapid Commun. Mass Spectrom.* **2002**, *16*, 655–662. [CrossRef]
54. Kammerer, D.; Carle, R.; Schieber, A. Characterization of Phenolic Acids in Black Carrots (*Daucus carota* ssp. *sativus* var. *atrorubens* Alef.) by High-Performance Liquid Chromatography/Electrospray Ionization Mass Spectrometry. *Rapid Commun. Mass Spectrom.* **2004**, *18*, 1331–1340. [CrossRef]
55. Gu, D.; Yang, Y.; Bakri, M.; Chen, Q.; Xin, X.; Aisa, H.A. A LC/QTOF–MS/MS Application to Investigate Chemical Compositions in a Fraction with Protein Tyrosine Phosphatase 1B Inhibitory Activity from *Rosa rugosa* Flowers. *Phytochem. Anal.* **2013**, *24*, 661–670. [CrossRef]
56. Innocenti, M.; La Marca, G.; Malvagia, S.; Giaccherini, C.; Vincieri, F.F.; Mulinacci, N. Electrospray Ionisation Tandem Mass Spectrometric Investigation of Phenylpropanoids and Secoiridoids from Solid Olive Residue. *Rapid Commun. Mass Spectrom.* **2006**, *20*, 2013–2022. [CrossRef]

57. Matos, P.; Figueirinha, A.; Paranhos, A.; Nunes, F.; Cruz, P.; Geraldes, C.F.G.C.; Cruz, M.T.; Batista, M.T. Bioactivity of *Acanthus Mollis*—Contribution of Benzoxazinoids and Phenylpropanoids. *J. Ethnopharmacol.* **2018**, *227*, 198–205. [CrossRef]
58. Seeram, N.P.; Lee, R.; Scheuller, H.S.; Heber, D. Identification of Phenolic Compounds in Strawberries by Liquid Chromatography Electrospray Ionization Mass Spectroscopy. *Food Chem.* **2006**, *97*, 1–11. [CrossRef]
59. Zhang, Y.; Shi, P.; Qu, H.; Cheng, Y. Characterization of Phenolic Compounds in *Erigeron breviscapus* by Liquid Chromatography Coupled to Electrospray Ionization Mass Spectrometry. *Rapid Commun. Mass Spectrom.* **2007**, *21*, 2971–2984. [CrossRef]
60. Zhang, Y.; Liu, C.; Zhang, Z.; Wang, J.; Wu, G.; Li, S. Comprehensive Separation and Identification of Chemical Constituents from *Apocynum venetum* Leaves by High-Performance Counter-Current Chromatography and High Performance Liquid Chromatography Coupled with Mass Spectrometry. *J. Chromatogr. B* **2010**, *878*, 3149–3155. [CrossRef]
61. Nijat, D.; Abdulla, R.; Liu, G.-Y.; Luo, Y.-Q.; Aisa, H.A. Identification and Quantification of Meiguihua Oral Solution Using Liquid Chromatography Combined with Hybrid Quadrupole-Orbitrap and Triple Quadrupole Mass Spectrometers. *J. Chromatogr. B* **2020**, *1139*, 121992. [CrossRef]
62. Parejo, I.; Jauregui, O.; Sánchez-Rabaneda, F.; Viladomat, F.; Bastida, J.; Codina, C. Separation and Characterization of Phenolic Compounds in Fennel (*Foeniculum vulgare*) Using Liquid Chromatography-Negative Electrospray Ionization Tandem Mass Spectrometry. *J. Agric. Food Chem.* **2004**, *52*, 3679–3687. [CrossRef]
63. Ibrahim, R.M.; Fayez, S.; Eltanany, B.M.; Abu-Elghait, M.; El-Demerdash, A.; Badawy, M.S.E.M.; Pont, L.; Benavente, F.; Saber, F.R. Agro-Byproduct Valorization of Radish and Turnip Leaves and Roots as New Sources of Antibacterial and Antivirulence Agents through Metabolomics and Molecular Networking. *Sci. Hortic.* **2024**, *328*, 112924. [CrossRef]
64. Wang, Z.; Yao, M.; Ouyang, H.; He, M.; Zhao, W.; Wei, W.; Cui, Y.; Yang, S.; Zhong, G.; Feng, Y.; et al. Characterization of Chemical Constituents and Metabolites in Rat Plasma after Oral Administration of *Ainsliaea fragrans* Champ by Using UHPLC-QTOF-MS/MS. *J. Chromatogr. B* **2024**, *1244*, 124259. [CrossRef] [PubMed]
65. Lei, H.; Xin, J.; Lv, Y.; Chen, W.; Xu, X.; Wang, J.; Tian, S.; Xie, B.; Shen, Y.; Zu, X. Effects of Processing on the Efficacy and Metabolites of *Cistanche tubulosa* Using Ultra-Performance Liquid Chromatography Coupled with Quadrupole Time-of-Flight Mass Spectrometry. *Biomed. Chromatogr.* **2023**, *37*, e5621. [CrossRef]
66. Schliemann, W.; Ammer, C.; Strack, D. Metabolite Profiling of Mycorrhizal Roots of *Medicago truncatula*. *Phytochemistry* **2008**, *69*, 112–146. [CrossRef]
67. Huhman, D.V.; Sumner, L.W. Metabolic Profiling of Saponins in *Medicago Sativa* and *Medicago Truncatula* Using HPLC Coupled to an Electrospray Ion-Trap Mass Spectrometer. *Phytochemistry* **2002**, *59*, 347–360. [CrossRef]
68. Zhao, D.; Chen, X.; Wang, R.; Pang, H.; Wang, J.; Liu, L. Determining the Chemical Profile of *Caragana jubata* (Pall.) Poir. by UPLC–QTOF–MS Analysis and Evaluating Its Anti-Ischemic Stroke Effects. *J. Ethnopharmacol.* **2023**, *309*, 116275. [CrossRef] [PubMed]
69. Saleri, F.D.; Chen, G.; Li, X.; Guo, M. Comparative Analysis of Saponins from Different *Phytolaccaceae* Species and Their Antiproliferative Activities. *Molecules* **2017**, *22*, 1077. [CrossRef] [PubMed]
70. Tavares-Silva, C.; Holandino, C.; Homsani, F.; Luiz, R.R.; Prodestino, J.; Farah, A.; Lima, J.d.P.; Simas, R.C.; Castilho, C.V.V.; Leitão, S.G.; et al. Homeopathic Medicine of *Melissa officinalis* Combined or Not with *Phytolacca decandra* in the Treatment of Possible Sleep Bruxism in Children: A Crossover Randomized Triple-Blinded Controlled Clinical Trial. *Phytomedicine* **2019**, *58*, 152869. [CrossRef]
71. Liu, R.; Cai, Z.; Xu, B. Characterization and Quantification of Flavonoids and Saponins in Adzuki Bean (*Vigna angularis* L.) by HPLC-DAD-ESI-MSn Analysis. *Chem. Cent. J.* **2017**, *11*, 93. [CrossRef] [PubMed]
72. Pham, H.N.; Tran, C.A.; Trinh, T.D.; Nguyen Thi, N.L.; Tran Phan, H.N.; Le, V.N.; Le, N.H.; Phung, V.T. UHPLC-Q-TOF-MS/MS Dereplication to Identify Chemical Constituents of Hedera Helix Leaves in Vietnam. *J. Anal. Methods Chem.* **2022**, *8*, 1167265. [CrossRef]
73. Kite, G.C. Characterization of phenylethanoid glycosides by multiple-stage mass spectrometry. *Rapid Commun. Mass Spectrom.* **2020**, *34*, e8563. [CrossRef]
74. Qi, M.; Xiong, A.; Geng, F.; Yang, L.; Wang, Z. A Novel Strategy for Target Profiling Analysis of Bioactive Phenylethanoid Glycosides in *Plantago* Medicinal Plants Using Ultra-Performance Liquid Chromatography Coupled with Tandem Quadrupole Mass Spectrometry. *J. Sep. Sci.* **2012**, *35*, 1470–1478. [CrossRef]
75. Pagliari, S.; Sicari, M.; Pansera, L.; Guidi Nissim, W.; Mhalhel, K.; Rastegar, S.; Germanà, A.; Cicero, N.; Labra, M.; Cannavacciuolo, C.; et al. A comparative metabolomic investigation of different sections of Sicilian *Citrus x limon* (L.) Osbeck, characterization of bioactive metabolites, and evaluation of in vivo toxicity on zebrafish embryo. *J. Food Sci.* **2024**, *89*, 3729–3744. [CrossRef]
76. Fu, Z.; Xue, R.; Li, Z.; Chen, M.; Sun, Z.; Hu, Y.; Huang, C. Fragmentation patterns study of iridoid glycosides in Fructus Gardeniae by HPLC-Q/TOF-MS/MS. *Biomed. Chromatogr.* **2014**, *28*, 1795–1807. [CrossRef]
77. Mohamed, A.S.; Elmi, A.; Spina, R.; Kordofani, M.A.Y.; Laurain-Mattar, D.; Nour, H.; Abchir, O.; Chtita, S. In Vitro and In Silico Analysis for Elucidation of Antioxidant Potential of Djiboutian *Avicennia marina* (Forsk.) Vierh. Phytochemicals. *J. Biomol. Struct. Dyn.* **2024**, *42*, 3410–3425. [CrossRef]

78. Zhang, Y.C.; Zhuang, L.H.; Zhou, J.J.; Song, S.W.; Li, J.; Huang, H.Z.; Chi, B.J.; Zhong, Y.H.; Liu, J.W.; Zheng, H.L.; et al. Combined Metabolome and Transcriptome Analysis Reveals a Critical Role of Lignin Biosynthesis and Lignification in Stem-like Pneumatophore Development of the Mangrove *Avicennia marina*. *Planta* **2024**, *259*, 12. [CrossRef] [PubMed]
79. Sun, Y.; Ding, Y.; Lin, W.H. Isolation and Identification of Compounds from Marine Mangrove Plant *Avicennia marina*. *Beijing Da Xue Xue Bao Yi Xue Ban J. Peking Univ. Health Sci.* **2009**, *41*, 221–225.
80. Kartikaningsih, H.; Djamaludin, H.; Fauziyah, J.N.; Audina, N.; Noviyanti, L.; Saputra, D. Green extraction of *Avicennia marina* leaves by natural deep eutectic solvents: Phytochemical profile, antioxidant activity, molecular docking and admet analysis. *Rasayan J. Chem.* **1123**, *17*, 1123–1133. [CrossRef]
81. Wu, J.; Huang, J.; Xiao, Q.; Zhang, S.; Xiao, Z.; Li, Q.; Long, L.; Huang, L. Complete Assignments of 1H and 13C NMR Data for 10 Phenylethanoid Glycosides. *Magn. Reson. Chem.* **2004**, *42*, 659–662. [CrossRef]
82. Vinh, L.B.; Nguyet, N.T.M.; Yang, S.Y.; Kim, J.H.; Van Thanh, N.; Cuong, N.X.; Nam, N.H.; Van Minh, C.; Hwang, I.; Kim, Y.H. Cytotoxic Triterpene Saponins from the Mangrove *Aegiceras corniculatum*. *Nat. Prod. Res.* **2019**, *33*, 628–634. [CrossRef]
83. Clemente, S.M.; Martínez-Costa, O.H.; Monsalve, M.; Samhan-Arias, A.K. Targeting Lipid Peroxidation for Cancer Treatment. *Molecules* **2020**, *25*, 5144. [CrossRef]
84. Kang, J.H.; Uddin, N.; Kim, S.; Zhao, Y.; Yoo, K.C.; Kim, M.J.; Hong, S.A.; Bae, S.; Lee, J.Y.; Shin, I.; et al. Tumor-Intrinsic Role of ICAM-1 in Driving Metastatic Progression of Triple-Negative Breast Cancer through Direct Interaction with EGFR. *Mol. Cancer* **2024**, *23*, 230. [CrossRef] [PubMed]
85. Tomlinson, P. *The Botany of Mangroves*; Cambridge University Press: Cambridge, UK, 2016; ISBN 1-316-79065-7.
86. Rosental, L.; Nonogaki, H.; Fait, A. Activation and Regulation of Primary Metabolism during Seed Germination. *Seed Sci. Res.* **2014**, *24*, 1–15. [CrossRef]
87. Sharif, Y.; Chen, H.; Deng, Y.; Ali, N.; Khan, S.A.; Zhang, C.; Xie, W.; Chen, K.; Cai, T.; Yang, Q.; et al. Cloning and Functional Characterization of a Pericarp Abundant Expression Promoter (AhGLP17-1P) From Peanut (*Arachis hypogaea* L.). *Front. Genet.* **2022**, *12*, 821281. [CrossRef] [PubMed]
88. Zietz, M.; Weckmuller, A.; Schmidt, S.; Rohn, S.; Schreiner, M.; Krumbein, A.; Kroh, L.W. Genotypic and climatic influence on the antioxidant activity of flavonoids in kale (*Brassica oleracea* var. *sabellica*). *J. Agric. Food Chem.* **2010**, *58*, 2123–2130. [CrossRef] [PubMed]
89. Wu, J.Y.; Wong, K.; Ho, K.P.; Zhou, L.G. Enhancement of saponin production in *Panax ginseng* cell culture by osmotic stress and nutrient feeding. *Enzym. Microb. Technol.* **2005**, *36*, 133–138. [CrossRef]
90. Oku 2003Oku, H.; Baba, S.; Koga, H.; Takara, K.; Iwasaki, H. Lipid composition of mangrove and its relevance to salt tolerance. *J. Plant Res.* **2003**, *116*, 37–45. [CrossRef]
91. Xue, Z.; Yang, B. Phenylethanoid Glycosides: Research Advances in Their Phytochemistry, Pharmacological Activity and Pharmacokinetics. *Molecules* **2016**, *21*, 991. [CrossRef] [PubMed]
92. Sova, M.; Saso, L. Natural Sources, Pharmacokinetics, Biological Activities and Health Benefits of Hydroxycinnamic Acids and Their Metabolites. *Nutrients* **2020**, *12*, 2190. [CrossRef]
93. Yang, B.; Liu, H.; Yang, J.; Gupta, V.K.; Jiang, Y. New Insights on Bioactivities and Biosynthesis of Flavonoid Glycosides. *Trends Food Sci. Technol.* **2018**, *79*, 116–124. [CrossRef]
94. Wang, C.; Gong, X.; Bo, A.; Zhang, L.; Zhang, M.; Zang, E.; Zhang, C.; Li, M. Iridoids: Research Advances in Their Phytochemistry, Biological Activities, and Pharmacokinetics. *Molecules* **2020**, *25*, 287. [CrossRef]
95. Sparg, S.G.; Light, M.E.; Van Staden, J. Biological Activities and Distribution of Plant Saponins. *J. Ethnopharmacol.* **2004**, *94*, 219–243. [CrossRef]
96. De Marino, S.; Festa, C.; Zollo, F.; Incollingo, F.; Raimo, G.; Evangelista, G.; Iorizzi, M. Antioxidant activity of phenolic and phenylethanoid glycosides from *Teucrium polium* L. *Food Chem.* **2012**, *133*, 21–28. [CrossRef]
97. Budzianowska, A.; Kikowska, M.; Budzianowski, J. Phenylethanoid glycosides accumulation and antiradical activity of fractionated extracts of *Plantago ovata* Forssk. callus cultures lines. *Plant Cell Tissue Organ Cult.* **2024**, *156*, 54. [CrossRef]
98. Lu, S.-H.; Zuo, H.-J.; Huang, J.; Li, W.-N.; Huang, J.-L.; Li, X.-X. Chemical constituents from the leaves of *Ligustrum robustum* and their bioactivities. *Molecules* **2023**, *28*, 362. [CrossRef]
99. Ji, S.L.; Cao, K.K.; Zhao, X.X.; Kang, N.X.; Zhang, Y.; Xu, Q.M.; Yang, S.L.; Liu, Y.L.; Wang, C. Antioxidant activity of phenylethanoid glycosides on glutamate-induced neurotoxicity. *Biosci. Biotechnol. Biochem.* **2019**, *83*, 2016–2026. [CrossRef]
100. Wei, W.; Lan, X.B.; Liu, N.; Yang, J.M.; Du, J.; Ma, L.; Zhang, W.J.; Niu, J.G.; Sun, T.; Yu, J.Q. Echinacoside Alleviates Hypoxic-Ischemic Brain Injury in Neonatal Rat by Enhancing Antioxidant Capacity and Inhibiting Apoptosis. *Neurochem. Res.* **2019**, *44*, 1582–1592. [CrossRef]
101. Momtazi-Borojeni, A.A.; Behbahani, M.; Sadeghi-Aliabadi, H. Antiproliferative Activity and Apoptosis Induction of Crude Extract and Fractions of *Avicennia marina*. *Iran. J. Basic Med. Sci.* **2013**, *16*, 1203.

102. Tanjung, I.B.; Azizah, N.N.; Arsianti, A.; Anisa, A.S.; Audah, K.A. Evaluation of the Ethyl Acetate Extract of the Roots of *Avicennia marina* as Potential Anticancer Drug. In Proceedings of the 6th International Conference of Food, Agriculture, and Natural Resource (IC-FANRES 2021), Tangerang, Indonesia, 4–5 August 2021; Atlantis Press: Dordrecht, The Netherlands, 2022; Volume 16, pp. 75–81. [CrossRef]
103. Geran, R.I.; Greenberg, N.H.; McDonald, M.M. Protocols for Screening Chemical Agents and Natural Products against Animal Tumors and Other Biological Systems. *Cancer Chemother. Rep.* **1972**, *3*, 1–103.
104. Niksic, H.; Becic, F.; Koric, E.; Gusic, I.; Omeragic, E.; Muratovic, S.; Miladinovic, B.; Duric, K. Cytotoxicity screening of *Thymus vulgaris* L. essential oil in brine shrimp nauplii and cancer cell lines. *Sci. Rep.* **2021**, *11*, 13178. [CrossRef] [PubMed]
105. Addy, B.S.; Firempong, C.K.; Komlaga, G.; Addo-Fordjour, P.; Domfeh, S.A.; Afolayan, O.; Emikpe, B.O. In vitro antiproliferative activities of some Ghanaian medicinal plants. *Clin. Phytosci* **2024**, *10*, 19. [CrossRef]
106. Du, J.R.; Long, F.Y.; Chen, C. Research Progress on Natural Triterpenoid Saponins in the Chemoprevention and Chemotherapy of Cancer. *Enzymes* **2014**, *36*, 95–130. [CrossRef]
107. da Silva Magedans, Y.V.; Phillips, M.A.; Fett-Neto, A.G. Production of Plant Bioactive Triterpenoid Saponins: From Metabolites to Genes and Back. *Phytochem. Rev.* **2020**, *20*, 461–482. [CrossRef]
108. Yang, X.W.; Dai, Z.; Wang, B.; Liu, Y.P.; Zhao, X.D.; Luo, X.D. Antitumor Triterpenoid Saponin from the Fruits of *Avicennia marina*. *Nat. Prod. Bioprospect* **2018**, *8*, 347–353. [CrossRef]
109. Duke, N.C. A Systematic Revision of the Mangrove Genus *Avicennia* (Avicenniaceae) in Australasia. *Aust. Syst. Bot.* **1991**, *4*, 299–324. [CrossRef]
110. Friis, G.; Vizueta, J.; Smith, E.G.; Nelson, D.R.; Khraiwesh, B.; Qudeimat, E.; Salehi-Ashtiani, K.; Ortega, A.; Marshell, A.; Duarte, C.M.; et al. A high-quality genome assembly and annotation of the gray mangrove, Avicennia marina. *G3 Genes Genomes Genet.* **2021**, *11*, jkaa025. [CrossRef]
111. Friis, G.; Smith, E.G.; Lovelock, C.E.; Ortega, A.; Marshell, A.; Duarte, C.M.; Burt, J.A. Rapid diversification of grey mangroves (*Avicennia marina*) driven by geographic isolation and extreme environmental conditions in the Arabian Peninsula. *Mol. Ecol.* **2024**, *33*, e17260. [CrossRef]
112. Che Sulaiman, I.S.; Basri, M.; Fard Masoumi, H.R.; Chee, W.J.; Ashari, S.E.; Ismail, M. Effects of Temperature, Time, and Solvent Ratio on the Extraction of Phenolic Compounds and the Anti-Radical Activity of *Clinacanthus nutans* Lindau Leaves by Response Surface Methodology. *Chem. Cent. J.* **2017**, *11*, 54. [CrossRef]
113. Lim, K.J.A.; Cabajar, A.A.; Lobarbio, C.F.Y.; Taboada, E.B.; Lacks, D.J. Extraction of Bioactive Compounds from Mango (*Mangifera indica* L. var. *Carabao*) Seed Kernel with Ethanol–Water Binary Solvent Systems. *J. Food Sci. Technol.* **2019**, *56*, 2536–2544. [CrossRef]
114. Plaskova, A.; Mlcek, J. New Insights of the Application of Water or Ethanol-Water Plant Extract Rich in Active Compounds in Food. *Front. Nutr.* **2023**, *10*, 1118761. [CrossRef]
115. Huamán-Castilla, N.L.; Díaz Huamaní, K.S.; Palomino Villegas, Y.C.; Allcca-Alca, E.E.; León-Calvo, N.C.; Colque Ayma, E.J.; Zirena Vilca, F.; Mariotti-Celis, M.S. Exploring a Sustainable Process for Polyphenol Extraction from Olive Leaves. *Foods* **2024**, *13*, 265. [CrossRef] [PubMed]
116. Palaiogiannis, D.; Chatzimitakos, T.; Athanasiadis, V.; Bozinou, E.; Makris, D.P.; Lalas, S.I. Successive Solvent Extraction of Polyphenols and Flavonoids from *Cistus creticus* L. Leaves. *Oxygen* **2023**, *3*, 274–286. [CrossRef]
117. Cannavacciuolo, C.; Pagliari, S.; Giustra, C.M.; Carabetta, S.; Guidi Nissim, W.; Russo, M.; Branduardi, P.; Labra, M.; Campone, L. LC-MS and GC-MS Data Fusion Metabolomics Profiling Coupled with Multivariate Analysis for the Discrimination of Different Parts of Faustrime Fruit and Evaluation of Their Antioxidant Activity. *Antioxidants* **2023**, *12*, 565. [CrossRef] [PubMed]
118. Verbanac, D.; Jain, S.C.; Jain, N.; Chand, M.; Paljetak, H.C.; Matijašic, M.; Peric, M.; Stepanic, V.; Saso, L. An efficient and convenient microwave-assisted chemical synthesis of (thio)xanthones with additional in vitro and in silico characterization. *Bioorg. Med. Chem.* **2012**, *20*, 3180–3185. [CrossRef]
119. Filimonov, D.A.; Lagunin, A.A.; Gloriozova, T.A.; Rudik, A.V.; Druzhilovskii, D.S.; Pogodin, P.V.; Poroikov, V.V. Prediction of the Biological Activity Spectra of Organic Compounds Using the PASS Online Web Resource. *Chem. Heterocycl. Compd.* **2014**, *50*, 444–457. [CrossRef]
120. Desai, T.H.; Joshi, S.V. In Silico Evaluation of Apoptogenic Potential and Toxicological Profile of Triterpenoids. *Indian J. Pharmacol.* **2019**, *51*, 181–207. [CrossRef] [PubMed]
121. Lagunin, A.; Stepanchikova, A.; Filimonov, D.; Poroikov, V. PASS: Prediction of Activity Spectra for Biologically Active Substances. *Bioinformatics* **2000**, *16*, 747–748. [CrossRef] [PubMed]

ChemSusChem

Review
doi.org/10.1002/cssc.202401065

Chemistry Europe
European Chemical Societies Publishing

www.chemsuschem.org

Microplastics in Cosmetics: Open Questions and Sustainable Opportunities

Marco Giustra,[a, b] Giulia Sinesi,[a] Francesca Spena,[a] Beatrice De Santes,[a] Lucia Morelli,[a] Linda Barbieri,[a] Stefania Garbujo,[a, b] Paolo Galli,[c, d, e] Davide Prosperi,*[a, b] and Miriam Colombo*[a, b]

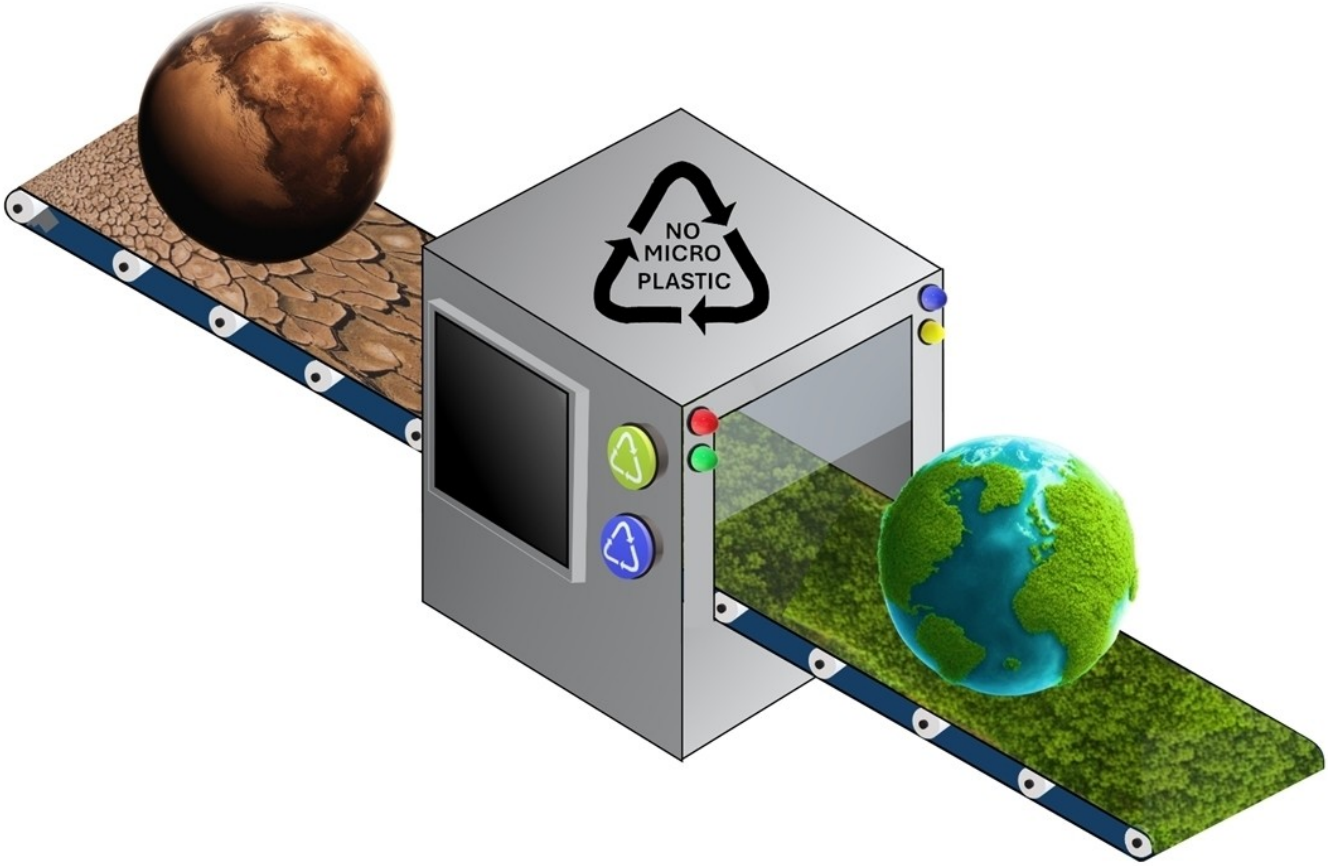

The cosmetic industry is now changing or rather having an ecological transition in which formulations such as creams, lotions, and powders for make-up, skin and hair care must not contain microplastics, now a taboo word in this field. Nowadays, many companies are intensifying their research and development (R&D) work to align with recent and future legislation that provides for their elimination to safeguard the ecosystem. The production of new eco-sustainable materials is currently a hot topic which finds its place in a market worth above 350 billion dollars which will reach more than 700 billion dollars in a very short time. This review offers an overview of the main advantages and adverse issues relating to the use of microplastics in cosmetics and of their impact, providing an insight into the properties of the polymeric materials that are currently exploited to improve the sensorial characteristics of cosmetic products. In addition, the various regulatory restrictions in the different geographical areas of the world are also described, which is matter for reflection on future direction. Finally, a prospective vision of possible solutions to replace microplastics with sustainable alternatives complete the picture of the next generation personal care products to support decision-making in the cosmetic marketplace.

1. Introduction

Cosmetics is a rapidly expanding economic and scientific sector, as also witnessed by the increasing number of brands and new products entering the marketplace every year, with the search for new materials and new effects capable of responding to new claims.[1]

Cosmetics play a significant role in the daily lives of people worldwide. The interest for their usage is no longer restricted to a concept of vanity and luxury. Indeed, psychological-social factors. Remarkably contribute to such constantly growing attractiveness for cosmetics. In fact, the daily consumption of these products has become a way to express and take care of oneself and increase self-esteem.[2,3] On this basis, the market is always evolving reflecting consumer needs.

Based on the data reported by Fortune Business Insights Pvt. Ltd., the global cosmetics market was estimated at $374.18 billion in 2023 and is projected to exceed $750 billion by 2032, exhibiting a Compound Annual Growth Rate (CAGR) of 9.8%. Notwithstanding the startling numbers, researchers and activists are still conducting studies on the problematic presence of microplastics in cosmetics highlighting their potential risks to the environment. Prior to the advent of microplastics, natural compounds have been used in cosmetic manufacturing since ancient times. Raw materials such as sugar, cellulose, starch, proteins, natural fats, and oils were processed by the chemical industry in various fields. For instance, some vegetable oils such as avocado, lauric, palm, soybean, and walnut were used. Among vegetable fats were hydrogenated vegetable oil and shea butter. Animal sources of fatty acids included lard and tallow.[4,5] Additionally, lanolin alcohols, derived from the fat of wool shearing, were introduced to the market as emollients after the Second World War.[6]

In the ′80s, microplastics replaced these natural ingredients in many products, both in formulations and in the packaging of cosmetic products, due to their versatility. They were used for various functions, including viscosity regulation, film forming, opacifying, bulking, and exfoliating.[7] For example, polyethylene glycols (PEGs) were used as humectants and moisturizers,[8] polyacrylates as film-forming agents,[9] and polyamides to lend substantivity to hair and skin.[10]

However, the first bans regarding marine litter began with the increase in plastic pollution. Countries and organizations have become more aware of the negative impact of plastic and microplastics on the environment. In 2015, the "Microbead-Free Waters Act" was the first ban on microbeads. Subsequently, prohibitions or restrictions on microbeads or microplastics in cosmetic and personal care products were implemented.

Beat the Microbead (http://www.beatthemicrobead.org) was one of the first campaigns published on April 2022 to put under the spotlight the problem of microplastics in cosmetics by promoting broad awareness on this issue to encourage consumers to choose products free of microplastics. *Greenpeace* and *Friends of the Earth* have also helped highlight the issue of microplastics in cosmetics through alertness campaigns, reports, and studies.[11] These efforts are encouraging institutions worldwide to fight against another widespread mystification, which offers new products dishonestly declared to be environmentally friendly – the so-called greenwashing. In 1986, Jay Westerveld coined the term "greenwashing" concerning the idea of encouraging the reuse of towels in hotels suggesting environmental care but actually done as a strategy to reduce laundry costs.[12] Although the concept is not yet formally defined, today this term is adopted to describe practices in which commitment to environmental sustainability is promoted, but all is done primarily for economic and marketing purposes.

The EU defines greenwashing as "*the practice whereby companies claim to be doing more for the Environment than they actually are*". In 2024, the European Parliament recognized its

[a] *NanoBioLab, Department of Biotechnology and Bioscience, University of Milano-Bicocca, Milano, Italy*
[b] *Nanobiotechnologies for Health Center, NANOMIB, University of Milano-Bicocca, Vedano al Lambro, MB, Italy*
[c] *Department of Earth and Environmental Sciences, University of Milano-Bicocca, Milano, Italy*
[d] *Dubai Business School, University of Dubai, United Arab Emirates Goumbook, Ras Al Khaimah, United Arab Emirates*
[e] *MaRHE Centre (Marine Research and High Education Center), Magoodhoo Island, Maldives*

Correspondence: *Davide Prosperi and Miriam Colombo, NanoBioLab, Department of Biotechnology and Bioscience, University of Milano-Bicocca, Piazza della Scienza, 2, 20126 Milano, Italy.*
Email: davide.prosperi@unimib.it and miriam.colombo@unimib.it

provisional agreement with the Council on the Directive Empowering Consumers for the Green Transition through Better Protection against Unfair Practices and Better Information ("Greenwashing Directive").[13] Nevertheless, a specific EU regulation focused on greenwashing in cosmetics does not exist, while just regulations and initiatives to ensure transparency and prevent deceptive marketing practices are being taken.

Over time, consumers have become increasingly aware of the above issue, seeking out products with specific labels such as Cruelty-Free, Vegan, Nickel Tested, Dermatologically & Ophthalmologically Tested, and free of Ethyl Alcohol, Silicone, and Petrochemicals. Additionally, consumers are increasingly choosing products with eco-sustainable packaging and/or made from recycled materials (Green Packaging).[14] In this review, we will focus on a fundamental component in the production of solid and semi-solid formulations: cosmetic powders. Cosmetic powders have been and continue to be at the forefront of sustainability concerns, leading various institutions to enact legislation addressing the issue.

Cosmetic powders are widely used in cosmetic formulations owing to their versatility, ability to enhance sensorial characteristics and skin benefits making the final products appreciated by the consumers. The main features of cosmetic powders include (Figure 1):

- Exfoliating: powders are able to remove dead cells on the skin surface promoting cell renewal and favouring smoother skin.
- Fixative: powders avoid smudging in semi-solid formulations and prolong their shelf life.
- Mattifying or brightening: powders can be used to reduce undesirable reflections on the skin or enhance brightness to the face, especially in the T-zone (forehead, nose and chin), where oiliness tends to accumulate more.

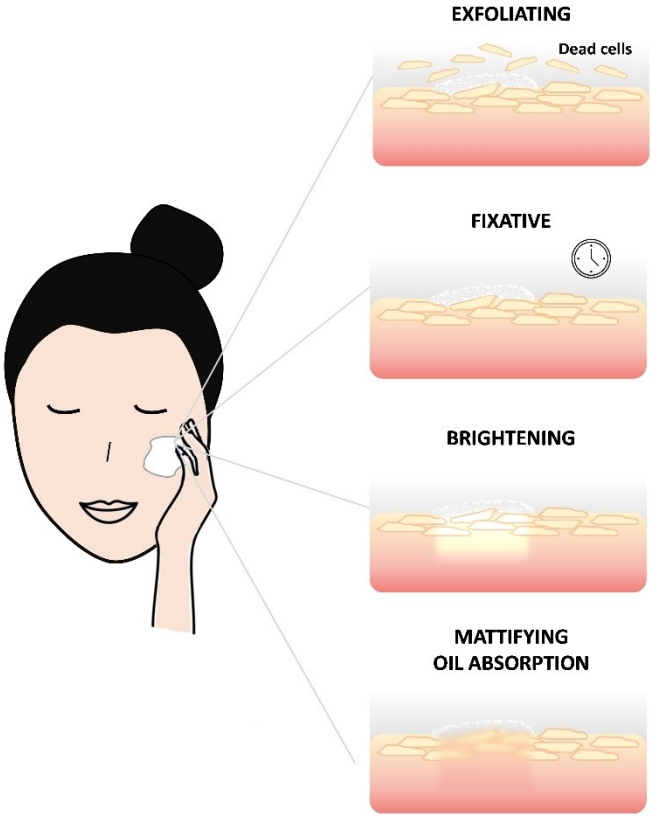

Figure 1. Main characteristics of cosmetic powders in formulation and relative effects on skin: exfoliating, fixative, brightening, mattifying and oil absorption.

- Oil absorption: sebum-normalizing products, some powders help to control oiliness maintaining an opaque and matte appearance.

Marco Giustra graduated in Chemistry from the University of Milano-Bicocca in 2018. He obtained a PhD in Nanotechnology and Materials Science in 2022, focusing on synthesizing inorganic nanoparticles and multi-branching polymers to enhance colloidal stability. His current research is centered on producing sustainable raw materials for cosmetic and pharmaceutical formulations, as well as developing alternative RNA nanodelivery methods for cancer treatment.

Davide Prosperi graduated in Chemistry in 1998 and obtained a PhD in Chemistry in 2002 at the University of Milan. Since 2019, he is Full Professor in Biochemistry at the University of Milan-Bicocca. He is Director of the Nanobiotechnologies for Health Center. His research is mainly focused on colloidal and biomimetic nanoparticles for use as drug delivery systems, molecular imaging and probes for the investigation of intracellular molecular mechanisms, including gene silencing and cell transduction and signaling. Current research topics in his laboratory are RNA therapy for cancer treatment and the development of sustainable materials for nanomedicine and cosmetics.

Prof. Miriam Colombo obtained her Master degree in 2008 in Medicinal Chemistry and Technology at the University of Milano and she made the PhD in Biology in 2012. She is full professor of Clinical Biochemistry at the University of Milano-Bicocca. Her scientific research focuses on developing nanoparticles for biomedical applications. This involves creating new systems for drug delivery and other therapeutic approaches, characterizing them, and bio-functionalizing them with various active bio-ligands. Additionally, she has explored alternative administration methods for nanoparticles and biomolecules, such as oral and topical administration, particularly for pharmaceutical and cosmetic applications.

These features can be combined to produce formulations capable of satisfying multiple needs, such as setting makeup, controlling skin oiliness, sculpting, and defining facial features.

Actives encapsulation or surface modification of cosmetic powders boost the final product's applicability and performance, such as wetting and anti-ageing effects.

Microplastics have often addressed the main appearances stated, presenting a global and pressing challenge (Figure 2). Currently, some R&D companies, alongside universities are striving to replace microplastics in cosmetic products while maintaining or even improving the powder performance, thus obtaining sustainable products.

2. Microplastics in Cosmetic Formulations – A Real Threat for the Environment and Human Health

In the last decade, microplastics (MPs) have emerged as a significant environmental and health problem worldwide. MPs are defined as small plastic particles ranging in size from 0.1 to 5 mm.[15] Microplastics derive from a variety of sources, including discarded plastic, the textile, and cosmetic industries. The generation of plastics and microplastics associated with the cosmetic industry is currently one of the most serious environmental issues, reinforced also by the increased number of consumers and the high demand in this sector.[16]

Microplastics can be found in primary form, as constituents of cosmetic formulations, such as exfoliating agents, or as secondary plastics, derived from cosmetic packaging. Among the primary sources, personal care products, including cleansing products, makeup cosmetics, shower gel, facial cleanser, hand sanitizer, soap, toothpaste, sunscreen and shampoo represent significant sources of microplastics in the environment.[17] These microplastics are specially designed and optimized in a spherical shape, to reduce skin scratches or disruption of the natural skin growth process. The use of microplastics in various personal care products has expanded beyond their initial scrubbing effects to include important functions such as binders, bulking agents, emulsifiers, film formers, viscosity regulators, opacifying agents, glitters, skin conditioning, tooth polishing in oral care, gellants in denture adhesives, moisturizers, sun filters, and stabilizers.[18]

The plastic ingredients used for the scrubbing function are commonly referred to as plastic microbeads. Microbeads made of polyethylene are the most common application, although polyurethane, polypropylene, polyethylene terephthalate, polymethyl methacrylate and nylon are used.[19] The advantages of using plastic microspheres for washing and exfoliation include their soft peeling effect, associated with good skin tolerance. They have a broad range of positive properties, they are chemically inert substances, odourless, non-sensitizing and non-irritating.[20]

Microbeads have the potential to improve the performance of a wide range of cosmetic products, but there are also some drawbacks to consider. In fact, microbeads, being tiny plastic particles, are difficult to filter out in wastewater treatment plants, entering water streams and eventually contaminating rivers.[21] They can be found in the ocean, soil, and even in the air we breathe.

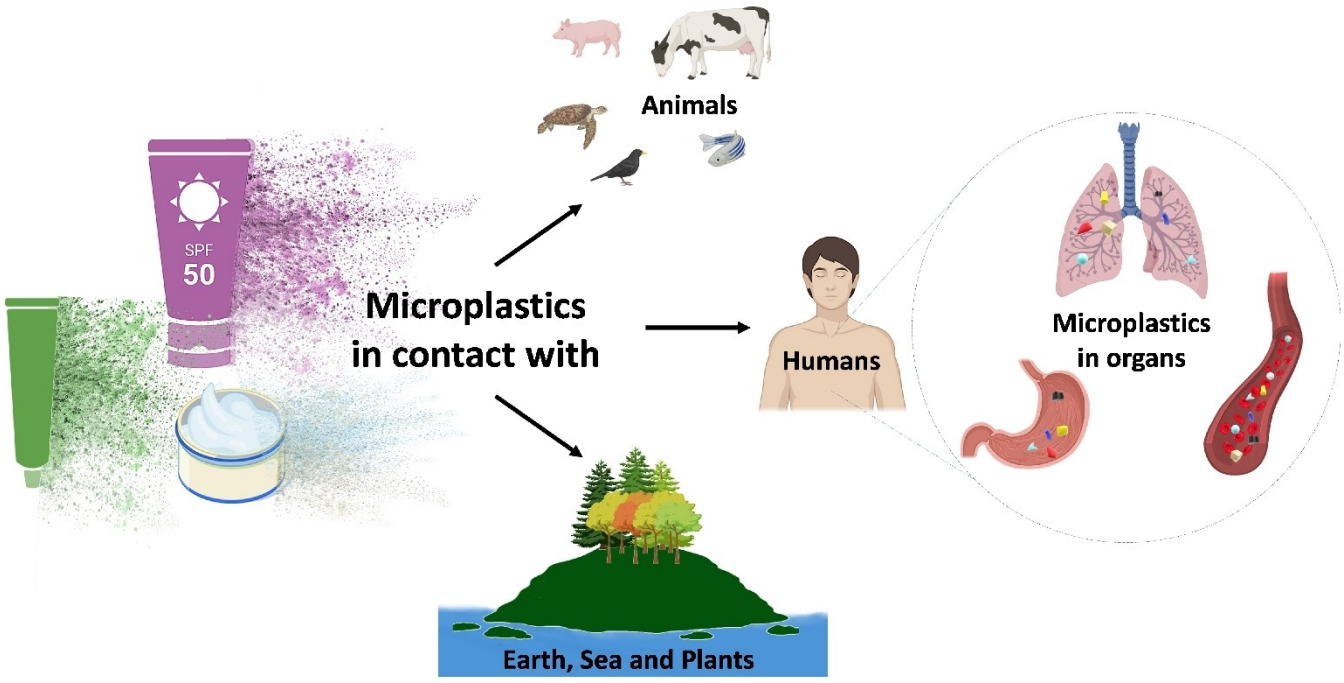

Figure 2. Microplastics from personal care and cosmetic products have the potential to infiltrate the entire ecosystem–reaching the earth, seas, plants, animals, and ultimately, humans. Especially, microplastics reach human organs.

Since there is no effective way to remove microplastic contaminants from the marine environment and they are highly resistant to degradation, microparticles can be adsorbed or ingested by many marine organisms. The introduction of these microparticles by marine animals, plankton, and other biota results in a negative effect on the entire food chain of the marine ecosystem. The presence of microplastics in different marine organisms, such as copepods,[22] bivalves,[23] fish,[24] and seabirds[25] has already been documented.

Another issue to be considered is that microplastics have large specific surface areas, making them easier to absorb hydrophobic chemicals (e.g., polychlorinated biphenyls) from aquatic environments. They can be considered as vectors for various harmful contaminants, such as heavy metals (Al, Cd, Co, Cr, Cu, Hg, Mn and Pb), polycyclic aromatic hydrocarbons, polychlorinated biphenyls, pesticides and persistent organic pollutants.[26,27]

Furthermore, particles of less than 130 mm, can accumulate in human tissue and diffused into bloodstream, lymphatic system, and organs through various mechanisms, such as ingestion, inhalation, and dermal absorption (Table 1). The implications for human health are substantial and multifaceted, as MPs may release the mentioned toxins, additives and monomers, which may have carcinogenic activity and trigger inflammatory responses.[28] In light of these considerations, there is obviously a need for consolidation of actions, changes and optimization in the production processes and products of the cosmetic industry.

2.1. Human Blood

A study by Leslie et al. provided the first evidence of plastic particles in the bloodstream. They quantified MPs in whole blood samples from 22 healthy individuals,[29] obtaining data for concentrations in blood for five polymers: poly (methyl methacrylate) (PMMA), polypropylene (PP), materials containing polystyrene (PS), polyethylene (PE) and polyethylene terephthalate (PET). PET was the most frequently detected polymer, with measurable values found in 50% of all tested donors. PMMA, PE, and PS were detected in 5%, 23%, and 36% of donors, respectively. The average polymer concentration in blood was 1.6 μg/mL. The study highlighted that plastic particles can enter the human body and be eliminated through the biliary tract, the kidneys or other organs at a slower rate than they are absorbed into the blood. Given the lack of information on the long-term health effects of MPs in human blood, further research is essential to better understand the risks. This involves investigating the sources and pathways by which MPs enter the bloodstream, analyzing their distribution and accumulation patterns, and assessing their potential impacts on various physiological and cardiovascular systems.

More recently, Yang et al. conducted a study which identified MPs in the human heart for the first time.[30] In this study, the presence of MPs in the human heart and its surrounding tissues was investigated by collecting blood venous samples from 15 cardiac surgery patients through a laser direct infrared chemical imaging system and scanning electron microscopy. The most common MPs were polyamide (49%) and PET (22%), making up over 70% of the total microplastic content. The composition of MPs changed significantly before and after surgery. Pre-surgery samples were dominated by PET (67%), whereas post-surgery samples were primarily polyamide (57%). The diameter of MPs also shifted, with pre-surgery MPs mostly between 30 and 50 μm and post-surgery MPs predominantly between 20 and 30 μm. These findings indicate the potential interactions between medical procedures and MP exposure, which can impact on post-operative recovery and cardiovascular health.

Table 1. Predominant microplastics found in human organs and fluids.

Organs and fluids	Detection technique	Particle types	References
Blood	Py-GC/MS	PE, PET, PMMA, PP and PS	Leslie et al.[29]
	LD-IR and SEM	PA, PC, PE, PET, PMMA, PP, PS, PU, and PVC	Yang et al.[30]
Vein tissue	μFTIR	Alkyd resin, Nylon EVA, PVAc, PVAE and PUR	Rotchell et al.[31]
Semen	μRaman	PC, PE, PET, POM, PP, PS, and PVC	Montano et al.[32]
	Py-GC/MS and LD-IR	PA, PE, PET, PP, PS, and PVC	Zhao et al.[33]
Testis	Py-GC/MS and LD-IR	PE, PP, PS and PVC	Zhao et al.[33]
Placenta	μRaman	PP and other fragments	Ragusa et al.[34]
	FTIR	PE, PP and PU	Braun et al.[35]
	VP-SEM and TEM	Fragments compatible with MPs	Ragusa et al.[36]
	LD-IR	PP and PVC	Zhu et al.[37]
	LD-IR	PA and PU	Liu et al.[38]
Pulmunary tissue	μRaman	PE and PP	Amato-Laurenço et al.[39]
Sputum	LD-IR and μFTIR	Alkyd varnish, CPE, PES and PU,	Huang et al.[40]
Urine and kidneys	μRaman	PE, PP, PVA and PVC	Pironti et al.[41]
	μRaman	PE and PS	Massardo et al.[42]

MPs have also been found in human vein tissue. Rotchell et al. discovered MPs in four out of five vein samples by using μFTIR. The MPs were mainly fragments ranging in size from 16 to 1074 μm. The most common polymers were alkyd resin, polyvinyl propionate/acetate (PVAc), and a tie layer of nylon EVA or ethylene vinyl alcohol (EVOH)-EVA.[31]

2.2. Testis and Semen

Montano et al. analyzed semen samples from men living in a polluted area of Southern Italy to determine the presence of MPs. Spherical and irregular microplastic fragments, ranging in size from 2 to 6 μm, were found in six out of ten samples.[32] Furthermore, the chemical composition analysis identified the presence of commonly used polymers including PP, PS, PET, PE, polyoxymethylene (POM), polyvinylchloride (PVC), and polycarbonate (PC).

In another study by Zhao et al., MPs were discovered in human testis and semen. 6 testis and 30 semen samples were used to detect MPs through pyrolysis-gas chromatography/mass spectrometry (Py-GC/MS) and laser direct infrared spectroscopy (LD-IR).[33] MPs were found in both testis and semen, with an average concentration of 0.23 ± 0.45 particles/mL in semen and 11.60 ± 15.52 particles/g in testis. The MPs in the testis were predominantly composed of PS at 67.7%, while PE and PVC were the main polymers in semen. The MPs were between 21.76 μm and 286.71 μm in size, with the majority (67% in semen and 80.6% in testis) being between 20 and 100 μm. This study is the first to reveal MP contamination in the human male reproductive system, highlighting the presence of various MP characteristics in different regions and providing essential data for assessing the risk of MPs to human health. Further investigation should be conducted to determine the potential implications for male reproductive health and fertility.

2.3. Human Placenta

The first evidence of MPs in human placenta was found in a study by Ragusa et al. in 2021. Six human placentas, collected from consenting women with normal pregnancies, were analyzed using Raman microspectroscopy to detect the presence of microplastics.[34]

The placenta regulates the fetal to maternal environment and, indirectly, the external environment. The potential presence of MPs in this organ can have an impact on embryo development, causing risks for the newborn. A total of 12 fragments, ranging from 5 to 10 μm in size and various shapes, were found in four of the placentas. Specifically, five fragments were located on the fetal side, four on the maternal side, and three within the chorioamniotic membranes. The analysis also revealed the presence of industrial pigments like iron hydroxide oxide and ultramarine blue, both applied for cosmetic formulations, such as BB creams, foundations, lipstick, mascara and eyeshadow.

Differently, Braun et al. used FTIR to analyze particles larger than 50 μm and discovered various MPs, including PE, PP, and polyurethane (PU) in two out of three placentas contained.[35]

More recently, three additional studies have been conducted on placentas using different techniques.

In another work, Ragusa et al. examined 10 human placentas using variable pressure scanning electron microscopy (PV-SEM) and transmission electron microscopy.[36] They detected MPs, ranging in size from 2.1 to 18.5 μm, in both intra- and extracellular compartments of different placental cellular layers, including lysosomes, peroxisomes, lipid droplets, multivesicular bodies (intracellular), stroma, endothelial cells, and pericytes (extracellular). Zhu et al. and Liu et al. used laser direct infrared spectroscopy (LD-IR) to investigate MPs in human placentas. Zhu et al.[37] identified PVC (43.27%) and PP (14.55 as the main polymer types (out of 11 types) found in the placenta. These microparticles ranged in diameter from 20.34 to 307.29 μm, with the majority (80.29%) being smaller than 100 μm. Liu et al. predominantly found polyamide and PU, which accounted for over 78% of the MPs.[38] Compared to previous studies, the laser direct infrared spectroscopy (LD-IR) technique detected a higher number of microplastics, suggesting that placentas may accumulate more microplastics than previously estimated. Therefore, it is crucial to gain a thorough understanding of the sources of microplastics in the human placenta, along with their potential health impacts on fetal development.

2.4. Respiratory and Gastrointestinal Systems

Several studies have focused on MP exposure in the respiratory and gastrointestinal systems, which are the primary entry routes for MPs.

In 2021, Amato-Laurenço et al. detected MPs in 13 out of 20 human pulmonary tissue samples obtained during autopsies.[39] These samples were collected from the distal and proximal regions of the left lung of non-smoking adults. Using μRaman spectroscopy, the most frequently determined polymers were PE (24.3%) and PP (35.1%). All particles were smaller than 5 μm, while fibers ranged between 8.1 and 16.8 μm.

In 2022, Huang et al.[40] conducted a study where they examined human sputum samples collected from 22 patients with various respiratory conditions to investigate inadvertent inhalation of MPs. FTIR microscopy and laser infrared imaging spectrometry were used to detect MPs in the respiratory tract. The study identified 21 different types of MPs in the sputum samples, with PU being the most common type, followed by polyester (PES), chlorinated polyethylene (CPE), and alkyd varnish, which together constituted 78.36% of all MPs detected. The study concluded that MPs are prevalent in sputum samples, indicating that inhalation could be a significant pathway for plastics to enter the human body. Moreover, statistical analysis ($p < 0.05$) indicated that the levels of specific MP types found in the respiratory tract were associated with factors such as smoking and invasive medical procedures.

2.5. Kidneys and Urine

Pironti et al.[41] examined urine samples from six volunteers residing in different cities in Southern Italy. The researchers utilized μRaman to analyze the samples and identify MPs. The results of the analysis revealed the presence of four pigmented microplastic fragments, ranging in size from 4 to 15 μm, with irregular shapes. Specifically, polyethylene vinyl acetate, PVC, PP, and PE were the polymers identified in the samples.

Massardo et al. investigated the presence of microplastics in human kidneys and urine using microRaman spectroscopy.[42] Healthy sections from ten nephrectomized kidneys and ten urine samples from healthy donors were analyzed using micro-Raman spectroscopy.

A total of 26 out of 66 microparticles were identified in both kidney and urine samples, with sizes ranging from 3 to 13 μm in urine and from 1 to 29 μm in kidneys. The most frequently detected polymers were polyethylene and polystyrene, while hematite and Cu-phthalocyanine were the most common pigments. This preclinical study demonstrates the presence of microplastics in renal tissues and confirms their presence in urine, providing evidence of microplastic deposition in human kidneys.

Based on these findings, there is a need for consolidation of actions and further research is necessary to enhance our understanding of the potential toxicity of MPs in humans.

3. Current Global Regulation on Microplastics in Cosmetic Formulations

As stated, microplastics are an emerging environmental and human health problem. Due to their small size, filtering them out in wastewater treatments is challenging, allowing easy access of microplastics to the sea.[16] As a result, for decades, governments and non-governmental organizations (NGOs) have reported the problem of marine pollution caused by plastics and microplastics (Figure 3).

The 2000s marked the beginning of international efforts to address marine litter and protect the aquatic environment. In 1972, the London Convention[43] listed materials considered marine waste including plastic or other synthetic substances. Both the Oslo Convention (1974)[44] and the MARPOL (Annex V-1978)[45] of the International Maritime Organization (IMO) forbade the dumping of materials such as plastics and garbage plastic bags in the sea. On November 3rd 1995,[46] 108 governments, the European Commission with various UN bodies and UN specialised agencies declared the "Global Programme of Action of the Marine Environment" to establish a global initiative on marine pollution in 2003. It stated that domestic wastewaters were discharged improperly. It was noted that 80% of plastic pollution originated from land, and uncontrolled combustion of plastic could generate Persistent Organic Pollutants (POPs), metals, and hydrocarbons. In 2016, UNEA (United Nations Environment Assembly) recognized the negative impacts of microplastics and encouraged countries to take

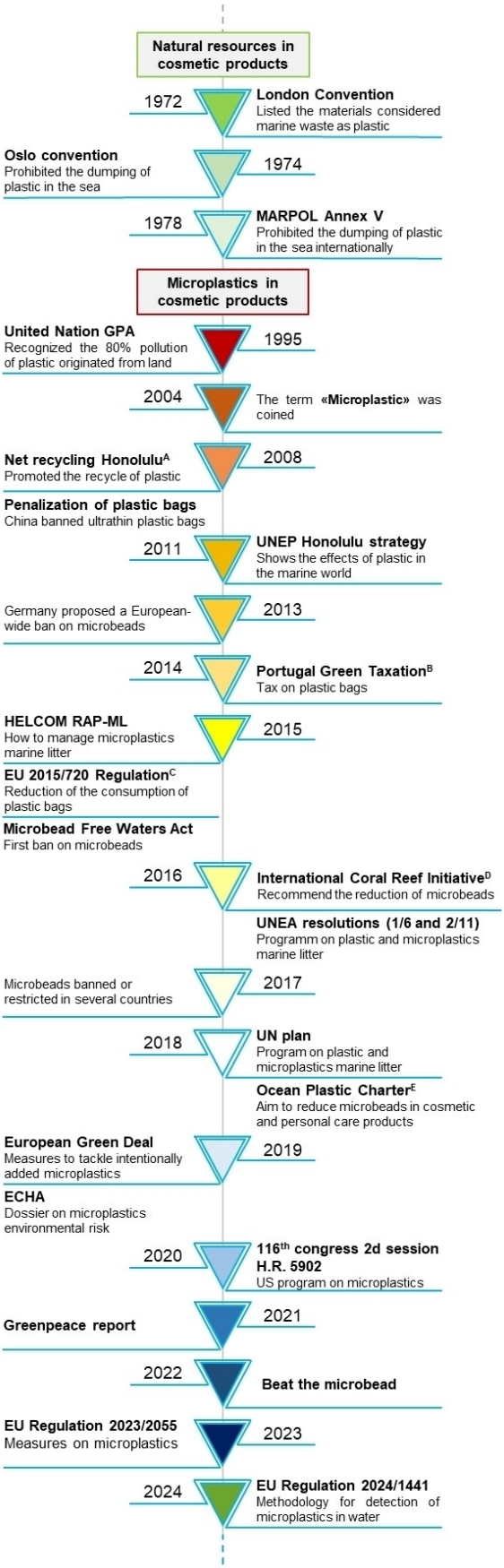

Figure 3. Main actions taken by governments, institutions and associations against microplastics since their introduction.

immediate actions.[47] In the following years, several documents were published such as the UN plan (2018), and European Green Deal (2019) which suggest solutions to reduce MPs.[48,49] In 2021, Greenpeace published a report where 664 cosmetic products were analyzed and found that 25% of them contained MPs, providing a list of toxic substances along with their relative percentages in each product.[11,50] Other NGOs are monitoring and fighting for marine litter such as "the Honolulu Strategy".[51] In 2019, the European Chemical Agency (ECHA) proposed the definition of microplastic as a "solid polymer-containing particle" and suggested their restrictions.[52,53] Countries have begun to establish new norms and prohibitions on the use of microplastics in commercial products, especially cosmetics(.

3.1. Europe

In 2013, the Dutch government was the first country to propose a European-wide ban on microbeads. A year later, the European Commission established the prohibition of the Ecolabel sign on rinse-off cosmetics.[54] Therefore, Austria, Belgium, Luxembourg and Sweden demanded a ban on microbeads in personal care products in a common statement. A few countries, including the Netherlands and the UK, declared themselves free from microbeads by 2017, while others proposed temporary bans, like Denmark. Italy decided to reduce the use of microplastics in rinse-off products (as well as cotton buds and detergent). From 2020, the marketing of rinse-off manufactures with microplastics are forbidden.[55] The Nordic Council, in January 2017, proposed a full ban on microplastic in cosmetic products.[56]

Two years later, Ireland was the first country to publish the definition of microplastic to form a national ban and in 2020, to eliminate in household and industrial cleaner microbeads.[57] Moreover, European personal care industries started reducing the use of microbeads by 82% by 2015 with Cosmetic Europe introducing further restrictions in 2017.

Furthermore, the European Commission accelerated the implementation of the "Circular Economy Action Plan" which was initially outlined in 2015.[58,59] HELCOM (Helsinki Commission) described how to manage marine litter. It defined "primary" and "secondary" microplastics and how to tackle this issue.[60] On November 9th 2017, the European Commission invited the European Chemical Agency (ECHA) to design a dossier for the restrictions on synthetic water-insoluble microparticle polymers of 5 mm. ECHA published the dossier highlighting the environmental risk of marketing synthetic solid microparticles. Specifically, it proposed a "prohibition of the placing on the market of any solid polymer contained in microparticles or microparticles which have a solid polymer surface coating, as a substance on their own or in a mixture in a concentration equal to or greater than 0,01% by weight".[61] Seven years later the European Union banned products containing added microplastics as cosmetics, personal care and single-use manufactures.[62] Europe aims to reduce the amount of MPs released in the environment by 30% by 2030.[63] Additionally, they established a methodology to measure MPs in water by 2024.[64]

3.2. America

In 2014, Illinois became the first state in the United States to ban non-biodegradable microbeads in personal care products.[65] In 2020, the use of daily chemical products containing microbeads smaller than 5 mm, such as rinse-off products, was banned. By December 2022, the sale of these products was also prohibited.[66] Later, California expanded this ban to biodegradable microplastics and in 2015 microbeads were banned in cosmetics and personal care products.[67,68] In the same year, the US government published the "Microbeads free-water Act" which prohibits the manufacture and sale of microbeads in rinse-off personal care items from 2018.[69] In 2015, Canada labelled microplastic as a toxic substance in the Canadian Environmental Act of 1999, but it was not simultaneously banned. Two years later, regulatory measures banned the manufacture, import, and sale of microbeads in toiletries by July 1, 2018.[70] In 2020, it proposed a system that reduce the use of microbeads in personal care products.[71] In 2016, the Brazilian government banned the use of non-biodegradable plastic in cleaning, bleaching, grinding, and exfoliating cosmetics. Four years later Argentina banned the production, import, and marketing of microbeads in toiletries and makeup items.

3.3. Asia and Oceania

In 2008, the Chinese government penalised plastic bags and launched microplastic monitoring in 2016.[72,73] It proposed guidance for industries to forbid the manufacture of household chemical products containing plastic microbeads. In 2020, banned daily chemical products with microbeads smaller than 5 mm like rinse-off products. In December 2022, their sale was forbidden. Taiwan and South Korea have already banned microbeads in rinse-off cosmetics, while India is still considering regulations to address them.[74] Since 2020, Thailand has forbidden microbeads in cosmetic products to reduce primary microplastics[75] In 2015, Australian government began to take action on microbeads through the NSW EPA.[76,77] During the Meeting of Environment Ministers in December, an agreement was reached to slowly get rid of microbeads in personal care, cosmetic, and cleaning products. Australia eliminated microbeads in rinse-off cosmetics and personal care products. However, New Zealand took action three years later, in 2018, by choosing to prohibit microbeads.[78] Other countries, like the United Arab Emirates (UAE), have not yet announced legal restrictions or bans on the phase-out of microplastics from cosmetics. The situation in South Africa is similar to India, where the government is still consulting on regulations against the use of microbeads in cosmetics.[79] Anyway, in active bans, there is not a universal document which states what microbeads are restricted and for what purpose. There is only an agreement between countries on the definition and size of microbeads.

4. Major Microplastics in Cosmetic Formulations

As previously mentioned, cosmetic powders are among the most relevant raw materials for the achievement of final formulations with specific properties distinguishable by the end consumer. The small size, shape, and chemistry of these materials are the characteristics that influence most of their properties. Microplastics have led to a drastic change in the performance of formulations, improving sensory attributes, albeit at the expense of sustainability. Table 2 summarizes the principal microplastics exploited in cosmetic products, showing their chemical formula and main effects in formulations.[7,80]

- Polyethylene (PE) is one of the most widely used synthetic polymers and is easy to produce. PE consists of repetitive units of ethylene groups, which give the polymer flexibility and strength. Indeed, the relative polymerization can yield branched or linear structures, leading to the production of high-density polyethene (HDPE), low-density polyethene (LDPE), and linear low-density polyethene (LLDPE), each contributing to different performances. In cosmetics, PE is a film-forming and viscosity-regulating agent.[7,80,81] Specifically, PE microparticles were used in formulations for facial and body scrubs as an exfoliating agent. But since 2018, they have been banned from cosmetic products due to their impact on marine ecosystems.[80]
- Polypropylene (PP) is a thermoplastic homopolymer produced from 1-propene, a gas derived from petroleum and natural gas. PP is known for its lightweight nature and resistance to corrosion, wear, and moisture. This polymer is used as a viscosity-controlling agent in foundations and nail polishes – also, employed as an exfoliant in some formulations.[80]
- Poly(methyl methacrylate) or PMMA is a transparent thermoplastic polymer obtained from methyl methacrylate. In cosmetics, this polymer is used in nail polish, lip gloss, and mascara due to its film-forming aptitude. PMMA microparticles are also used as absorbent agents for transporting active ingredients and as brightness/mattifying regulators, reducing imperfections caused by ageing. Additionally, they modulate the texture of formulations due to their small size.[7,80,82]
- Polytetrafluoroethylene (PTFE) is a homopolymer derived from the polymerization of tetrafluoroethylene. This polymer is used as a hair conditioning and additive in makeup products,[80] including foundations, face powders, and primers, to offer a matte finish. PTFE microparticles can enhance the sensorial experience of cosmetic formulations by improving the texture with a smooth and silky sensation. Additionally, they exhibit non-stick, free-flowing, moisture-resistant, and long-lasting properties, which well-suite for most products.[83,84]
- Polyethylene Terephthalate (PET) is derived from terephthalic acid and ethylene glycol. PET microparticles can be utilized in various formulations due to their properties.[7,80,85] They can enhance the texture of semi-solid formulations and serve as exfoliating agents in skincare products like face and body scrubs. Additionally, they can function as mattifying agents in creams, lotions, and foundations. These microplastics can be used also to deliver and release active ingredients. In addition, they can be coloured and used as additives in the formulation of leg and body paints, nail polish, lip gloss, and hair colouring products.
- Polyamides (Nylon) are synthetic polymers containing amide bonds as repeating units, and various types can be obtained based on the starting monomers; eminent examples are Nylon-6 and Nylon-12.[7,80] The first one is derived from the ring-opening of caprolactam, serves as a viscosity-controlling, bulking, thinning, and moisturizing agent. Nylon-12, a synthetic polymer derived from ω-amino lauric acid monomers, possesses bulking and opacifying properties and is commonly found in skin creams and face powders.
- Polyurethane (PU) is a synthetic polymer made from the reaction between polyols and diisocyanates. In cosmetics, PU microbeads are used as exfoliating, texture enhancement, and/or binding agents. They are capable of absorbing excess sebum from the skin, making them useful in oil-control formulations. Polyurethane can also be used as a colour additive to enhance the effects in products such as nail polish, lip gloss, and eyeshadows.[86]
- An example is PU cross polymer-1, a synthetic copolymer made of isophthalic acid, adipic acid, hexylene glycol, neopentyl glycol, dimethylolpropanoic acid, and isophorone diisocyanate units, which is used as a binding, film-forming, and hair-fixing agent.[80]
- Polyacrylates are a family of synthetic polymers made up of acrylate monomers, which are used as film-forming, antistatic, binding, hair fixative, and suspending agents.[7,82] There are various acrylate copolymers such as styrene-acrylates copolymers, used as colour opacification and filming agents; and ethylene/acrylate copolymers, used as a binding, emulsion stabilizing, thickening, film-forming, and opacifying agent.
- Polyethylene glycols (PEGs) and polypropylene glycols (PPGs), synthetic polymers of ethylene glycol broadly used also in pharmaceutical formulations for drug delivery. They are employed in cosmetic products as humectants or emulsifiers formulated as creams, lotions, and serums. PEGs and PPGs are soluble in aqueous and organic phases, favoring the solubilization of active ingredients and fragrances in formulations.[87]
- Polymethylsilsesquioxane is a synthetic silicone obtained from the hydrolysis and condensation of silicone methyltrimethoxysilane. This synthetic polymer is used for film-forming, texturing, opacifying, skin and hair conditioning.[80,88,89]
- Other microplastics of common usage[7,80] are polybutylene terephthalate (PBT), polystyrene (PS), various types of Nylon, acrylates[82,86,90] and polyurethane crosspolymers.[90]

Table 2. Main formulation effects of principal microplastic in cosmetic products.

Microplastic	Formulation effects
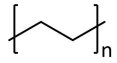 Polyethylene (PE)	Abrasive, film-forming and viscosity-regulating
Polyethylene (PE)	
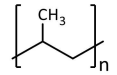 Polypropylene (PP)	Exfoliating and viscosity-regulating
Polypropylene (PP)	
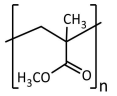 Polymethyl methacrylate (PMMA)	Brightness/mattifying regulators, carrier of actives, film-forming and texturizing
Polymethyl methacrylate (PMMA)	
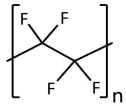 Polytetrafluoroethylene (PTFE)	Binding, bulking, hair and skin conditioning, long-lasting, moisture-resistance and texturizing
Polytetrafluoroethylene (PTFE)	
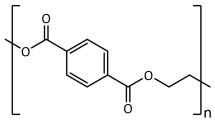	Absorbent, film-forming, mattifying and texturizing
Polyethylene Terephthalate (PET)	
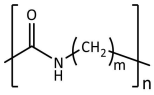 Polyamides (Nylon)	Bulking, conditioning, opacifying, texturizing and viscosity controlling
Polyamides (Nylon)	
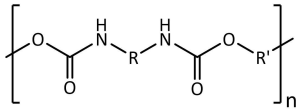	Binding agent, film-forming, hair fixing and conditioning and viscosity controlling
Polyurethane (PU)	
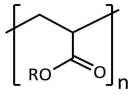 Polyacrylates	Absorbent, binding agent, emollient, emulsifying filming, hair and skin conditioning, opacifying and viscosity controlling
Polyacrylates	
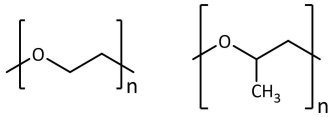 Polyethylene glycols (PEGs) Polypropylene glycols (PPGs)	Emulsifying, hair and skin conditioning, humectant and solvent
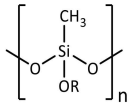 Polymethylsilsesquioxane	Film-forming, hair and skin conditioning, opacifying and texturing
Polymethylsilsesquioxane	

5. Eco-friendly Cosmetic Powders – Alternatives to Microplastic

The regulatory restrictions applied to plastic microbeads stem from growing scientific evidence of their environmental release and harm. However, the presence of alternative materials has played a key role in driving the implementation of these regulations.[91] Numerous initiatives are underway to address the harmful impacts of microplastics, including those originating from personal care and cosmetic products, on marine environments and other ecosystems. Leading these efforts is the replacement of traditional synthetic microplastics with eco-friendly, sustainable, and biodegradable materials.[79] In the cosmetic industry, there is active seeking of alternatives to traditional microplastic ingredients, distinguishing natural, semi-synthetic and synthetic alternatives as Figure 4 shows.[92]

5.1. Natural Alternatives

Consumer consciousness about the detrimental impact of synthetic polymers on the environment is pushing for the improvement of biopolymer production from natural sources. The eco-friendly, safe, and biocompatible traits of natural polymers make them particularly significant in cosmetic formulations. Natural polymers like starch, cellulose, alginate, chitosan, lignin, pectin, xanthan gum, agar, hyaluronic acid, guar gum, gelatine, collagen, and keratin can be modulated as microparticles[93–95] and formulated for the cosmetic industry.[96] These versatile materials can be employed in skincare, haircare, and makeup, serving as stabilizers and modifiers. Their safety, biocompatibility, eco-friendliness, and appeal to consumers make them highly suitable for various cosmetic applications. Introducing small molecules or polymers can modify natural alternatives, resulting in semi-synthetic materials. Celluloses and starches are commonly modified to gain properties for skin sensoriality and formulation purposes.

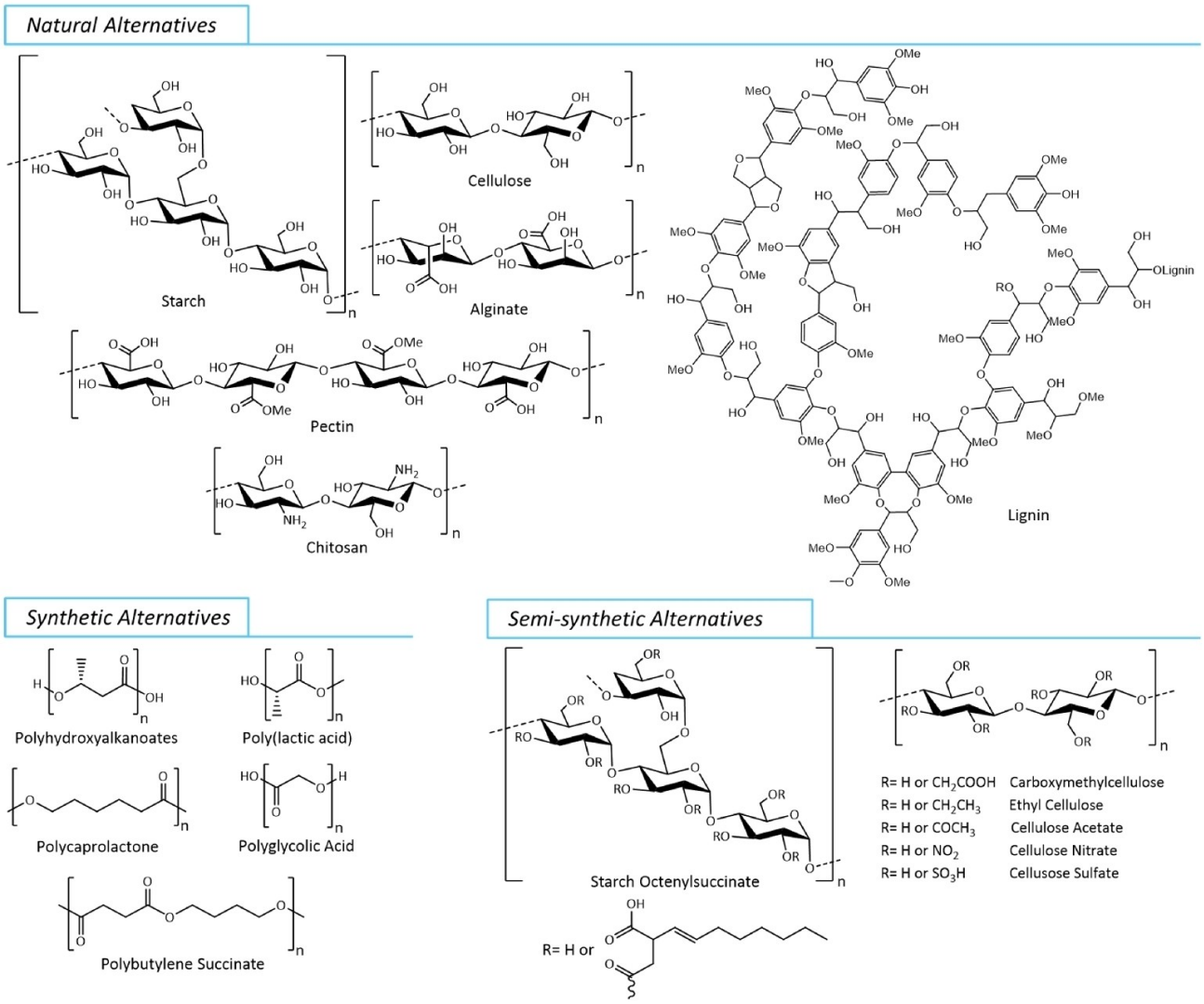

Figure 4. Main natural, semi-synthetic and synthetic alternatives used to replace microplastics in cosmetic products.

5.2. Starch

Starch is a natural polysaccharide obtained from plant sources such as corn, rice, maize, wheat, and barley. This biopolymer usually exhibits size distribution in the order of micrometers.[97] It is utilized as a versatile cosmetical component, applied in skincare, hair care, and personal care formulations. Starch beads have garnered significant attention in cosmetic formulations due to their biodegradability, renewability, and potential to replace non-biodegradable microplastics in personal care products.[96,98]

A study by Junlapong et al. investigated the biodegradation of starch-based hydrogels resulting in environmentally friendly alternatives to synthetic microplastics.[99] This feature aligns with the growing consumer demand for sustainable and eco-friendly cosmetic products. Studies have also shown that controlling parameters such as starch source, processing techniques, and crosslinking agents can influence the size, shape, and texture of starch beads, thereby affecting their suitability for various cosmetic formulations.[100] For example, Farrag et al. pointed out that the source of starch significantly influences the self-assembling behavior of this polymer at the nanometric level due to different amylose/amylopectin ratios. Starch beads have been explored as carriers for active ingredients in cosmetics, improving stability, controlled release, efficacy, and longevity.[101] For instance, Adejoro et al. succeeded in producing starch-based systems enabling the production of homogeneous microcapsules trapping tannins.[102] Pueknang and Saewan encapsulated folic acid in phosphorylated rice starch producing a semi-solid formulation. They evaluated the improvement of human skin noticing the melanin content, scaliness, and wrinkle.[103] Starch beads can also serve as texture enhancers in cosmetic formulations by providing desirable sensory properties such as smoothness, spreadability, and a luxurious feel. Studies have investigated the rheological properties of starch-based gels and emulsions, demonstrating their potential to improve the texture and consistency of creams, lotions, and other cosmetic products.[104] Research by Marto et al. has focused on assessing the compatibility and stability of starch-based emulsions (St-BV) in various cosmetic formulations. The physicochemical characteristics and the toxicological profile of ingredients combined with the risk characterization and the evaluation of tissue viability resulted in being safe for human use. Furthermore, an increase in skin hydration and microcirculation has been observed.[105]

Besides the above-mentioned advantages, starch is one of the easily modifiable polymers due to its simple structure and abundance in nature. Different physical properties could be achieved by to the polymer through the grafting of molecules and/or macromolecules, making the resulting starch derivatives one of the most versatile alternatives in the formulation field.[106] A common modification involves the insertion of octenyl succinic acid (OSA) to confer hydrophobic character to starches, leading to a smart product primarily employed as an emulsifier. Mu et al. modified waxy maize and corn starches with 3% OSA to create oil-in-water emulsions and studied their stability under various conditions (pH change, electrolyte concentration, and enzymatic treatment). OS-starches can be customized for the release of active ingredients by controlling their destabilization rate.[107]

5.3. Cellulose

Cellulose is a natural polymer found in the cell walls of plants and is derived from abundant sources, including wood, hemp, cotton, and linen. Macro- and nanofibers originated from cellulose are a highly appealing substrate for cosmetics, as they are biodegradable, non-toxic,[108] and offer gentle exfoliation without causing harm to the environment. Celluloses are mainly employed as emulsifiers, film-forming and thickeners agents in cosmetic formulation, i.e. facial scrubs and exfoliating cleansers.[96,109]

OBrien et al. produced spherical cellulose microbeads by a scalable membrane emulsification−phase inversion process as an eco-friendly alternative to microplastics.[110] Recently, bacterial cellulose (BC) is taking place in this field due to its purity, porosity tensile strength. BC has identical chemical composition with pure plant-derived cellulose, differing solely in molecular weight.[111] This polymer can be used in cosmetic products as Personal Care formulations, facial scrubs and mask.[112,113]

As already mentioned, cellulose is often modified to achieve characteristics useful for formulating cosmetic products, i.e. improved solubility – some examples are sodium carboxymethylcellulose, ethyl cellulose, and cellulose esters.

Sodium carboxymethylcellulose (NaCMC) is the sodium salt of carboxymethylcellulose (CMC), resulting from the etherification of cellulose with sodium monochloroacetate in an alkaline solution (NaOH). NaCMC is a water-soluble biopolymer used in cosmetics as a moisturizer, humectant, and emulsifier. In a study by Martins and Rocha, CMC was tested with bacterial cellulose, as an emulsifier in a cosmetic cream. This combination was able to completely replace commercial surfactants maintaining the rheological properties of the formulations.[114] Aguiar et al. produced spherical Na-CMC microparticles by spray drying to encapsulate three natural antioxidants – caffeic acid (CAF), chlorogenic acid (CGA) and rosmarinic acid (RA). They obtained high encapsulation efficiency and evaluated the total release and the antioxidant activity.[115] Instead, Costa et al. used CMC as a bioactive cosmetic ingredient for skincare formulation. They studied the effects in HaCat and HDFa cells showing no cytotoxic effect, intracellular production of procollagen I α I and modulation HaCat immune response.[116]

Ethylcellulose (EC) is a non-ionic water-insoluble cellulose ether obtained from the etherification of alkali cellulose with ethyl chloride.[117] Juleaha et al. encapsulated essential oils isolated from the peel of *C. aurantifolia* in ethyl cellulose microparticles by coacervation method for cosmetotextile products.[118]

Cellulose esters are obtained from the reaction of natural cellulose with organic acids, anhydrides, and acid chlorides. Generally, they are water-insoluble polymers, characterized by excellent film-forming properties.[119] These polymers are mostly used as gelling agents, bioadhesive, thickening, and stabilizing

agents applied in cosmetic formulations (creams, shampoos, and lotions).[92] Some examples of cellulose esters are cellulose acetate (CA), cellulose sulfate (CS), and cellulose nitrate (CN).

5.4. Alginate

Alginate is an indigestible polysaccharide naturally produced and typically harvested from brown algae. The molecular structure consists of unbranched linear binary copolymers comprising β-D-mannuronic acid (M) and α-L-glucuronic acid (G) residues linked by 1,4-glycosidic bonds. In algal alginate structures, three uronic acid blocks are present, including homopolymeric regions of M and G blocks, as well as alternating MG blocks containing both polyuronic acids. Typically, bacterial alginates contain O-acetyl groups absent in algal alginates, with bacterial polymers exhibiting higher molecular weights.[120] The ability of sodium alginate (SA) to create a physical hydrogel through ionic crosslinks, particularly with divalent cations like Ca^{2+}, is well-documented. These alginate hydrogels undergo biodegradation through the hydrolysis of glycosidic linkages and are also subject to degradation due to the release of divalent cations.[121] In their study, Bae et al. produced sodium alginate (SA) microbeads (MB) by using an aqueous solution of SA and electrospraying it into a Calcium water solution. An increase in microbead size from 640 to 880 μm was observed by the SA concentration and the nozzle diameter, showing how these parameters can influence the final dimension and shape of the product.[122] Given their mucous consistency, cost-effectiveness, non-toxic nature, and biocompatibility, alginate hydrogels find extensive use in various biomedical and environmental applications such as drug delivery systems, cell encapsulation, and cosmetics.

5.5. Chitosan

Chitosan is a biopolymer derived from deacetylation of chitin, a natural polysaccharide found in the exoskeletons of crustaceans like shrimp, crab, and lobster, as well as in the cell walls of fungi.[123] Chitosan can be used in cosmetic formulations for skin and hair care products. Specifically, it is utilized as a texturizer, emulsifier, film-forming and humectant agent.[124,125] Gomaa et al. utilized chitosan microparticles as carriers of Ensulinzol (PBSA) to apply sunscreen products.[126] Ju et al. prepared chitobeads (CBs) using chitin, which, after re-acetylation, exhibited higher cleansing efficiency compared to polyethylene beads able to remove potentially toxic elements.[127] Instead, Wisuitiprot et al. tested a cream containing chitosan microparticles loaded green tea extract on human facial skin, demonstrating anti-wrinkle effects and improved skin elasticity and lightening after 2 months treatment period.[128]

5.6. Lignin

Lignin is a polyphenolic material present as main component in the plant cell walls and obtained by oxidative coupling of three monolignols, para-coumaryl alcohol (H), coniferyl alcohol (G) and synapyl alcohol (S). Depending on the degree of these monomers (H, G and S), the lignin can be classified in Grass Lignin, Softwood and Hardwood. In general, lignin presents several properties useful for topic applications in cosmetics. In fact, it is an emulsion stabilizer, antimicrobial and UV shield agent.[129] Antunes et al. exploited lignin from sugarcane bagasse in a semisolid formulation demonstrating its activity to scavenge ABTS and DPPH radicals. Moreover, their study revealed an in vivo Sun Protection Factor (SPF) value of 9.6 ± 0.8, indicating a broad-spectrum UV protection capability.[130] Lee et al. employed lignin under mild conditions (MWL) as sunscreen agent, demonstrating synergistic effects with commercial ones, and enhancing SPF activity of commercial product.[131]

5.7. Pectin

Pectin is a natural polysaccharide present in the cell walls of fruits and vegetables, such as apples and berries and is made of a network of galacturonic acid with side chains of other sugars, such as rhamnose, arabinose, and galactose.[132] This conformation provides specific properties making pectin employing as a gelling agent, thickener, and stabilizer.[95]

In literature, there are few techniques to produce pectin microparticles (i.e., ionic gelation, spray drying, and extrusion), especially for encapsulating active ingredients, but mostly related to the pharmacological field as drug delivery systems.[95,132,133]

5.8. Synthetic Alternatives

Synthetic polymers deriving from renewable sources such as polyhydroxyalkanoates and poly(lactic acid), are gaining attention as an alternative to petrochemical-based plastic due to their biocompatibility, biodegradability, and non-toxicity.[96,134]

5.9. Polyhydroxyalkanoates (PHA)

Polyhydroxyalkanoates (PHAs) are polyesters of hydroxyalkanoates (HAs) and naturally produced by various Gram-positive and Gram-negative bacteria. PHAs can be obtained by fermenting renewable sources making them a sustainable alternative to petrochemical-based plastics such as PET. The number of carbon atoms in the chain determines the structure and types of PHAs. PHA is biodegradable and biocompostable, making it an eco-friendly option for a range of products including cosmetics. PHAs are used in many beauty products such as beauty masks or sanitary pads, as well as in heat-sensitive adhesives, smart gels, and surfactants.[135,136] They have antiox-

idant and moisturizing properties and products containing PHAs can have an antibacterial effect.[96] PHA has tiny pore sizes, high dependability, and high surfactancy. They offer many advantages like easy manufacturing, good UV resistance, and hydrophobicity.[137] Phothong et al. investigated astaxanthin-loaded PHB microbeads, from crude glycerol, for facial scrubs not observing skin irritation and sensitization during a human repeated insult patch test (HRIPT).[138]

5.10. Poly(Lactic Acid) (PLA)

Poly(lactic acid) (PLA) is an aliphatic thermoplastic polyester composed of lactic acid (2-hydroxy propionic acid) units obtainable from renewable and degradable resources like corn and rice. PLA has a low environmental impact because its degradation yields mainly water and carbon dioxide. Poly(lactic acid) is commonly employed in cosmetic packaging due to its mechanical resistance and good rigidity. PLA is ideal for applications on skin, hair, and nails finding use in cosmetic products including makeup, scrub soaps, creams, gels, and lotions.[139]

5.11. Polyglycolic Acid (PGA)

Poly(glycolic acid) (PGA) is a biopolymer synthesized via the condensation of glycolic acid or by the ring-opening of glycolide. PGA is insoluble in a wide range of solvents because of its high porosity, hydrophobicity, and high crystalline structure (between 45% and 55%).[140] PGA has better mechanical qualities and a faster rate of deterioration than polylactic acid (PLA).

5.12. Polycaprolactone (PCL)

Polycaprolactone (PCL) is an aliphatic polyester made of hexanoate units, characterized by its hydrophobic and semi-crystalline structure. PCL is an eco-friendly biopolymer obtainable from renewable materials.[141] For example, Forigua et al. produced PCL microparticles w/o cargo exploiting a microfluidic system. The size distribution below 50 μm and the spherical shape obtained are very promising not only in drug delivery and tissue engineering, but also in cosmetics.[142] Nam and Park produced PLA and PCL MBs using an eco-friendly melt electrospraying process, without the need for any organic solvent. These aliphatic polyester-based biodegradable MBs showed high skin hydration and minimal irritation, making them suitable for use in cosmetics.[143]

5.13. Polybutylene Succinate (PBS)

Polybutylene Succinate (PBS) is a biopolymer derived from the polycondensation between 1,4-butanediol and succinic acid, obtainable from renewable sources such as sugar cane. It degrades in non-toxic products such as water, carbon dioxide, and biomass. PBS is known for strength, stiffness, toughness, biodegradability properties showing resistance to various chemicals, and compatibility with a wide range of additives.[144] Dutra et al. proposed a new production of PBS microparticles through a water-free suspension polycondensation process with an average size of 80–180 μm.[145] Gan et al. synthesized four polyester microparticles, including PBS and poly(butylene succinate adipate) (PBSA), and tested their degradation under marine and enzymatic conditions, showing promising results compared to the common microplastics used in cosmetics.[146]

6. Summary and Perspectives

Although many natural alternatives exist and can be modified using functional groups like amines, carboxylic acids, aldehydes, and thiols, there are currently fewer patents in this area compared to the number of products on the market.This occurs because companies, both for reasons of trade secrecy and for a rapid transition to plastic-free and vegan products, utilize natural microbeads without making modifications. However, products or formulation examples containing microplastics or 'skeptical microplastics' (synthetic polymers lacking enough available information and are under investigation) are still observed, to enhance properties (i.e. film forming, long-lasting effects, and others).

Despite the challenging and rapid transition to sustainable formulations, there has been an increase in patents where both natural and synthetic alternatives are discussed to be employed in the final product, contributing to its main characteristics.

Starches and celluloses are receiving increased attention due to their wide availability from various plant sources globally. Different types of starches like ginger, turmeric, wheat, and mung bean are used to make solid and semi-solid products such as eyeshadow and emulsions.[147] Additionally, starches can be used to create innovative solid formulations for hair products, primarily composed of polyols, fatty alcohols and/or acids, improving the shelf life and avoiding the transport of a liquid composition.[148] In combination with xanthan gum and cellulose, starch is used as a thickening agent to obtain an eco-sustainable stabilizing component for make-up products such as mascara, powder foundation, lipstick, lip gloss, and nail polish, as well as for hair and skin care.[149]

Celluloses also find their application in producing cosmetic products,[150,151] often with other ingredients, as previously cited to create products like sunscreen and waterproof formulations without polyacrylates, carbomers, and polyvinylpyrrolidones[152] Other celluloses, such as sodium carboxymethylcellulose and microcrystalline cellulose, combined with Diutan gum, ensure high stability in personal care formulations.[153] Sustainable alternatives such as lignin,[154,155] alginate,[156,157] and pectin[158,159] are already exploited in patented products for these applications.

Synthetic alternatives are gaining ground in cosmetics, particularly polyhydroxyalkanoates (PHA) and polycaprolactone (PCL). PHAs offer several advantages, including the ability to

adsorb oils, adjust the viscosity of certain thickening agents, and enhance opacity, and uniformity of pigmentation.[160] PHA microparticles are utilized in anhydrous formulations, free of polyamides and acrylic polymers, such as lipsticks, which require good dispersibility, viscosity, moldability, and mechanical properties.[161]

On the other hand, PCL can create spherical microparticles[162] and is used to encapsulate collagen peptides[163] or vitamin C[164] as dermal fillers, as well as metal oxide particles as opacifiers.

As noted, the challenge of removing microplastics from beauty care products is a current topic in the cosmetic industry worldwide. Institutions work to eliminate all components harmful to the ecosystem and promote a sustainable transition. In cosmetics, this approach represents a significant opportunity for innovation due to green consumers pushing companies to reconsider their formulations, also in response to government bans.

The fact that microplastics have now entered the human food and vascular cycle is a cause for serious global alarm.[165] However, scientific literature remains lacking in terms of alternatives aimed at replacing microplastics, especially concerning the necessary sensory characteristics requested by the cosmetic market.

In this review, we have summarized the main types of microplastics (as shown Figure 5a–c), and their characteristics utilized in current cosmetic products such as make-up, skincare, and hair care. We highlight three categories of alternatives (natural, semi-synthetic, and synthetic) that include the most promising solutions currently under investigation (as shown Figure 5d–h). The newly explored biopolymers applied as microplastic substitutes and their main characteristics have been discussed herein.

Natural resources derived from plants, such as starches, cellulose, and lignin, are emerging as the primary alternatives to reformulating cosmetic products, especially for their broad availability in comparison to other ones. These natural ingredients not only offer an ecological solution to the problem of microplastics but also have the potential to improve the overall performance and sustainability of finished cosmetic products.

The pressing need to adopt more eco-friendly approaches is pushing researchers to focus more on current claims. We anticipate a significant increase in literature on sustainable cosmetics in the next few years, as the interest in sustainable cosmetic products is rapidly increasing. Presumably, studies will primarily focus on new production methodologies, the use of natural and biodegradable ingredients, as well as the studies of the environmental impact of new cosmetic formulations. This growing research interest aims to provide companies and consumers with detailed information to support informed and sustainable choices in cosmetic products.

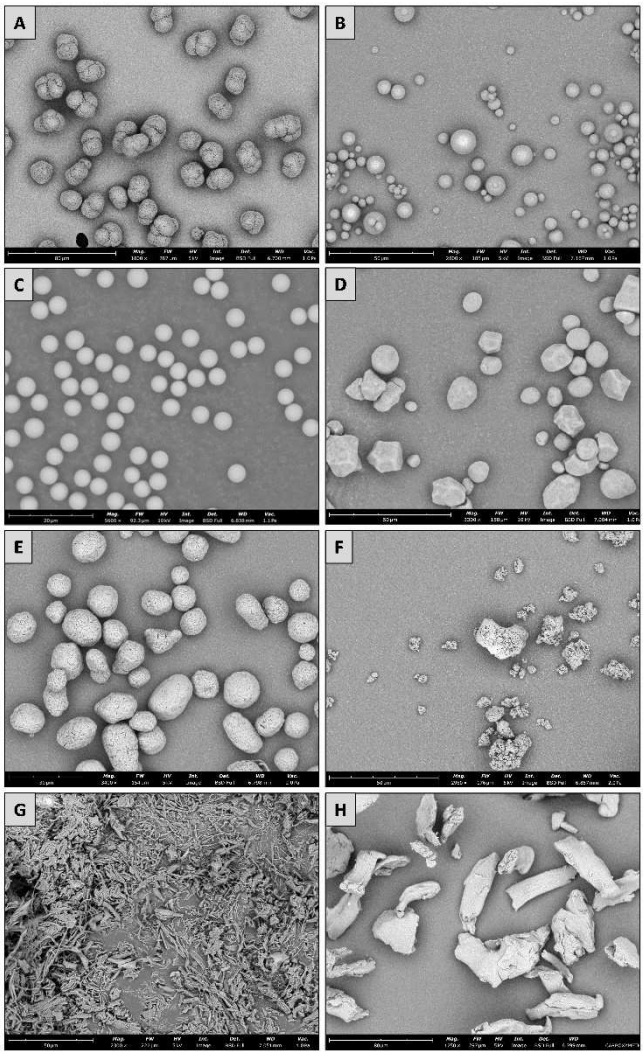

Figure 5. SEM images of A) Nylon 12, B) PMMA, C) polymethylsilsequioxane, D) Corn starch, E) Cellulose beads, F) Lignin, G) PLA, H) Sodium carboxymethylcellulose. Pictures taken in the NanoBioLab using Phenom Pro G6 Desktop SEM.

Acknowledgments

This research was funded by MUSA – Multilayered Urban Sustainability Action – project, funded by the European Union – NextGenerationEU, under the National Recovery and Resilience Plan (NRRP) Mission 4 Component 2 Investment Line 1.5: Strenghtening of research structures and creation of R&D "innovation ecosystems", set up of "territorial leaders in R&D" Open Access publishing facilitated by Università degli Studi di Milano-Bicocca, as part of the Wiley - CRUI-CARE agreement. Open Access publishing facilitated by Università degli Studi di Milano-Bicocca, as part of the Wiley - CRUI-CARE agreement.

Conflict of Interests

The authors declare no conflict of interest.

Keywords: Microplastics · Natural products · Sustainable chemistry · Cosmetic formulations · Regulatory measures

[1] M. Ferreira, A. Matos, A. Couras, J. Marto, H. Ribeiro, *Cosmetics* **2022**, *9*, 1–15.
[2] Z. D. Draelos, *Essential Psychiatry for the Aesthetic Practitioner* **2021**, pp. 34–41.
[3] A. L. I. Al-Samydai, M. N. A. Hajleh, M. A. Othman, D. Marie, E. Altatar, H. Taher, R. H. R. Alharairy, R. O. Yousif, M. Al-Samydai, *Int. J. Pharm. Res.* **2021**, *13*(1), 09752366.
[4] H. Baumann, M. Bühler, H. Fochem, F. Hirsinger, H. Zoebelein, J. Falbe, *Angew. Chemie Int. Ed. English* **1988**, *27*, 41–62.
[5] J. Knaut, H. J. Richtler, *J. Am. Oil Chem. Soc.* **1985**, *62*, 317–327.
[6] M. G. Denavarre, *J. Am. Oil Chem. Soc.* **1978**, *55*, 435–437.
[7] H. A. Leslie, *IVM Inst. Environ. Stud.* **2014**, *476*, 1–33.
[8] J. P. Guillot, J. Y. Giauffret, M. C. Martini, J. F. Gonnet, G. Soulé, *Int. J. Cosmet. Sci.* **1982**, *4*, 53–66.
[9] H. Lautenschlager, *J. Appl. Cosmetol.* **1990**, *8*, 1–9.
[10] P. J. Petter, *Int. J. Cosmet. Sci.* **1989**, *11*, 35–48.
[11] Greenpeace **2021**.
[12] S. V. de Freitas Netto, M. F. F. Sobral, A. R. B. Ribeiro, G. R. da L. Soares, *Environ. Sci. Eur.* **2020**, *32*, 1–12.
[13] The European Parliament and The Council of the European Union, *Official Journal of the European Union* **2024/825**, 1–16.
[14] G. Wandosell, M. C. Parra-Meroño, A. Alcayde, R. Baños, *Sustainability* **2021**, *13*, 1–191.
[15] M. Kumar, H. Chen, S. Sarsaiya, S. Qin, H. Liu, M. K. Awasthi, S. Kumar, L. Singh, Z. Zhang, N. S. Bolan, A. Pandey, S. Varjani, M. J. Taherzadeh, *J. Hazard. Mater.* **2021**, *409*, 124967
[16] A. L. V. Cubas, R. T. Bianchet, I. M. A. S. dos Reis, I. C. Gouveia, *Polymers (Basel)* **2022**, *14*, 4576.
[17] L. Nizzetto, M. Futter, S. Langaas, *Environ. Sci. Technol.* **2016**, *50*, 10777–10779.
[18] L. Tian, R. J. van Putten, G. J. M. Gruter, *Biodegradable Polymers in the Circular Plastics Economy* **2022**, 59–81.
[19] C. M. Hung, C. W. Chen, C. P. Huang, S. L. Hsieh, C. Di Dong, *Environ. Pollut.* **2022**, *307*, 119522.
[20] P. Sweety Joseant, *Microplastics: Sources and Solutions* **2021**, *6*.
[21] L. S. Fendall, M. A. Sewell, *Mar. Pollut. Bull.* **2009**, *58*, 1225–1228.
[22] M. Cole, P. Lindeque, C. Halsband, T. S. Galloway, *Mar. Pollut. Bull.* **2011**, *62*, 2588–2597.
[23] M. A. Browne, A. Dissanayake, T. S. Galloway, D. M. Lowe, R. C. Thompson, *Environ. Sci. Technol.* **2008**, *42*, 5026–5031.
[24] P. Davison, R. G. Asch, *Mar. Ecol. Prog. Ser.* **2011**, *432*, 173–180.
[25] J. A. Van Franeker, C. Blaize, J. Danielsen, K. Fairclough, J. Gollan, N. Guse, P. L. Hansen, M. Heubeck, J. K. Jensen, G. Le Guillou, B. Olsen, K. O. Olsen, J. Pedersen, E. W. M. Stienen, D. M. Turner, *Environ. Pollut.* **2011**, *159*, 2609–2615.
[26] H. Golwala, X. Zhang, S. M. Iskander, A. L. Smith, *Sci. Total Environ.* **2021**, *769*, 144581.
[27] E. Guzzetti, A. Sureda, S. Tejada, C. Faggio, *Environ. Toxicol. Pharmacol.* **2018**, *64*, 164–171.
[28] C. E. Enyoh, A. Devi, H. Kadono, Q. Wang, M. H. Rabin, *Environments* **2023**, *10*, 1–18.
[29] H. A. Leslie, M. J. M. van Velzen, S. H. Brandsma, A. D. Vethaak, J. J. Garcia-Vallejo, M. H. Lamoree, *Environ. Int.* **2022**, *163*(1195), 107199.
[30] Y. Yang, E. Xie, Z. Du, Z. Peng, Z. Han, L. Li, R. Zhao, Y. Qin, M. Xue, F. Li, K. Hua, X. Yang, *Environ. Sci. Technol.* **2023**, *57*, 10911–10918.
[31] J. M. Rotchell, L. C. Jenner, E. Chapman, R. T. Bennett, I. O. Bolanle, M. Loubani, L. Sadofsky, T. M. Palmer, *PLoS One* **2023**, *18*, 1–12.
[32] L. Montano, E. Giorgini, V. Notarstefano, T. Notari, M. Ricciardi, M. Piscopo, O. Motta, *Sci. Total Environ.* **2023**, *901*, 165922.
[33] Q. Zhao, L. Zhu, J. Weng, Z. Jin, Y. Cao, H. Jiang, Z. Zhang, *Sci. Total Environ.* **2023**, *877*, 162713.
[34] A. Ragusa, A. Svelato, C. Santacroce, P. Catalano, V. Notarstefano, O. Carnevali, F. Papa, M. C. A. Rongioletti, F. Baiocco, S. Draghi, E. D'Amore, D. Rinaldo, M. Matta, E. Giorgini, *Environ. Int.* **2021**, *146*, 106274.
[35] T. Braun, L. Ehrlich, W. Henrich, S. Koeppel, I. Lomako, P. Schwabl, B. Liebmann, *Pharmaceutics* **2021**, *13*, 1–12.
[36] A. Ragusa, M. Matta, L. Cristiano, R. Matassa, E. Battaglione, A. Svelato, C. De Luca, S. D'Avino, A. Gulotta, M. C. A. Rongioletti, P. Catalano, C. Santacroce, V. Notarstefano, O. Carnevali, E. Giorgini, E. Vizza, G. Familiari, S. A. Nottola, *Int. J. Environ. Res. Public Health* **2022**, *19*, 11593.
[37] L. Zhu, J. Zhu, R. Zuo, Q. Xu, Y. Qian, L. AN, *Sci. Total Environ.* **2023**, *856*, 159060.
[38] S. Liu, X. Liu, J. Guo, R. Yang, H. Wang, Y. Sun, B. Chen, R. Dong, *Environ. Sci. Technol.* **2023**, *57*, 17774–17785.
[39] L. F. Amato-Lourenço, R. Carvalho-Oliveira, G. R. Júnior, L. dos Santos Galvão, R. A. Ando, T. Mauad, *J. Hazard. Mater.* **2021**, *416*, 126124.
[40] S. Huang, X. Huang, R. Bi, Q. Guo, X. Yu, Q. Zeng, Z. Huang, T. Liu, H. Wu, Y. Chen, J. Xu, Y. Wu, P. Guo, *Environ. Sci. Technol.* **2022**, *56*, 2476–2486.
[41] C. Pironti, V. Notarstefano, M. Ricciardi, O. Motta, E. Giorgini, L. Montano, *Toxics* **2023**, *11*, 1–9.
[42] S. Massardo, D. Verzola, S. Alberti, C. Caboni, M. Santostefano, E. Eugenio Verrina, A. Angeletti, F. Lugani, G. M. Ghiggeri, M. Bruschi, G. Candiano, N. Rumeo, M. Gentile, P. Cravedi, S. La Maestra, G. Zaza, G. Stallone, P. Esposito, F. Viazzi, N. Mancianti, E. La Porta, C. Artini, *Environ. Int.* **2024**, *184*, 108444.
[43] H. O. Bergesen, G. Parmann, Ø. B. Thommessen, Convention on the Prevention of Marine Pollution by Dumping of Wastes and Other Matter (London Convention 1972) in*Year B. Int. Co-Operation Environ. Dev.* **2018**, 98–100.
[44] H. O. Bergesen, G. Parmann, Ø. B. Thommessen, Convention for the prevention of marine pollution by dumping from ships and aircraft (Oslo Convention 1974) in*Year B. Int. Co-Operation Environ. Dev.* **2018**, 118–119.
[45] M. Julian, *Maritime Studies* **2000**, 16–23.
[46] *United Nations Environment Programme, Intergovernmental Conference to Adopt a Global Programme of Action for the Protection of the Marine Environment. from Land- Based Activities* (Washington, D.C.) **1995**, 341.7622 GLO
[47] UNEP, Environment Assembly, *United Nations Environ. Program* (2nd sess.: 2016: Nairobi) **2016**.
[48] K. Raubenheimer, N. Oral, A. Mcllgorm, *UN Environment* **2017**, 1–131
[49] *EUROPEAN COMMISSION, The European Green Deal* **2019**, 1–24.
[50] R. Z. Habib, J. A. K. Aldhanhani, A. H. Ali, F. Ghebremedhin, M. Elkashlan, M. Mesfun, W. Kittaneh, R. Al Kindi, T. Thiemann, *Environ. Sci. Pollut. Res.* **2022**, *29*, 89614–89624.
[51] United Nations Environment Programme (UNEP), National Oceanic and Atmospheric Administration (NOAA), The Honolulu Strategy **2011**, 1–57.
[52] I. Conti, C. Simioni, G. Varano, C. Brenna, E. Costanzi, L. M. Neri, *Environ. Pollut.* **2021**, *288*, 117708.
[53] ECHA, *ANNEX XV RESTRICTION REPORT*, **2019**, 1-145.
[54] The European Commision, Official Journal of the European Union **2015**, *L354*, 47–61.
[55] C. Guerranti, T. Martellini, G. Perra, C. Scopetani, A. Cincinelli, *Environ. Toxicol. Pharmacol.* **2019**, *68*, 75–79.
[56] Nordic Council of Ministers, Nordisk Ministerråd **2017**, 1–24.
[57] Y. Li, *Water* **2022**, *14*, 2790.
[58] D. Xanthos, T. R. Walker, *Mar. Pollut. Bull.* **2017**, *118*, 17–26.
[59] L. Anagnosti, A. Varvaresou, P. Pavlou, E. Protopapa, V. Carayanni, *Mar. Pollut. Bull.* **2021**, *162*, 111883.
[60] Baltic Marine Environment Protection Commission **2015**, 1–15
[61] Committee for Risk Assessment (RAC), Committee for Socio-economic Analysis (SEAC), *Eur. Chem. Agency* **2020**, 1–78
[62] D. R. Osuna-Laveaga, V. Ojeda-Castillo, V. Flores-Payán, A. Gutiérrez-Becerra, E. D. Moreno-Medrano, *Front. Environ. Sci.* **2023**, *11*, 1–16.
[63] The European Commission, *Off. J. Eur. Union* **2023**, *L*, 67–88.
[64] The European Commision, *Off. J. Eur. Union* **2024**, *L*, 1–7.
[65] C. M. Rochman, S. M. Kross, J. B. Armstrong, M. T. Bogan, E. S. Darling, S. J. Green, A. R. Smyth, D. Veríssimo, *Environ. Sci. Technol.* **2015**, *49*, 10759–10761.
[66] J. Halfar, K. Brožová, K. Čabanová, S. Heviánková, A. Kašpárková, E. Olšovská, *Int. J. Environ. Res. Public Health* **2021**, *18*, 7608.
[67] N. Girard, S. Lester, A. Paton-Young, M. Saner, *Institute for Science, Society and Policy*: Ottawa, ON, Canada, **2016**, 210–230.
[68] K. Syberg, S. F. Hansen, T. B. Christensen, F. R. Khan, *Freshwater Microplastics: Emerging Environmental Contaminants?* **2017**, 203–221.
[69] US Congress Microbead-free waters act of 2015. *Public Law*, **2015**, 114–231.
[70] Government of Canada, SOR/2017-111 **2018**.
[71] J. N. Meegoda, M. C. Hettiarachchi, *Int. J. Environ. Res. Public Health* **2023**, *20*, 5555.
[72] H. He, *Environ. Dev. Econ.* **2012**, *17*, 407–431.
[73] C. Liu, C. Liu, *Sustainability* **2023**, *15*, 9087.
[74] E. Kentin, *Proceedings of the International Conference on Microplastic Pollution in the Mediterranean Sea* **2018**, 245–250.

[75] C. H. Ng, M. A. Mistoh, S. H. Teo, A. Galassi, A. Ibrahim, C. S. Sipaut, J. Foo, J. Seay, Y. H. Taufiq-Yap, J. Janaun, *Front. Environ. Sci.* **2023**, *11*, 1142071.
[76] C. S. Lam, S. Ramanathan, M. Carbery, K. Gray, K. S. Vanka, C. Maurin, R. Bush, T. Palanisami, *Water. Air. Soil Pollut.* **2018**, *229*, 1–19.
[77] State of NSW and Enviroment Protection Authority, *EPA Annual Report* **2016**.
[78] D. Drohmann, *Int. Chem. Regul. Law Rev.* **2018**, *1*, 79–86.
[79] Y. Zhou, V. Ashokkumar, A. Amobonye, G. Bhattacharjee, R. Sirohi, V. Singh, G. Flora, V. Kumar, S. Pillai, Z. Zhang, M. K. Awasthi, *Environ. Pollut.* **2023**, *320*, 121106.
[80] M. Guzik, O. Czerwińska-Ledwig, A. Piotrowska, *Cosmetics* **2023**, *10*, 67.
[81] C. L. Burnett, W. F. Bergfeld, D. V. Belsito, R. A. Hill, C. D. Klaassen, D. C. Liebler, J. G. Marks, R. C. Shank, T. J. Slaga, P. W. Snyder, L. J. Gill, B. Heldreth, *Int. J. Toxicol.* **2020**, *39*, 59S–90S.
[82] L. C. Becker, W. F. Bergfeld, D. V. Belsito, R. A. Hill, C. D. Klaassen, D. C. Liebler, J. G. Marks, R. C. Shank, T. J. Slaga, P. W. Snyder, F. A. Andersen, *Int. J. Toxicol.* **2011**, *30*, 54S–65S.
[83] W. Johnson, W. F. Bergfeld, D. V. Belsito, R. A. Hill, C. D. Klaassen, D. C. Liebler, J. G. Marks, R. C. Shank, T. J. Slaga, P. W. Snyder, M. Fiume, B. Heldreth, *Int. J. Toxicol.* **2023**, *42*, 144S–161S.
[84] C. A. Cody, W. Neuberg, M. Sui, Y. Aead, Shamrock Technologies Inc *U.S. Pat. No. 6,881,784 Washington, DC: U.S. Patent and Trademark Office* **2005**, *2*.
[85] L. C. Becker, W. F. Bergfeld, D. V. Belsito, R. A. Hill, C. D. Klaassen, D. C. Liebler, J. G. Marks, R. C. Shank, T. J. Slaga, P. W. Snyder, F. A. Andersen, L. J. Gill, *Int. J. Toxicol.* **2014**, *33*, 36S–47S.
[86] A. Patil, M. S. Ferritto, *ACS Symp. Ser.* **2013**, *1148*, 3–11.
[87] H. J. Jang, C. Y. Shin, K. B. Kim, *Toxicol. Res.* **2015**, *31*, 105–136.
[88] M. Kanji, C. Orr, S. Plains, V. Robert, L'Oreal S.A. *U.S. Pat. Appl. No. 11/227,232*, **2006**.
[89] A. Olejnik, B. Sztorch, D. Brząkalski, R. E. Przekop, *Materials (Basel)* **2022**, *15*, 1–18.
[90] A. Patil, R. W. Sandewicz, *ACS Symp. Ser.* **2013**, *1148*, 13–37.
[91] C. F. Hunt, W. H. Lin, N. Voulvoulis, *Nat. Sustain.* **2021**, *4*, 366–372.
[92] T. F. R. Alves, M. Morsink, F. Batain, M. V Chaud, T. Almeida, D. A. Fernandes, C. F. Silva, E. B. Souto, *Cosmetics* **2020**, *7*, 1–16.
[93] M. Yamada, A. Hori, S. Sugaya, Y. Yajima, R. Utoh, M. Yamato, M. Seki, *Lab Chip* **2015**, *15*, 3941–3951.
[94] S. Sharma, A. Gupta, S. M. S. T. Chik, C. G. Kee, B. M. Mistry, D. H. Kim, G. Sharma, *Int. J. Biol. Macromol.* **2017**, *104*, 189–196.
[95] K. Gutierrez-Alvarado, R. Chacón-Cerdas, R. Starbird-Perez, *Chem.* **2022**, *4*, 121–136.
[96] S. Gupta, S. Sharma, A. Kumar Nadda, M. Saad Bala Husain, A. Gupta, *Mater. Today Proc.* **2022**, *68*, 873–879.
[97] A. Apriyanto, J. Compart, J. Fettke, *Plant Sci.* **2022**, *318*, 111223.
[98] J. B. Olivato, *Starch Industries: Processes and Innovation Products in Food Non-Food Uses. Academic Press* **2024**, 255–269.
[99] K. Junlapong, P. Maijan, C. Chaibundit, S. Chantarak, *Int. J. Biol. Macromol.* **2020**, *158*, 258–264.
[100] P. Chavan, A. Sinhmar, M. Nehra, R. Thory, A. K. Pathera, A. A. Sundarraj, V. Nain, *Food Chem.* **2021**, *364*, 130416.
[101] Y. Farrag, W. Ide, B. Montero, M. Rico, S. Rodríguez-Llamazares, L. Barral, R. Bouza, *Int. J. Biol. Macromol.* **2018**, *114*, 426–433.
[102] F. A. Adejoro, A. Hassen, M. S. Thantsha, *Asian-Australasian J. Anim. Sci.* **2019**, *32*, 977–987.
[103] J. Pueknang, N. Saewan, *Molecules* **2022**, *27*, 3463.
[104] L. Gilbert, C. Picard, G. Savary, M. Grisel, *J. Sens. Stud.* **2012**, *27*, 392–402.
[105] J. Marto, P. Pinto, M. Fitas, L. M. Gonçalves, A. J. Almeida, H. M. Ribeiro, *Toxicol. Appl. Pharmacol.* **2018**, *342*, 14–21.
[106] M. A. V. T. Garcia, C. F. Garcia, A. A. G. Faraco, *Starch/Staerke* **2020**, *72*, 1–15.
[107] M. Mu, P. Karthik, J. Chen, M. Holmes, R. Ettelaie, *Food Hydrocoll.* **2021**, *111*, 106363.
[108] K. S. Min, G. E. Ji, J. S. Hwan, L. S. Mock, S. W. Jong, K. J. Sik, *J. Toxicol. Risk Assess.* **2019**, *5*, 1–6.
[109] S. Wiechers, F. Unger, J. Meyer, *United States Apl. Publ.* **2015**, *1*, 30.
[110] J. Coombs OBrien, L. Torrente-Murciano, D. Mattia, J. L. Scott, *ACS Sustain. Chem. Eng.* **2017**, *5*, 5931–5939.
[111] D. Andriani, A. Y. Apriyana, M. Karina, *Cellulose* **2020**, *27*, 6747–6766.
[112] P. Perugini, M. Bleve, R. Redondi, F. Cortinovis, A. Colpani, *J. Cosmet. Dermatol.* **2020**, *19*, 725–735.
[113] H. Ullah, H. A. Santos, T. Khan, *Cellulose* **2016**, *23*, 2291–2314.
[114] D. Martins, C. Rocha, F. Dourado, M. Gama, *Colloids Surfaces A Physicochem. Eng. Asp.* **2021**, *617*, 126380.
[115] J. Aguiar, R. Costa, F. Rocha, B. N. Estevinho, L. Santos, *Powder Technol.* **2017**, *313*, 287–292.
[116] E. M. Costa, C. F. Pereira, A. A. Ribeiro, F. Casanova, R. Freixo, M. Pintado, O. L. Ramos, *Appl. Sci.* **2022**, *12*, 6560.
[117] H. Seddiqi, E. Oliaei, H. Honarkar, J. Jin, L. C. Geonzon, R. G. Bacabac, J. Klein-Nulend, *Cellulose* **2021**,*28*, 1893–1931.
[118] E. Julaeha, N. S. Pandiangan, D. R. Eddy, N. Permadi, A. Harja, T. Wahyudi, J. Al-Anshori, *Polymer (Guildf)* **2023**, *283*, 126265.
[119] K. J. Edgar, *Encycl. Polym. Sci. Technol.* **2003**, *9*, 129–151
[120] T. Saha, M. E. Hoque, T. Mahbub, *Advanced Processing, Properties, and Applications of Starch and Other Bio-Based Polymers* **2020**, 197–214.
[121] A. Łętocha, M. Miastkowska, E. Sikora, *Polymers* **2022**, *14*, 3834.
[122] S. Bin Bae, H. C. Nam, W. H. Park, *Int. J. Biol. Macromol.* **2019**, *133*, 278–283.
[123] K. Kulka, A. Sionkowska, *Molecules* **2023**, *28*, 1817.
[124] I. Aranaz, N. Acosta, C. Civera, B. Elorza, J. Mingo, C. Castro, M. de los, L. Gandía, A. H. Caballero, *Polymers* **2018**, *10*, 213.
[125] E. Guzmán, F. Ortega, R. G. Rubio, *Cosmetics* **2022**, *9*, 99.
[126] Y. A. Gomaa, L. K. El-Khordagui, N. A. Boraei, I. A. Darwish, *Carbohydr. Polym.* **2010**, *81*, 234–242.
[127] S. Ju, G. Shin, M. Lee, J. M. Koo, H. Jeon, Y. S. Ok, D. S. Hwang, S. Y. Hwang, D. X. Oh, J. Park, *Green Chem.* **2021**, *23*, 6953–6965.
[128] W. Wisuitiprot, K. Ingkaninan, S. Jones, N. Waranuch, *J. Cosmet. Dermatol.* **2022**, *21*, 4001–4008.
[129] D. Piccinino, E. Capecchi, E. Tomaino, S. Gabellone, V. Gigli, D. Avitabile, R. Saladino, *Antioxidants* **2021**, *10*, 1–19.
[130] F. Antunes, I. F. Mota, J. F. Fangueiro, G. Lopes, M. Pintado, P. S. Costa, *Int. J. Biol. Macromol.* **2023**, *234*, 0–9.
[131] S. C. Lee, T. M. T. Tran, J. W. Choi, K. Won, *Int. J. Biol. Macromol.* **2019**, *122*, 549–554.
[132] R. Sun, Y. Niu, M. Li, Y. Liu, K. Wang, Z. Gao, Z. Wang, T. Yue, Y. Yuan, *Trends Food Sci. Technol.* **2023**, *134*, 80–97.
[133] Zulham, G. Wilar, Y. Susilawati, A. Subarnas, A. Y. Chaerunisaa, *Pharmacogn. J.* **2021**, *13*, 285–295.
[134] A. Asti, L. Gioglio, *Int. J. Artif. Organs* **2014**, *37*, 187–205.
[135] K. Sudesh, K. Bhubalan, J. A. Chuah, Y. K. Kek, H. Kamilah, N. Sridewi, Y. F. Lee, *Appl. Microbiol. Biotechnol.* **2011**, *89*, 1373–1386.
[136] H. Park, H. He, X. Yan, X. Liu, N. S. Scrutton, G. Q. Chen, *Biotechnol. Adv.* **2024**, *71*, 108320.
[137] K. Saravanan, M. Umesh, P. Kathirvel, Journal of Polymers and the Environment **2022**, G2gbio Inc *30*, 4903–4935.
[138] N. Phothong, T. Boontip, P. Chouwatat, D. Aht-Ong, S. C. Napathorn, *Int. J. Biol. Macromol.* **2024**, *257*, 128709.
[139] M. N. Abu Hajleh, A. AL-Samydai, E. A. S. Al-Dujaili, *J. Cosmet. Dermatol.* **2020**, *19*, 2805–2811.
[140] K. J. Jem, B. Tan, *Adv. Ind. Eng. Polym. Res.* **2020**, *3*, 60–70.
[141] M. O. Christen, F. Vercesi, *Clin. Cosmet. Investig. Dermatol.* **2020**, *13*, 31–48.
[142] A. Forigua, A. Dalili, R. Kirsch, S. M. Willerth, K. S. Elvira, *ACS Appl. Polym. Mater.* **2022**, *4*, 7004–7013.
[143] H. C. Nam, W. H. Park, *ACS Biomater. Sci. Eng.* **2020**, *6*, 2440–2449.
[144] K. Shen, *MATEC Web Conf.* **2023**, *386*, 01005.
[145] L. Dutra, M. Nele, J. C. Pinto, *Macromol. Symp.* **2018**, *381*, 1–8.
[146] H. Gan, T. Okada, S. Kimura, K. Kasuya, T. Iwata, *Polym. Degrad. Stab.* **2023**, *208*, 110239.
[147] G. DiStefano, P. Valsesia, Intercos SpA *US Patent App. 17/908,132*, **2023**.
[148] S. Scheele, M. Mette, P. Westphal, T. Schroeder, Henkel AG and Co KGaA *U.S. Patent No. 11,701,321*, **2023**.
[149] L. Mentink, A.-M. Lheritier, M. Lavarde, S. Piot, Roquette Freres SA *U.S. Patent No. 11,690,795*, **2023**.
[150] T. Tsuji, T. Nogita, Chuetsu Pulp and Paper Co Ltd*U.S. Patent Application No. 16/606,291*, **2022**.
[151] T. Sudo, Y. Hirama, S. Niinobe, Shin Etsu Chemical Co Ltd *U.S. Patent Application No. 18/155,109*, **2023**.
[152] D. Schlenker, S. Von der Fecht, H. Volbrich, S. Sprock, Beiersdorf AG *U.S. Patent Application No. 17/904,039*, **2023**.
[153] J. C. Puche, L. Dupin, J. L. Viladot Petit, P. Guardeño Mingueza, M. Casanovas Gassó, Lubrizol Advanced Materials Inc *U.S. Patent Application No. 18/018,663*, **2023**.
[154] M. H. Padilha, C. Scliar Sasson, B. Correa Da Cruz, Janny Fernanda Stangherlin Santucci, Botica Comercial Farmaceutica Ltda *U.S. Patent Application No. 18/257,931*, **2024**.

[155] X. Qiu, Y. Qian, Y. Li, D. Yang, H. Lou, S. Zhu, W. Liu, South China University of Technology SCUT *U.S. Patent No. 10,729,624*, **2020**.
[156] R. S. Blackburn, C. M. Rayner, Keracol Ltd *U.S. Patent Application No. 18/085,214*, **2023**.
[157] P. Wong, Tula Life Inc *U.S. Patent Application No. 17/583,125*, **2023**.
[158] L. Caisey, M. Cabannes, L. Poulet, F. Guyon, J.-Y. Berthon, A. Martin, Freedge Sas *U.S. Patent Application No. 17/433,819*, **2022**.
[159] K. Booten, Creasearch BV *U.S. Patent Application No. 17/791,703*, **2023**.
[160] P. Saettone, M. Comes Franchini, Bio On SpA *U.S. Patent Application No. 17/967,834*, **2023**.
[161] H. T. Lam, L. A. McCullough, Y. L. Lee, J. Gu, L'Oreal S.A. *U.S. Patent Application No. 17/387,420*, **2023**.
[162] H. Super, P. W. Mijnen, P. G. Zijlstra, D. W. Grijpma, Aqtis IP BV *U.S. Patent No. 11,998,638*, **2024**.
[163] H. Lee, E. Seol, K. Yoon, Y. Na, G2gbio Inc *U.S. Patent Application No. 16/960,379*, **2020**.
[164] H. Lee, E. Seol, K. Yoon, Y. Na, G2gbio Inc *U.S. Patent No. 11,590,258*, **2023**.
[165] Y. Li, L. Tao, Q. Wang, F. Wang, G. Li, M. Song, *Environ. Heal.* **2023**, *1*, 249–257.

Manuscript received: May 17, 2024
Revised manuscript received: July 18, 2024
Accepted manuscript online: September 2, 2024
Version of record online: September 24, 2024